Universidad de Cantabria

Escuela Técnica Superior de Ingenieros Industriales y de Telecomunicación

Departamento de Ingenierías Química y Biomolecular

TRACEABILITY OF PCDD/Fs FORMATION IN THE ADVANCED OXIDATION OF TRICLOSAN IN AQUEOUS SAMPLES

Trazabilidad de la formación de PCDD/Fs durante la oxidación avanzada de Triclosan en fase acuosa

Memoria de Tesis Doctoral presentada para optar al título de
Doctor por la Universidad de Cantabria. Programa Oficial de Doctorado
en Ingeniería Química, de la Energía y de Procesos.

Claudia Solá Gutiérrez

Directoras de la Tesis Doctoral:

Prof. Dr. Inmaculada Ortiz Uribe

Dr. Mª Fresnedo San Román San Emeterio

Santander, 2019

Programa Oficial de Doctorado en Ingeniería Química, de la Energía y de Procesos (BOE núm. 16, de 19 de enero de 2015. RUCT: 5601000)

This research was financially supported by the Spanish Ministry of Science, Innovation and Universities through the Projects: CTM2014-58029-R (MINECO-FEDER, UE) "Identificación y Cuantificación de las Variables Responsables de la Potencial Formación de PCDD/Fs en Procesos de Oxidación Avanzada" and CTM2017-87740-R (AEI/FEDER, UE) "Aplicación de Tecnologías Ambientales a Matrices Líquidas Conteniendo Contaminantes Orgánicos Emergentes Precursores de la Formación de Derivados Clorados (PCDD/Fs)".

The author of the thesis would also like to express her gratitude to the Spanish Ministry of Science, Innovation and Universities for the FPI postgraduate research grant (BES-2015-072920). Thanks to this financial aid, a predoctoral short stay have been conducted. This research stay was developed in the Institute of Biogeochemistry and Pollutant Dynamics at the Eidgenössische Technische Hochschule (ETH, Zürich) over the period September-December 2018, under the supervision of Professor Kristopher McNeill.

Due to all these, a warm thanks towards these institutions is extended.

Agradecimientos

Me gustaría expresar mi más sincero agradecimiento a mis directoras de tesis, la Prof. Dra. Inmaculada Ortiz Uribe y la Dra. María Fresnedo San Román San Emeterio, por brindarme la oportunidad de realizar este trabajo, pero sobre todo por su ayuda, dedicación y paciencia durante toda esta etapa investigadora. Sin vuestros consejos y sugerencias la obtención de esta tesis no hubiera sido posible. Muchas gracias por todo vuestro tiempo invertido, que finalmente, ha permitido alcanzar con éxito el fin de esta etapa.

I would like to acknowledge Prof. Dr. Kristopher McNeill and Dr. Jennifer Apell for giving me the opportunity to work at the Institute of Biogeochemistry and Pollutants Dynamics in the Department of Environmental Systems Science (ETH, Zürich). I would like to highlight their help, devotion and support to develop this work. I would also like to thank all members of the research group for the willingness to always help me, especially to Kathi, Prachi, Taylor, Gordon and Ale. It was a great experience, professionally as well as personally.

Ampliar mi agradecimiento al personal administrativo, personal técnico y profesorado del Departamento de Ingenierías Química y Biomolecular de la Universidad de Cantabria, por la asistencia recibida. Especialmente, me gustaría dar las gracias a Gema, siempre dispuesta a echarme una mano en todo lo que he necesitado, y a Sonia, por el esfuerzo dedicado en la compleja tarea de análisis de muestras. A Pablo, quien me enseñó con gran paciencia y detalle el infinito método EPA 1613, pero que, con tan buena compañía, ¡cada muestra era un paseo! Y, por supuesto, agradecer a todos mis compañeros del 335-H y alrededores, siempre dispuestos a apoyarme poniéndole un toque de humor al día a día: Laura, Cris, Alba, Miguel, Juan… Jenni, aunque ya no estés en el "seminario", has dejado una huella difícil de borrar. No sólo sois buenos compañeros, si no que me llevo muy buenos amigos.

No puedo dejar pasar esta oportunidad para dar las gracias a mi compañera y mi gran amiga Sophie. Hemos luchado y aprendido mucho juntas (creo que nos llevamos el récord en horas dedicadas al HPLC). Gracias por hacerlo todo fácil, por tus consejos, por tirar de mi en los momentos más difíciles y por ser siempre mi apoyo, desde el 21 de septiembre de 2009. ¡Gracias por estos años!

Quería agradecer a mis amigos Jose, Iván, Javi, Carmen y Bea, por estar siempre ahí para compartir nuevas experiencias y seguir creciendo juntos. A mi “comando” de chicas, apoyo fundamental desde hace ya muchos años. A Maitane, por escucharme y aconsejarme siempre que lo he necesitado, y, además, como buena navarra, acabar teniendo siempre la razón. A mi “Familia por el mundo”, siempre presente. Porque los buenos amigos duran siempre.

A Luca, por su paciencia, apoyo y fuerza en todo momento. Gracias por ser mi mejor acompañante en nuestra nueva aventura. “I bi immer für di da. Immer. Ey tag länger aus für immer!”. Finalmente, quiero agradecer a toda mi familia, por su incondicional apoyo. A Abu, porque aunque sea difícil entender lo que hago, siempre estás ahí para apoyarme, y a Tere, porque por mucho que pasen los años, tus recuerdos siguen vivos. A mi hermano, por tener la gran habilidad de revolucionar todo por donde pasa, pero al final acabar haciéndonos reír a todos. Y especialmente a mis padres, mi respaldo, porque si he llegado hasta aquí ha sido gracias a ellos. El camino de la vida se recorre de una manera mucho más fácil con vuestros sabios consejos.

A todos, ¡muchas gracias!

Claudia

Table of contents

Summary

Triclosan (TCS) is an emerging antimicrobial pollutant; it belongs to the group of Pharmaceutical and Personal Care Product (PCPP), commonly added to many consumer goods, such as cosmetics, hand wash, deodorant, soaps and toothpaste, among others. The extensive use of TCS has caused its presence in many water sources, especially in wastewater, wastewater treatment plant effluents, lakes, rivers and in sediments throughout the world, posing a risk to the environment and human health. Advanced Oxidation Processes (AOPs), defined as aqueous phase oxidation technologies based on the formation of highly reactive species, especially hydroxyl radicals (·OH), have been successfully applied to wastewaters containing recalcitrant organic compounds, such as TCS. Together with the complete removal of the pollutant, the generation of by-products during the degradation of the primary pollutant is another issue of concern in the application of AOPs. In fact, the presence of these by-products could increase the final toxicity of the treated wastewater. In this way, TCS has been related to the formation of polychlorinated dibenzo-p-dioxins and dibenzofurans (PCDD/Fs), which are a family of unintentionally persistent organic pollutants regulated internationally by the Stockholm Convention (2001). They belong to the so-called “dirty-dozen” and, even though they are emitted at low concentrations, they are characterized by their high persistency, bioaccumulation in the environment and high toxicity.

Hence, this thesis aims to generate knowledge to help in the safe implementation of remediation technologies to remove TCS from wastewater. Specifically, it is focused on the study of oxidation treatments, electrochemical and photo-oxidation, in terms of TCS degradation rate and by-products formation, paying special attention to the potential formation of PCDD/Fs.

Firstly, in chapter 1, an overview of the main aspects related to PPCPs as precursors of PCDD/Fs during the application of AOPs is detailed. Additionally, the fundamentals of AOPs and, specifically, of electrochemical and photolytic oxidation (photolysis and photocatalysis), focused on the degradation of TCS and the formation of PCDD/Fs and related by-products, are presented.

Chemical reagents, experimental set-up as well as analytical methods and techniques are detailed in chapter 2, paying special attention to liquid and gas chromatography techniques, as well as to PCCD/Fs analytical method.

Although the high effectiveness of electrochemical oxidation applied to organic compounds has been reported by many authors, the literature that focuses on TCS degradation

by-products is scarce, and is still more scarce in relation to the final toxicity of the treated water. In this sense, the electrochemical oxidation of TCS solutions using boron-doped diamond anodes, focused on the quantitative traceability of chlorinated derivatives, is reported in chapter 3. The role of two widely applied electrolytes, NaCl and Na_2SO_4, has been studied. Besides, and motivated by the extended presence of copper in wastewaters and industrial effluents, the influence of the presence of this metal in the treated solution has been analysed. Of the three variables, it is the presence of NaCl as electrolyte the one with a more pronounced contribution to the formation of chlorinated by-products, and, more specifically, to the formation of low and highly chlorinated PCDD/Fs, analysed following the 1613 EPA method (specialized to analyse species from tetra-PCDD/Fs to OCDD/Fs). In this way, and working at these conditions, the toxicity equivalent index (TEQ) reached values between 4.4 and $3.8 \cdot 10^2$ pg L^{-1}, being between 10 and 320 times higher with respect to the untreated water that contained TCS. Additionally, coupled to the determination of 2,7/2,8-dichlorodibenzo-p-dioxin congener, classified as a low chlorinated PCDD/Fs, the results of the concentration of 0.67 mg L^{-1} obtained after GC/MS analysis were not supported by the HPLC technique that works at milder temperature; thus, further analytical efforts are needed to corroborate the formation of this compound.

In chapter 4, based on literature reports that highlight the effective degradation of a wide range of organic pollutants, the performance of photolysis (direct) and photocatalysis (indirect) oxidation of TCS samples was analysed. The study was focused on establishing the oxidation routes that lead to the potential formation of PCDD/Fs and related compounds shedding light into the mechanistic degradation of TCS. Firstly, an exhaustive and critical analysis of the state-of-the-art related to the photo-degradation techniques applied to TCS solutions, as well as to the formation of different intermediate products during the application of these treatments, is presented. Then, once the best pH and wavelength conditions had been determined, a deep experimental study of the photolysis of TCS was performed, focused on the understanding of the reaction pathways that are behind the photolysis of TCS. These results led to a consistent proposal of the oxidation route of TCS based on the experimental data obtained, and, specifically, on the formation pathway of 2,8-dichlorodibenzo-p-dioxin through the analysis of the three different chlorine positions of the TCS molecule. Finally, in order to study the influence of a catalyst on the reaction medium, TiO_2 photocatalytic treatment of TCS was carried out. The obtained results showed better results in terms of TCS degradation and lower PCDD/Fs formation as the catalyst loading increased. In this regard, TEQ reached values between 0.5 and 6.3 pg L^{-1}, being between 10 and 104 times higher with respect to untreated water that initially contained TCS.

This thesis contains novel results regarding the potential formation of PCDD/Fs in the application of AOPs to aqueous solutions containing PPCPs, emphasizing the importance of the quantitative traceability of by-products formation and the resulting toxicity depending on the treatment and conditions applied. Besides, it contributes with new information on the controversial formation of low chlorinated dioxin, 2,8-dichlorodibenzo-p-dioxin, during the oxidation of TCS aqueous samples, highlighting the relevance of the analytical technique and opening the way for further research.

Resumen

Triclosán (TCS) es un contaminante emergente antimicrobiano perteneciente al grupo de los Productos Farmacéuticos y de Cuidado Personal (PPCPs en inglés), y comúnmente añadido a una gran cantidad de artículos de consumo, tales como cosméticos, jabones, desodorantes y pasta de dientes, entre otros. Como consecuencia de su extensivo uso, el TCS se ha encontrado en muchas fuentes de agua, especialmente en aguas residuales, efluentes de Estaciones Depuradoras de Aguas Residuales (EDAR), lagos, ríos y sedimentos en todo el mundo, siendo un riesgo para el medio ambiente y la salud humana. Los Procesos de Oxidación Avanzada (POAs), que se definen como tecnologías de oxidación en fase acuosa basadas en la formación de especies altamente reactivas, fundamentalmente radicales hidroxilo (·OH), han sido aplicadas satisfactoriamente a aguas residuales que contienen compuestos orgánicos recalcitrantes, como el TCS. Junto con la completa eliminación del contaminante, la generación de subproductos durante la degradación del contaminante primario en la aplicación de POAs es motivo de preocupación. En efecto, la presencia de estos subproductos puede aumentar la toxicidad final del agua residual tratada. En este sentido, el TCS ha sido relacionado con la formación de dibenzo-p-dioxinas y dibenzofuranos policlorados (PCDD/Fs), una familia de contaminantes orgánicos persistentes regulados internacionalmente por el Convenio de Estocolmo (2001). Pertenecen a los llamados “dirty-dozen” y, aunque son emitidos en bajas concentraciones, están caracterizados por su gran persistencia, bioacumulación en el medio ambiente y elevada toxicidad.

En este sentido, esta tesis tiene como objetivo generar conocimiento en la implementación segura de tecnologías de remediación para eliminar TCS de aguas residuales. Concretamente se centra en el estudio de tratamientos oxidativos, oxidación electroquímica y oxidación fotoquímica, en términos de degradación de TCS y de formación de subproductos, con especial interés en la potencial formación de PCDD/Fs.

En primer lugar, en el capítulo 1 se detalla una perspectiva general de los aspectos principales relacionados con los PPCPs como precursores de PCDD/Fs durante la aplicación de POAs. Además, se exponen los principios básicos de los POAs y, más concretamente, la oxidación electroquímica y oxidación fotoquímica (fotólisis y fotocatálisis), centrados en la degradación del TCS y en la formación de PCDD/Fs y subproductos relacionados.

Los reactivos empleados, las configuraciones experimentales, así como los métodos y técnicas analíticas, son detallados en el capítulo 2, con especial interés en las técnicas de cromatografía líquida y de gases, y al método análitico empleado en el análisis de PCDD/Fs.

Varios autores han reportado la alta efectividad de la oxidación electroqímica aplicada a compuestos orgánicos, sin embargo, la literatura centrada en los suproductos de degradación del TCS es escasa, siendo aún más escasa enfocada a la toxicidad final del agua tratada. En este sentido, en el capíutlo 3 se expone la oxidación electroquímica de soluciones de TCS utilizando ánodos de diamante dopados con boro, centrados en la trazabilidad cuantitativa de derivados clorados. Se ha estudiado la influencia de dos electrolitos comúnmente utilizados debido a su extendida presencia en gran variedad de matrices acuosas, NaCl and Na_2SO_4. Además, e incentivado por la extensa presencia de cobre en aguas residuales y efluentes industriales, la influencia de este metal en la disolución ha sido analizada. De las tres variables estudiadas, la presencia de NaCl como electrolito es la que presentó una mayor contribución a la formación de subproductos clorados y, más específicamente, a la formación de PCDD/Fs de baja y alta cloración, analizados siguiendo el método EPA 1613 (específico para el análisis desde tetra-PCDD/Fs hasta octa-PCDD/Fs). Trabajando con estas condiciones de operación, el Equivalente Tóxico (en inglés, Toxic Equivalent, TEQ) alcanzó valores entre 4.4 and $3.8 \cdot 10^2$ pg L^{-1}, siendo entre 10 y 320 veces mayor con respecto al agua con TCS sin tratar. Además, la determinación del congéner 2,7/2,8-diclorodibenzo-p-dioxina, clasificado como PCDD/Fs de baja cloración, resultó en una concentración de 0.67 mg L^{-1}, obtenido a través del análisis con GC/MS. Este resultado no fue contrastado con la técnica analítica HPLC, que funciona a temperaturas más bajas, y, por lo tanto, mostrando que se requiere una mayor investigación en este área para poder corroborar la formación de este compuesto.

En el capítulo 4, se analizaron los resultados obtenidos en la literatura aplicados a la oxidación por fotólisis (oxidación directa) y por fotocatálisis (oxidación indirecta) de muestras que contienen TCS, los cuales destacan la degradación efectiva de una amplia gama de contaminantes orgánicos. El estudio se centró en establecer las rutas de oxidación que conducen a la potencial formación de PCDD/Fs y compuestos relacionados, arrojando luz sobre los

mecanismos de reacción del TCS. En primer lugar, se presenta un análisis exhaustivo y crítico del estado del arte relacionado con las técnicas de foto-degradación aplicadas a soluciones con TCS, así como a la formación de diferentes productos intermedios durante la aplicación de estos tratamientos. Después, una vez determinadas las mejores condiciones de pH y longitud de onda, se realizó un profundo estudio experimental enfocado a la fotólisis de TCS y a las rutas de degradación que están detrás de este proceso. Estos resultados dieron lugar a una propuesta consistente de rutas de oxidación de TCS basada en los datos experimentales obtenidos y, específicamente, se propuso una vía de formación de la 2,8-diclorodibenzo-p-dioxina a través del análisis de las tres posibles posiciones del cloro en la molécula de TCS. Finalmente, se llevó a cabo el tratamiento fotocatalítico de TCS con TiO_2 con el fin de estudiar la influencia de un catalizador en el medio de reacción. Los resultados obtenidos mostraron una mejora en los resultados en términos de degradación de TCS, y una menor formación de PCDD/Fs a medida que aumentaba la carga de catalizador. En este sentido, el TEQ alcanzó valores entre 0.5 y 6.3 pg L^{-1}, siendo entre 10 y 104 veces mayor con respecto al agua sin tratar que contiene TCS.

Esta tesis contiene resultados novedosos con respecto a la potencial formación de PCDD/Fs en la aplicación de POAs a soluciones acuosas que contienen PPCPs, enfatizando en la importancia de la trazabilidad cuantitativa de la formación de subproductos, además de en la toxicidad resultante dependiendo del tratamiento y de las condiciones aplicadas. Además, contribuye con información nueva sobre la controvertida formación de dioxinas de baja cloración, especialmente 2,8-diclorodibenzo-p-dioxina, durante la oxidación de muestras acuosas que contienen TCS, destacando la importancia de las técnicas analíticas que abren el camino para futuras investigaciones.

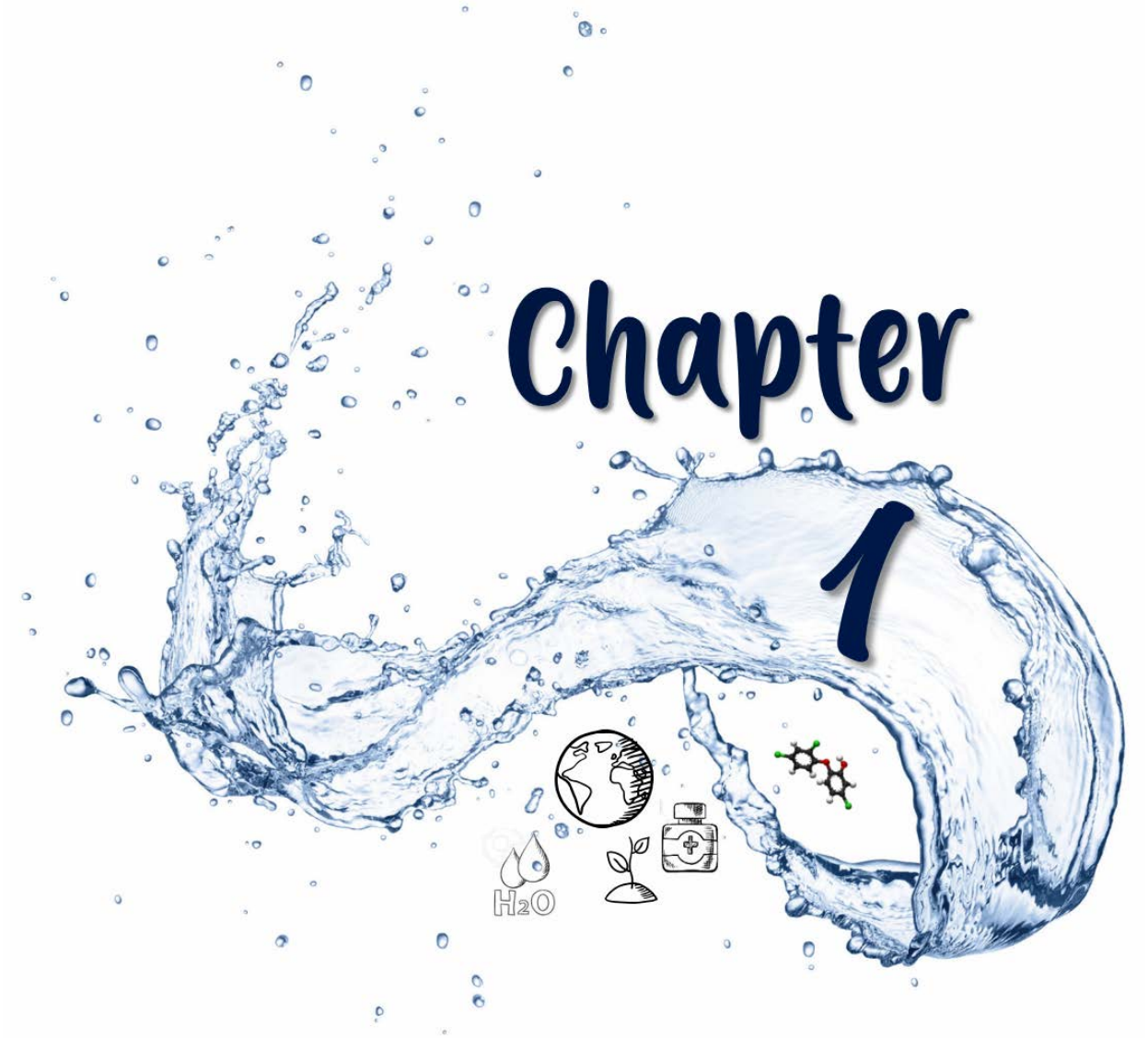

Chapter 1

MOTIVATION

1.1. Water contamination with emerging and persistent pollutants

Water pollution may be defined as the contamination of water with chemical compounds or other substances that are harmful to human, plant or animal health (National Institute of Environmental Health Sciences, 2019). Due to the rising global demand of water, the wastewater production is increasing and, as a consequence, the pollution load around the world, is constantly growing (UNESCO, 2017). According to the 2017 edition of the United Nations World Water Development Report, over 80 % of the world's wastewater is discharged to the environment free of treatment, entering into lakes, rivers, aquifers and sea, causing adverse consequences for the environment (UNESCO, 2017). Moreover, as described by the World Health Organization (WHO) and the United Nations International Children´s Emergency Fund (UNICEF) in the Joint Monitoring Programme report updated in 2017, 2.1 billion people lack access to safe and easy available water at home, and 4.5 billion people lack safe sanitation (World Health Organization (WHO) and United Nations Children's Fund (UNICEF), 2017). In addition, it is expected that 90 % of the 3 billion people to be added to the world´s population by 2050 might be in countries that are already experiencing water stress (World Water Assessment Programme (WWAP), 2017).

In addition, associated with the population increase of the last decade, the occurrence of new and emerging pollutants in the aquatic environment is becoming a serious concern. Emerging pollutants may be defined as chemicals that are not commonly monitored but have the potential to enter the environment and cause adverse ecological and human health effects, possibly being regulated by future legislation (Geissen et al., 2015; Teodosiu et al., 2018). Its source could be attributed to the increase of industrial and household wastewater, agriculture water discharge, aquaculture, hospital effluents and landfill leachates (Ribeiro et al., 2015), since these emerging pollutants may be found in pesticides, cosmetics, industrial compounds, and pharmaceutical and personal care products (PPCPs), among others (Yap et al., 2019).

The significance of this issue needs to be addressed in the context of the large number of emerging pollutants that already exist and, unfortunately, keep growing as new chemicals are identified. According to the biannual review of emerging pollutants in water, Table 1.1 shows a brief classification of these substances as well as the most representative chemicals belonging to each group (Richardson and Ternes, 2018). PCPPs are of special relevance, since the list of

these compounds is very large and between 60 and 80 % of them end up in urban wastewater (Marín Galvín, 2017).

Table 1.1. Major emerging pollutant groups classification (Stefanakis and Becker, 2015; Ebele et al., 2017).

Emerging contaminant groups	Commercial name	Chemical name
Pharmaceuticals and Personal Care Products (PCPPs)	Amoxicillin	*(2S,5R,6R)-6-[[(2R)-2-amino-2-(4-hydroxyphenyl) acetyl]amino]-3,3-dimethyl-7-oxo-4-thia-1-azabicyclo[3.2.0]heptane-2-carboxylic acid*
	Diclofenac	*2-[2-(2,6-dichloroanilino)phenyl]acetic acid*
	Ibuprofen	*(RS)-2-(4-(2-methylpropyl)phenyl)propanoic acid*
	Paracetamol	*N-(4-hydroxyphenyl)ethanamide, N-(4-hydroxyphenyl)acetamide*
	Salbutamol	*4-[2-(tert-butylamino)-1-hydroxyethyl]-2-(hydroxymethyl)phenol*
	Diatrizoate	*3,5-bis(acetylamino)-2,4,6-triiodobenzoic acid*
	Benzophenone	*Diphenylmethanone*
	N,N-diethyltoluamide (DEET)	*N,N-Diethyl-3-methylbenzamide*
	Triclosan	*5-chloro-2-(2,4-dichlorophenoxy)phenol*
	DEHP	*Bis(2-ethylhexyl)phthalate*
	Estradiol	*(17β)-estra-1,3,5(10)-triene-3,17-diol*
	Estrone	*(8R,9S,13S,14S)-3-hydroxy-13-methyl-7,8,9,11,12,14,15,16-octahydro-6H-cyclopenta[a]phenanthren-17-one*
	Estriol	*(8R,9S,13S,14S,16R,17R)-13-methyl-6,7,8,9,11,12,14,15,16,17-decahydrocyclopenta[a]phenanthrene-3,16,17-triol*
	Diethylstilbestrol	*4,4'-(3E)-hex-3-ene-3,4-diyldiphenol*
Perfluoronated compounds	PFOA	*Perfluorooctanoic acid*
	PFOS	*Perfluorooctane sulfonate*
Surfactants and surfactant metabolites	APEO	*Alkylphenol ethoxylates*
	4-nonylphenol	-
Flame retardants	PBDEs	*Polybrominated diphenyl ethers*
	PBBs	*Polybrominated biphenyls*
	PBDDs	*Polybrominated dibenzo-p-dioxins*
	PBDFs	*Polybrominated dibenzofurans*
	HBCD	*Hexabromocyclododecane*
Industrial additives and agents	EDTA	*Ethylenediaminetetraacetic acid*
	Aromatic sulfonates	-
Gasoline additives	Dialkyl ethers	-
	MTBE	*Methyl tert-butyl ether*

The European Union along with the United States Environmental Protection Agency (USEPA) have highlighted some of the emerging pollutants, developing a priority pollutant list. Priority pollutants are defined as a wide range of chemicals that are present in wastewater and surface waters, among other sources, characterized by special persistence, bioaccumulation and toxicity criteria (Ebele et al., 2017). Their presence, due to being eco-toxicological and harming human health effects, pose a risk throughout the environment (Teodosiu et al., 2018). If emerging pollutants are relatively new and not well regulated, priority pollutants, which are mostly part of emerging pollutants, are regulated at international and national levels. In 2001, the initial lists consisted of 33 priority chemicals established by the European Union Water Framework Directive (EU WFD) (2455/2001/CE). This directive was updated being extended to 45 priority substances by 2013/39/UE Directive. Then, in 2015, 10 substances were identified as future priority candidates to add to the list by the 2015/495/UE Directive. In the same way, the 2015/495/UE Directive was updated and 8 more substances were added to the list (2018/840/UE) (Ebele et al., 2017). In addition, only a small part of emerging pollutants have been classified as Persistent Organic Pollutants (POPs), defined as chemicals that persist in the environment, bioaccumulate through the food chain and cause adverse effects to human health and the environment (Stockholm Convention, 2008). Initially, 12 POPs were included in the list. Currently, 28 POPs comprises the list and they are classified into 3 categories: pesticides, industrial chemicals and unintentional chemical by-products (Stockholm Convention, 2017). A brief scheme summarizing the three different pollutant groups with their respective legislation is displayed in Figure 1.1.

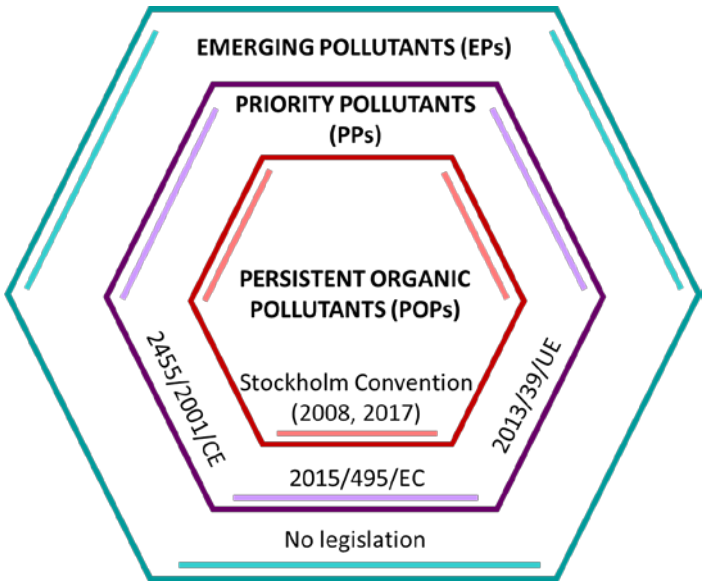

Figure 1.1. Scheme of emerging, priority and persistent pollutants and their respective regulations.

1.1.1. Pharmaceutical and Personal Care Products: Triclosan

Pharmaceutical and Personal Care Products (PCPPs) are defined by the U.S. EPA as any product used by individuals for personal health, cosmetic use or utilized to enhance growth or health of livestock. PCPPs are characterized by their extensively and increasingly use; however, due to their physicochemical properties, many of them are not easily removed. As a result, they reach the environment, being found in water, sediments and biota (Ebele et al., 2017). PCPPs may be classified in many groups including antibiotics, hormones, anti-inflammatory drugs, antimicrobial agents or preservatives (Table 1.2) (Liu and Wong, 2013). Although most of them are emerging environmental pollutants that are extensively and progressively being used in human and animals medicine, some of them already been classified as priority pollutants, as in the case of diclofenac (Nikolaou et al., 2007).

Table 1.2. Classification of Pharmaceutical and Personal Care Products (PCPPs) (Liu and Wong, 2013).

Pharmaceutical	Antibiotics	*Clarithromycin, Erythromycin, Sulfamethoxazole, Sulfadimethoxine, Ciprofloxacin, Norfloxacin, Chloramphenicol*
	Hormones	*Estrone, Estradiol, Ethinylestradiol*
	Analgesics and anti-inflammatory drugs	*Diclofenac, Ibuprofen, Acetaminophen, Acetylsalicylic acid*
	Antiepileptic drugs	*Carbamazepine, Primidone*
	Blood lipid regulators	*Clofibrate, Gemfibrozil*
	B-blockers	*Metoprolol, Propanolol*
	Constrast media	*Diatrizoate, Iopromide*
	Cytostatic drugs	*Ifosfamide, Cyclophosphamide*
Personal Care Products (PCPs)	Antimicrobial agents/Disinfectants	*Triclosan, Triclocarban*
	Synthetic musks/Fragrances	*Galaxolide, Toxalide*
	Insect repellants	*N,N-diethyl-m-toluamide*
	Preservatives	*Parabens*
	Sunscreen UV filters	*2-ethyl-hexyl-4-trimethoxycinnamate, 4-methyl-benzilidine-camphor*

From all antimicrobial agents, Triclosan (TCS) that acts as disinfectant, preservative or antiseptic (Scientific Committee on Consumer Safety, 2010), have been commonly added to many consumer goods, such cosmetics, hand wash, deodorant soaps, detergents, toothpaste, textiles, plastic consumer goods, as well as toys, (Figure 1.2). Triclosan production started in 1964 and, approximately, in 1998, 1500 tons were produced annually worldwide (Bester, 2005). Among them, 350 and 450 tons were produced in Europe and U.S., respectively (Dhillon et al., 2015). Its worldwide production annually increased due to its multiple uses. However, the industrial development was not accompanied by a rigorous legislation regarding its use and its permissible levels and thus, the production and environmental management of Triclosan-based products has not been safely controlled yet (Halden, 2014).

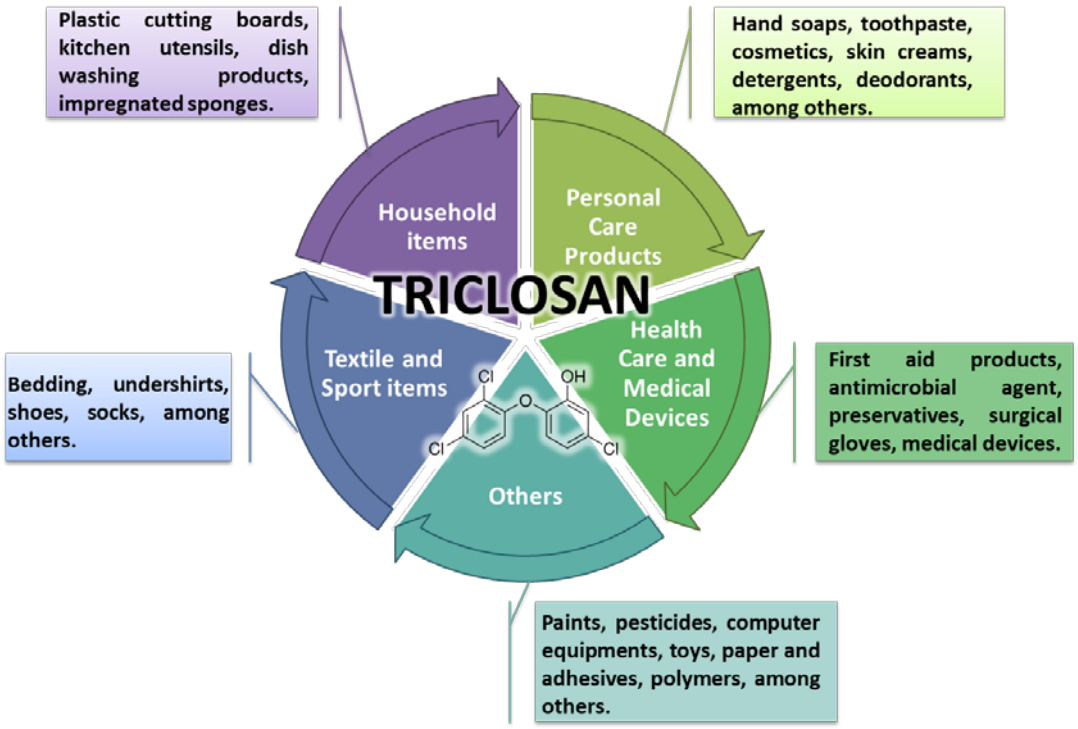

Figure 1.2. Different applications of Triclosan (Dhillon et al., 2015).

Triclosan has been related to numerous human health problems, including dermatitis, skin irritation, increase of allergic reactions, thyroid hormone metabolisms alterations, and it has been defined as an endocrine disruptor (Weatherly and Gosse, 2017). The Food and Drug Administration (FDA) and the Environmental Protection Agency (EPA) have been working together in various regulatory issues related to Triclosan. In May 2015, EPA replied to the Citizen Petition that requested the cancelation of registered pesticide products that contained Triclosan and assessing risk under the Federal Food, Drug, and Cosmetic Act, Clean Water Act, Safe

Drinking Water Act, among others. EPA approved some petitions, including the evaluation of a biological assessment of the potential effects of Triclosan registered products, and disapproved others, like the cancelation of registered pesticides products that contain Triclosan due to the lack of available information that support this petition. Then, in 2016, the FDA issued a final ruling that was eventually effective in 2017: consumer antiseptic wash products containing an antibacterial active ingredient like Triclosan, since they are not recognized as safe and effective, can no longer be marketed. In the same way, according to the European Commission the maximum concentration of Triclosan is restricted to 0.2 % in mouthwashes and 0.3 % in other cosmetic products, such as toothpastes, face powders or hand soaps (Table 1.3) (358/2014/EU (2014)). Then, in 2016, the European Commission (EC) disapproved Triclosan for use in human hygiene biocidal products (2015/110/EU (2016)). Beginning in February 2017, Triclosan will no longer be allowed in such products in the EU.

Table 1.3. Maximum concentration of TCS and proportion contained in products based on the EU legislation (358/2014/UE).

Product type	Maximum concentration in ready for use preparation	Proportion of TCS-containing products (%) (Codecheck Database)
Toothpaste	0.3 %	3.4 %
Hand soaps		0.4 %
Body soaps / Shower gels		0.1 %
Deodorants (non-spray)		2.2 %
Face powder and blemish concealers		0.2 %
Nails products for fingernails cleaning before the artificial nail system application[1]		-
Mouthwashes	0.2 %	0.5 %

[1] No nail products registered in the consumer Codecheck Database.

The extensive use of Triclosan has caused its presence in many water sources, especially in wastewater, wastewater treatment plant effluents, lakes, rivers, and in sediments throughout the world, posing a risk to the environment and human health (Montaseri and Forbes, 2016). The worldwide concentration of Triclosan reaches values between 1.4 - 40000 ng L^{-1} in surface water, 20 - 86161 ng L^{-1} in wastewater influents, 23 - 5370 ng L^{-1} in wastewater effluents, <100 ng L^{-1} in sea water, 100 - 53000 µg kg^{-1} dry weight in sediments from lakes and rivers, 0.02 - 35 µg kg^{-1} dry weight in marine sediments, 20 - 133000 µg kg^{-1} dry weight in biosolids from wastewater treatment plants, 580 - 15600 µg kg^{-1} dry weight in activated sludge and up to 100

mg L^{-1} in industrial effluents (Dhillon et al., 2015; Martín de Vidales, 2015; Montaseri and Forbes, 2016). Because of its harmful and persistent attributed, Triclosan constitutes an environmental and health hazard, requiring to find new ways to reduce its input into the environment. For all these reasons stated above, this work focuses on the study of Triclosan removal as a model PCPPs.

1.1.2. Polychlorodibenzo-p-dioxins and polychlorodibenzofurans (PCDD/Fs)

Polychlorinated dibenzo-p-dioxins (PCDDs) and polychlorinated dibenzofurans (PCDFs), PCDD/Fs, also known as dioxins and furans, are a group of organic chemical substances that are classified as POPs. They are characterized by a particular combination of physical and chemical properties; they remain long periods in the environment and become widely distributed through it and they accumulate in the fatty tissue of humans, being highly toxic to both humans and wildlife (Stockholm Convention, 2008). PCDD/Fs are associated to a number of adverse illnesses in humans, including immune disorders, reproductive and development problems, or even cancer (World Health Organization (WHO), 2016). PCDD/Fs are highly toxic and ubiquitous compounds, and originally, they were thought to come totally from anthropogenic origin (Zheng et al., 2018). PCDDs comprise 75 congeners and PCDFs comprise 135 congeners (210 congeners in total), which can have up to eight chlorine atoms attached to any carbon atom of the molecule (Figure 1.3). Congeners with the same number of chlorines are called homologues, thus, homologues are the group of PCDDs and PCDFs classified by the number of chlorines presented in the molecule. The Table 1.4 summarizes the names, abbreviations and number of congeners in each homologue.

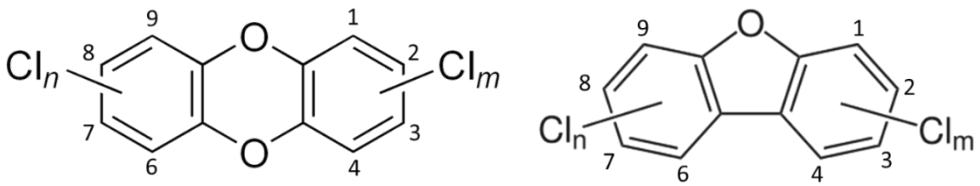

PCDD **PCDF**

Figure 1.3. Structures of PCDD/Fs molecules.

Table 1.4. Homologue PCDD/Fs names, abbreviation and number of congeners in each homologue group.

Homologue	Abbreviation	Chlorines	Number of congeners
Monochlorodibenzo-p-dioxin	MCDD	1	2
Dichlorodibenzo-p-dioxin	DCDD	2	10
Trichlorodibenzo-p-dioxin	TrCDD	3	14
Tetrachlorodibenzo-p-dioxin	TCDD	4	22
Pentachlorodibenzo-p-dioxin	PeCDD	5	14
Hexachlorodibenzo-p-dioxin	HxCDD	6	10
Heptachlorodibenzo-p-dioxin	HpCDD	7	2
Octachlorodibenzo-p-dioxin	OCDD	8	1
		TOTAL	**75**
Monochlorodibenzofuran	MCDD	1	4
Dichlorodibenzofuran	DCDD	2	16
Trichlorodibenzofuran	TrCDD	3	28
Tetrachlorodibenzofuran	TCDD	4	38
Pentachlorodibenzofuran	PeCDD	5	28
Hexachlorodibenzofuran	HxCDD	6	16
Heptachlorodibenzofuran	HpCDD	7	4
Octachlorodibenzofuran	OCDD	8	1
		TOTAL	**135**

The dominant source of PCDD/Fs proceeds from human activity, especially related to combustion processes, but can also come from natural action, like volcanic eruptions or forest fires. There are two well-known pathways of PCDD/Fs formation: on the one hand, formation via “novo synthesis”, described as the degradation of unburned carbon species in the presence of a chlorine source (chlorine, metal chlorides) at temperatures within 200 – 600 ºC (Weber, 2007); or, on the other hand, formation via precursors, including compounds such as chlorophenols (CPs), chlorobenzenes (CBzs), chlorinated diphenyl ethers and polychlorinated biphenyls (PCBs), by the application of oxidative or reductive remediation technologies (Addink and Olie, 1995; Iino et al., 2000; Weber, 2007; Vallejo et al., 2015). According to the literature, four main categories of PCDD/Fs sources can be distinguished: incineration; combustion; industrial; and reservoir sources (Kulkarni et al., 2008) (See Figure 1.4).

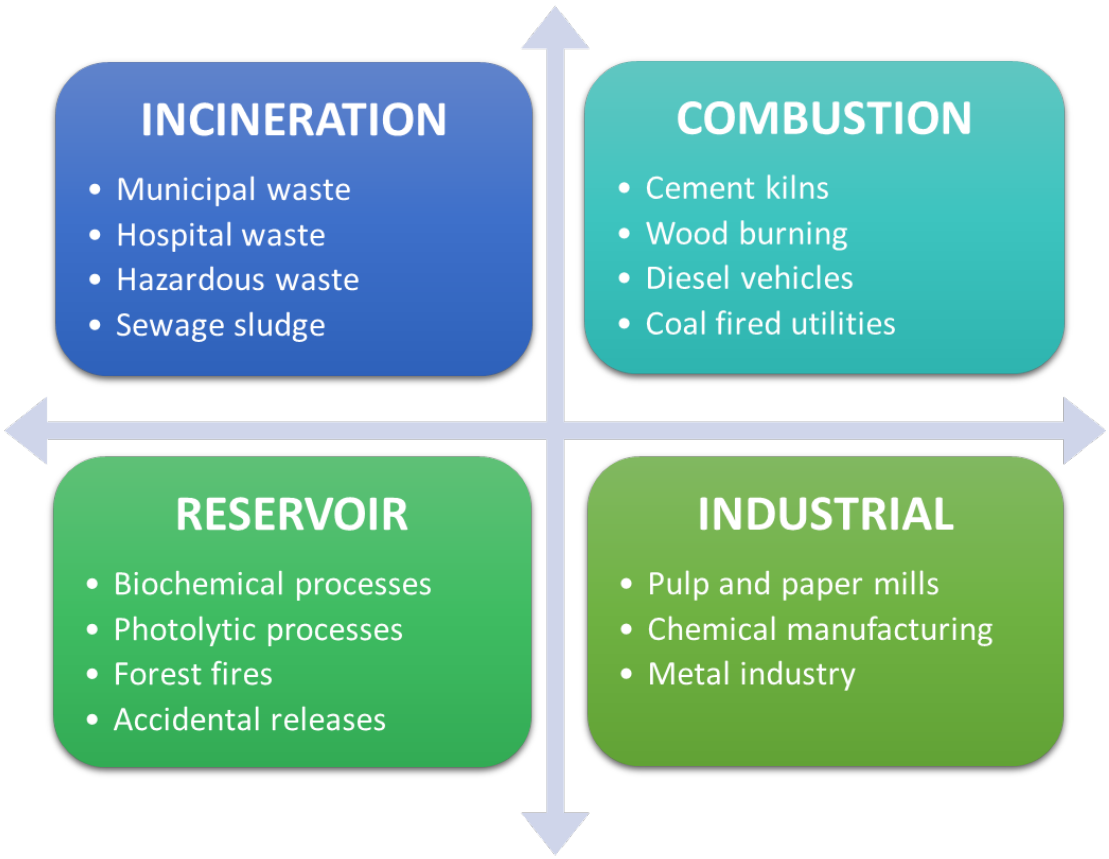

Figure 1.4. PCDD/Fs sources.

Although incineration is an effective way of reducing municipal solid waste, it is the largest source of PCCD/Fs emission in the environment. In particular, they are predominantly produced by municipal solid waste, hospital waste, hazardous waste and sewage sludge incinerators, burning high content of chlorine waste and toxic metals (Stanmore and Clunies-Ross, 2000; Fullana et al., 2007). In the same way, combustion sources, such as cement kilns, wood burning, diesel vehicles, crematoria and coal-fired utilities, are considered an important source of PCDD/Fs release (Abad et al., 2004; Chen, 2004; Lavric et al., 2004). In spite of the low solubility of PCDD/Fs in water, the manufacture of bleached pulp and paper industry results in PCDD/Fs formation through the chlorination of natural phenolic compounds in aqueous phase, like those present in wood pulp (Zheng et al., 2001). The metallurgical industry, which requires high temperature processes to produce steel, is identified as a typical source of PCDD/Fs in aqueous medium (Anderson and Fisher, 2002). Furthermore, although the manufacture of many chlorinated phenolic compounds is nowadays banned in many countries, for example, the production of lindane (γ-hexachlorocyclohexane) in Spain (Gómez-Lavín et al., 2018), former disposal of these substances might result in the formation of PCDD/Fs in the environment (Sidhu and Edwards, 2002). Last but not least, reservoir sources represent a potential formation of

PCDD/Fs, including biological and photochemical natural processes, accidental origin or landfills, among others (Baker and Hites, 2000; Balmer et al., 2000).

Due to the ubiquitous presence of PCDD/Fs, they are found throughout the environment; however, not all PCDD/Fs present the same toxicity. The number of chlorines and their respective position also determine the PCDD/Fs physical and chemical properties, and, as a consequence, the toxicity and persistence of the 210 different congeners. Among all PCDD/Fs congeners, those with a chlorine atom in the position 2, 3, 7 and 8, accounting for a total of 17 congeners, have received special attention due to their higher toxicity and extremely negative effects (Berntssen and Lundebye, 2008). Specifically, 2,3,7,8-TCDD is considered one of the most toxic man-made substance with the highest acute toxicity. Commonly, PCDD/Fs are present in samples as a mixture of the most toxic 2,3,7,8-PCDD/Fs congeners. In order to facilitate the risk assessment and considering that not all PCDD/Fs have the same toxicity, the toxic equivalency factor (TEF) and toxic equivalents (TEQ) were defined. The overall toxicity of a mixture of congeners is expressed as the 2,3,7,8-TCDD TEQ concentration, where 2,3,7,8-TCDD is the most toxic congener. A value of TEF of 1 is given to 2,3,7,8-TCDD, and the TEFs for the other 16 congeners, generally ranged from 0.0003 to 1, are assigned based on their toxicity related to the toxicity of 2,3,7,8-TCDD (Bhavsar et al., 2008). There are two different TEF defined: the International Toxicity Equivalency Factor (I-TEF), established by a scientific research committee called NATO Committee on the Challenges of Modern Society (NATO/CCMS); and the most recently, the World Health Organization Toxicity Equivalency Factor (WHO-TEF), which also includes PCBs, re-evaluated in the International Programme on Chemical Safety meeting in 2005 (Van den Berg et al., 2006). These TEFs values are summarized in Table 1.5. A total TEQ is calculated by summing the product of the congener concentration times the specific TEF of the congener, providing an overall view of the toxicity of the sample.

Table 1.5. Toxic equivalency factors (TEF) for the 17 2,3,7,8-PCDD/Fs congeners.

Congener	I-TEF	WHO-TEF 2005
2,3,7,8-TCDD	1	1
1,2,3,7,8-PeCDD	0.5	1
1,2,3,4,7,8-HxCDD	0.1	0.1
1,2,3,6,7,8-HxCDD	0.1	0.1
1,2,3,7,8,9-HxCDD	0.1	0.1
1,2,3,4,6,7,8-HpCDD	0.01	0.01
OCDD	0.001	0.0003
2,3,7,8-TCDF	0.1	0.1
1,2,3,7,8-PeCDF	0.05	0.03
2,3,4,7,8-PeCDF	0.5	0.3
1,2,3,4,7,8-HxCDF	0.1	0.1
1,2,3,6,7,8-HxCDF	0.1	0.1
1,2,3,7,8,9-HxCDF	0.1	0.1
2,3,4,6,7,8-HxCDF	0.1	0.1
1,2,3,4,6,7,8-HpCDF	0.01	0.01
1,2,3,4,7,8,9-HpCDF	0.01	0.01
OCDF	0.001	0.0003

Since the 1980s, countries are struggling to estimate the emission of PCDD/Fs with the aim to mitigate their effects and release in their territories (Fiedler, 2007). The earliest inventories were made in Canada, Germany, Sweden and USA (Sheffield, 1985; Fiedler and Hutzinger, 1992; Thomas and Spiro, 2011). In the mid-1990s, national agencies established inventories reporting to the requirements of international conventions, such as the Stockholm Convention on Persistent Organic Pollutants (POPs) (Fiedler, 2007). The objective of this Convention consists on the protection of human health and environment from the adverse effects of POPs by reducing or mitigating their release to the environment (Stockholm Convention, 2009). In the case of PCCD/Fs, an unintentionally POP, measures wanted to be taken with the aim to reduce the total releases derived from anthropogenic sources in an attempt to achieve their total elimination. In accordance with the Stockholm Convention, the European Union approved the Regulation 850/2004/EC of 29 April 2004 on POPs, promoting the necessity of eliminate this kind of compounds. More recently, PCDD/Fs have been included as new priority substances in the field of water policy in the Directive 2013/39/EU, which updates the Directives 2000/60/EC and 2008/105/EC. With regard to the U.S. EPA regulation, the Safe Drinking Water Act (SDWA) established a maximum contaminant level goal for 2,3,7,8-TCDD in drinking water of zero, however, considering cost, benefits and the ability of public water systems to remove this kind of compounds, a new maximum level of 30 pg L^{-1} was set.

1.2. Advanced oxidation processes for wastewater treatment

Conventional wastewater treatment plants (WWTPs) are considered to be the most significant emerging pollutant emitters (Luo et al., 2014). These chemicals, due to the ineffectiveness of conventional physical and biological treatments, are partially removed and remain in WWTPs effluents, being discharged into the aquatic environment (Zhang et al., 2008). The need to improve conventional treatments to avoid the presence of emerging pollutants in the ecosystem is required. With this purpose, Advanced Oxidation Processes (AOPs) came out as new technologies that provide effective and powerful treatments to wastewater containing emerging organic pollutants, such as pesticides, PPCPs, industrial chemicals, among others (Comninellis et al., 2008; Klavarioti et al., 2009; Yang et al., 2014; Giannakis et al., 2015). The main challenge currently is to ensure the successful implementation regarding their operational costs (energy consumption, chemicals required), sustainability (carbon footprint, resources uses) or common feasibility (by-products formation) (Miklos et al., 2018).

AOPs might be defined as aqueous phase oxidation technologies that are based on the formation of highly reactive species, especially hydroxyl radicals (·OH), leading to the elimination of the target pollutant (Comninellis et al., 2008). ·OH is one of the most reactive oxidizing agent present in water treatments, with an oxidation potential between 2.8 V and 1.95 V (Deng and Zhao, 2015). This radical has the advantage of being non-selective and rapidly reacts with numerous species. Figure 1.5 illustrates some characteristics of hydroxyl radicals that make AOPs powerful technologies for the removal of refractory pollutants (Buthiyappan et al., 2016).

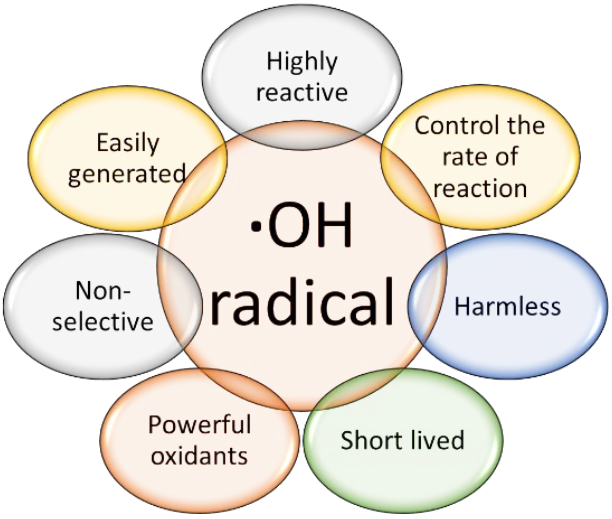

Figure 1.5. Key features of hydroxyl radical.

The four basic attack pathways, which depends on the structure and ionization potential of the target pollutant, are: radical addition, hydrogen abstraction, electron transfer and radical combination (Gao et al., 2014). AOPs might be classified based on the way to generate ·OH radicals: (i) photolytic and photocatalytic processes; (ii) Fenton processes that include conventional Fenton, photo-Fenton and sono-Fenton; (iii) ozone technologies that include different combinations based on ozone applications; (iv) electrochemical processes, such as electro-Fenton, photo-electrocatalysis, photo-electro-Fenton, sono-electro-Fenton and anodic oxidation; and (v) other different AOPs like sonolysis, wet oxidation and supercritical oxidation (Figure 1.6).

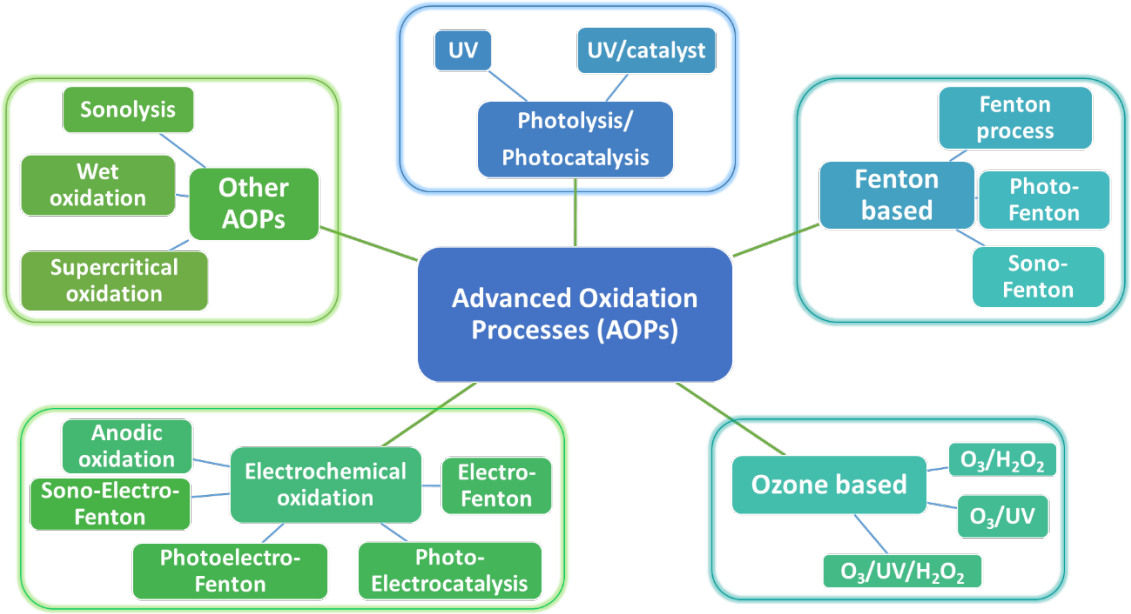

Figure 1.6. Classification of Advanced Oxidation Processes.

Among the numerous advantages of applying AOPs, it should be mentioned the fast reaction rates, the potential to reduce toxicity and the possibility to achieve a complete mineralization of organic compounds, or the non-selectivity oxidation, offering the possibility to treat more than one pollutant at the same time (Sharma et al., 2011). However, although the mineralization of the organic compounds by AOPs can be achieved, it should be also taken into consideration the formation of intermediates that tend to be more resistant to chemical degradation. This disadvantage makes the process more expensive due to the increase of the energy and chemical reagent consumption (Oller et al., 2011). In order to avoid this issue, the integration of a pre-treatment based on AOPs could improve the biodegradability of the initial wastewater, applying then a secondary conventional treatment. The integration of different combination processes, especially AOPs together with biological treatments, results in cost-

effective alternatives that have already been employed in industrial activities (Kestioğlu et al., 2005; Oller et al., 2011).

From the range of options that AOPs offer, electrochemical and photolytic oxidations are among the treatments widely considered by many researchers, increasing the attention within the last two decades. Electrochemical oxidation offers a versatile, efficient, cost-effective safe and clean technology (Comninellis et al., 2008; Muff, 2014), whereas photolytic treatments provide high feasibility for the oxidative degradation of organic pollutants in water (Kurt et al., 2017). Hence, these two AOPs have been studied and applied in this thesis.

1.2.1. Electrochemical oxidation

Electrochemical oxidation has deserved particular attention due to its high effectiveness in the degradation and complete mineralization of emerging and persistent organic pollutants (Anglada et al., 2009; Vallejo et al., 2013; Solá-Gutiérrez et al., 2018, 2019). Electrochemistry is based on redox chemistry, where electrons are transferred from one species to others, oxidizing the specie that loses electrons, and reducing those which gain electrons (Muff, 2014). In particular, electrochemical oxidation is a process in which the chemical reaction is ensured by an imposed voltage (Vallejo et al., 2013). The charge of electrons pass through an electrochemical cell consisting of two electrodes: an anode (oxidation) and a cathode (reduction).

Electrochemical oxidation of organic matter takes place by two different mechanisms (see Figure 1.7):

- Direct electrolysis, where the organic matter exchanges electrons directly with the anode surface without involvement of other substances. Direct oxidation involved the following steps: i) diffusion of organic matter from the bulk solution to the anode surface and ii) oxidation of the organic matter at the anode surface. The chemical oxidation takes place once it has been adsorbed on the anode surface.

  $$Pollutants \rightarrow Anode \rightarrow Degradation\ products$$

- Indirect electrolysis, where the organic matter does not exchange electrons directly with the anode surface but rather through electro-active species generated on the anode

surface (Panizza, 2010; Vallejo et al., 2013; Solá-Gutiérrez et al., 2018, 2019). It involves the formation of ·OH radicals from water discharge on the anode surface that act as intermediate species between the electrodes and the organic matter.

$$H_2O \rightarrow Anode \rightarrow \cdot OH\ (radicals)$$
$$\cdot OH\ (radicals) \rightarrow Pollutants \rightarrow Degradation\ products$$

During electrochemical oxidation of aqueous solutions both oxidation mechanisms may occur (Anglada et al., 2009).

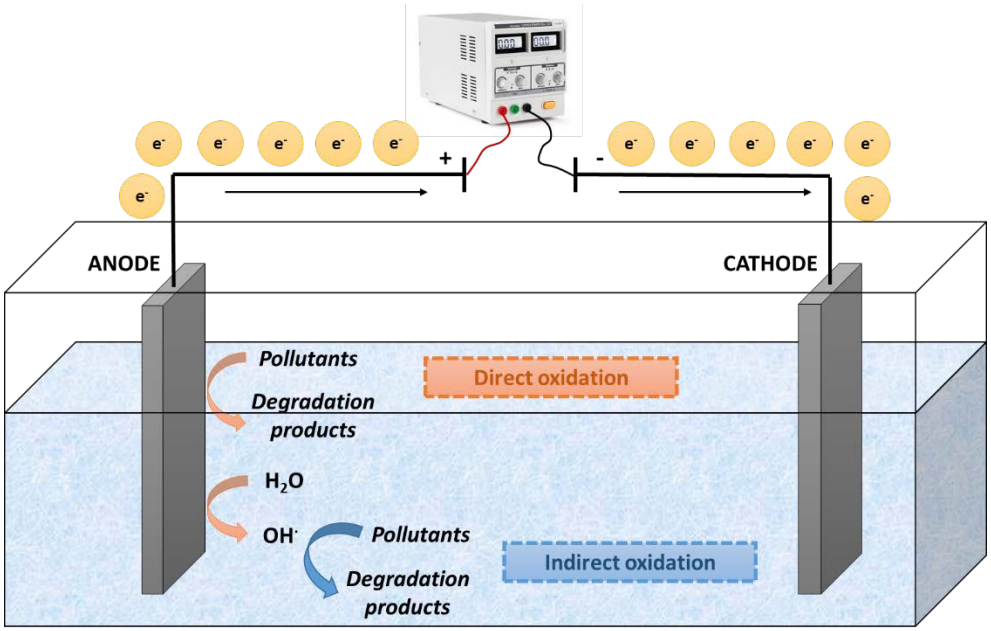

Figure 1.7. Scheme of the two possible electrochemical oxidation mechanisms.

One of the factors that has a stronger influence on the selectivity and effectiveness of the electrochemical process is the nature of the electrode material. In the literature, different electrode materials were used for wastewater treatments. They are usually noble metals electrodes, carbon and graphite electrodes, boron-doped diamond (BDD) and mixed type of materials (Shestakova and Sillanpää, 2017). However, the most common materials are BDD and mixed metal oxide electrodes, such as Ti/Ta_2O_5-IrO_2, Ti/SnO_2-IrO_2, Ti/RuO_2-IrO_2, Ti/Sb-SnO_2, Ti/SnO_2-Sb_2O_5-RuO_2 and Ti/TiO_2-IrO_2, among others (Bogdanovskii et al., 2001; Kong et al., 2007; Pereira et al., 2012; da Silva et al., 2013; Yahiaoui et al., 2013). The use of these materials is largely due to their long service life, corrosion resistance and high overpotential towards oxygen evolution reactions. The activity of the electrodes is related to the interactions between ·OH radicals and the anode surfaces. ·OH radicals adsorb strongly on active electrodes and they can

interact with the anode material forming higher metal oxides, which then oxidize the organic matter (Martínez-Huitle and Ferro, 2006). This is a typical behaviour for anodes with a lower oxygen evolution overpotential (RuO_2, IrO_2, carbon) (see Figure 1.8), and, in consequence, lower activities toward the organic matter. However, non-active electrodes (PbO_2, SnO_2-SbO_2 or BDD) (see Figure 1.8), those which have a higher oxygen evolution overpotential, weakly absorbs ·OH radicals. Thus, the reaction between the organic matter and the ·OH radicals is direct, promoting a higher reactivity between the radicals and the organic compounds.

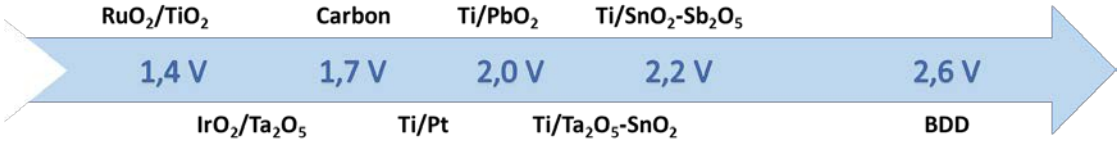

Figure 1.8. Oxygen evolution overpotential for different electrode materials.

According to Figure 1.8, BDD anodes have the highest overpotential for the oxygen evolution reaction among other existing electrode materials used in electrochemical oxidation. This results in a higher electrocatalytic activity and a higher efficiency in comparison to other electrodes in the oxidation of organic matter, demonstrated by a large number of studies (Santana et al., 2005; Haidar et al., 2013; Urtiaga et al., 2014; Labiadh et al., 2016). BDD anodes have proved to be stable, corrosion-resistant, they have exceptional conducting properties in a wide range of temperatures and low operational costs (Panizza and Cerisola, 2008). But BDD anodes have the disadvantage of being expensive due to the high diamond and boron dopant contents (boron: 10^{19} – 10^{21} atoms/cm^2) (Patel et al., 2013) (see Figure 1.9).

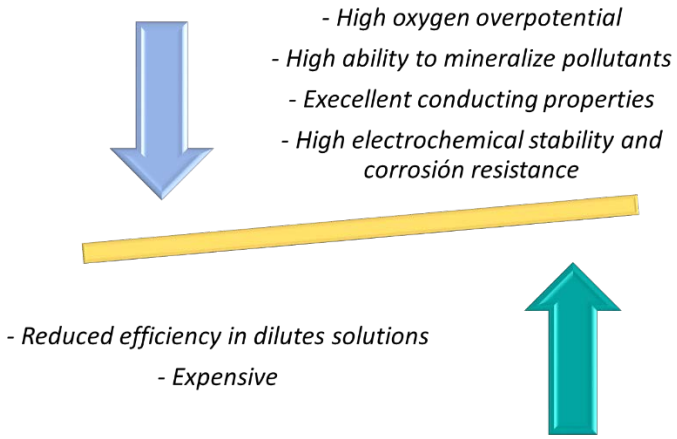

Figure 1.9. Advantages and disadvantages of boron-doped diamond (BDD) anodes.

During electrochemical oxidation in the region of water discharge, BDD anodes promote the generation of ·OH radicals, which unselectively could achieve a completely mineralization of organic pollutants. A mechanism for the oxidation or organic matter on BDD anodes has been proposed by Comninellis (2008). The model assumes the following reactions:

$$BDD + H_2O \rightarrow BDD(OH\cdot) + H^+ + e^- \quad (1.1)$$

$$BDD(OH\cdot) + R \rightarrow BDD + mCO_2 + nH_2O \quad (1.2)$$

$$BDD(OH\cdot) \rightarrow BDD + {}^1/_2\, O_2 + H^+ + e^- \quad (1.3)$$

The reaction between the organic matter (R) and ·OH radicals competes with the ·OH radicals discharge in the anode to lead oxygen. During the electrochemical reaction using BDD anodes, a high amount of ·OH radicals are produced in the potential region of oxygen evolution, and due to the weakly adsorption on the anode surface, the efficient wastewater treatment is achieved (Panizza and Cerisola, 2009).

1.2.2. Photolytic oxidation

Photolytic treatments have been pointed out as alternative effective treatment processes for the removal of a wide range of organic pollutants, including PCPPs (V. J. Pereira et al., 2012; Sanches et al., 2013; Wols et al., 2015). They provide the capability to achieve high mineralization rates, the chemicals required are relatively low cost and easily available, the energy consumption is not very high and the process is non-selective being able to eliminate any organic molecule.

Photochemical technologies are based on light-induced chemical reactions, driven by UV/Vis radiation or auxiliary chemicals like catalyst, which accelerate the degradation of the organic matter. UV/Vis is often used because most of the molecules absorb in the UV/Vis wavelength range. UV extend from 100 – 400 nm (UV-C (200 – 280 nm), UV-B (280 – 315 nm) and UV-A (315 – 380 nm)) and visible spectrum from 380 – 850 nm. The photochemical processes that have been studied in this thesis are as follows:

- *Photolysis oxidation*, direct photolysis starts with the absorption of a photon emitted from the light source by the target molecule. Then, the photons produce an electronically excited state of the molecule, causing the cleavage of the molecule bonds and starting the transformation pathway to form degradation products (Wong-Wah-Chung et al., 2007; Chen et al., 2018). Thus, the first step of the photolysis mechanism consists on the production of an electronically excited state of the target molecule:

$$X + h\nu \rightarrow X^* \quad (1.4)$$

where X is the target molecule and X* is the excited state of X; as the lifetime of X* is very short the general photolysis reaction might be expressed as follows:

$$X + h\nu \rightarrow Y + Z \quad (1.5)$$

where Y and Z are the products in which X is transformed.

- *Photocatalytic oxidation*, photocatalysis occurs when a photochemical reaction is accelerated by the presence of a catalyst, which absorbs photons. The catalyst is usually a semiconductor material that has an orbital with an electronic band structure. There are two bands that describe the electronic structure of the material: i) conduction band (C_B), the band of orbitals that are high in energy and generally empty; and ii) valence band (V_B), which is the band of electron orbitals where electrons can jump out of. In this sense, the band gap energy is the energy difference between these two bands. When a photon with an energy equal or higher than the band gap is absorbed by the catalyst (or light is emitted at a wavelength shorter than its ban gap); an electron from the V_B is promoted to the C_B, leaving a photogenerated hole (h^+) in the V_B and producing electron-hole pairs. The holes (h^+) generated in the catalyst react with H_2O resulting in the formation of reactive oxygen species (ROS), such as ·OH radicals, responsible for the breakage and transformation of the target molecule, whereas the electrons form species like superoxides radicals, such as O_2· or O· (see Figure 1.10 for TiO_2 photocatalyst) (Fernández-Castro et al., 2016; Ribao et al., 2018b, 2018a). These electrons can also recombine between themselves, liberating the energy as heat or light and avoiding the photochemical reactions.

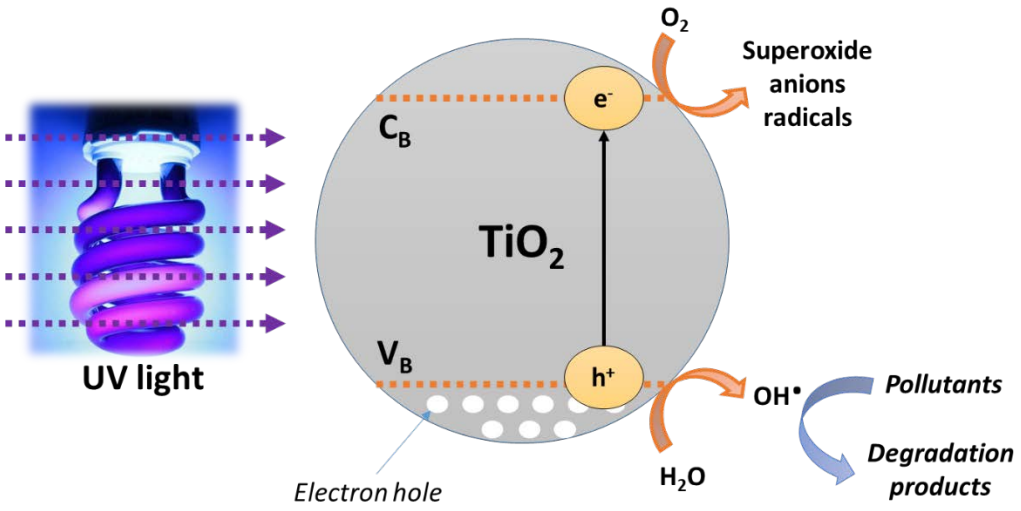

Figure 1.10. Photocatalytic mechanisms of electron-hole pair formation in TiO_2 catalyst.

The main reactions involved in the photolytic treatments are as follows:

$$Catalyst + hv \rightarrow h^+ + e^- \quad (1.6)$$

$$h^+ + H_2O \rightarrow ROS\ (OH^{\cdot}) \quad (1.7)$$

$$ROS\ (OH^{\cdot}) + X \rightarrow Y + Z \quad (1.8)$$

where h^+ and e^- are the hole and electron generated, respectively, ROS is the reactive oxygen specie, mainly hydroxyl radicals (·OH), X is the target molecule and Y and Z are the products in which X is transformed.

Of the many different photocatalyst, TiO_2 has been the most widely studied and used in many applications due to its strong oxidizing abilities on the degradation of organic pollutants, in addition to its chemical stability, long durability, non-toxicity and low cost (Nakata and Fujishima, 2012). Nevertheless, TiO_2 photocatalyst is only activated under UV radiation, which represents from 4 % to 8 % of the solar sprectrum. For this reason, the use of artificial UV lamps are required. Specifically, for TiO_2 photocatalyst, wavelengths between 300 and 400 nm are of interest (Kanakaraju et al., 2014). Thus, some strategies to modify TiO_2 for the use of visible light including nonmetal and/or metal doping to the material are being implemented (Oturan and Aaron, 2014).

1.3. PCDD/Fs and related by-products formation during the advanced oxidation of Triclosan

Emerging pollutants removal from wastewater, such as PCPPs, is one of the current major challenges in the scientific community. Among all PCPPs, different studies have addressed the removal of Triclosan from different matrices by using multiple technologies based on AOPs, including photolysis, photocatalysis, Fenton reaction, electro-oxidation, and different combinations between them (Maharana et al., 2015; Alfiya et al., 2017; Kosera et al., 2017; Solá-Gutiérrez et al., 2018, 2019; Vega et al., 2019). However, the generation of by-products when trying to degrade Triclosan by AOPs is one of the main issues of concern. Triclosan oxidation has been related to the formation of chlorinated phenols (CPs), a group of organic compounds, with high toxicity and carcinogenic characteristics, bioaccumulation and poor biodegradability, specifically, 2-chlorophenol, 2,4-dichlorophenol, 2,4,6-trichlorophenol and pentachlorophenol. In addition, Triclosan has been also related to the likely formation of PCDD/Fs (Vallejo et al., 2013; Solá-Gutiérrez et al., 2018, 2019). An exhaustive and critical analysis of the state of the art related to AOPs techniques of Triclosan and the formation of different by-products during these treatments has been undertaken, being photolytic processes among the most studied treatments on Triclosan degradation.

By this, deepens in the formation of intermediate products during the application of a direct photolytic treatment, as photolysis, two main pathways might be produced, leading to the formation of different by-products: (i) breakage of the molecule, which lead to the formation of smaller molecules, mainly 2,4-dichlorophenol and 4-chlorocatechol, among others (Son et al., 2007; Chen et al., 2018, 2016; Iovino et al., 2019). These results were obtained working under a large range of pH (5 – 12) and usually at wavelengths ranging from 254 to 400 nm; (ii) non-breakage of the molecules, such as cyclization or polymerization reactions, which lead to the formation of DCDD or polymerized Triclosan products (Latch et al., 2003; Mezcua et al., 2004; Latch et al., 2005; Lores et al., 2005; Sanchez-Prado et al., 2006; Son et al., 2007; Chen et al., 2010; Kliegman et al., 2013; Iovino et al., 2019; Wu et al., 2019). Results obtained when usually working at a pH above 6.5 and at wavelengths ranging from 254 to 400 nm.

On the other hand, the application of photocatalysis as an indirect oxidation treatment to Triclosan solutions, the formation of smaller molecules might be the predominant degradation pathway. In this way, the formation of 2,4-dichlorophenol, 4-chlorocatechol and chlorobenzenes have been reported as the main photo-products after the photocatalytic

treatment of Triclosan (Rafqah et al., 2006; Son et al., 2009; Stamatis et al., 2014; Constantin et al., 2018). However, scarce authors have observed the formation of PCDD/Fs, like DCDD, when applying photocatalysis as AOP (Yu et al., 2006; Sankoda et al., 2011; Constantin et al., 2018). For these studies, the predominant catalyst loading ranged between 0.03 and 1 g L^{-1} and at wavelength ranging from 300 to 400 nm.

Finally, although the literature reporting the application of an electrochemical oxidation treatment to solutions containing Triclosan is scarce, the formation of different by-products has been observed. In the same way, the formation of 2,4-dichlorophenol, catechol, 4-chlorocatechol and chlorohydroquinone, among others, have been identified as Triclosan intermediate products (Martín de Vidales et al., 2013; Maharana et al., 2015). Current densities ranging from 2 to 150 mA cm^{-2} were applied. Besides, the effect of two electrolytes (NaCl and Na_2SO_4) as well as the pH solution (pH values from 3 to 12) were studied.

More details related to the formation of by-products formed during the application of AOPs to Triclosan solutions are summarized in table 1.6.

Table 1.6. Summary of the main by-products formed during the advanced oxidation treatments of TCS.

References	AOP	Conditions	Matrix	By-products
Iovino et al., 2019	Photolysis	λ= 254 nm; UV doses: 400 mJ/m^2	**[TCS]**= 4.5 - 18 ppm; **pH**: 6-10; **NO_3^-**: 0-50 ppm; **HA*****: 0-10 ppm; **TiO_2**: 0-100 ppm	DCDD*; 2,4-dichlorophenol
Chen et al., 2018	Photolysis	Hg lamp (350 W); 25ºC	**[TCS]**= 1 ppm; **pH**= 7 (adjusted with perchloric or NaOH); **Anions NO_3^- or HCO_3^-**: 10 and 50 ppm; **Cl^-**: 50 and 100 ppm	Chlorophenol; 2,4- dichlorophenol; 2,4,6-trichlorophenol; dichlorohydroxydiphenyl ether
Chen et al., 2016	Photolysis	$\lambda_{Xenon\ lamp\ (500\ W)}$ > 290 nm; 25 ºC	**[TCS]**= 1 ppm; **HA*****: 0, 1, 5 or 10 ppm; **pH**: 5, 7 or 11 (adjusted perchloric or NaOH); **Trapping studies**: 2-propanol, 2,4,6-trimethylphenol, furfuryl alcohol or B-carotene	4-chlorocatechol (just at pH 5 and 7); 2,4-dichlorophenol; chlorophenol; dichlorohydroxydiphenyl ether; DCDD* (not a pH 5)
Son et al., 2009	Photolysis and photocatalysis	Medium-pressure Hg-vapor UVA lamp (450 W), λ_{max} 365 nm	**[TCS]**= 5 ppm; **Adsorption or photocatalysis**: 0.1 g/L; 2-propanol as scavenger (1,3 mM if used); **pH**: neutral	Benzoic acid, phenol, chlorophenol, 2,4-dichlorophenol, MCDD** (not in photocatalysis w/o 2-propanol) and DCDD* (not in photocatalysis w/o 2-propanol)
Son et al., 2007	Photolysis	Medium-pressure Hg-vapor UV lamps (450 W): UVC (λ= 254 nm) and UVA (λ= 365 nm)	**[TCS]**= 1 ppm (in MeOH; H_2O or MeOH:H_2O); time: 60 min	DCDD* (only at 365 nm), MCDD** (only at 365 nm), chlorophenol, dichlorophenol and phenol
Chen et al., 2010	Photolysis	UV light (15 W) λ= 292 nm; 20 ºC	**[TCS]**= 30 ppm; **pH**= 8.7 and 10.5; time: 60 min	Polymerized products and DCDD*

*DCDD: 2,7/2,8-dichlorodibenzo-p-dioxin; **MCDD: monochlorodibenzo-p-dioxin; ***HA: Humic acid.

Table 1.4. Summary of the main by-products formed during the advanced oxidation treatments of TCS (cont.).

References	AOP	Conditions	Matrix	By-products
Kosera et al., 2017	Photolysis and photocatalysis	Hg vapor lamp (125W); range of 200 to 300 nm	**[TCS]**= 10 ppm; If **catalyst**: 30 ppm	After 800 min, stable intermediates formed (2,4-dichlorophenol and dioxin reported in literature)
Constantin et al., 2018	Photocatalysis	Medium pressure Hg-lamp (λ= 300-400 nm)	**[TCS]**= 31.8 ppm; **pH**: 6.5; **TiO_2**: 200 ppm; 2-propanol (scavenger): 3 mM (if used)	2,4-dichlorophenol, 4-chlorocatechol, 3,5-dichlorobenzene-1,2-diol, 4,6-dichlorobenzene-1,3-diol, TCS derivatives, DCDD*
Stamatis et al., 2014	Photocatalysis	Solar simulator with Xenon lamp (filters restricting below λ= 290 nm)	**[TCS]**= 1 ppm; **TiO_2**: 550 ppm; **I**: 700 W/m^2; **pH**: 6.6; some **scavengers** including 2-propanol (slower degradation)	2,4-dichlorophenol, chlorocatechol, 2-chloro-dihydroxy-1,4-benzoquinone. Pathways: hydroxylation of TCS; multistep-hydroxylation of TCS; dechlorination; scission of the ether bond
Sankoda et al., 2011	Photolysis and photocatalysis	UV light	**[TCS]**= 1 ppm; **TiO_2**: -	Mono-chlorinated derivatives of TCS, 2,4-dichlorophenol (main product), other derivatives with higher m/z. DCDD* increased at 60 min and maximum at 120 min to 0,25 µg/L
Rafqah et al., 2006	Photocatalysis	Fluorescent lamp (λ= 300-450 nm)	**[TCS]**= 4.6 ppm; **TiO_2**: 1 g/L; **pH**: 5.7	Chlorocatechol (10 % of conversion, RT 3 min) and 2,4-dichlorophenol (25 % of conversion, Retention Time: 4,9 min)

*DCDD: 2,7/2,8-dichlorodibenzo-p-dioxin.

Table 1.4. Summary of the main by-products formed during the advanced oxidation treatments of TCS (cont.).

References	AOP	Conditions	Matrix	By-products
Yu et al., 2006	Photocatalysis	1L UV reactor 15 W λ= **365 nm** or 254 nm	**[TCS]**= 9 ppm; **TiO_2**: 100 ppm;	DCDD* only detected at λ= 254 nm (167.7 ng/L by photolysis and 26.45 ng/L by photocatalysis). 2,4-dichlorophenol maximum of 0.98 ppm after 2 h and then dropped slowly to 0.34 ppm. Quinone of TCS (0,12 ppm) and hydroquinone of TCS (0.05 ppm) (all at λ= 365 nm)
Wang and Wang, 2018	Photolysis and Biological treatment	Gamma irradiation (similar to UV or X-ray, electromagnetic radiation) 1, 2, 3, 4 and 5 kGy	**[TCS]**= 10 ppm (in water)	Two main intermediates; difficult to quantify due to the unavailability of commercial standards (TCS derivatives)
Bianco et al., 2015	Photochemistry	Xenon lamp filtered to remove wavelength lower than λ= 285 nm (λ=290-400 nm)	**[TCS]**= 15 ppm; **pH**: 10.5	DCDD*
Latch et al., 2005	Photolysis	Hg-lamp (450W) or four Hg-lamps (175W) (λ>300nm) or natural sunlight	**[TCS]**= 0.9-29 ppm; **pH**: 4-12 (experiments in natural sunlight pH: 8)	DCDD* and 2,4-dichlorophenol (0.3 ppm at 2h and then decay). TCS may form photocoupled products (with other TCS molecules) that may account for some to the TCS mass balance
Latch et al., 2003	Photolysis	Filters λ> 280, λ> 290 or λ> 320 nm from Hg-lamp (450 W)	**[TCS]**= 1-22 ppm; Experiment time: 6 min	DCDD* above pH 8

*DCDD: 2,7/2,8-dichlorodibenzo-p-dioxin.

Table 1.4. Summary of the main by-products formed during the advanced oxidation treatments of TCS (cont.).

References	AOP	Conditions	Matrix	By-products
Constantin et al., 2015	Photocatalysis	Hg lamp; I_o: 1.05e^{-6} Einstein/s	**[TCS]**= 1-13.5 ppm; **pH**: 5.3-8.7; **TiO_2**: 100-500 ppm; **Irradiation time**: 30-180 min; **Q_{air}**: 50 L/h	-
Maharana et al., 2015	Electrochemical oxidation	Ti/SnO_2-Sb/Ce-PbO_2 5 x 5 cm (anode) and Ti 5 x 5 cm (cathode)	**[TCS]**= 0.5-5 ppm; **pH**: 3, 5, 7, 9, 11; **Current density**: 2, 4, 6, 8, 10 mA/cm^2; **NaCl or Na_2SO_4**: 10 mmol/L	2,4-dichlorophenol, 5-chloro-3-(chlorohydroquinone) phenol, 2-chloro-5-(2,4-dichlorophenoxy) benzene-1,4-diol
Wang and Farrell, 2004	Electrochemical oxidation	BDD electrode (1 cm^2)	**[TCS]**= 1158 ppm; **pH**:12; **Current density**: 2, 6, 15 mA/cm^2; **NaCl**: 0,2 M	-
Martín de Vidales et al., 2013	Electrochemical oxidation and Sonoelectrolysis	Si-BDD as anode and SS as cathode (78 cm^2)	**[TCS]**= 0,1-100 ppm (0.37-37 % MeOH); **NaCl and Na_2SO_4**: 0.035 mol/L; **Current density**: 15-100 mA/cm^2	Catechol, chlorohydroquinone and 4-chlorocatechol
Lores et al., 2005	Photolysis	Fiber exposed to irradiation (SPME), two mercury lamp 10 and 8 W; λ= **254 nm**	**[TCS]**= 5, 20 y 200 ng/L;	DCDD* formation; no basic media is required to observe the formation of DCDD* at least at λ= 254 nm
Sanchez-Prado et al., 2006	Photolysis	Hg lamp λ= 254 nm and sunlight simulated in Xenon lamp	Real urban wastewater and synthetic water. In urban water pH: 3, 7.1 and 8.5	DCDD* formed in urban water and synthetic water and in both light sources. DCDD* observed in all the pH, even at 3 (independently of the pH). Monochlorophenol and 2,4-dichlorophenol

*DCDD: 2,7/2,8-dichlorodibenzo-p-dioxin.

Table 1.4. Summary of the main by-products formed during the advanced oxidation treatments of TCS (cont.).

References	AOP	Conditions	Matrix	By-products
Kliegman et al., 2013	Photolysis	λ= 300 nm	**[TCS]**=15 ppm (10:90 MeOH:H_2O and buffer solution); **pH**: 10.6	DCDD* (4 % conversion) (intermediate)
Wu et al., 2019	Photolysis + chlorine	16 lamps (8 W), 365 nm	**[TCS]**= 0.2 and 2 µg/mL (in MeOH below 0.1 %); **pH**: between 7.5 and 8.4	DCDD* and PCDDs including 2,3,7,8-TCDD***
Mezcua et al., 2004	Photolysis	UV: λ= 320-400 nm	Wastewater and water (8.2 ppm). pH 5 and 7 in distilled water samples	DCDD* only at pH 7 because at pH 5 no TCS degradation. Faster DCDD formation in wastewater due to the faster TCS degradation
Aranami and Readman, 2007	Photolysis	Fluorescent lamp (UV: λ= 250-370 nm)	Pure water, fresh water and sea water spiked with 9.4 ppm	0.08 ppm of DCDD* observed after 12 days. Less DCDD in fresh water and no observed in pure water (kinetics)
Alfiya et al., 2017	Photolysis	Mercury lamps: λ= 254 nm or 254 + 180 nm. Output intensity: 30 mW/cm^2 (λ= 254 nm) and 1.3 mW/cm^2 (λ= 180 nm)	**[TCS]**= 2.5 ppm in deionized water; **pH**: 5.6-5.7	Higher DCDD* concentration found with both lamps due to the faster degradation of TCS
Wong-Wah-Chung et al., 2007	Photolysis	λ= 254 nm lamp (6 W)	**[TCS]**= 3-10 ppm	DCDD* observed at samples irradiated at pH 11.8. Besides other TCS isomers were observed

*DCDD: 2,7/2,8-dichlorodibenzo-p-dioxin; ***2,3,7,8-TCDD: 2,3,7,8-tetrachlorodibenzo-p-dioxin.

1.4. Background, thesis scope and outline

This thesis aims to contribute to the knowledge necessary for the safe implementation of remediation processes of Triclosan contaminated waters. More specifically, it is focused on the study of the by-products formation, paying special attention to the potential formation of PCDD/Fs, during electrochemical and photolytic treatments of model aqueous solutions containing Triclosan, a common PCPPs and precursor of PCDD/Fs.

Chapter 1 describes the main aspects related to PCPPs as precursors of PCDD/Fs during the application of AOPs. The fundamentals of AOPs, specifically, of electrochemical and photolytic oxidation, focused on the degradation of Triclosan, the formation of PCDD/Fs and related by-products, are presented.

Chapter 2 describes the chemicals and the experimental and analytical methods used in the present thesis.

Chapter 3 reports the study of the electrochemical oxidation of synthetic aqueous solutions containing Triclosan on BDD anodes. The influence of two common electrolytes, NaCl and Na_2SO_4, as well as the presence of copper in the solution, a widely used metal found in many industrial effluents, has been studied. Also, the initial concentration of Triclosan has been analysed. The distribution of the main by-products and PCDD/Fs formed during the electrochemical oxidation treatment has been qualitative and quantitative assessed. In this way, the toxicity of the samples before and after the treatment has been evaluated. Finally, a scheme of the reaction mechanism of Triclosan based on the identified compounds and the related literature is proposed.

Chapter 4 reports an exhaustive analysis of the state-of-the-art related to the photo-degradation techniques applied to Triclosan solutions as well as to the formation of different by-products during these treatments. In addition, photolytic oxidation (direct oxidation) experiments of model aqueous solutions containing Triclosan has been performed. This study has been focused on the analysis of different by-products formed during the treatment as well as on the reaction mechanisms involved on it. Next, photocatalytic oxidation (indirect oxidation) applied to model aqueous solutions containing Triclosan has been assessed. The effect of TiO_2 dosis has been studied. In addition, the analysis of the main by-products formed during the photocatalytic treatment, focusing on the formation of PCDD/Fs and the final toxicity, has been

evaluated. Finally, a reaction pathway based on the main experimental results obtained and corroborated by the literature is proposed.

Chapter 5 reports a comparative assessment between electrochemical and photocatalytic oxidation technologies applied to model aqueous solutions containing Triclosan, focused on the potential formation of PCCD/Fs. In addition, the final toxicity of the samples treated with both technologies is compared.

Finally, **chapter 6** summarizes the main conclusions obtained in this thesis.

1.5. References

Abad, E., Martínez, K., Caixach, J., Rivera, J., 2004. Polychlorinated dibenzo-p-dioxin/polychlorinated dibenzofuran releases into the atmosphere from the use of secondary fuels in cement kilns during clinker formation. Environ. Sci. Technol. 38, 4734–4738. https://doi.org/10.1021/es049641a

Addink, R., Olie, K., 1995. Mechanisms of formation and destruction of polychlorinated dibenzo-p-dioxins and dibenzofurans in heterogeneous systems. Environ. Sci. Technol. 29, 1425–1435. https://doi.org/10.1021/es00006a002

Alfiya, Y., Friedler, E., Westphal, J., Olsson, O., Dubowski, Y., 2017. Photodegradation of micropollutants using V-UV/UV-C processes; Triclosan as a model compound. Sci. Total Environ. 601–602, 397–404. https://doi.org/10.1016/j.scitotenv.2017.05.172

Anderson, D.R., Fisher, R., 2002. Sources of dioxins in the United Kingdom: the steel industry and other sources. Chemosphere 46, 371–381. https://doi.org/10.1016/S0045-6535(01)00178-3

Anglada, Á., Urtiaga, A., Ortiz, I., 2009. Contributions of electrochemical oxidation to waste-water treatment: Fundamentals and review of applications. J. Chem. Technol. Biotechnol. 84, 1747–1755. https://doi.org/10.1002/jctb.2214

Aranami, K., Readman, J.W., 2007. Photolytic degradation of triclosan in freshwater and seawater. Chemosphere 66, 1052–1056. https://doi.org/10.1016/j.chemosphere.2006.07.010

Baker, J.I., Hites, R.A., 2000. Is combustion the major source of polychlorinated dibenzo-p-dioxins and dibenzofurans to the environment? A mass balance investigation. Environ. Sci. Technol. 34, 2879–2886. https://doi.org/10.1021/es9912325

Balmer, M.E., Goss, K.U., Schwarzenbach, R.P., 2000. Photolytic transformation of organic pollutants on soil surfaces - An experimental approach. Environ. Sci. Technol. 34, 1240–1245. https://doi.org/10.1021/es990910k

Berntssen, M.H.G., Lundebye, A.K., 2008. Environmental contaminants in farmed fish and potential consequences for seafood safety, Improving Farmed Fish Quality and Safety. Woodhead Publishing Limited. https://doi.org/10.1533/9781845694920.1.39

Bester, K., 2005. Fate of triclosan and triclosan-methyl in sewage treatment plants and surface waters. Arch. Environ. Contam. Toxicol. 49, 9–17. https://doi.org/10.1007/s00244-004-0155-4

Bhavsar, S.P., Reiner, E.J., Hayton, A., Fletcher, R., MacPherson, K., 2008. Converting Toxic

Equivalents (TEQ) of dioxins and dioxin-like compounds in fish from one Toxic Equivalency Factor (TEF) scheme to another. Environ. Int. 34, 915–921. https://doi.org/10.1016/j.envint.2008.02.001

Bianco, A., Fabbri, D., Minella, M., Brigante, M., Mailhot, G., Maurino, V., Minero, C., Vione, D., 2015. New insights into the environmental photochemistry of 5-chloro-2-(2,4-dichlorophenoxy)phenol (triclosan): Reconsidering the importance of indirect photoreactions. Water Res. 72, 271–280. https://doi.org/10.1016/j.watres.2014.07.036

Bogdanovskii, G.A., Savel'eva, T. V., Saburova, T.S., 2001. Phenol conversions during electrochemical generation of active chlorine. Russ. J. Electrochem. 37, 865–869. https://doi.org/10.1023/A:1016703623573

Buthiyappan, A., Abdul Aziz, A.R., Wan Daud, W.M.A., 2016. Recent advances and prospects of catalytic advanced oxidation process in treating textile effluents. Rev. Chem. Eng. 32, 1–47. https://doi.org/10.1515/revce-2015-0034

Chen, C.M., 2004. The emission inventory of PCDD/PCDF in Taiwan. Chemosphere 54, 1413–1420. https://doi.org/10.1016/j.chemosphere.2003.10.039

Chen, L., Wang, Z., Qian, C., He, Y., 2018. Effects of inorganic anions on the photolysis of triclosan under UV irradiation. Water Sci. Technol. 78, 1476–1480. https://doi.org/10.2166/wst.2018.421

Chen, L., Wang, Zheng, Wang, Zhulai, Gu, X., 2016. Influence of humic acid on the photolysis of Triclosan in different dissociation forms. Water. Air. Soil Pollut. 227, 1–7. https://doi.org/10.1007/s11270-016-3024-7

Chen, Z., Cao, G., Song, Q., 2010. Photo-polymerization of triclosan in aqueous solution induced by ultraviolet radiation. Environ. Chem. Lett. 8, 33–37. https://doi.org/10.1007/s10311-008-0187-5

Comninellis, C., Kapalka, A., Malato, S., Parsons, S.A., Poulios, I., Mantzavinos, D., 2008. Advanced oxidation processes for water treatment: advances and trends for R&D. J. Chem. Technol. Biotechnol. 83, 769–776. https://doi.org/10.1002/jctb.1873

Constantin, L., Nitoi, I., Cristea, I., Oancea, P., Orbeci, C., Nechifor, A.C., 2015. Degradation of triclosan by TiO_2 - UV irradiation in aqueous solutions. Rev. Chim. 66, 597–600.

Constantin, L.A., Nitoi, I., Cristea, N.I., Constantin, M.A., 2018. Possible degradation pathways of triclosan from aqueous systems via TiO_2 assisted photocatalyis. J. Ind. Eng. Chem. 58, 155–162. https://doi.org/10.1016/j.jiec.2017.09.020

da Silva, A.J.C., dos Santos, E.V., de Oliveira Morais, C.C., Martínez-Huitle, C.A., Castro, S.S.L., 2013. Electrochemical treatment of fresh, brine and saline produced water generated by petrochemical industry using Ti/IrO_2-Ta_2O_5 and BDD in flow reactor. Chem. Eng. J. 233, 47–55. https://doi.org/10.1016/j.cej.2013.08.023

Deng, Y., Zhao, R., 2015. Advanced Oxidation Processes (AOPs) in wastewater treatment. Curr. Pollut. Reports 1, 167–176. https://doi.org/10.1007/s40726-015-0015-z

Dhillon, G.S., Kaur, S., Pulicharla, R., Brar, S.K., Cledón, M., Verma, M., Surampalli, R.Y., 2015. Triclosan: Current status, occurrence, environmental risks and bioaccumulation potential. Int. J. Environ. Res. Public Health 12, 5657–5684. https://doi.org/10.3390/ijerph120505657

Ebele, A.J., Abou-Elwafa Abdallah, M., Harrad, S., 2017. Pharmaceuticals and personal care products (PPCPs) in the freshwater aquatic environment. Emerg. Contam. 3, 1–16. https://doi.org/10.1016/j.emcon.2016.12.004

European Commision. Commission regulation (EU) No 258/2014/EU of the European Parliament and of the Council of 3 April 2014 establishing a Union programme to support specific activities in the field of financial reporting and auditing for the period of 2014-20 and repealing Decision No 716/2009/EC, 2014. URL https://eur-lex.europa.eu/legal-content/EN/TXT/PDF/?uri=CELEX:32014R0358&from=ES.

European Commission. Commission implementing decision (EU) 2016/110 of 27 January 2016 not approving triclosan as an existing active substance for use in biocidal products for product-type 1, 2016. https://doi.org/http://eur-lex.europa.eu/pri/en/oj/dat/2003/l_285/l_28520031101en00330037.pdf

Fernández-Castro, P., San Román, M.F., Ortiz, I., 2016. Theoretical and experimental formation of low chlorinated dibenzo-p-dioxins and dibenzofurans in the Fenton oxidation of chlorophenol solutions. Chemosphere 161, 136–144. https://doi.org/10.1016/j.chemosphere.2016.07.011

Fiedler, H., 2007. National PCDD/PCDF release inventories under the Stockholm Convention on Persistent Organic Pollutants. Chemosphere 67. https://doi.org/10.1016/j.chemosphere.2006.05.093

Fiedler, H., Hutzinger, O., 1992. Sources and sinks of dioxins: Germany. Chemosphere 25, 1487–1491. https://doi.org/10.1016/0045-6535(92)90174-P

Fullana, A., Conesa, J.A., Font, R., Sidhu, S., 2007. Formation and destruction of chlorinated pollutants during sewage sludge incineration. Environ. Sci. Technol. 38, 2953–2958.

https://doi.org/10.1021/es034896u

Gao, Y., Ji, Y., Li, G., An, T., 2014. Mechanism, kinetics and toxicity assessment of OH-initiated transformation of triclosan in aquatic environments. Water Res. 49, 360–370. https://doi.org/10.1016/j.watres.2013.10.027

Geissen, V., Mol, H., Klumpp, E., Umlauf, G., Nadal, M., van der Ploeg, M., van de Zee, S.E.A.T.M., Ritsema, C.J., 2015. Emerging pollutants in the environment: A challenge for water resource management. Int. Soil Water Conserv. Res. 3, 57–65. https://doi.org/10.1016/j.iswcr.2015.03.002

Giannakis, S., Gamarra Vives, F.A., Grandjean, D., Magnet, A., De Alencastro, L.F., Pulgarin, C., 2015. Effect of advanced oxidation processes on the micropollutants and the effluent organic matter contained in municipal wastewater previously treated by three different secondary methods. Water Res. 84, 295–306. https://doi.org/10.1016/j.watres.2015.07.030

Gómez-Lavín, S., San Román, M.F., Ortiz, I., Fernández, J., de Miguel, P., Urtiaga, A., 2018. Dioxins and furans legacy of lindane manufacture in Sabiñánigo (Spain). The Bailín landfill site case study. Sci. Total Environ. 624, 955–962. https://doi.org/10.1016/j.scitotenv.2017.12.162

Haidar, M., Dirany, A., Sirés, I., Oturan, N., Oturan, M.A., 2013. Electrochemical degradation of the antibiotic sulfachloropyridazine by hydroxyl radicals generated at a BDD anode. Chemosphere 91, 1304–1309. https://doi.org/10.1016/j.chemosphere.2013.02.058

Halden, R.U., 2014. On the need and speed of regulating triclosan and triclocarban in the United States. Environ. Sci. Technol. 48, 3603–3611. https://doi.org/10.1021/es503494j

Iino, F., Imagawa, T., Gullett, B.K., 2000. Dechlorination-controlled polychlorinated dibenzofuran isomer patterns from municipal waste incinerators. Environ. Sci. Technol. 34, 3143–3147. https://doi.org/10.1021/es9913131

Iovino, P., Chianese, S., Prisciandaro, M., Musmarra, D., 2019. Triclosan photolysis: operating condition study and photo-oxidation pathway. Chem. Eng. J. In press. https://doi.org/10.1016/j.cej.2019.02.132

Kanakaraju, D., Glass, B.D., Oelgemöller, M., 2014. Titanium dioxide photocatalysis for pharmaceutical wastewater treatment. Environ. Chem. Lett. 12, 27–47. https://doi.org/10.1007/s10311-013-0428-0

Kestioğlu, K., Yonar, T., Azbar, N., 2005. Feasibility of physico-chemical treatment and Advanced Oxidation Processes (AOPs) as a means of pretreatment of olive mill effluent (OME). Process

Biochem. 40, 2409–2416. https://doi.org/10.1016/j.procbio.2004.09.015

Klavarioti, M., Mantzavinos, D., Kassinos, D., 2009. Removal of residual pharmaceuticals from aqueous systems by advanced oxidation processes. Environ. Int. 35, 402–17. https://doi.org/10.1016/j.envint.2008.07.009

Kliegman, S., Eustis, S.N., Arnold, W.A., McNeill, K., 2013. Experimental and theoretical insights into the involvement of radicals in triclosan phototransformation. Environ. Sci. Technol. 47, 6756–6763. https://doi.org/10.1021/es3041797

Kong, J., Shi, S., Zhu, X., Ni, J., 2007. Effect of Sb dopant amount on the structure and electrocatalytic capability of Ti/Sb-SnO_2 electrodes in the oxidation of 4-chlorophenol. J. Environ. Sci. 19, 1380–1386.

Kosera, V.S., Cruz, T.M., Chaves, E.S., Tiburtius, E.R.L., 2017. Triclosan degradation by heterogeneous photocatalysis using ZnO immobilized in biopolymer as catalyst. J. Photochem. Photobiol. A Chem. 344, 184–191. https://doi.org/10.1016/j.jphotochem.2017.05.014

Kulkarni, P.S., Crespo, J.G., Afonso, C.A.M., 2008. Dioxins sources and current remediation technologies - A review. Environ. Int. 34, 139–153. https://doi.org/10.1016/j.envint.2007.07.009

Kurt, A., MErt, B.K., Özengin, N., Sivrioglu, Ö., Yonar, T., 2017. Treatment of antibiotics in wastewater using Advanced Oxidation Processes (AOPs). https://doi.org/10.5772/67538

Labiadh, L., Barbucci, A., Carpanese, M.P., Gadri, A., Ammar, S., Panizza, M., 2016. Comparative depollution of Methyl Orange aqueous solutions by electrochemical incineration using $TiRuSnO_2$, BDD and PbO_2 as high oxidation power anodes. J. Electroanal. Chem. 766, 94–99. https://doi.org/10.1016/j.jelechem.2016.01.036

Latch, D., Packer, J., Stender, B., VanOverbeke, J., Arnold, W., McNeill, K., 2005. Aqueous photochemistry of Triclosan: Formation of oligomerization products. Environ. Toxicol. Chem. 24, 517–525.

Latch, D.E., Packer, J.L., Arnold, W.A., McNeill, K., 2003. Photochemical conversion of triclosan to 2,8-dichlorodibenzo-p-dioxin in aqueous solution. J. Photochem. Photobiol. A Chem. 158, 63–66. https://doi.org/10.1016/S1010-6030(03)00103-5

Lavric, E.D., Konnov, A.A., De Ruyck, J., 2004. Dioxin levels in wood combustion - A review. Biomass Bioenergy 26, 115–145. https://doi.org/10.1016/S0961-9534(03)00104-1

Liu, J.L., Wong, M.H., 2013. Pharmaceuticals and personal care products (PPCPs): A review on environmental contamination in China. Environ. Int. 59, 208–224. https://doi.org/10.1016/j.envint.2013.06.012

Lores, M., Llompart, M., Sanchez-Prado, L., Garcia-Jares, C., Cela, R., 2005. Confirmation of the formation of dichlorodibenzo-p-dioxin in the photodegradation of triclosan by photo-SPME. Anal. Bioanal. Chem. 381, 1294–1298. https://doi.org/10.1007/s00216-004-3047-6

Luo, Y., Guo, W., Ngo, H.H., Nghiem, L.D., Hai, F.I., Zhang, J., Liang, S., Wang, X.C., 2014. A review on the occurrence of micropollutants in the aquatic environment and their fate and removal during wastewater treatment. Sci. Total Environ. 473–474, 619–641. https://doi.org/10.1016/j.scitotenv.2013.12.065

Maharana, D., Niu, J., Rao, N.N., Xu, Z., Shi, J., 2015. Electrochemical degradation of Triclosan at a Ti/SnO_2-Sb/Ce-PbO_2 anode. Clean - Soil, Air, Water 43, 958–966. https://doi.org/10.1002/clen.201400180

Marín Galvín, R., 2017. Contaminación emergente: sustancias prioritarias y preferentes, productos farmacéuticos, drogas de abuso, disruptores endocrinos, microplásticos y patógenos emergentes. TECNOAQUA 24, 66–77.

Martín de Vidales, M.J., 2015. Eliminación de contaminantes orgánicos persistentes de aguas residuales mediante oxidación electroquímica con ánodo de diamante dopado con boro. Doctoral Thesis, University of Castilla la Mancha.

Martín de Vidales, M.J., Sáez, C., Cañizares, P., Rodrigo, M.A., 2013. Removal of triclosan by conductive-diamond electrolysis and sonoelectrolysis. J. Chem. Technol. Biotechnol. 88, 823–828. https://doi.org/10.1002/jctb.3907

Martínez-Huitle, C.A., Ferro, S., 2006. Electrochemical oxidation of organic pollutants for the wastewater treatment: Direct and indirect processes. Chem. Soc. Rev. 35, 1324–1340. https://doi.org/10.1039/b517632h

Mezcua, M., Gómez, M.J., Ferrer, I., Aguera, A., Hernando, M.D., Fernández-Alba, A.R., 2004. Evidence of 2,7/2,8-dibenzodichloro-p-dioxin as a photodegradation product of triclosan in water and wastewater samples. Anal. Chim. Acta 524, 241–247. https://doi.org/10.1016/j.aca.2004.05.050

Miklos, D.B., Remy, C., Jekel, M., Linden, K.G., Drewes, J.E., Hübner, U., 2018. Evaluation of advanced oxidation processes for water and wastewater treatment – A critical review. Water

Res. 139, 118–131. https://doi.org/10.1016/j.watres.2018.03.042

Montaseri, H., Forbes, P.B.C., 2016. A review of monitoring methods for triclosan and its occurrence in aquatic environments. Trends Anal. Chem. 85, 221–231. https://doi.org/10.1016/j.trac.2016.09.010

Muff, J., 2014. Electrochemical oxidation - A versatile technique for aqueous organic contaminant degradation, chemistry of advanced environmental purification processes of water: Fundamentals and Applications. https://doi.org/10.1016/B978-0-444-53178-0.00003-1

Nakata, K., Fujishima, A., 2012. TiO_2 photocatalysis: Design and applications. J. Photochem. Photobiol. C Photochem. Rev. 13, 169–189. https://doi.org/10.1016/j.jphotochemrev.2012.06.001

National Institute of Environmental Health Sciences, 2019. Water Pollution. URL https://www.niehs.nih.gov/health/topics/agents/water-poll/index.cfm (accessed 6.25.19).

Nikolaou, A., Meric, S., Fatta, D., 2007. Occurrence patterns of pharmaceuticals in water and wastewater environments. Anal. Bioanal. Chem. 387, 1225–1234. https://doi.org/10.1007/s00216-006-1035-8

Oller, I., Malato, S., Sánchez-Pérez, J.A., 2011. Combination of Advanced Oxidation Processes and biological treatments for wastewater decontamination - A review. Sci. Total Environ. 409, 4141–4166. https://doi.org/10.1016/j.scitotenv.2010.08.061

Oturan, M.A., Aaron, J.J., 2014. Advanced oxidation processes in water/wastewater treatment: Principles and applications. A review. Crit. Rev. Environ. Sci. Technol. 44, 2577–2641. https://doi.org/10.1080/10643389.2013.829765

Panizza, M., 2010. Importance of Electrode Material in the Electrochemical Treatment of Wastewater Containing Organic Pollutants. https://doi.org/10.1007/978-0-387-68318-8_2

Panizza, M., Cerisola, G., 2009. Direct and mediated anodic oxidation of organic pollutants. Chem. Rev. 109, 6541–6569. https://doi.org/10.1021/cr9001319

Panizza, M., Cerisola, G., 2008. Electrochemical degradation of methyl red using BDD and PbO_2 anodes. Ind. Eng. Chem. Res. 47, 6816–6820. https://doi.org/10.1021/ie8001292

Patel, P.S., Bandre, N., Saraf, A., Ruparelia, J.P., 2013. Electro-catalytic materials (electrode materials) in electrochemical wastewater treatment. Procedia Eng. 51, 430–435. https://doi.org/10.1016/j.proeng.2013.01.060

Pereira, G.F., Rocha-Filho, R.C., Bocchi, N., Biaggio, S.R., 2012. Electrochemical degradation of bisphenol A using a flow reactor with a boron-doped diamond anode. Chem. Eng. J. 198–199, 282–288. https://doi.org/10.1016/j.cej.2012.05.057

Pereira, V.J., Galinha, J., Barreto Crespo, M.T., Matos, C.T., Crespo, J.G., 2012. Integration of nanofiltration, UV photolysis, and advanced oxidation processes for the removal of hormones from surface water sources. Sep. Purif. Technol. 95, 89–96. https://doi.org/10.1016/j.seppur.2012.04.013

Rafqah, S., Wong-Wah-Chung, P., Nelieu, S., Einhorn, J., Sarakha, M., 2006. Phototransformation of triclosan in the presence of TiO_2 in aqueous suspension: Mechanistic approach. Appl. Catal. B Environ. 66, 119–125. https://doi.org/10.1016/j.apcatb.2006.03.004

Ribao, P., Corredor, J., Rivero, M.J., Ortiz, I., 2018a. Role of reactive oxygen species on the activity of noble metal-doped TiO_2 photocatalysts. J. Hazard. Mater. 372, 45–51. https://doi.org/10.1016/j.jhazmat.2018.05.026

Ribao, P., Rivero, M.J., Ortiz, I., 2018b. Enhanced photocatalytic activity using GO/TiO_2 catalyst for the removal of DCA solutions. Environ. Sci. Pollut. Res. 25, 34893–34902. https://doi.org/10.1007/s11356-017-0901-6

Ribeiro, A.R., Nunes, O.C., Pereira, M.F.R., Silva, A.M.T., 2015. An overview on the advanced oxidation processes applied for the treatment of water pollutants defined in the recently launched Directive 2013/39/EU. Environ. Int. 75, 33–51. https://doi.org/10.1016/j.envint.2014.10.027

Richardson, S.D., Ternes, T.A., 2018. Water Analysis: Emerging Contaminants and Current Issues. Anal. Chem. 90, 398–428. https://doi.org/10.1021/acs.analchem.7b04577

Sanches, S., Penetra, A., Rodrigues, A., Cardoso, V. V., Ferreira, E., Benoliel, M.J., Barreto Crespo, M.T., Crespo, J.G., Pereira, V.J., 2013. Removal of pesticides from water combining low pressure UV photolysis with nanofiltration. Sep. Purif. Technol. 115, 73–82. https://doi.org/10.1016/j.seppur.2013.04.044

Sanchez-Prado, L., Llompart, M., Lores, M., García-Jares, C., Bayona, J.M., Cela, R., 2006. Monitoring the photochemical degradation of triclosan in wastewater by UV light and sunlight using solid-phase microextraction. Chemosphere 65, 1338–1347. https://doi.org/10.1016/j.chemosphere.2006.04.025

Sankoda, K., Matsuo, H., Ito, M., Nomiyama, K., Arizono, K., Shinohara, R., 2011. Identification

of triclosan intermediates produced by oxidative degradation using TiO_2 in pure water and their endocrine disrupting activities. Bull. Environ. Contam. Toxicol. 86, 470–475. https://doi.org/10.1007/s00128-011-0249-4

Santana, M.H.P., Faria, L.A.D., Boodts, J.F.C., 2005. Electrochemical characterisation and oxygen evolution at a heavily boron doped diamond electrode. Electrochim. Acta 50, 2017–2027. https://doi.org/10.1016/j.electacta.2004.08.050

Scientific Committee on Consumer Safety, 2010. Opinion on triclosan. Antimicrobial Resistence. Brussels. https://doi.org/10.2772/11162

Sharma, S., Ruparelia, J., Patel, M., 2011. A general review on advanced oxidation processes for waste water treatment. International Conference on Current Trends in Technology. 1–7.

Sheffield, A., 1985. Sources and releases of PCDD's and PCDF's to the Canadian environment. Chemosphere 14, 811–814. https://doi.org/10.1016/0045-6535(85)90193-6

Shestakova, M., Sillanpää, M., 2017. Electrode materials used for electrochemical oxidation of organic compounds in wastewater. Rev. Environ. Sci. Biotechnol. 16, 223–238. https://doi.org/10.1007/s11157-017-9426-1

Sidhu, S., Edwards, P., 2002. Role of phenoxy radicals in PCDD/F formation. Int. J. Chem. Kinet. 34, 531–541. https://doi.org/10.1002/kin.10083

Solá-Gutiérrez, C., Schröder, S., San Román, M.F., Ortiz, I., 2019. PCDD/Fs traceability during triclosan electrochemical oxidation. J. Hazard Mater. 369, 584–592. https://doi.org/10.1016/j.jhazmat.2019.02.066

Solá-Gutiérrez, C., San Román, M.F., Ortiz, I., 2018. Fate and hazard of the electrochemical oxidation of triclosan. Evaluation of polychlorodibenzo‐p‐dioxins and polychlorodibenzofurans (PCDD/Fs) formation. Sci. Total Environ. 626, 126–133. https://doi.org/10.1016/j.scitotenv.2018.01.082

Son, H.S., Choi, S.B., Zoh, K.D., Khan, E., 2007. Effects of ultraviolet intensity and wavelength on the photolysis of triclosan. Water Sci. Technol. 55, 209–216. https://doi.org/10.2166/wst.2007.034

Son, H.S., Ko, G., Zoh, K.D., 2009. Kinetics and mechanism of photolysis and TiO_2 photocatalysis of triclosan. J. Hazard. Mater. 166, 954–960. https://doi.org/10.1016/j.jhazmat.2008.11.107

Stamatis, N., Antonopoulou, M., Hela, D., Konstantinou, I., 2014. Photocatalytic degradation

kinetics and mechanisms of antibacterial triclosan in aqueous TiO_2 suspensions under simulated solar irradiation. J. Chem. Technol. Biotechnol. 89, 1145–1154. https://doi.org/10.1002/jctb.4387

Stanmore, B.R., Clunies-Ross, G., 2000. An empirical model for the de novo formation of PCDD/F in medical waste incinerators. Environ. Sci. Technol. 34, 4538–4544. https://doi.org/10.1021/es001160d

Stefanakis, A.I., Becker, J.A., 2015. A review of emerging contaminants in water: Classification, sources and potential risks (pp. 55–80). https://doi.org/10.4018/978-1-4666-9559-7.ch003

Stockholm Convention, 2017. The 16 New POPs: An introduction to the chemicals added to the Stockholm Convention as Persistent Organic Pollutants by the Conference of the Parties, Stockholm Convention, Geneve, Switzerland.

Stockholm Convention, 2009. Stockholm convention on Persistent Organic Pollutants (POPs) as amended in 2009. https://www.wipo.int/edocs/lexdocs/treaties/en/unep-pop/trt_unep_pop_2.pdf

Stockholm Convention, 2008. Stockholm Convention on Persistent Organic Pollutants, Stockholm Convention, Geneve, Switzerland. https://doi.org/10.1351/goldbook.s06019

Teodosiu, C., Gilca, A.F., Barjoveanu, G., Fiore, S., 2018. Emerging pollutants removal through advanced drinking water treatment: A review on processes and environmental performances assessment. J. Clean. Prod. 197, 1210–1221. https://doi.org/10.1016/j.jclepro.2018.06.247

Thomas, V.M., Spiro, T.G., 2011. The U.S. Dioxin Inventory: Are There Missing Sources? Environ. Sci. Technol. 30, 82A-85A. https://doi.org/10.1021/es962098g

UNESCO, 2017. The United Nations world water development report, Wastewater: The untapped resource. UNESCO, Paris. https://unesdoc.unesco.org/ark:/48223/pf0000247153

Urtiaga, A., Fernandez-Castro, P., Gómez, P., Ortiz, I., 2014. Remediation of wastewaters containing tetrahydrofuran. Study of the electrochemical mineralization on BDD electrodes. Chem. Eng. J. 239, 341–350. https://doi.org/10.1016/j.cej.2013.11.028

Vallejo, M., Fresnedo San Román, M., Ortiz, I., Irabien, A., 2015. Overview of the PCDD/Fs degradation potential and formation risk in the application of advanced oxidation processes (AOPs) to wastewater treatment. Chemosphere 118, 44–56. https://doi.org/10.1016/j.chemosphere.2014.05.077

Vallejo, M., San Román, M.F., Ortiz, I., 2013. Quantitative assessment of the formation of polychlorinated derivatives, PCDD/Fs, in the electrochemical oxidation of 2-chlorophenol as function of the electrolyte type. Environ. Sci. Technol. 47, 12400–12408. https://doi.org/10.1021/es403246g

Van den Berg, M., Birnbaum, L.S., Denison, M., De Vito, M., Farland, W., Feeley, M., Fiedler, H., Hakansson, H., Hanberg, A., Haws, L., Rose, M., Safe, S., Schrenk, D., Tohyama, C., Tritscher, A., Tuomisto, J., Tysklind, M., Walker, N., Peterson, R.E., 2006. The 2005 World Health Organization reevaluation of human and mammalian toxic equivalency factors for dioxins and dioxin-like compounds. Toxicol. Sci. 93, 223–241. https://doi.org/10.1093/toxsci/kfl055

Vega, L.P., Soltan, J., Peñuela, G.A., 2019. Sonochemical degradation of triclosan in water in a multifrequency reactor. Environ. Sci. Pollut. Res. 26, 4450–4461. https://doi.org/10.1007/s11356-018-1281-2

Wang, J., Farrell, J., 2004. Electrochemical inactivation of triclosan with boron doped diamond film electrodes. Environ. Sci. Technol. 38, 5232–5237. https://doi.org/10.1021/es035277o

Wang, S., Wang, J., 2018. Degradation of triclosan and its main intermediates during the combined irradiation and biological treatment. Environ. Technol. 39, 1115–1122. https://doi.org/10.1080/09593330.2017.1321692

Weatherly, L.M., Gosse, J.A., 2017. Triclosan exposure, transformation, and human health effects. J. Toxicol. Environ. Health B Crit. Rev. 20(8), 447–469.

Weber, R., 2007. Relevance of PCDD/PCDF formation for the evaluation of POPs destruction technologies - Review on current status and assessment gaps. Chemosphere 67, 109–117. https://doi.org/10.1016/j.chemosphere.2006.05.094

Wols, B.A., Harmsen, D.J.H., Beerendonk, E.F., Hofman-Caris, C.H.M., 2015. Predicting pharmaceutical degradation by UV (LP)/H_2O_2 processes: A kinetic model. Chem. Eng. J. 263, 336–345. https://doi.org/10.1016/j.cej.2014.10.101

Wong-Wah-Chung, P., Rafqah, S., Voyard, G., Sarakha, M., 2007. Photochemical behaviour of triclosan in aqueous solutions: Kinetic and analytical studies. J. Photochem. Photobiol. A Chem. 191, 201–208. https://doi.org/10.1016/j.jphotochem.2007.04.024

World Health Organization (WHO), 2016. Dioxins and their effects on human health. URL https://www.who.int/news-room/fact-sheets/detail/dioxins-and-their-effects-on-human-health (accessed 6.28.19)

World Health Organization (WHO) and United Nations Children's Fund (UNICEF), 2017. Progress on Drinking Water, Sanitation and Hygiene: 2017 updated and SDG baselines. Geneva. https://apps.who.int/iris/bitstream/handle/10665/258617/9789241512893-eng.pdf;jsessionid=B175DB9F2B438AB0172EC34594D5675D?sequence=1

Wu, J. lin, Ji, F., Zhang, H., Hu, C., Wong, M.H., Hu, D., Cai, Z., 2019. Formation of dioxins from triclosan with active chlorine: A potential risk assessment. J. Hazard. Mater. 367, 128–136. https://doi.org/10.1016/j.jhazmat.2018.12.088

World Water Assessment Programme (WWAP), 2017. Fact 31: Population increase & water stress. URL http://www.unesco.org/new/en/natural-sciences/environment/water/wwap/facts-and-figures/all-facts-wwdr3/fact-31-population-increase-water-stress/ (accessed 6.25.19)

Yahiaoui, I., Aissani-Benissad, F., Fourcade, F., Amrane, A., 2013. Removal of tetracycline hydrochloride from water based on direct anodic oxidation (Pb/PbO_2 electrode) coupled to activated sludge culture. Chem. Eng. J. 221, 418–425. https://doi.org/10.1016/j.cej.2013.01.091

Yang, Y., Pignatello, J.J., Ma, J., Mitch, W.A., 2014. Comparison of halide impacts on the efficiency of contaminant degradation by sulfate and hydroxyl radical-based advanced oxidation processes (AOPs). Environ. Sci. Technol. 48, 2344–2351. https://doi.org/10.1021/es404118q

Yap, H.C., Pang, Y.L., Lim, S., Abdullah, A.Z., Ong, H.C., Wu, C.H., 2019. A comprehensive review on state-of-the-art photo-, sono-, and sonophotocatalytic treatments to degrade emerging contaminants. Int. J. Environ. Sci. Technol. 16, 601–628. https://doi.org/10.1007/s13762-018-1961-y

Yu, J.C., Kwong, T.Y., Luo, Q., Cai, Z., 2006. Photocatalytic oxidation of triclosan. Chemosphere 65, 390–399. https://doi.org/10.1016/j.chemosphere.2006.02.011

Zhang, Y., Geißen, S.U., Gal, C., 2008. Carbamazepine and diclofenac: Removal in wastewater treatment plants and occurrence in water bodies. Chemosphere 73, 1151–1161. https://doi.org/10.1016/j.chemosphere.2008.07.086

Zheng, H., Liu, B., Liu, G., Cai, Z., Zhang, C., 2018. Potential Toxic Compounds in Biochar: Knowledge gaps between biochar research and safety, Biochar from biomass and waste. Elsevier Inc. https://doi.org/10.1016/b978-0-12-811729-3.00019-4

Zheng, M.H., Bao, Z.C., Zhang, B., Xu, X.B., 2001. Polychlorinated dibenzo-p-dioxins and dibenzofurans in paper making from a pulp mill in China. Chemosphere 44, 1335–1337. https://doi.org/10.1016/S0045-6535(00)00488-4

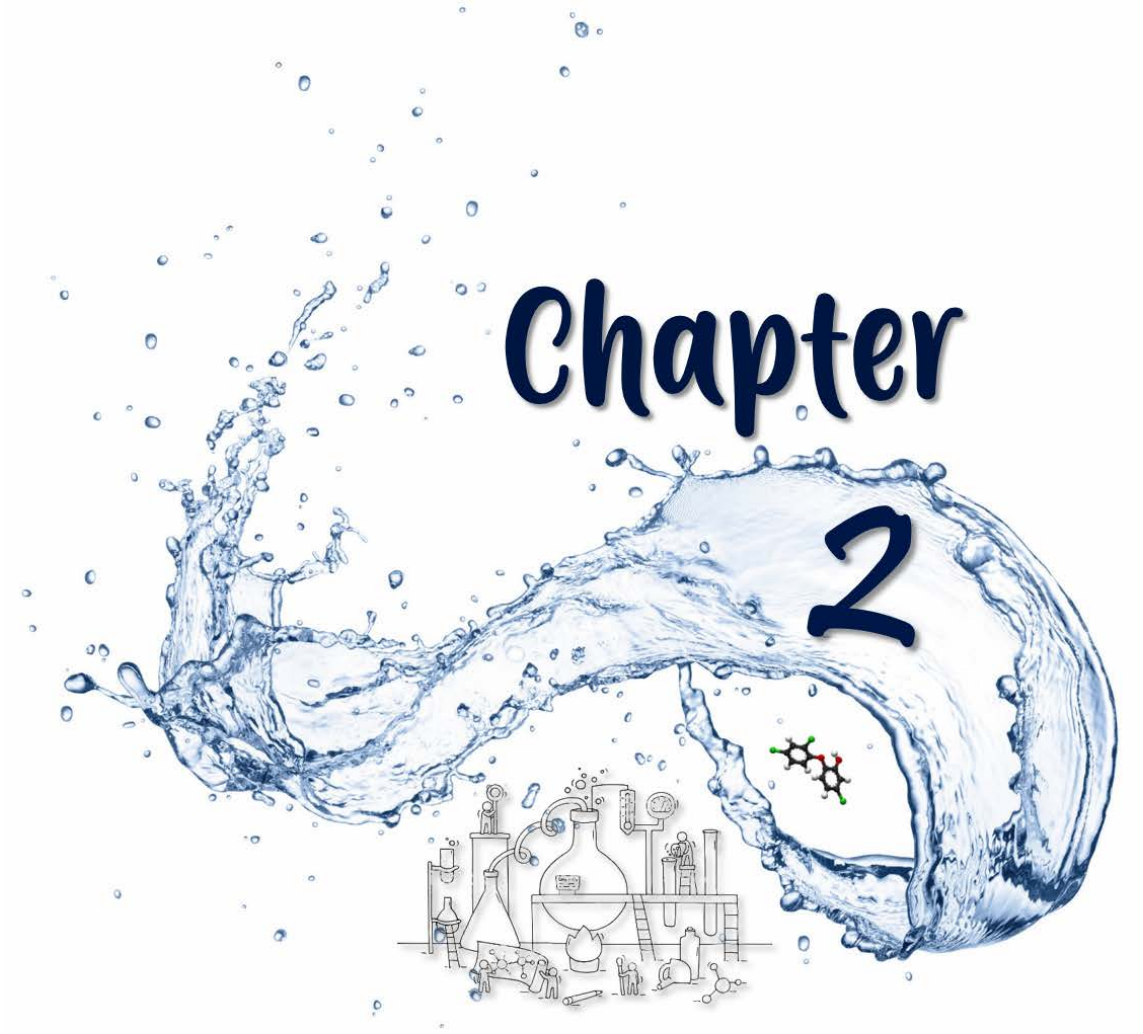

Chapter 2

Materials and Methods

2.1. Chemical reagents

This chapter details the characteristics of the chemicals used in electrochemical and photolytic experiments as well as the standards employed for the analytical measurements. These reagents are listed in Table 2.1, the specific chemicals used for PCDD/Fs analysis are detailed in Table 2.2. All solutions were prepared using ultrapure water (Q-POD Millipore).

Table 2.1. Summary of the chemicals used in this thesis.

Name	Chemical formula	Purity	Supplier
Acetic acid	$C_2H_4O_2$	100 %	Merck
Acetonitrile	C_2H_3N	99.9 %	Panreac
Copper sulphate pentahydrate	$CuSO_4 \cdot 5H_2O$	99 %	Merck
Phenol	C_6H_6O	>99.5 %	Sigma-Aldrich
2-chlorophenol	C_6H_5ClO	>99 %	Sigma-Aldrich
3-chlorophenol	C_6H_5ClO	>98 %	Sigma-Aldrich
4-chlorophenol	C_6H_5ClO	>99 %	Sigma-Aldrich
2,4-dichlorophenol	$C_6H_4Cl_2O$	99 %	Sigma-Aldrich
2,2´-biphenol	$C_{12}H_{10}O_2$	99 %	Sigma-Aldrich
Dibenzo-p-dioxin	$C_{12}H_8O_2$	>98 %	AccuStandard
Monochlorodibenzo-p-dioxin	$C_{12}H_7ClO_2$	>98 %	AccuStandard
2,8-dichlorodibenzo-p-dioxin	$C_{12}H_6Cl_2O_2$	>98 %	AccuStandard/Wellington Laboratories
Formic acid	CH_2O_2	98 %	Panreac
Methanol	CH_4O	99.5 %	Panreac
Nitric acid	HNO_3	65 %	Scharlau
Sodium chloride	NaCl	99.5 %	Panreac
Sodium hydroxide	NaOH	32 % w/v	Panreac
Sodium sulphate	Na_2SO_4	99 %	Merck
Sulphuric acid	H_2SO_4	98 %	Merck-Millipore
Titanium dioxide (TiO_2) P25	TiO_2	20 % rutile/80 % anatase	Evonik Industries
5-chloro-2-(2,4-dichlorophenoxy)phenol (Triclosan, TCS)	$C_{12}H_7Cl_3O_2$	99 %	Thermo Fisher

Table 2.2. Reagents used for PCDD/Fs analysis.

Reagent	Supplier
Acetone (Suprasolv)	Merck-Millipore
Dichloromethane (Unisolv)	Merck-Millipore
Ethyl acetate (Pestinorm)	VWR Chemicals
n-Hexane (Unisolv)	Merck-Millipore
Toluene (Unisolv)	Merck-Millipore
EPA 1613 CLS-CS4: calibration standard solutions	Wellington Laboratories
EPA 1613 ISS: internal standard spiking solution	Wellington Laboratories
EPA 1613 LCS: labelled compound stock solution	Wellington Laboratories
DDF-MDT: native PCDD/PCDF solution/mixture	Wellington Laboratories
MDDF-MDT: mass-labelled PCDD/FCDF solution/mixture	Wellington Laboratories

Some chemicals used in photolysis experiments had been previously synthesized in ETH laboratories. These compounds are listed in Table 2.3, where the molecular structures are also depicted.

Table 2.3. Chemicals synthesized for photolysis experiments.

Name	Acronym used in the text	Chemical formula	Molecular structure
4,5´-dichloro-[1,1´-biphenyl]-2,2´-diol	$(OH)_2$PCB13	$C_{12}H_8Cl_2O_2$	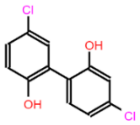
2-phenoxy phenol	OH	$C_{12}H_{10}O_2$	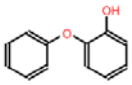
5-chloro-2-phenoxy phenol	OHCl	$C_{12}H_9ClO_2$	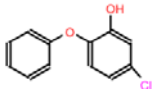
2-(2-chlorophenoxy) phenol	2ClOH	$C_{12}H_9ClO_2$	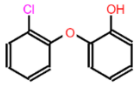
5-chloro-2-(2-chlorophenoxy) phenol	2ClOHCl	$C_{12}H_8Cl_2O_2$	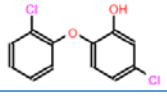
2-(4-chlorophenoxy) phenol	4ClOH	$C_{12}H_9ClO_2$	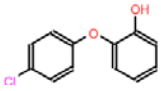
5-chloro-2-(4-chlorophenoxy) phenol	4ClOHCl	$C_{12}H_8Cl_2O_2$	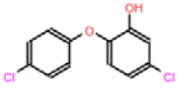

2.2. Electrochemical oxidation experiments

The flow diagram of the experimental set-up used in the electrochemical experiments is shown in Figure 2.1. It consists of a feed tank in which the sample was placed before beginning the treatment, then, water containing TCS is pumped into the electrochemical cell using a magnetic pump. The electrochemical cell used, shown in Figure 2.2, is a labELOX 1/176 cell manufactured by APRIA Systems S.L. (Spain). The cell was comprised of two rectangular electrodes disposed in parallel with an area of 176 cm^2 each and an electrode gap of 2 mm. The anode is made on boron-doped-diamond (BDD) and the cathode is made on titanium (Vallejo, 2014; Solá-Gutiérrez et al., 2018).

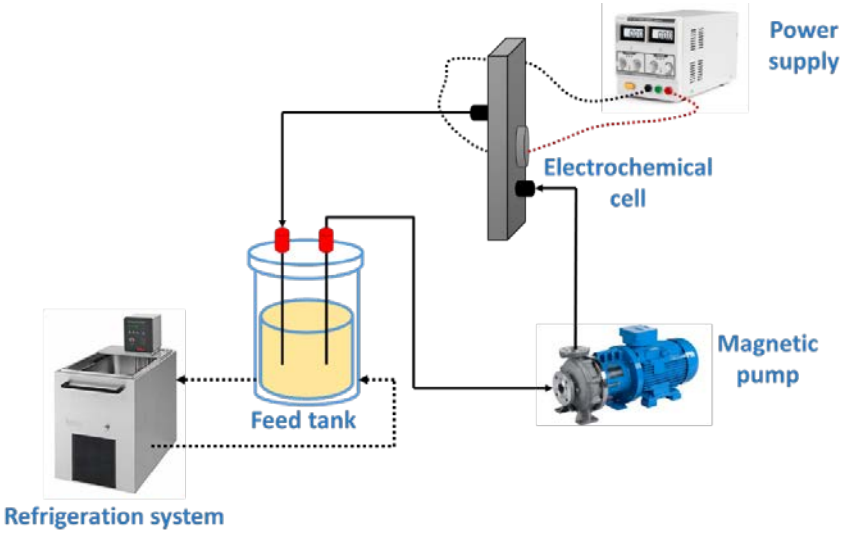

Figure 2.1. Schematic diagram of the electrochemical oxidation experimental set-up.

Figure 2.2. Experimental set-up employed in the electrochemical oxidation experiments (LabELOX 1/176 electrochemical cell, APRIA Systems, S.L.).

The experiments were conducted in batch mode at constant temperature of 20 °C. Experiments were ran at constant current density (J) equal to 6, 60 and 90 A m^2 depending on the initial concentration of TCS (10, 100 and 150 mg L^{-1}, respectively, dissolved in 3.7, 37.0 and 55.5 % of methanol) and the flow rate was kept constant at 9 L min^{-1} for all the experiments (Solá-Gutiérrez et al., 2019). Samples were collected from the feed tank at regular time intervals and analysed according to the pertinent analytical technique. The experimental conditions developed on the electrochemical experiments are summarized in Table 2.4.

Table 2.4. Experimental conditions applied on electrochemical experiments.

Electrochemical experiments	
$[TCS]_0$ (mg L^{-1})	10 (in 3.7 % methanol) 100 (in 37 % methanol) 150 (in 55 % methanol)
J (A m^{-2})	6 60 90
Volume (L)	1
Temperature (°C)	20
Flow rate (L min^{-1})	9
Electrolyte (mM)	NaCl: 56.3 Na_2SO_4: 21.1
Cu (mg L^{-1}) (if present)	10

2.3. Photolytic oxidation experiments

Photolysis experiments

Photolysis experiments were performed at the Institute of Biogeochemistry and Pollutant Dynamics (ETH, Zurich). The solutions were photolyzed in a photoreactor Rayonet Srinivasan-Griffin manufactured by The Southern New England Ultraviolet Company (U.S.A.) fitted with a merry-go-round apparatus and 300 nm wavelength bulbs (Figures 2.3 and 2.4).

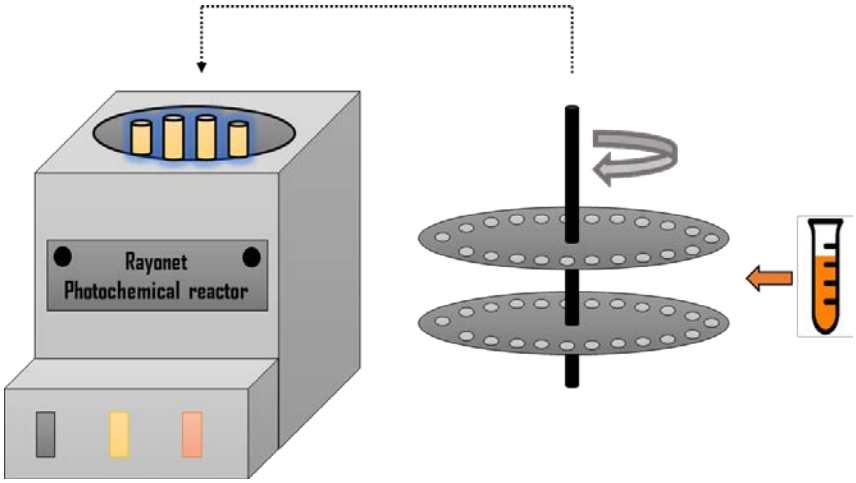

Figure 2.3. Schematic diagram of the photolytic oxidation experimental set-up.

Figure 2.4. Experimental set-up employed in the photolytic oxidation experiments (Rayonet photochemical reactor).

The photolysis solutions consisted of TCS and its hydrodehalogenation products (50 µM) dissolved separately in 20 mL Pyrex tubes in carbonate buffer (0.01 M, pH 10.6; $NaHCO_3$ (121.3 mg), Na_2CO_3 (293.1 mg), water (1 L)) containing 10 % acetonitrile (see operational conditions details in Table 2.5). The merry-go-round device containing the samples was placed in the photoreactor, the lamps were switched on and the experiment started. Different samples were taken out over the course of the experiments. To take samples, the light was turned off, then, to continue the experiment, the lamps were turned on again. All the experiments were performed in duplicate.

Table 2.5. Experimental conditions applied in the photolysis experiments.

Photolysis experiments		
Initial compound concentration (µM)	TCS OH OHCl 2ClOH 2ClOHCl 4ClOH 4ClOHCl	50 (in 10 / 90 (ACN: buffer solution))
Volume (mL)		20
Temperature (°C)		Room temperature
Lamps wavelength (nm)		300

Photocatalysis experiments

Photocatalysis experiments were carried out in a photoreactor as illustrated in Figure 2.5 (APRIA System S.L. laboratory UV LED reactor). It consist of a 1 L Pyrex glass cylindrical vessel and 180 1st generation LEDs (OCU-400 UA375, OSA Opto Light) assembled into 10 strips mounted around a dark PVC. LEDs had an emission wavelength between 375 and 380 nm. Total radiation ranged between $4 \cdot 10^{-3}$ and $2.4 \cdot 10^{-2}$ mW cm^{-2}, with an electrical power between 2.38 and 11.9 W.

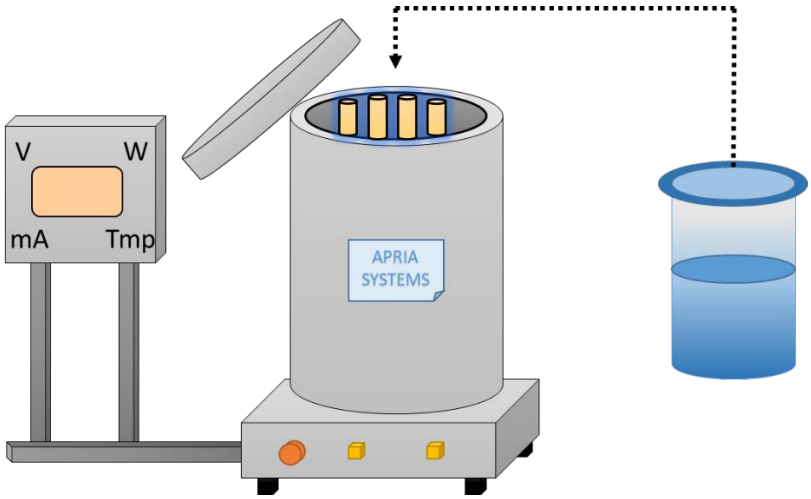

Figure 2.5. Experimental set-up employed in the photocatalytic oxidation experiments.

The solution containing the target compound was mixed with a given amount of TiO_2 photocatalyst and kept for 2.0 min in the dark to reach adsorption equilibrium. To test this phenomenon, samples before and after the addition of TiO_2 were taken. Then, the catalyst

suspension was added to the reactor, the reactor was closed and the light was switched on, giving rise to the beginning of the photocatalytic experiment. Time points were taken over the course with a pipette and filtered through a 1 µm syringe filter (AC Millex APFB, Millipore) to remove the suspended photocatalyst prior to analysis. Table 2.6 details the operational conditions. All experiments were performed in duplicate at room temperature.

Table 2.6. Experimental conditions applied on photocatalysis experiments.

Photocatalysis experiments	
$[TCS]_0$ (mg L^{-1})	10 (in 1 % acetonitrile)
TiO_2 (gr L^{-1})	0.75 1.0 1.5
Volume (L)	1
Temperature (°C)	Room temperature
LED electrical power (W)	6
Reactor electrical power (W)	50

2.4. Analytical measurements

2.4.1. Liquid chromatography analysis

High-Performance Liquid Chromatography (HPLC)

TCS samples oxidized by electrochemical and photocatalytic treatments were quantitatively analysed using an Agilent Series 1100 High-Performance Liquid Chromatograph (HPLC) coupled to a Diode Array Detector (DAD) (Figure 2.6). Separation occurred with a Zorbax Extend-C18 column (L = 150 mm; $Ø_i$ = 3 mm; 5 µm). To analyse TCS, an isocratic elution method of acetonitrile (60 %) and ultrapure water (40 %) at a flow rate of 1 mL min^{-1} was applied. The analysis of by-products also followed a gradient elution method with acetonitrile and formic acid (0.1 % v/v) as mobile phase at a flow rate of 1 mL min^{-1}: 80 % of formic acid solution (0.1 % v/v) was eluted during 3 min with acetonitrile, 80 % to 20 % of formic acid solution (0.1 % v/v) was eluted in the next 12 min followed by elution with 20 % to 0 % formic acid for another 5 min. Finally, 100 % acetonitrile was eluted for 6 min. The selected wavelengths were 210, 230, 254 and 280 nm and the column was kept at 30 °C. The volume injection was 50 µL. Products were identified using authentic standards by matching their retention time and absorbance spectra.

Figure 2.6. High-Performance Liquid Chromatograph (Agilent Series 1100) employed for the analysis of TCS and its by-products.

TCS samples oxidized by photolysis were quantitatively analysed in the Institute of Biogeochemistry and Pollutant Dynamics (ETH, Zurich) without further processing using HPLC with diode array detection. In this case, HPLC was a Dionex Ultimate 3000 Pump, Ultimate 3000 Photodiode Array Detector, Ultimate 3000 Autosampler HPLC system fitted with a Dionex Hypersil GOLD aQ C18 (L = 150 mm; $Ø_i$ = 4.6 mm; 5 µm) (Figure 2.7). A gradient elution method using acetonitrile: formic acid (0.1% v/v) as mobile phase at a flow rate of 1 mL min^{-1} was used. 65 % of formic acid solution (0.1 % v/v) was eluted during 2 min with acetonitrile, from 65 % to 30 % of formic acid solution (0.1 % v/v) was eluted in the next 25 min followed by 65 % held in another 5 min. By-products were identified using authentic standards by matching their retention time and absorbance spectra.

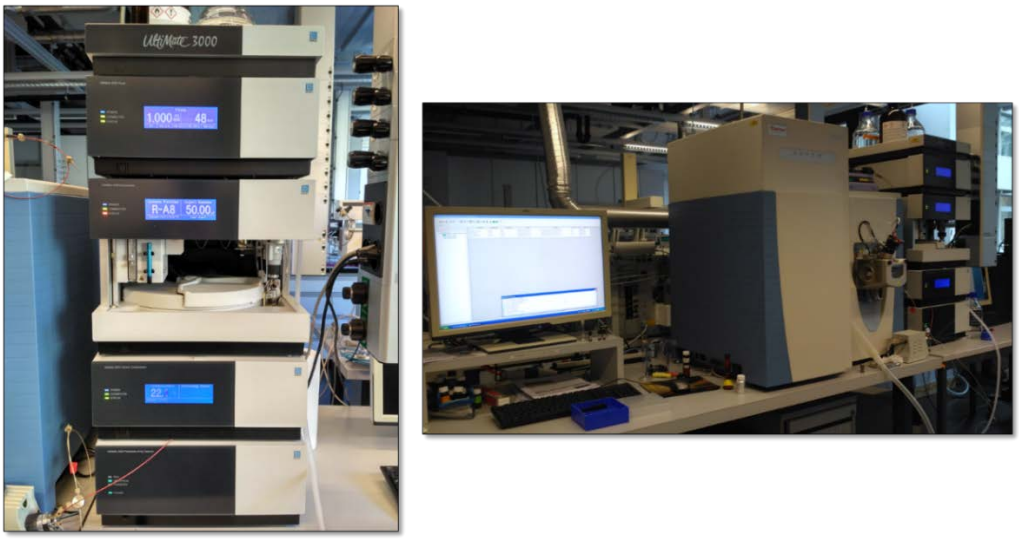

Figure 2.7. High-Performance Liquid Chromatograph (Thermo Scientific™ Ultimate™ 3000) employed for the analysis of TCS and its by-products.

2.4.2. Gas chromatography analysis

Qualitative analysis for intermediate organic compounds formed during the electrochemical and photocatalytic experiments for oxidation of TCS solutions was performed by gas chromatography coupled to mass spectrometry (GC-MS). The GC-MS was a Shimadzu QP2010 Ultra equipped with an auto-sampler (Figure 2.8). Separation occurred in a HP-5MS column (L = 30 m; Øi = 0.25 mm; 0.25 µm). The temperature program of the GC-MS oven was 80 °C, hold 2 min, rate 12.5 °C min^{-1} to 300 °C, hold 1.5 min. Helium was used as carrier gas at a flow rate of 1 mL min^{-1}. A volume sample of 2 µL was injected in splitless mode and the injector temperature was set at 250 °C. The mass spectrometer (MS) was operated in the electron impact ionization mode (70 eV). The transfer line and ion source temperatures were 290 and 230 °C, respectively. Data acquisition was in full scan mode with a range from m/z 50 to 350. Confirmation of all structural assignments for the identified compounds was verified using the NIST08 spectra library.

Figure 2.8. GC-MS Shimadzu QP2010 Ultra employed for the analysis of TCS and its by-products.

2.4.3. Atomic absorption spectroscopy

The presence of copper in the solution was monitored by atomic absorption spectroscopy using a Perkin Elmer 3110B (Figure 2.9). Copper was atomized by an air-acetylene flame. A hallow cathode lamp, Perkin Elmer Lumina^{TM} lamp, with a wavelength of 324.8 nm working with an intensity of 30 mA was employed. The slit width was set at 0.7 nm. Copper solutions ranging from 0.5 to 5 mg L^{-1} were used for calibration.

Figure 2.9. Atomic absorption spectroscopy (Perkin Elmer 3110B).

2.4.4. UV-Vis measurements

The pKa of Triclosan and its hydrodehalogenation derivatives was determined in the Institute of Biogeochemistry and Pollutant Dynamics (ETH, Zurich) by absorbance using a Varian Cary 100 Bio UV-Visible spectrophotometer (Figure 2.10) in the wavelength range between 200 and 800 nm, monitoring the absorbance under each pH in the range of 7-11. Solutions of 5 µM

Triclosan and 10 µM for hydrodehalogenation products of TCS were prepared in a 5 mM phosphate buffer solution. pH measurements were performed using a Metrohm 691 pH Meter. NaOH and HCl were used to adjust the pH value.

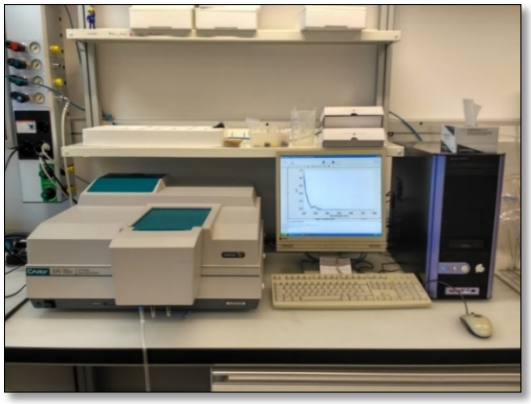

Figure 2.10. UV-Visible spectrophotometer (Varian Cary 100 Bio) employed for the absorbance analysis of TCS and its hydrodehalogenation derivatives.

2.5. Analysis of PCDD/Fs

PCDD/Fs were determined following the Standard Method U.S. EPA 1613 by isotope dilution and high-resolution gas chromatography coupled to a high-resolution mass spectrometry (HRGC-HRGS) (U.S. EPA 1613 1994). This method consists of successive meticulous steps summarized in Figure 2.11, which include extraction, concentration and purification stages in order to prepare the samples before the analysis by HRGC-HRGS (Vallejo et al., 2013; Vallejo, 2014; Fernández-Castro et al., 2016).

To ensure the analysis of PCDD/Fs, different standard solutions have been used: 1613 LCS, which contain a solution/mixture of 15 $^{13}C_{12}$-labelled chlorinated dibenzo-p-dioxins (2,3,7,8-$^{13}C_{12}$-PCDDs) and dibenzofurans (2,3,7,8-$^{13}C_{12}$-PCDFs) (Table I.1, Annexes) used to determine the recoveries of the labelled compounds obtained during the multiple steps followed to prepare the sample before analysis; DDF-MDT, a native PCDD/PCDF solution/mixture (Table I.2, Annexes); MDDF-MDT, a mass-labelled PCDD/PCDF solution/mixture (Table I.3, Annexes) used to determine the recoveries of the labelled compounds obtained during the multiple steps followed to prepare the sample before analysis; and ISS, an internal standard solution (Table I.4, Annexes), added to the sample before the chromatographic analysis. EPA 1613 CLS-CS4 have been used as calibration standard solutions (Table I.5, Annexes). Details of the methodology applied for the analysis of PCDD/Fs are explained below.

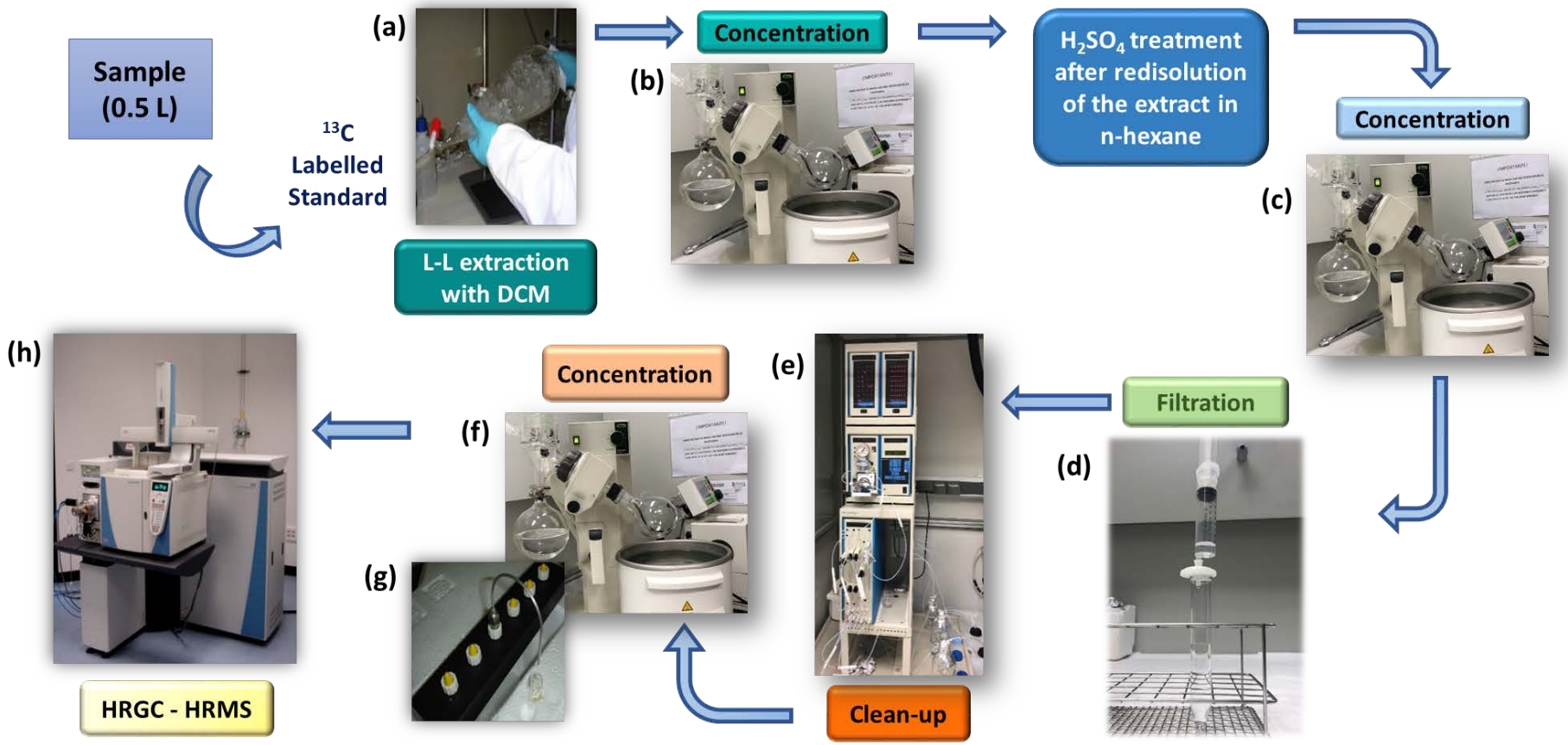

Figure 2.11. Analytical methodology scheme for the determination of PCDD/Fs (EPA 1613 method).

Extraction of PCDD/Fs

0.5 L samples placed in a 2 L separating funnel were spiked with 10 µL of 1613 LCS solution (15 mass ^{13}C-labeled PCDD/F solution, from TCDD/Fs to OCDD/Fs) and, in those samples were the less chlorinated species were also analysed, they were spiked with 5 µL of MDDF-MDT solution (mass-labelled PCDD/Fs standard, from unchlorinated and mono- to tri-CDD/Fs) dissolved in acetone. Then, 60 mL aliquots of dichloromethane were added to the separating funnel and mixed by carefully shaking for 3 min. Through this process, PCDD/Fs were extracted from the aqueous phase to the organic phase (Figure 2.11(a)). The organic phase was transferred to a rotary evaporator flask (Figure 2.12). This procedure was repeated three times.

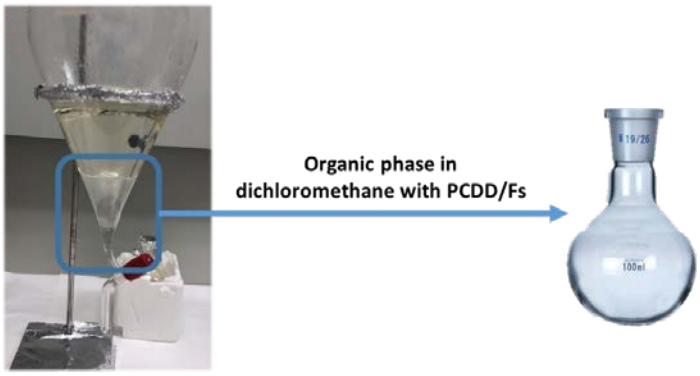

Figure 2.12. Extraction of PCDD/Fs from aqueous phase to organic phase (EPA 1613 method).

Concentration

The organic extract, placed in the rotary evaporator flask, was concentrated in a rotatory evaporator Büchi R-210 near to dryness at 35 °C and 750-600 mbar. At this point, the extract was rinsed with dichloromethane and concentrated again to almost dryness (Figure 2.11(b) and 2.13). This procedure was repeated three times.

Figure 2.13. Concentration step in a rotatory evaporator Büchi R-210 (EPA 1613 method).

H_2SO_4 treatment

In this step, in order to remove the organic matter, the evaporated extracts were treated with H_2SO_4 and with n-hexane. First, the evaporated extract was transferred to a separating funnel and, then, a 75 mL aliquot of n-hexane was added. Next, a 50 mL aliquot of H_2SO_4 was carefully added to the separating funnel. The mixture was shacked for 3 min. This procedure was repeated three times. Finally, the organic phase was transferred to a flask and then dried with Na_2SO_4 in a filter funnel (Figure 2.14).

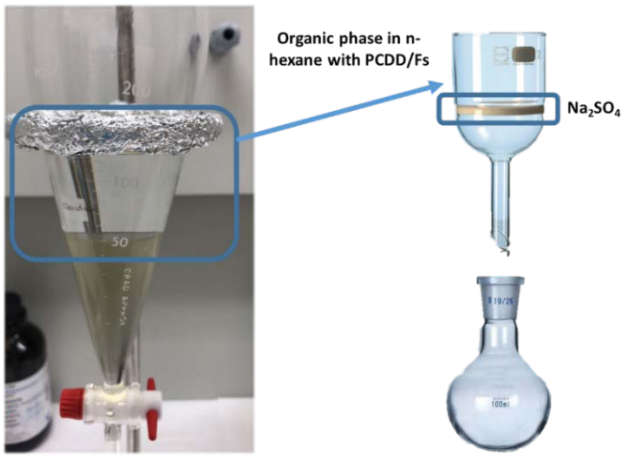

Figure 2.14. H_2SO_4 and drying with Na_2SO_4 treatments (EPA 1613 method).

Concentration

The organic phase, dissolved in n-hexane, was concentrated once again in the rotatory evaporator at 35 °C and at a pressure of 600 – 300 mbar. Next, the extract was rinsed with n-hexane and concentrated again to almost dryness to approximately 1 – 2 mL (Figure 2.11(c) and 2.15). This procedure was repeated three times.

Figure 2.15. Concentration step in a rotatory evaporator Büchi R-210 (EPA 1613 method).

Filtration

The concentration extract was filtered through a 0.45 µm PTFE filter and transferred to a test tube with 12 mL of n-hexane (Figure 2.11(d) and 2.16).

Figure 2.16. PCDD/Fs filtration step (EPA 1613 method).

Extract clean-up

The purification step of the filtered extract was performed through a solid-liquid adsorption chromatography using the automated system Power-Prep™ (Fluid Management Systems Inc., Waltham) (Figure 2.11(e) and 2.17). This automated clean-up system was based on the sequential use of multilayer silica, basic alumina and PX-21 carbon adsorbents. The filtered extract was pumped from the vial through the columns using the following solvents and their mixtures: n-hexane, n-hexane/dichloromethane (90/10 v/v), n-hexane/dichloromethane (50/50 v/v), toluene/ethyl acetate (50/50 v/v) and toluene. The purified extract was eluted from the carbon column in 75 mL of toluene.

Figure 2.17. Automated clean-up system (Power-Prep™, Fluid Management Systems Inc., Waltham) (EPA 1613 method).

Concentration and drying

Toluene was then evaporated in the rotatory evaporator at 35 °C and at a pressure of 150–85 mbar to almost dryness (Figure 2.11(f) and 2.18). After that, it was transferred into a vial to be concentrated to dryness under a nitrogen stream in a minivap unit (Figure 2.11(g) and 2.18).

Figure 2.18. PCDD/Fs concentration and drying steps (EPA 1613 method).

HRGC-HRMS analysis

Purified samples were analysed in the Chromatography Service (SERCROM) of the University of Cantabria. Before the chromatographic analysis, internal syringe standards (EPA 1613 ISS) were added to the sample. The analysis was carried out by HRGC-HRMS on a TRACE GC UltraTM gas chromatograph equipped with a split/splitless injector (Thermo Electron S.p.A.) and a DB-5 fused silica capillary column (J&W Scientific) (Figure 2.12 (h)). The initial temperature of the column (120 °C) was kept constant for 2 min and then it was increased sequentially in 3 steps to 210 °C, 230 °C and 310 °C at 15, 1 and 3 °C min^{-1}, respectively, for the analysis from tetra- to octa-CDD/Fs, and to 212, 232 and 233 °C at 6, 1 and 0.5 °C min^{-1}, respectively, for the analysis from unchlorinated and mono-CDD/Fs to tri-CDD/Fs. The column was connected through a heated transfer line kept at 270 °C to a DFS high-resolution magnetic sector mass spectrometer with a BE geometry (Figure 2.12 (h)). A positive electron ionization (EI+) mode with ionization energy of 45 eV was used in the source and its temperature was set at 270 °C. The mass spectrometer was operated in the SIM mode at 10,000 resolution power (10 % valley definition). Detection limits were calculated as the concentration values that gave instrumental responses within a signal-to-noise ratio of 3.

Figure 2.20. HRGC-HRMS (Thermo Fisher).

Quantitative determination was carried out by isotopic dilution method, an analytical technique applied to determine the quantity of chemical substances by adding a known amount

of an isotopically substance to the analysed sample. Relative response factors (RRFs), obtained from the calibration curve by analysing 1613CSL-CS4 standard solution mixtures for tetra to octa-CDD/Fs and the dilutions prepared from DDF-MDT for unchlorinated and mono- to tri-CDD/Fs, were used to determine the target compounds concentration in the samples. The recoveries of labelled standards were calculated using a mixture of two labelled PCDD/Fs included in the ISS that were added to the samples before the chromatographic analysis. Final results were expressed both in pg L^{-1} and in terms of toxicity equivalents (TEQ) in pg I-TEQ L^{-1}.

2.6. Quality control and quality assurance in the analysis of PCDD/Fs

The reliability of PCDD/Fs analysis was assured by means of the use of EPA 1613 LCS standard and the development of method blanks. The average recoveries were within the range established in the EPA 1613 method. Furthermore, blanks covering the whole sample preparation methodology showed that congeners were either not detected or below the detection limits, indicating the absence of contamination. In the same way, the recoveries obtained during electrochemical and photocatatalytic oxidation experiments were within the range proposed by EPA 1613 method.

2.7. References

EPA Method 1613. Tetra-trough octa-chlorinated dioxins and furans by isotope dilution HRGC-HRMS, 1994. U.S. Environmental Protection Agency. Office of Water. Engineering and Analysis Division (4303). 401 Street S.W. Washington, D.C.

Fernández-Castro, P., San Román, M.F., Ortiz, I., 2016. Theoretical and experimental formation of low chlorinated dibenzo-p-dioxins and dibenzofurans in the Fenton oxidation of chlorophenol solutions. Chemosphere 161, 136–144. https://doi.org/10.1016/j.chemosphere.2016.07.011

Solá-Gutiérrez, C., San Román, M.F., Ortiz, I., 2018. Fate and hazard of the electrochemical oxidation of triclosan. Evaluation of polychlorodibenzo‐p‐dioxins and polychlorodibenzofurans (PCDD/Fs) formation. Sci. Total Environ. 626, 126–133. https://doi.org/10.1016/j.scitotenv.2018.01.082

Solá-Gutiérrez, C., Schröder, S., San Román, M.F., Ortiz, I., 2019. PCDD/Fs traceability during triclosan electrochemical oxidation. J. Hazard. Mater. 369, 584–592. https://doi.org/10.1016/j.jhazmat.2019.02.066

Vallejo, M., 2014. Assessment of polychlorinated dibenzo-p-dioxins and dibenzofurans, PCDD/Fs, in the application of advanced oxidation processes. Doctoral Thesis, University of Cantabria.

Vallejo, M., San Román, M.F., Ortiz, I., 2013. Quantitative assessment of the formation of polychlorinated derivatives, PCDD/Fs, in the electrochemical oxidation of 2-chlorophenol as function of the electrolyte type. Environ. Sci. Technol. 47, 12400–12408. https://doi.org/10.1021/es403246g

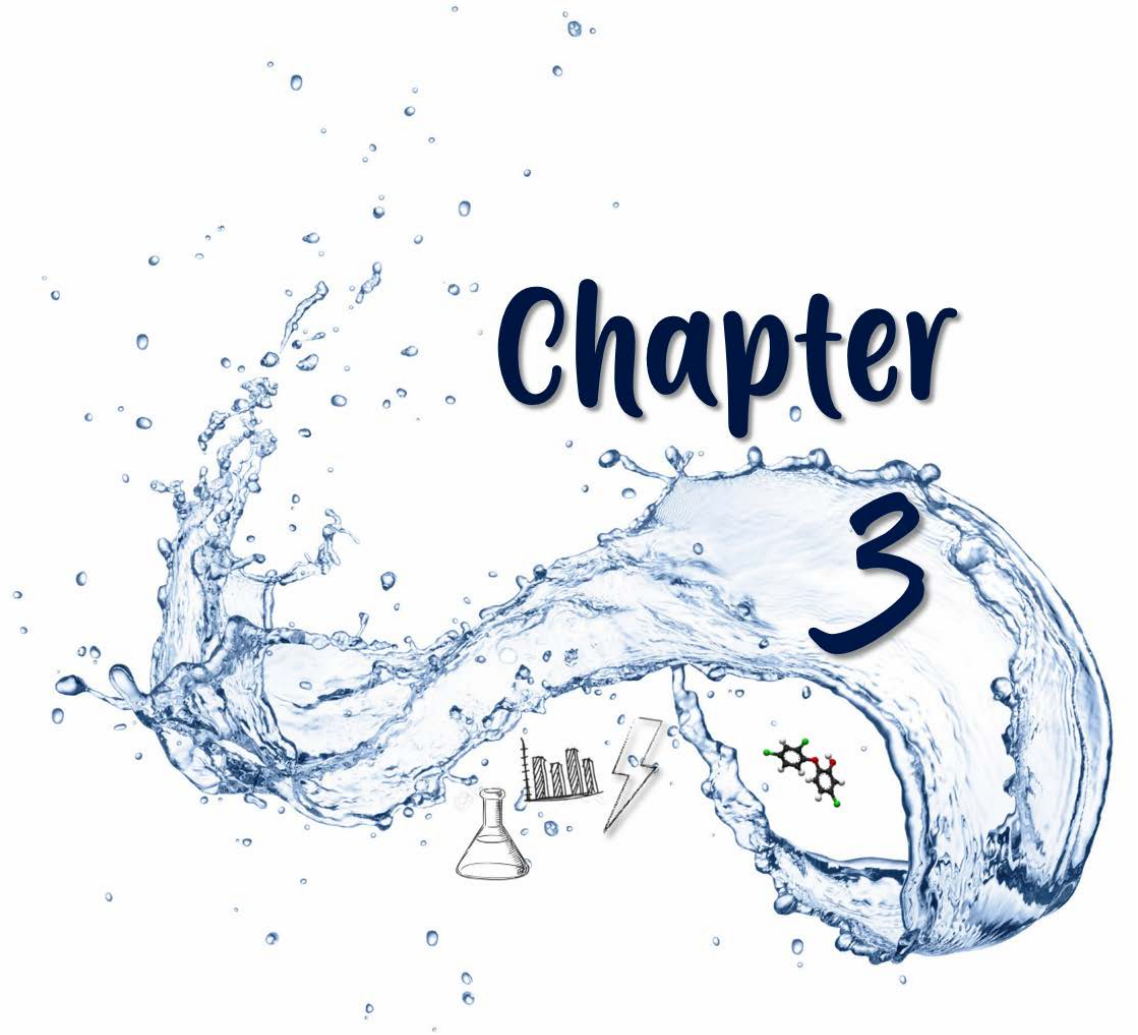

ELECTROCHEMICAL OXIDATION OF TRICLOSAN

In this chapter, the electrochemical oxidation of Triclosan has been assessed, paying special attention to the formation of intermediate products as well as the potential formation of PCDD/Fs. In the environment, Triclosan is typically found in highly variable concentrations ranging from µg L^{-1} to ng L^{-1}, particularly it is present in municipal wastewater treatment plants, surface water, sea water, or lakes and rivers (Mezcua et al., 2004; Lores et al., 2005; Sanchez-Prado et al., 2006; Wu et al., 2019). Nevertheless, the concentration of Triclosan could be several orders of magnitude greater if it proceeds from industrial effluents, reaching concentrations of mg L^{-1} (Martín de Vidales, 2015). In this work, different initial concentrations of Triclosan have been studied: 10; 100; and 150 mg L^{-1}. The overall objective of this study is to move forward on the influence of the initial concentration of Triclosan on its degradation rate, as well as on the generation of chlorinated organic intermediates and final oxidation products, including the potential formation of PCDD/Fs. The evaluation will be conducted in terms of concentration as well as toxicity of the oxidised samples. As well as the initial concentration of Triclosan, the electrolyte type is an important variable that has to be taken into account when applying electrochemical oxidation treatments. In this thesis, NaCl and Na_2SO_4, two common salts usually found in wastewater (Comninellis and Nerini, 1995; Kapałka et al., 2010; Govindaraj et al., 2013), have been used as electrolytes. Additionally and motivated by the extended presence of copper in wastewater and industrial effluents (Beyazit, 2014; Nawaz et al., 2016; Abdel-Aziz et al., 2017; Lee et al., 2017), the influence of this metal in the target solution has been analysed. Experiments have been carried out working with current densities (J) of 6, 60 and 90 A m^{-2}, depending on the initial concentration of Triclosan, as described next.

3.1. Calculation of the limiting current density

Before the experiments were stated, the limiting current density (J_{lim}) was determined. J_{lim} establishes the limit between two different operating regimes: electric current control ($J<J_{lim}$) or mass-transport control ($J>J_{lim}$). In this context, Panizza and Cerisola (2009) proposed a theoretical method for a process under mass-transport control, it means working with a current density higher than the J_{lim}, and for solutions with a unique compound present in the solution, which is consistent with the following equation:

$$J_{lim} = n \cdot F \cdot k_m \cdot C_{org} \quad (3.1)$$

where n is the number of electrons involved in the electrochemical oxidation of the target compound, F is the Faraday constant (96485 C mol^{-1}), k_m is the mass transport coefficient (m s^{-1}) and C_{org} is the concentration of the target compound in the solution (mol m^{-3}).

The number of electrons exchanged depend on the target compound, which is 51 electrons in the case of Triclosan (Martín de Vidales, 2015), as it is indicated in the following equation:

$$C_{12}H_7Cl_3O_3 + 22\,H_2O \rightarrow 12\,CO_2 + 51\,H^+ + {}^3/_2\,Cl_2 + {}^1/_2\,O_2 + 51\,e^- \quad (3.2)$$

k_m for the electrochemical cell used in this thesis was determined following the protocol proposed by Oduoza and Wragg (2000) for rectangular cells according to the results reported in previous works developed by the research group (Escudero, 2017). This protocol was based on a ferrocyanide/ferricyanide redox system. This technique consists on driving an electrochemical reaction to the maximum possible rate to guarantee the mass transport control (Cañizares et al., 2006). At this point, the rate of the electrochemical process only depends on the limiting current (I_{lim}), the number of electrons exchanged (n) and the Faraday constant (F). In the same way, the rate of the component transfers is dependent of the mass transport coefficient (k_m), the electrode area (A) and the concentration of the bulk solution (C_b) (Cañizares et al., 2006). Thus, the equation bellow was used to estimate the mass transport kinetic coefficient:

$$k_m = I_{lim}/(n \cdot F \cdot A \cdot C_b) \quad (3.3)$$

where I_{lim} is the limiting current (A), n the is the number of electrons involved in the electrochemical oxidation of the target compound, F is the Faraday constant (96485 c mol^{-1}), A is the electrochemical cell area (0.0176 m^2), C_b is the concentration of the compound that is oxidized ($K_4Fe(CN)_6$: 50 mol m^{-3}). I_{lim} was obtained experimentally resulting in 2.4 A. In addition, the number of electrons exchanged is equal to 1 as described in the following reactions:

$$Fe(CN)_6^{3-} + e^- \rightarrow Fe(CN)_6^{4-} \quad (3.4)$$

$$Fe(CN)_6^{3-} \rightarrow Fe(CN)_6^{4-} + e^- \quad (3.5)$$

As a result, a value of k_m of $2.83 \cdot 10^{-5}$ m s^{-1} was obtained. Therefore, for initial concentration of Triclosan of 10, 100 and 150 mg L^{-1}, the J_{lim} was 4.8, 48.1 and 72.2 A m^{-2}, respectively, by the equation 3.3. To ensure that the process was mass-transfer controlled, the final J applied was higher than the J_{lim} values, resulting in 6.0, 60.0 and 90.0 A m^{-2}.

3.2. Degradation of Triclosan

The electrochemical oxidation of Triclosan model solutions with initial concentrations of 10, 100 and 150 mg L^{-1}, that was dissolved in 3.7, 37.0 and 55.0 % (v/v) of methanol (values obtained experimentally by Martín de Vidales (2015)), respectively, was carried out under galvanostatic conditions (J: 6.0; 60.0; 90 A m^{-2}) using a BDD anode. Methanol was used to ensure the complete dissolution of Triclosan in the aqueous sample due to its low solubility (10 mg L^{-1} in water at 20 °C). Figure 3.1 shows the results of Triclosan degradation as a function of the supporting electrolyte (NaCl: 56.3 mM; Na_2SO_4: 21.1 mM). The concentration of these salts was chosen to provide a conductivity of 7.5 mS cm^{-1}, according to previous studies developed in the research group (Vallejo, 2014). As expected, the specific electrical charge (Q) needed to achieve a complete degradation of Triclosan increased with its initial concentration; however, it was independent of the supporting electrolyte as also reported by Maharana et al. (2015). 15, 45 and 60 minutes were required to reduce the initial Triclosan concentration, 10, 100 and 150 mg L^{-1}, by 50 %. In order to completely degrade the target compound, the treatment took 1, 3 and 4 hours for the three Triclosan concentrations studied. Experimental data are depicted together with error bars, which have been obtained after replication of the experiments.

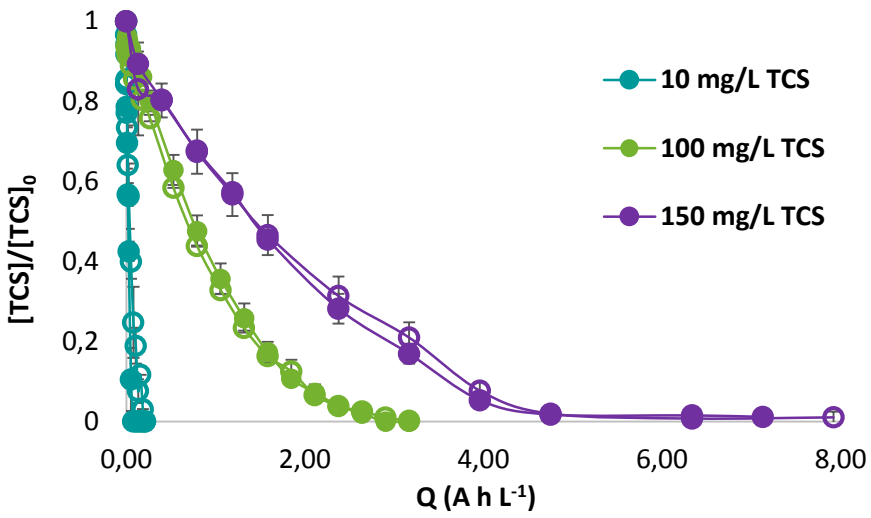

Figure 3.1. Influence of the initial concentration of TCS and the supporting electrolyte on Triclosan removal with the specific electric charge. Solid dots: NaCl; empty dots: Na_2SO_4.

3.2.1. Effect of copper on Triclosan degradation

Currently, water pollution by toxic heavy metals continues to be a worrisome environmental problem. This fact is due to the direct discharge of industrial effluents without any treatment to water (Basha et al., 2011; Chan et al., 2014; Nawaz et al., 2016; Rodrigues Pires da Silva et al., 2016). Specially, copper is one of the most toxic heavy metals that enter into the aquatic environment through many sources and it is usually found in concentrations ranging from mg L^{-1} to gr L^{-1} (See more details in Table 3.1). Among all different sources of copper, the following are highlighted: corrosion of water piping; fertilizer industries; paints and pigments or ceramic and glass industries; among others (Kamar et al., 2016; Abdel-Aziz et al., 2017; Adeli et al., 2017). Moreover, in particular, copper has been used as catalyst in the synthesis of ethers, useful intermediates in different organic synthesis (Marcoux et al., 1997). The U.S. EPA together with the Safe Drinking Water Act (SDWA) has established a Maximum Contaminant Level Goal (MCLG) for copper of 1.3 mg L^{-1}. Furthermore, copper is also regulated as an aesthetic contaminant under the U.S. EPA and the National Secondary Drinking Water Regulations (NSDWRs) at a Secondary Maximum Contaminant Level (SMCL) of 1.0 mg L^{-1}.

Table 3.1. Source classification and concentration of copper in aqueous phase.

Reference	Source				Copper concentration
	Synthetic water	Wastewater	Industrial effluent	Other source	
(Abdel-Aziz et al., 2017)	X				50 - 150 mg L^{-1} ($CuSO_4 \cdot 5H_2O$)
(Tonini and Ruotolo, 2017)	X				200 - 800 mg L^{-1} ($CuSO_4 \cdot 5H_2O$)
(Adeli et al., 2017)	X				10 mg L^{-1} ($Cu(NO_3)_2 \cdot 3H_2O$)
		X			0.01 – 0.02 mg L^{-1}
(Peng et al., 2015)	X				200 mg L^{-1}
(Kazeminezhad and Mosivand, 2017)	X				$CuSO_4 \cdot 5H_2O$: -
(Dong et al., 2017)	X				800 - 5000 mg L^{-1} ($CuCl_2$)
(Lee et al., 2017)			X		1.1 mg L^{-1}
(Hansen et al., 2017)			X		≈400 mg L^{-1}
(Šerbula et al., 2016)				X	0.276 – 333.5 mg L^{-1}
(Moneer et al., 2016)	X				3 - 10 g L^{-1}

Table 3.1. Source classification and concentration of copper in aqueous phase (cont.).

Reference	Source				Copper concentration
	Synthetic water	Wastewater	Industrial effluent	Other source	
(Nawaz et al., 2016)	X				50.16 - 252.09 g L^{-1} (Cu(II))
			X		0.95 mg L^{-1}
(Rodrigues Pires da Silva et al., 2016)	X				200 - 600 mg L^{-1}
(Kamar et al., 2016)	X				50 mg L^{-1} (Cu(II))
(Tokalıoğlu et al., 2016)		X			190 µg L^{-1}
(Chan et al., 2014)		X			56.8 µg L^{-1}
(Beyazit, 2014)			X		12.6 mg L^{-1}
(Arulmozhi et al., 2014)	X				10 mg L^{-1}
			X		10 mg L^{-1}
(Vadiraj et al., 2014)			X		0.27 -0.45 mg L^{-1}
(Basha et al., 2011)			X		164.48 mg L^{-1}
(Lin et al., 2019)	X				10 mg L^{-1} (Cu(II))

In order to study the influence of heavy metals on the electrochemical degradation of Triclosan, a model wastewater containing copper was prepared. To this aim, 10 mg L^{-1} of copper was dissolved in the aqueous solution of Triclosan (the equivalent amount to 39.63 mg L^{-1} of $CuSO_4 \cdot H_2O$). This analysis was made for an average initial concentration of 100 mg L^{-1} of Triclosan for both electrolytes, NaCl and Na_2SO_4. In order to ensure that copper was not deposited on the cathode surface during the electrochemical treatment, copper concentration has been monitored over time. According to the results depicted in Figure 3.2, with the slight differences shown on the specific electric charge no influence of the metal on the degradation of Triclosan is attributed.

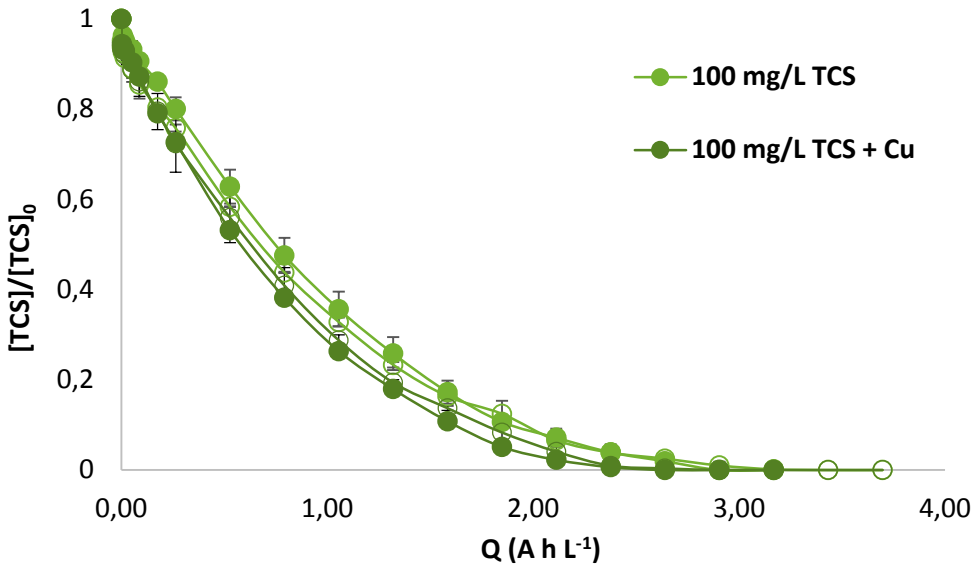

Figure 3.2. Influence of the presence of copper on Triclosan removal with the specific electric charge. Solid dots: NaCl; empty dots: Na_2SO_4.

3.3. Major intermediate products in the electrochemical oxidation of Triclosan

Although Triclosan disappeared completely, different oxidation by-products could be formed during the electrochemical oxidation, which could give rise to an increase of the final toxicity. In the scarce literature existing so far, some intermediate products have been identified. For instance, during the electrochemical oxidation of 100 mg L^{-1} of Triclosan, and working at 300 A m^{-2} with Na_2SO_4 as electrolyte, catechol, chlorohydroquinone and 4-chlorocatechol have been identified as intermediate products (Martín de Vidales, 2015). Sirés et al. (2007) proposed a reaction sequence for the degradation of Triclosan (50 mg L^{-1} in 20:80 (v/v) acetonitrile/water) by the electro-Fenton technology, working between 30 and 45 A m^{-2}, 0.2 mM of Fe^{+3} and Na_2SO_4 as electrolyte type. This reaction pathway was initiated by the rupture of the Triclosan molecule

to form 4-chlorocatechol and 2,4-dichlorophenol. In the same way, Maharana et al. (2015) studied the formation of some intermediate products during the electrochemical degradation of 4 mg L^{-1} of Triclosan at constant current density of 60 A m^{-2} and NaCl as electrolyte type, identifying 2,4-dichlorophenol, 5-chloro-3-(chlorohydroquinone)phenol and 2-chloro-5-(2,4-dichlorophenoxy)-benzene-1,4-diol.

In this thesis, along with the quantitative determination of the change in Triclosan concentration, GC–MS analysis were performed to identify the intermediate products that could be formed during the electrochemical oxidation of 100 mg L^{-1} of Triclosan. To study the influence of the electrolyte type present in the solution, these runs were performed with NaCl and Na_2SO_4. The qualitative analysis confirmed the formation of chloro-aromatic intermediary species, such as 2,4-dichlorophenol, 4-chlorocatechol, 2-chlorohydroquinone, 2-chloro-4-methoxyphenol and 1-chloro-2,5-dimethoxybenzene, for both electrolytes, NaCl and Na_2SO_4. Besides non-chlorinated products have been also detected, including 2-ethyl-hexanol, signal observed at 4.15 min. This compound had not been previously observed in the literature and it could be attributed to the presence of methanol as a co-solvent in the medium. Finally, the presence of diphenyl ether benzene, observed at 12.38 min, was also assessed. In Figure 3.3 the chromatogram of Triclosan samples after 3 hours of treatment, when no Triclosan remained in the solution, with NaCl as electrolyte, is shown.

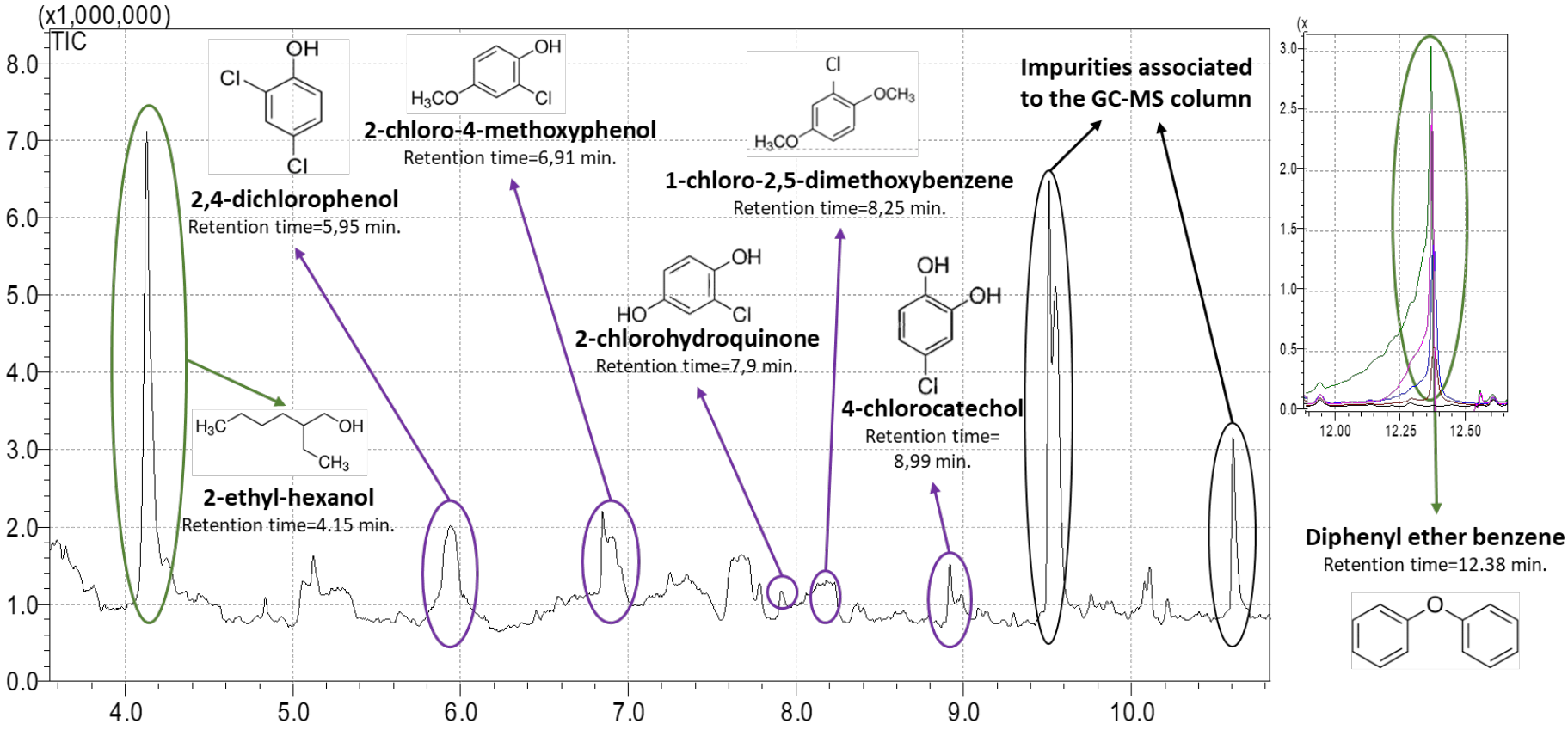

Figure 3.3. Chlorinated organic intermediate compounds detected by GC-MS analysis of 100 mg L^{-1} of Triclosan sample after 3 hours of treatment. Electrolyte used: NaCl.

3.4. Formation of highly chlorinated PCDD/Fs during the electrochemical oxidation of Triclosan

Recent works have directed the attention to the formation of PCDD/Fs during the oxidation of Triclosan as a result of the application of AOPs as previously reported in section 1.3 (Weber, 2007; Vallejo et al., 2013; Vallejo, 2014; Solá-Gutiérrez et al., 2018, 2019). Hence, this work focuses on the analysis and quantification of PCDD/Fs generated during the electrochemical oxidation of aqueous Triclosan samples. First, the influence of the initial concentration of Triclosan and the electrolyte employed have been studied. Additionally, and motivated by the extended presence of copper in wastewater and industrial effluents, the influence on the potential formation of PCDD/Fs of this metal in the target solution has been analysed. The analytical method employed for the analysis of PCDD/Fs was EPA 1613, explained in depth in section 2.5. The possible contamination of the experimental system by the accumulation of PCDD/Fs was determined before the experiments. With this purpose, a blank solution was pumped through the electrochemical cell and the concentration of PCDD/Fs was then determined (EPA 1613 recoveries presented in Table I.1 of the annexes). The results obtained showed negligible concentrations of PCDD/Fs. Figure 3.4 (when using NaCl as electrolytes) and Figure 3.5 (when using Na_2SO_4 as electrolyte) shows the concentration of the homologues, from TCDD/F to OCDD/F (tetra to octachlorinated dibenzo-p-dioxins and dibenzofurans), that have been identified in the untreated and electrochemically oxidized Triclosan samples (for 10, 100 and 150 mg L^{-1} of Triclosan) when Triclosan has completely disappeared, that is at 1, 3 and 4 hours, respectively. EPA 1613 recoveries obtained for these analysis are presented in the annexes (Table II.2 and II.3). Experimental data are depicted together with error bars, which have been obtained after replication of the experiments.

a)

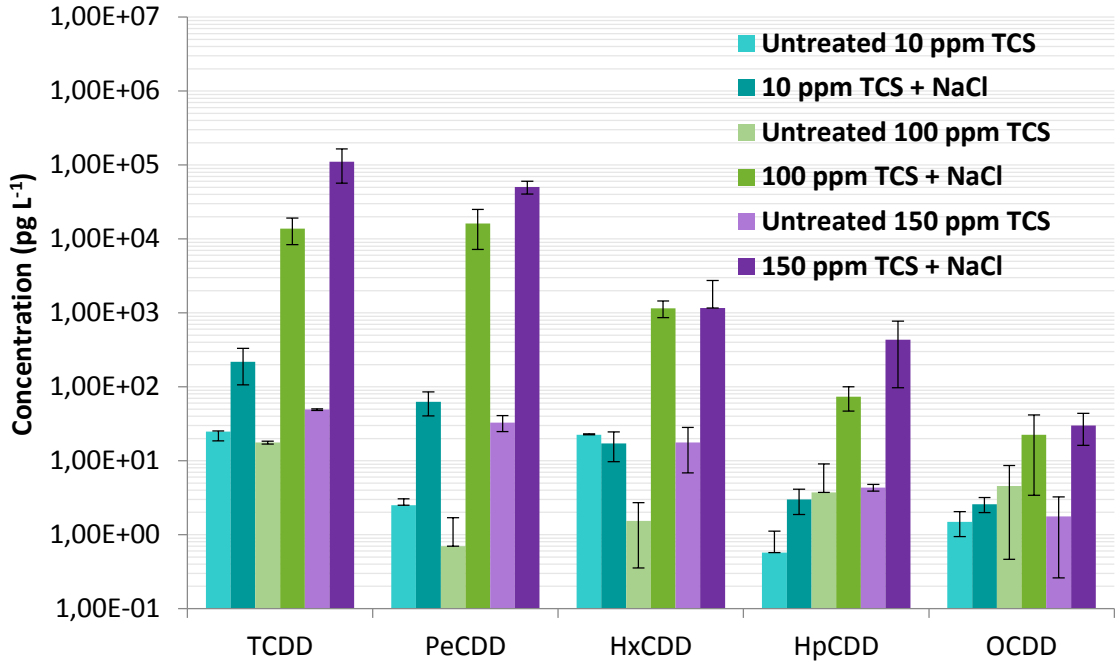

b)

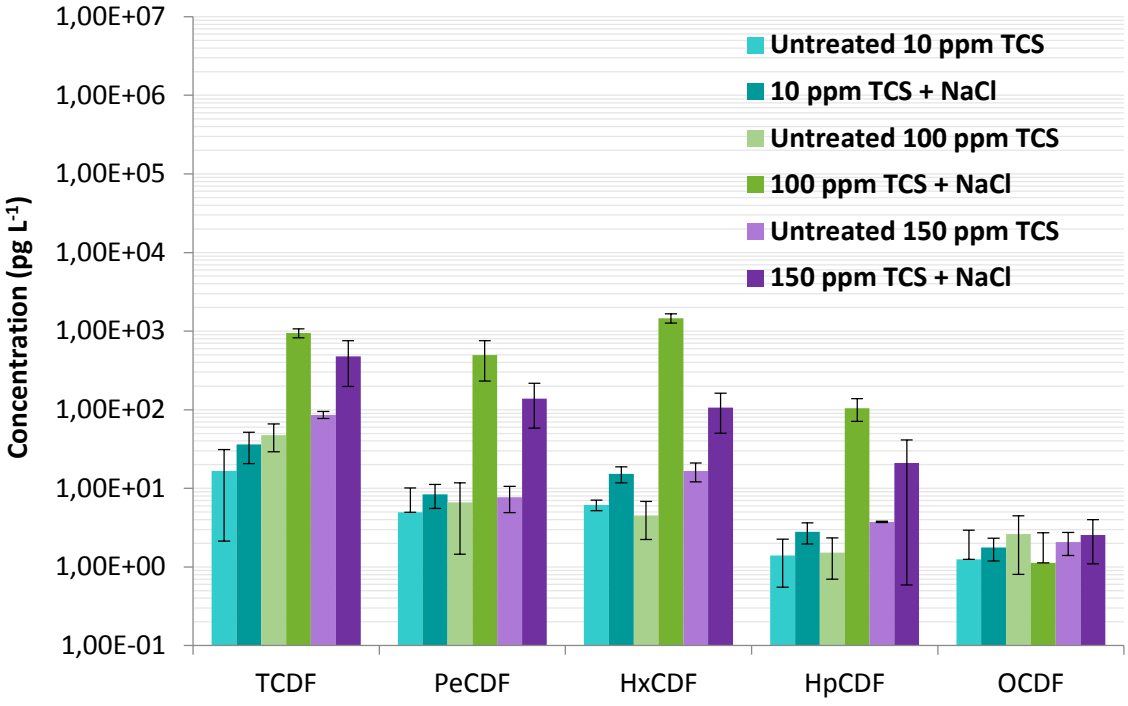

Figure 3.4. Concentration of highly chlorinated dioxins (a) and furans (b) as function of the initial concentration of TCS (10, 100 and 150 mg L^{-1}), oxidation time of 1, 3 and 4 h, respectively. Supporting electrolyte: NaCl.

According to the results depicted in Figure 3.4, low concentrations of highly chlorinated PCDD/Fs have been found in the untreated sample ($8.2 \cdot 10^1$, $9.1 \cdot 10^1$ and $2.2 \cdot 10^2$ pg L^{-1} for initial concentrations of Triclosan of 10, 100 and 150 mg L^{-1}). Of the total PCDD/Fs, 63.0, 28.1 and 47.5 % corresponded to the PCDDs profile for the three untreated Triclosan concentrations, respectively. Within all the homologue groups, TCDD was found at concentrations of $2.4 \cdot 10^1$, $1.7 \cdot 10^1$ and $4.9 \cdot 10^1$ pg L^{-1} to then decrease to 1.3, 2.6 and 2.1 pg L^{-1} for OCDD homologue, for 10, 100 and 150 mg L^{-1} untreated Triclosan samples, respectively. For these three Triclosan concentrations studied, TCDD accounted for 30.1, 19.4 and 22.1 % of the total PCDD/Fs profile. However, the concentration of all the homologue groups increased after the treatment in comparison to the untreated sample. When NaCl was used as electrolyte, the total PCDD/Fs concentration was $3.7 \cdot 10^2$, $3.4 \cdot 10^4$ and $1.6 \cdot 10^5$ pg L^{-1} for the three Triclosan concentrations studied in this thesis. Actually, the PCDD profile (Figure 3.4(a)) accounted for more than 82.5 % of the total PCCD/Fs concentration, specifically, 82.5, 91.2 and 99.5 % when using 10, 100 and 150 mg L^{-1} of Triclosan, respectively. Within all the homologue groups, TCDD the homologue group that presented the highest concentration, and then decrease as the chlorination degree increased. In addition, the PCDDs profile shows an increase in the homologue concentrations as the initial concentration of Triclosan increased, achieving the maximum values for the higher concentration of Triclosan, 150 mg L^{-1}, as well expected. Thus, the total concentration of TCDD was $2.2 \cdot 10^2$, $1.4 \cdot 10^4$ and $1.1 \cdot 10^5$ pg L^{-1} in the range of Triclosan initial concentrations studied in this work, accounting for 59.3, 40.4 and 67.7 % of the total PCDD/Fs concentration, respectively. As shown in Figure 3.4(a), the homologues concentration decreased as the chlorinated degree increased from TCDD to OCDD; the latter showed average concentration values of 2.6, $2.3 \cdot 10^1$ and $3.0 \cdot 10^1$ pg L^{-1}, that is 0.7, 0.1 and 0.1 % of the total PCDD/Fs concentration, for 10, 100 and 150 mg L^{-1} Triclosan samples, respectively. In the case of PCDFs profile (Figure 3.4(b)), the concentration of the homologue groups did not change appreciably, however, in comparison with the PCDD profile, the homologue concentrations are considerably lower. For 10 and 150 mg L^{-1} of initial concentration of Triclosan, TCDF was the group of homologues that presented the highest concentration of the total PCDFs profile, achieving values of $3.6 \cdot 10^1$ and $4.8 \cdot 10^2$ pg L^{-1}, respectively, accounting for 9.8 % and 0.3 % of the total PCDD/Fs concentration, respectively. Despite this, when using 100 mg L^{-1} of Triclosan as initial concentration, HxCDF was found at the highest concentration of the total PCDFs profile ($1.5 \cdot 10^3$ pg L^{-1}). The lowest concentrations were found in the OCDF homologue group, which decreased to 1.8, 1.1 and 2.5 pg L^{-1}, for 10, 100 and 150 mg L^{-1} Triclosan samples, respectively, values close to those in the untreated sample.

a)

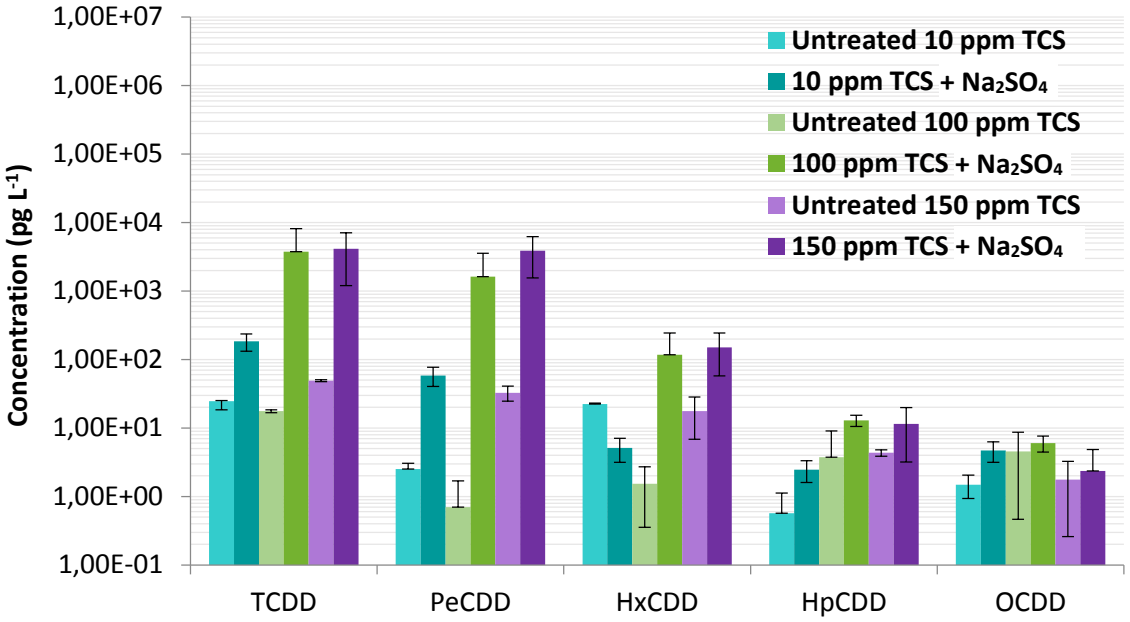

b)

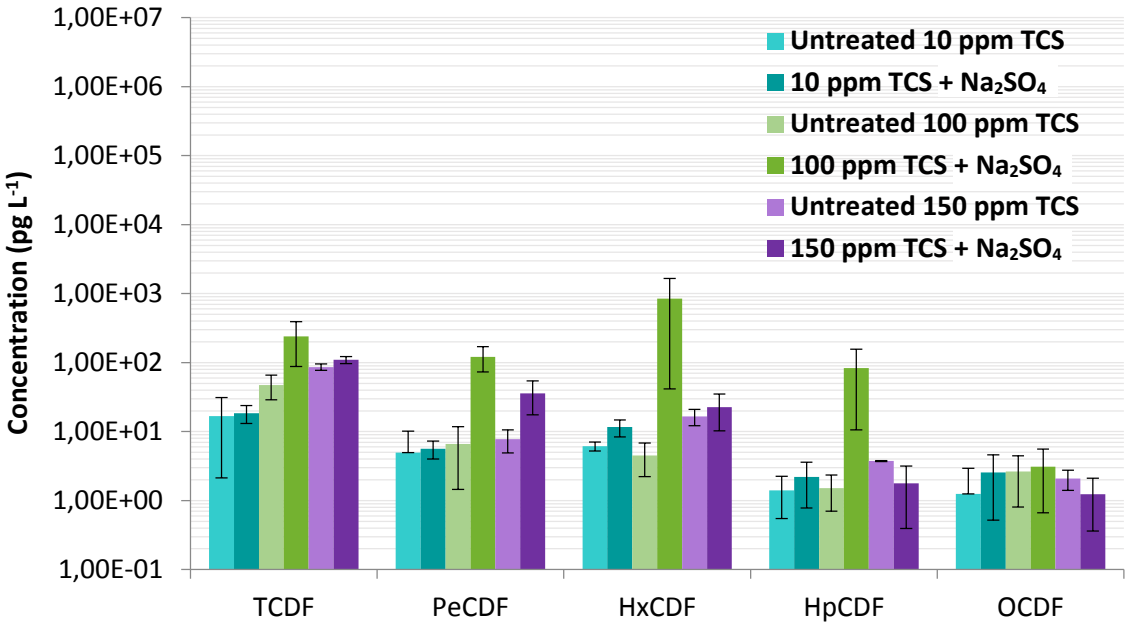

Figure 3.5. Concentration of highly chlorinated dioxins (a) and furans (b) as function of the initial concentration of TCS (10.0, 100.0 and 150.0 mg L^{-1}), oxidation time of 1, 3 and 4 h, respectively. Supporting electrolyte: Na_2SO_4.

When Na_2SO_4 was used as electrolyte (Figure 3.5), a similar behaviour was observed in both profiles (PCDD and PCDF); however, the total PCDD/Fs formation after the treatment was noticeably lower than for the case of NaCl electrolyte ($2.9 \cdot 10^2$, $8.6 \cdot 10^3$ and $8.4 \cdot 10^4$ pg L^{-1} for the

three Triclosan concentrations studied in this thesis). Actually, the same trend was observed when using NaCl as electrolyte, the PCDD profile accounted for more than 80.9 % of the total PCCD/Fs concentration, specifically, 86.3, 80.9 and 97.9 % when using 10, 100 and 150 mg L^{-1} of Triclosan, respectively. Additionally, after the data shown in Figure 3.5(a), it is concluded that the total concentration of homologues also decreases as the chlorination degree increases. TCDD reported the highest concentration in comparison to the rest of homologue groups. Thus, the total concentration of TCDD was $1.8 \cdot 10^2$, $3.7 \cdot 10^3$ and $4.1 \cdot 10^4$ pg L^{-1} in the range of Triclosan initial concentrations studied in this work, accounting for 62.3, 55.2 and 49.7 % of the total PCDD/Fs concentration, respectively. As shown in Figure 3.5(a), OCDD showed average concentration values of 2.6, 6.1 and 2.4 pg L^{-1}, that is 0.8, 0.1 and 0.1 % of the total PCDD/Fs concentration, for 10, 100 and 150 mg L^{-1} Triclosan samples, respectively. In the case of PCDFs profile (Figure 3.5(b)), the profile of the concentration of the homologue groups shows a similar trend to PCDDs, however, in comparison with the PCDD profile, the homologue concentrations are considerably lower. For 10 and 150 mg L^{-1} of initial concentrations of Triclosan, TCDF was the group of homologues that presented the highest concentration of the total PCDFs profile, achieving values of $1.8 \cdot 10^1$ and $1.1 \cdot 10^2$ pg L^{-1}, respectively, accounting for 6.2 and 1.3 % of the total PCDD/Fs concentration. Nevertheless, when using 100 mg L^{-1} of Triclosan as initial concentration, HxCDF was found at the highest concentration of the total PCDFs profile ($8.4 \cdot 10^2$ pg L^{-1}). However, in this case, the trend differences observed related to the concentration decrease as the number of chlorines increase (from TCDF to OCDF), could be attributed to the experimental error determined for the HxCDF homologue group. Finally, the OCDF homologue group showed the lowest concentration, decreasing to 2.6, 3.1 and 1.2 pg L^{-1}, for 10, 100 and 150 mg L^{-1} Triclosan samples, respectively.

Congeners with chlorine at 2,3,7,8 positions, recognised as the most toxic ones, are depicted in Figure 3.6. This analysis was made to Triclosan samples (for 10, 100 and 150 mg L^{-1} of Triclosan) when Triclosan had completely disappeared, that is at 1, 3 and 4 hours, respectively.

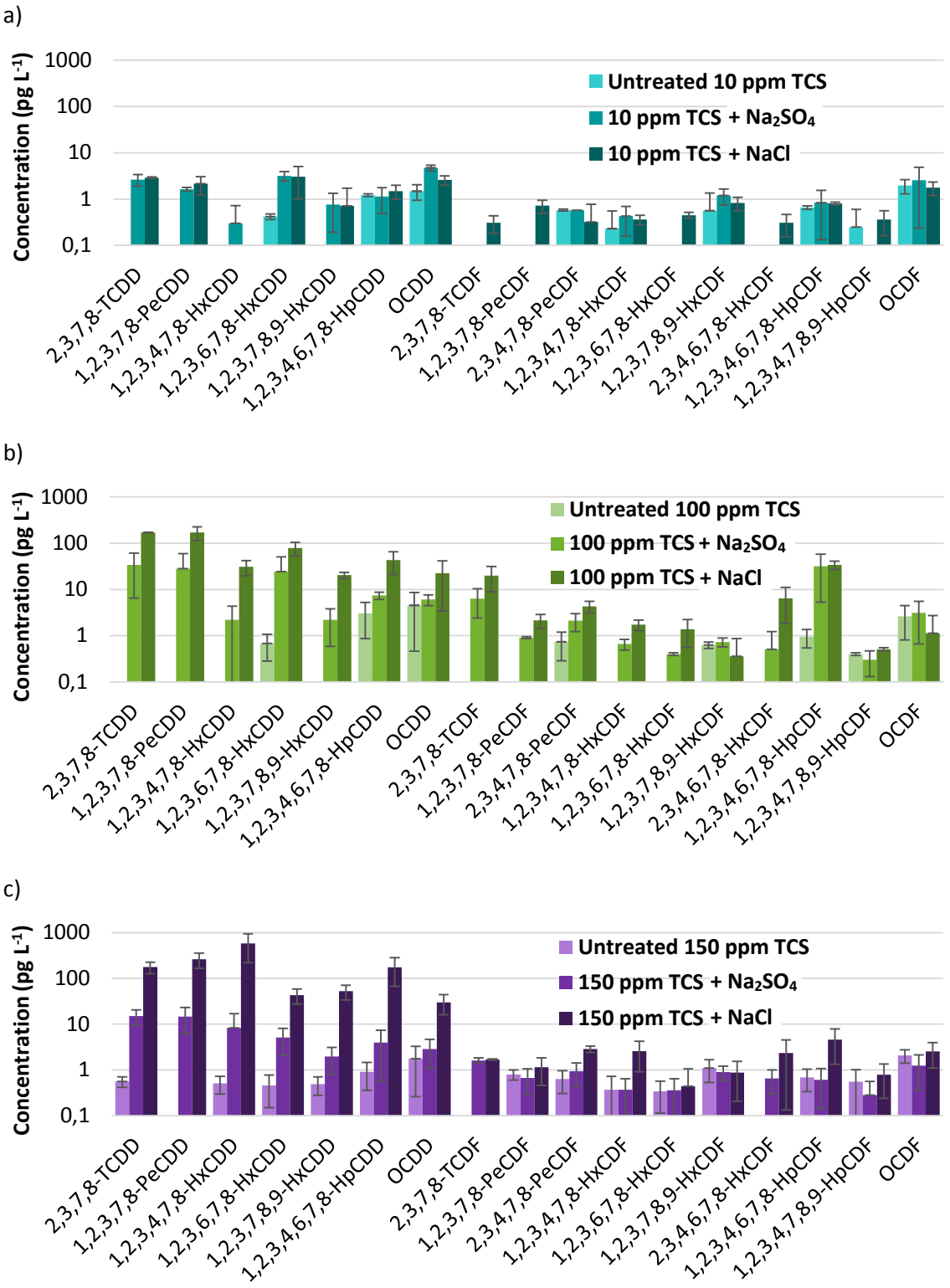

Figure 3.6. Concentration of 2,3,7,8-PCDD/Fs congeners as a function of the supporting electrolyte (NaCl and Na_2SO_4) and the initial concentration of TCS: (a) 10.0 mg L^{-1}; (b) 100.0 mg L^{-1}; and (c) 150.0 mg L^{-1}; oxidation time of 1, 3 and 4 h, respectively.

Figure 3.6 collects data of the untreated samples, which serve as reference together with the presence of the congeners in the oxidized samples working with both electrolytes. Firstly, for 10 mg L^{-1} Triclosan untreated sample, 1,2,3,4,6,7,8-HpCDD, OCDD and OCDF congeners were detected at the highest concentrations (1.2 – 2.0 pg L^{-1}). The same congeners were also detected for 100 mg L^{-1} (2.6 – 4.5 pg L^{-1}) and for 150 mg L^{-1} (0.9 – 2.1 pg L^{-1}). As it can be observed, the total concentration of 2,3,7,8-PCDD/Fs congeners increased considerably with the initial concentration of Triclosan (Figure 3.6(a–c)), increasing from less than 10 pg L^{-1} to more tha 100 pg L^{-1}. For 10 mg L^{-1} of Triclosan, the total concentration of 2,3,7,8-PCDD/Fs accounted for 5.2 and 6.7 % of the total PCDD/Fs concentration when NaCl and Na_2SO_4 was used as electrolyte, respectively. For this initial concentration of Triclosan (Figure 3.6(a)), 2,3,7,8-TCDD, 1,2,3,6,7,8-HxCDD and OCDD were the congeners that presented the highest concentrations for both electrolytes, Na_2SO_4 and NaCl, achieving average values up to 4.7 pg L^{-1}. Specifically, 2,3,7,8-congener profile was dominated by 1,2,3,6,7,8-HxCDD when NaCl was present in the reaction medium (16.0 % of the total 2,3,7,8-PCDD/Fs concentration) and by OCDD when using Na_2SO_4 as electrolyte (23.6 % of the total 2,3,7,8-PCDD/Fs concentration).

Figure 3.6(b) shows the results for 100 mg L^{-1} Triclosan samples. The total concentration of 2,3,7,8-PCDD/Fs represented the 1.8 and 1.7 % of the total PCDD/Fs concentration when NaCl and Na_2SO_4 were dissolved in the aqueous sample, respectively. In this way, 2,3,7,8-TCDD, 1,2,3,7,8-PeCDD, 1,2,3,6,7,8-HxCDD and 1,2,3,4,6,7,8-HpCDD were the predominant congeners observed after the oxidation treatment. The maximum concentration was observed for the most toxic congener, 2,3,7,8-TCDD, reaching average values of $3.4 \cdot 10^1$ (22.4 % of the total 2,3,7,8-PCDD/Fs concentration) and $1.7 \cdot 10^2$ pg L^{-1} (27.7 % of the total 2,3,7,8-PCDD/Fs concentration) for those samples treated with Na_2SO_4 and NaCl, respectively.

On the other hand, the total concentration of 2,3,7,8-PCDD/Fs accounted for 0.8 and 0.7 % of the total PCDD/Fs concentration for both electrolytes, NaCl and Na_2SO_4, respectively, when the initial concentration of Triclosan was 150 mg L^{-1} (Figure 3.6(c)). The dominant profile still being 2,3,7,8-TCDD, as well as 1,2,3,7,8-HpCDD, 1,2,3,4,7,8-HxCDD and 1,2,3,4,6,7,8-HpCDD. In this case, $5.8 \cdot 10^2$ pg L^{-1} (43.4 % of the total 2,3,7,8-PCDD/Fs concentration) was the maximum concentration observed, corresponding to the 1,2,3,4,7,8-HxCDD congener when NaCl was utilized as electrolyte.

To summarize, it can be observed that, for all cases, the concentration of 2,3,7,8-congeners increased after the electrochemical treatment, reaching concentrations that were even more pronounced when NaCl was present in the solution. Thus, the use of Na_2SO_4 led to an increase in the total concentration of the congener group from 3 to 11 times depending on the initial concentration of Triclosan, whereas the observed increase went from 3 to 119 times when NaCl was present in the oxidation medium with regard to the untreated sample.

In addition, the toxicity equivalent index (TEQ) has been calculated as previously detailed in chapter 2. Figure 3.7 depicts TEQ levels. A significant increase in TEQ in the electrooxidized samples with the initial concentration of Triclosan is clearly observed, especially for oxidized samples using NaCl as electrolyte. The maximum calculated value of TEQ was $3.8 \cdot 10^2$ pg L^{-1} (NaCl and 150 mg L^{-1} of Triclosan) that is considerably higher than the value corresponding to the untreated sample and to the limit of 30.0 pg L^{-1} recommended for drinking water by the U.S EPA. Furthermore, it should be taken into account that this value is also noticeably higher when compared to previous reported data performed in this research group for the electro-oxidation of 2-chlorophenol, commonly used as pesticide. 2000 mg L^{-1} of 2-chlorophenol were electrochemically oxidized with NaCl as electrolyte, achieving TEQ values up to $2.2 \cdot 10^2$ pg L^{-1} (Vallejo, 2014). These results indicated that much lower concentrations of Triclosan resulted in much higher toxicities values after the oxidation treatment than in the case of 2-chlorophenol.

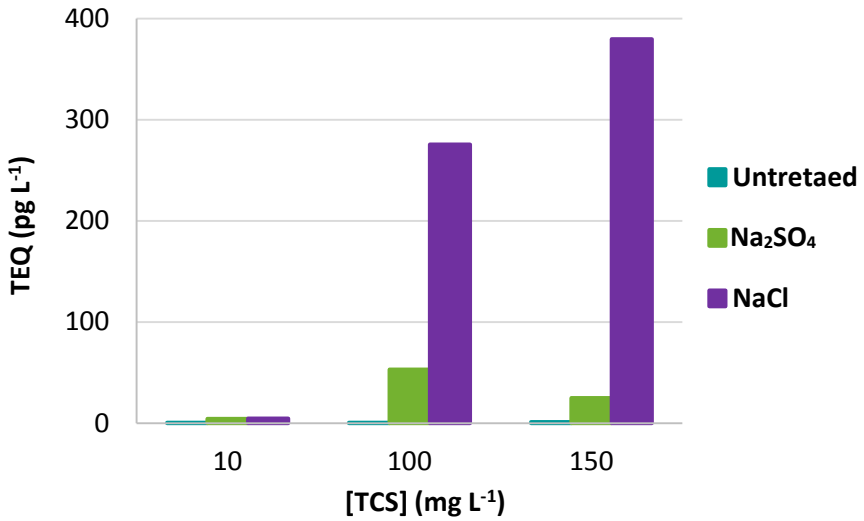

Figure 3.7. TEQ values as function of the initial concentration of TCS and the supporting electrolyte: NaCl (56.3 mM) and Na_2SO_4 (21.1 mM). Oxidation time of 1, 3 and 4 h for initial concentrations of 10, 100 and 150 mg L^{-1}, respectively.

3.4.1. Effect of copper on highly chlorinated PCDD/Fs formation

The influence of copper on the potential formation of PCDD/Fs has been studied for both electrolytes, NaCl and Na_2SO_4, and for those solutions which were prepared with an initial concentration of 100 mg L^{-1} of Triclosan. These results are shown in Figure 3.8.

a)

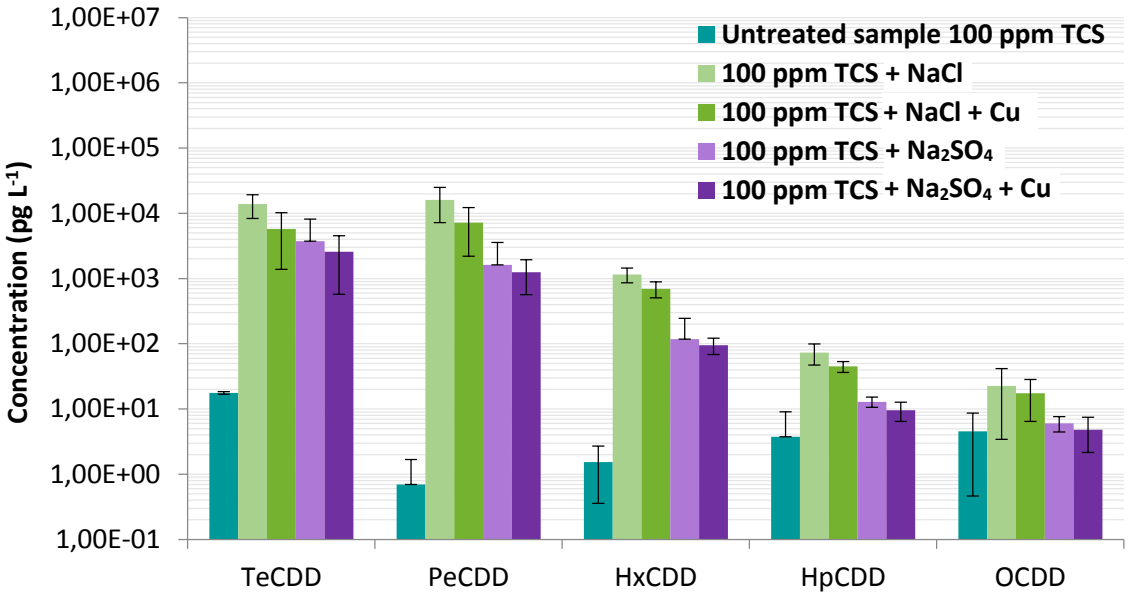

b)

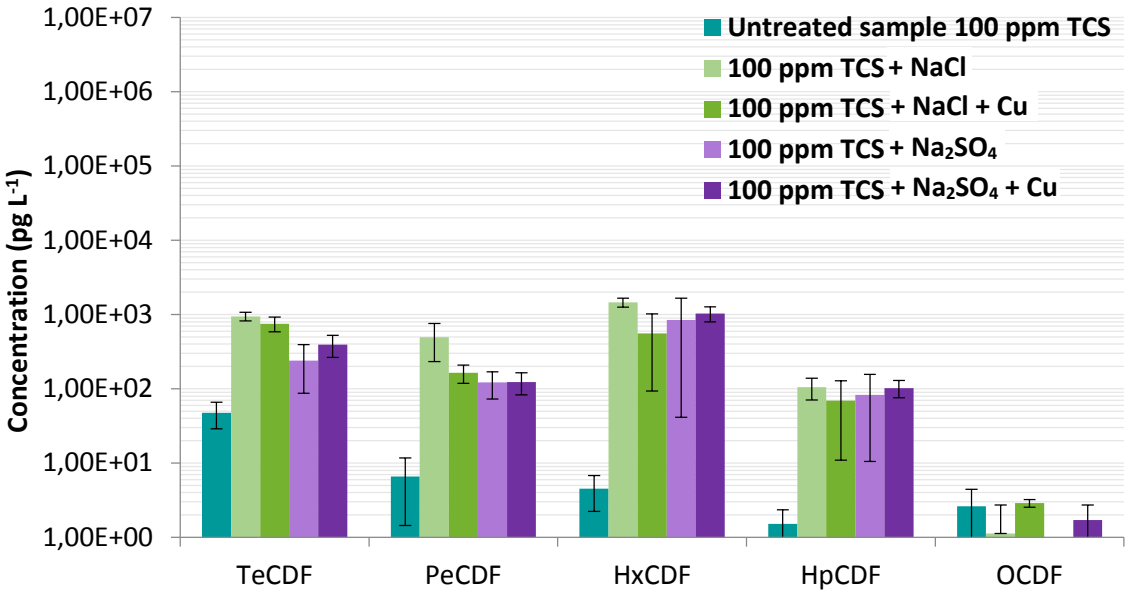

Figure 3.8. Influence of the electrolyte type and copper on the formation of highly chlorinated dioxins (a) and furans (b) during electrochemical oxidation. $[TCS]_0$=100 mg L^{-1}.

When copper is present in the reaction medium, the total concentration of PCDD/Fs decreased from $3.4 \cdot 10^4$ to $1.5 \cdot 10^4$ pg L^{-1} in the presence of NaCl (corresponding to a decrease of 55.8 %). In the same way, and using Na_2SO_4, this value decreased again from $8.6 \cdot 10^3$ to $5.6 \cdot 10^3$ pg L^{-1} in the presence of copper (corresponding to a decrease of 35.1 %). On the other hand, from TCDD to OCDD homologues (Figure 3.8(a)), the concentration tended to decrease as the chlorines increase in all the samples, independently on the electrolyte type used. Furthermore, a decrease in the total PCDDs concentration can be observed in comparison to those samples without copper. When NaCl was used as electrolyte, TCDD concentration decreased to $5.8 \cdot 10^3$ pg L^{-1} in the presence of copper (from $1.4 \cdot 10^4$ pg L^{-1} when no copper was dissolved in the target solution). At the same conditions, OCDD concentration was $1.7 \cdot 10^1$ pg L^{-1} with regard to $2.3 \cdot 10^1$ pg L^{-1} without copper salt in the medium. In the PCDFs profile (Figure 3.8(b)), as the chlorination degree increases, PCDFs concentration tended to decrease, except for HxCDF homologues. This homologue group presented also the highest concentration without the salt dissolved in the solution and decreased from $1.5 \cdot 10^3$ to $5.6 \cdot 10^2$ pg L^{-1} in the presence of it. In the case of having Na_2SO_4 in the reaction medium, TCDD concentration decreased to $2.5 \cdot 10^3$ pg L^{-1} in the presence of the salt (from $3.7 \cdot 10^3$ pg L^{-1} when no copper was dissolved in the solution). At the same conditions, OCDD concentration was 4.8 pg L^{-1}. In the PCDFs profile (Figure 3.8(b)), HxCDF presented the highest concentration achieving values up to $1.0 \cdot 10^3$ pg L^{-1} in the presence of copper.

The concentration of 2,3,7,8-PCDD/Fs congeners for these runs has been also analysed and results are depicted in Figure 3.9. When copper was added to the solution treated with NaCl as electrolyte, the total 2,3,7,8-PCDD/Fs concentration has almost decreased by 50.0 % (from $6.1 \cdot 10^2$ without copper to $3.6 \cdot 10^2$ pg L^{-1} in the presence of the salt). The dominant profile of 2,3,7,8-PCDD/Fs still being 2,3,7,8-TCDD ($1.1 \cdot 10^2$ pg L^{-1}; 30.0 % of the total 2,3,7,8-PCDD/Fs concentration), 1,2,3,7,8-PeCDD ($9.7 \cdot 10^1$ pg L^{-1}; 27.0 % of the total 2,3,7,8-PCDD/Fs concentration) and 1,2,3,6,7,8-HxCDD ($3.3 \cdot 10^1$ pg L^{-1}; 9.1 % of the total 2,3,7,8-PCDD/Fs concentration). When Na_2SO_4 was present in the reaction medium as electrolyte, the dominant 2,3,7,8-PCDD/Fs profile was: 2,3,7,8-TCDD ($3.0 \cdot 10^1$ pg L^{-1}; 21.4 % of the total 2,3,7,8-PCDD/Fs concentration), 1,2,3,7,8-PeCDD ($2.0 \cdot 10^1$ pg L^{-1}; 14.2 % of the total 2,3,7,8-PCDD/Fs concentration), and 1,2,3,4,6,7,8-HpCDF ($4.2 \cdot 10^1$ pg L^{-1}; 29.3 % of the total 2,3,7,8-PCDD/Fs concentration). TEQ levels decreased in the presence of copper from $2.76 \cdot 10^2$ pg L^{-1} to $1.67 \cdot 10^2$ pg L^{-1} in the sample with NaCl (accounting for a decrease of 41.3 %), and from $5.31 \cdot 10^1$ pg L^{-1} and $4.53 \cdot 10^1$ pg L^{-1} in the sample with Na_2SO_4 (accounting for a decrease of 14.7 %).

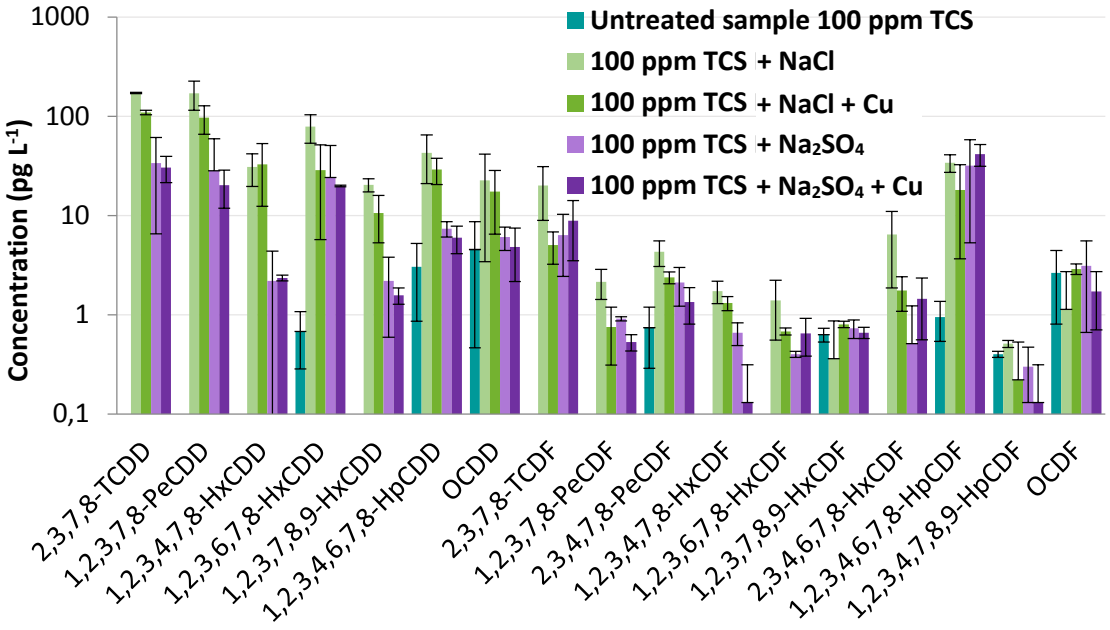

Figure 3.9. Influence of electrolyte type and copper in the 2,3,7,8-PCDD/Fs congeners profile. $[TCS]_0$= 100 mg L^{-1}.

Based on the results shown above, and taking into account the total concentration of highly chlorinated PCDD/Fs, copper could act as a catalyst in the electrochemical oxidation of Triclosan, having a significant influence on its decrease, independently on the electrolyte employed. In the same way, toxicity values in terms of dioxins and furans were less in the presence of the metal, decreasing by 41.3 and 14.7 % for NaCl and Na_2SO_4, respectively.

3.5. Formation of low chlorinated PCDD/Fs during the electrochemical oxidation of Triclosan

This section deepens in the formation of low chlorinated PCDD/Fs: non-chlorinated (DD/Fs) and low chlorinated dibenzo-p-dioxins and dibenzofurans (CDD/Fs), from mono- to tri-chlorinated congeners. EPA 1613 method, which is a procedure specific for the analysis of highly chlorinated species (from TCDD/F to OCDD/F), has been expanded to analyse unchlorinated and low chlorinated species as reported by Buth et al. (2010) and Fernández-Castro et al. (2016). Figure 3.10 (when using NaCl as electrolytes) and Figure 3.11 (when using Na_2SO_4 as electrolyte) show the concentration of the homologues, from DD/F to CDD/F (mono- to tri-chlorinated dibenzo-p-dioxins and dibenzofurans), that have been identified in the untreated and electrochemically oxidized Triclosan samples (for 10, 100 and 150 mg L^{-1} of Triclosan) when Triclosan has completely disappeared. EPA 1613 recoveries obtained for these analysis are presented in the annexes (Table II.4, II.5 and II.6).

a)

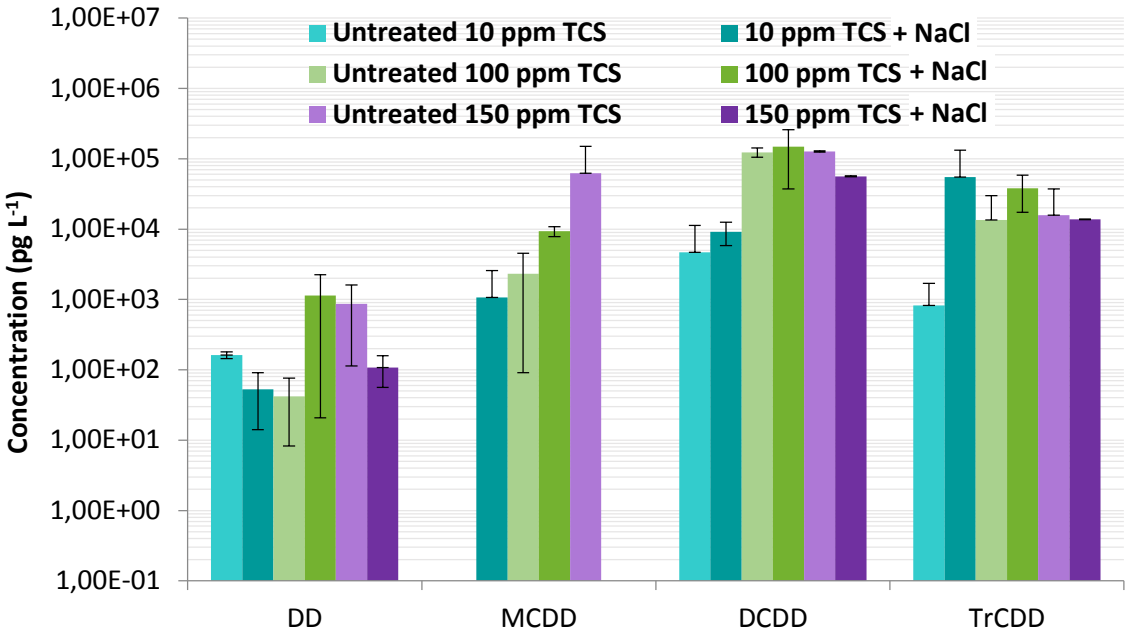

b)

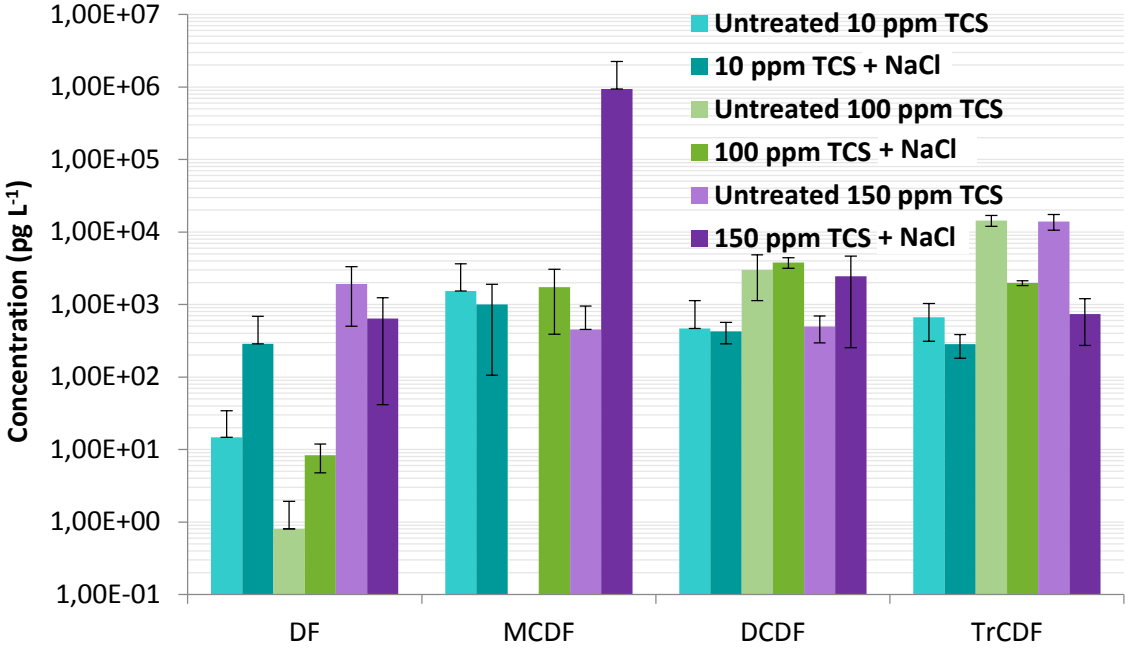

Figure 3.10. Concentration of low chlorinated dioxins (a) and furans (b) as function of the initial concentration of TCS (10.0, 100.0 and 150.0 mg L^{-1}), oxidation time of 1, 3 and 4 h, respectively. Supporting electrolyte: NaCl.

a)

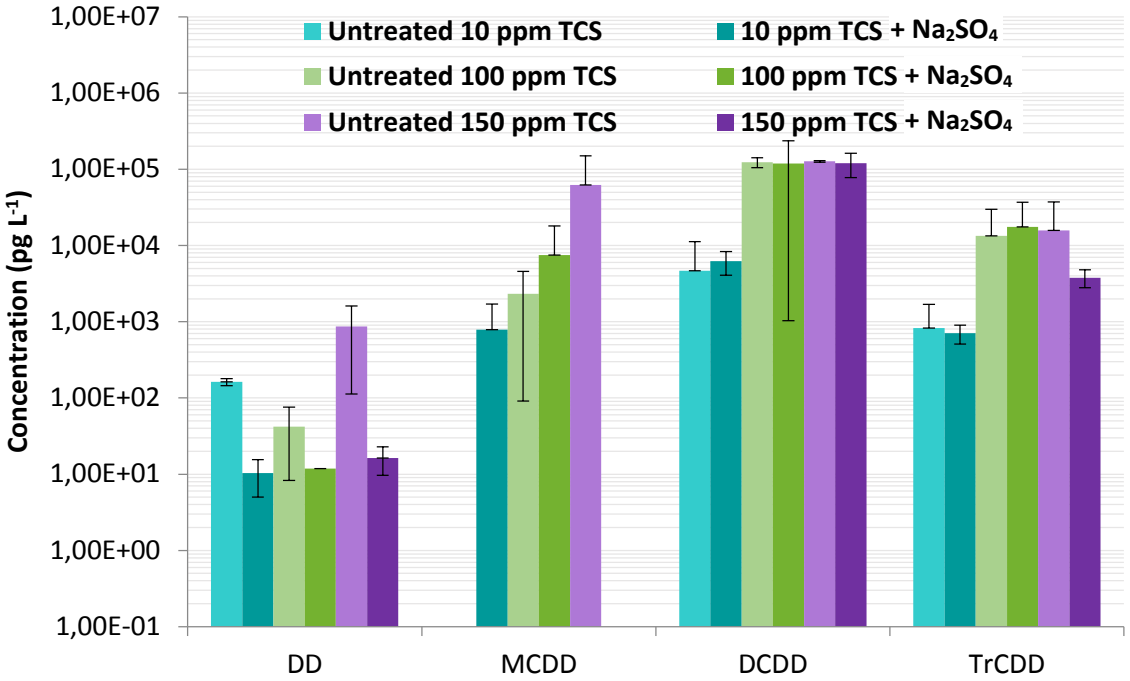

b)

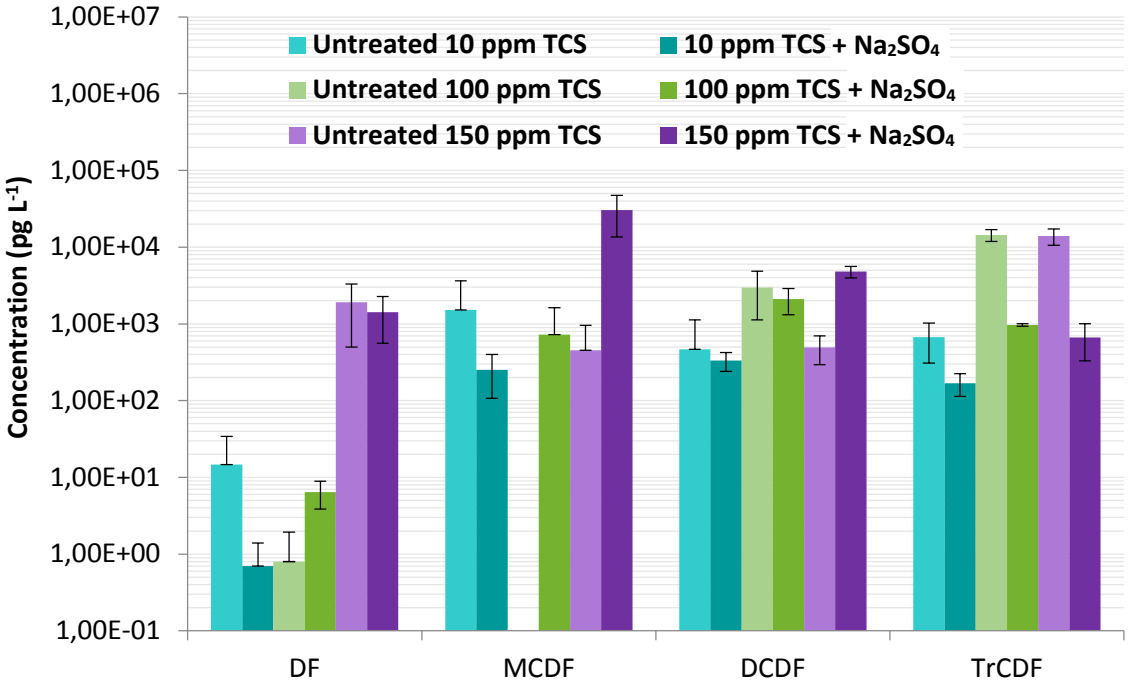

Figure 3.11. Concentration of low chlorinated dioxins (a) and furans (b) as function of the initial concentration of TCS (10, 100 and 150 mg L^{-1}), oxidation time of 1, 3 and 4 h, respectively. Supporting electrolyte: Na_2SO_4.

First, low chlorinated PCDD/Fs concentration was determined in the untreated samples containing 10, 100 and 150 mg L^{-1} of Triclosan, detecting for the three cases that DCDD/Fs and

TrCDD/Fs are the groups of homologues with the highest concentrations. Specially, DCDDs and TrCDDs reached values up to $1.26 \cdot 10^5$ and $1.58 \cdot 10^4$ pg L^{-1} in the untreated sample with 150 mg L^{-1} of Triclosan. The results obtained for the untreated samples for the three initial concentrations of Triclosan studied in this work are the same for both electrolytes, NaCl and Na_2SO_4, thus, these data are available in Figures 3.10 and 3.11. Then, the analysis has been carried out in samples withdrawn after the oxidation treatment, when no Triclosan remained in the solution (1, 3 and 4 hours for an initial concentration of Triclosan of 10, 100 and 150 mg L^{-1}, respectively). In most of the cases, low chlorinated PCDDs were the predominant group of homologues, counting for 76.8 % to 97.4 % of the total low chlorinated PCDD/Fs, except for the case of 150 mg L^{-1} of initial concentration of Triclosan and NaCl as electrolyte, where the predominant homologue group is PCDFs (93.1 %) (See Figures 3.10 and 3.11).

It can be observed in Figure 3.10 that, when NaCl was used as electrolyte, the total concentration of low chlorinated PCDD/Fs increased from $8.33 \cdot 10^3$, $1.56 \cdot 10^5$ and $2.23 \cdot 10^5$ pg L^{-1} for the untreated samples to $6.75 \cdot 10^4$, $2.04 \cdot 10^5$ and $1.01 \cdot 10^6$ pg L^{-1} when the initial concentration was 10, 100 and 150 mg L^{-1}, respectively. In the low chlorinated PCDDs profile (Figure 3.10(a)), for any of the three Triclosan concentrations studied, DCDD and TrCDD were found at the highest concentrations. In the case of DCDD homologue group, it achieved values up to $9.2 \cdot 10^3$ (13.6 % of the total low chlorinated PCDD/Fs), $1.5 \cdot 10^5$ (72.7 % of the total low chlorinated PCDD/Fs) and $5.6 \cdot 10^4$ pg L^{-1} (5.6 % of the total low chlorinated PCDD/Fs) for 10, 100 and 150 mg L^{-1} of Triclosan, respectively. On the other hand, TrCDD reached values up to $5.5 \cdot 10^4$ (81.7 % of the total low chlorinated PCDD/Fs), $3.8 \cdot 10^4$ (18.6 % of the total low chlorinated PCDD/Fs) and $1.4 \cdot 10^4$ pg L^{-1} (1.4 % of the total low chlorinated PCDD/Fs) for 10, 100 and 150 mg L^{-1} of Triclosan, respectively. In the low chlorinated PCDFs profile (Figure 3.10(b)), as a general rule, the concentration of PCDFs is lower when compared to the PCDDs concentration. For initial concentrations of 10 and 100 mg L^{-1} of Triclosan, the concentration of furans varied between $2.8 \cdot 10^2 - 1.0 \cdot 10^3$ pg L^{-1} and $8.3 - 3.8 \cdot 10^3$ pg L^{-1}, respectively. On the other hand, when the initial concentration of Triclosan was 150 mg L^{-1}, the concentration of MCDF was considerably higher in comparison to the rest of homologue groups ($9.4 \cdot 10^5$ pg L^{-1}; 92.2 % of the total low chlorinated PCDD/Fs).

In the presence of Na_2SO_4 (Figure 3.11), the total concentration of low chlorinated species remained constant or decreased slightly to $8.47 \cdot 10^3$, $1.48 \cdot 10^5$ and $1.61 \cdot 10^5$ pg L^{-1} for the three initial concentrations of Triclosan studied. DCDD was the predominant homologue group presented in the low chlorinated PCDDs profile (Figure 3.11(a)): $6.2 \cdot 10^3$ (73.3 % of the total low

chlorinated PCDD/Fs), $1.2 \cdot 10^5$ (80.4 % of the total low chlorinated PCDD/Fs) and $1.2 \cdot 10^5$ pg L^{-1} (74.4 % of the total low chlorinated PCDD/Fs) for the three concentration of Triclosan studied in this work. On the other hand, Figure 3.11(b) shows the low chlorinated PCDFs profile, once again, the concentration tends to be lower in comparison to the PCDDs profile. For initial concentrations of 10 and 100 mg L^{-1} of Triclosan, the concentration of furans varied between 0.7 – $3.3 \cdot 10^2$ pg L^{-1} and 6.4 – $2.1 \cdot 10^3$ pg L^{-1}, respectively. In the same way, working with NaCl as electrolyte and for the initial concentration of Triclosan of 150 mg L^{-1}, the concentration of MCDF was considerably higher ($3.1 \cdot 10^4$ pg L^{-1}; 18.9 % of the total low chlorinated PCDD/Fs).

3.5.1. Effect of copper on lower PCDD/Fs formation

In order to study the influence of copper on the formation of DD/Fs and CDD/Fs the analysis has been carried out for both electrolytes, NaCl and Na_2SO_4, and for an initial concentration of 100 mg L^{-1} of Triclosan. The results are shown in Figure 3.12. EPA 1613 recoveries obtained for these analysis are presented in the annexes (Table II.4, II.5 and II.6).

As it can be observed in Figure 3.12(a), when the sample contained NaCl, the presence of copper led to a decrease of the total concentration of low chlorinated PCDD/Fs from $2.04 \cdot 10^5$ to $7.01 \cdot 10^4$ pg L^{-1} (accounting for 65.6 %). In the presence of Na_2SO_4 as electrolyte (Figure 3.12(b), this value was reduced from $1.48 \cdot 10^5$ to $6.50 \cdot 10^4$ pg L^{-1} (accounting for 56.1 %). The presence of copper salt therefore leads to a relative decrease in the total concentration of low chlorinated species, probably attributed to absence of MCDD, DCDD, MCDF and TrCDF, which were not detected when NaCl was employed as electrolyte. TrCDD was the homologue group which presented the highest concentration: $6.0 \cdot 10^4$ pg L^{-1}, that is 86.0 % of the total low chlorinated PCDD/Fs. In the same way, no DCDD were identified using Na_2SO_4. In these cases, MCDD and TrCDD were observed at the highest concentrations: $3.9 \cdot 10^4$ and $2.1 \cdot 10^4$ pg L^{-1}, respectively. Based on these results, copper could act as catalyst in the electrochemical oxidation of Triclosan, having a significant influence on the decrease in the total concentration of low chlorinated PCDD/Fs, as observed also for highly chlorinated PCDD/Fs.

a)

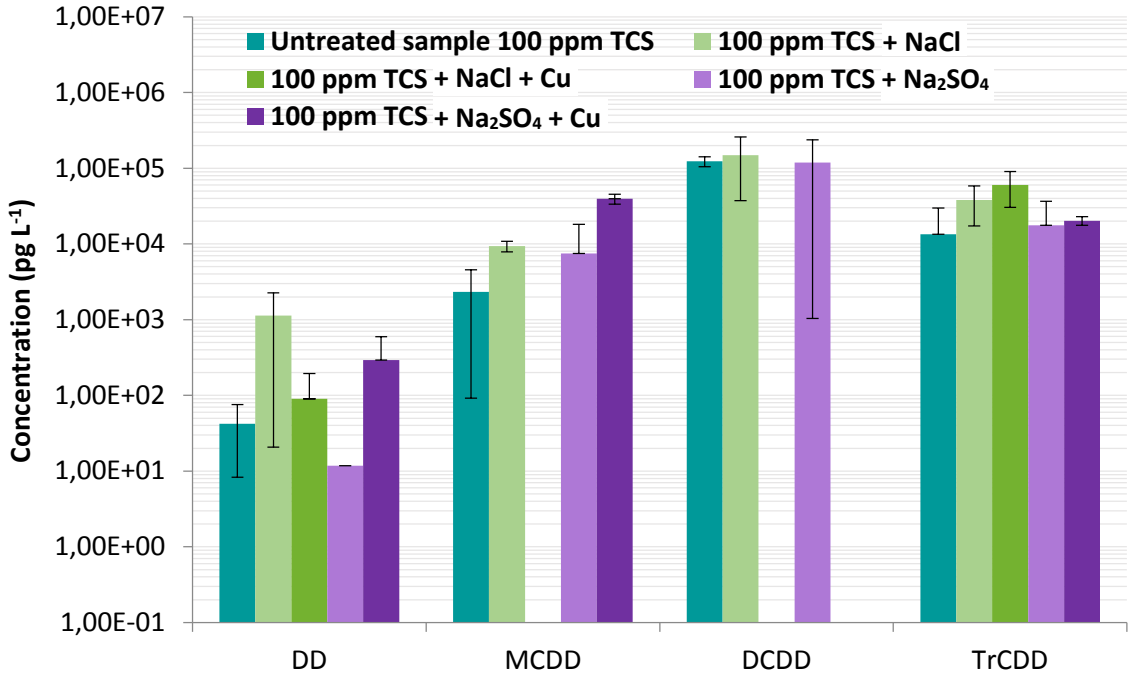

b)

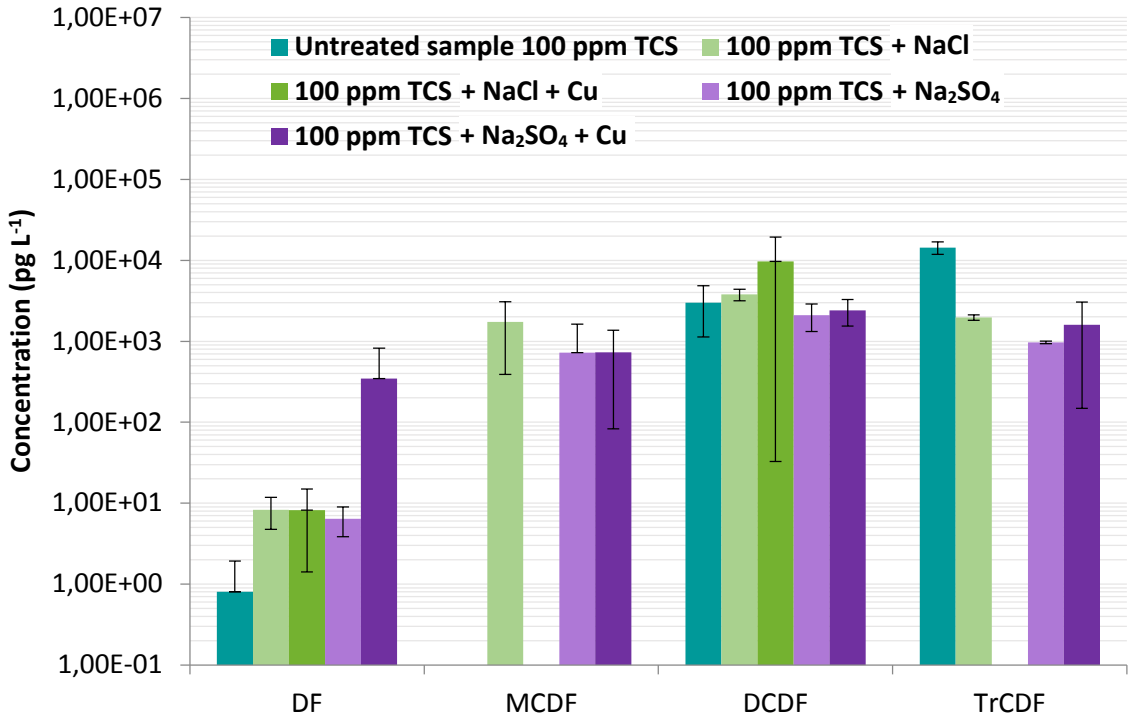

Figure 3.12. Influence of the electrolyte type and copper on the formation of lower chlorinated dioxins (a) and furans (b) during electrochemical oxidation. $[TCS]_0$= 100 mg L^{-1}.

According to the results shown above, the high concentrations obeserved in low chlorinated PCDD/Fs for the untreated samples as well as for the oxidized samples was inevitably the focus of attention. Besides, EPA 1613 recoveries were lower as the chlorinated degree

decreased (see recoveries in Tables II.4, II.5 and II.6 in Annexes), making more uncertain the reliability of this method for those species with less chlorines in the molecule, especially for unchlorinated and mono-chlorinated dibenzo-p-dioxins and dibenzofurans. This, together with recent works that have focused on the formation of 2,7/2,8-dichlorodibenzo-p-dioxin as a consequence of Triclosan oxidation, a congener that belongs to the DCDD (dichlorodibenzo-p-dioxin) homologue group, has led to an exhaustive analysis of this congener with the oxidation time. Ding et al. (2015) identified 2,8-dichlorodibenzo-p-dioxin as one of the major by-products in the degradation of Triclosan by Fe and Mn oxides at ambient temperature; the dioxin was detected using GC–MS technique. Also, the photochemical conversion of Triclosan into dichlorodibenzo-p-dioxin has been studied employing photo-solid-phase-microextraction as well as employing different surfactants and ultraviolet irradiation (Lores et al., 2005; Qiao et al., 2014). Recently, Wu et al. (2019) reported the presence of several chlorinated dibenzo-p-dioxins (2,8-dichlorodibenzo-p-dioxin, 2,3,7-trichlorodibenzo-p-dioxin, 1,2,8-trichlorodibenzo-p-dioxin, 2,3,7,8-tetrachlorodibenzo-p-dioxin and 1,2,3,8-tetrachlorodibenzo-p-dioxin) in the degradation of Triclosan under ultraviolet light conditions; these authors followed the presence of these by-products by GC-MS and HRGC/HRMS techniques (Wu et al., 2019). Buth et al. (2009) studied the photoformation of tri- and tetra-chlorinated dibenzo-p-dioxins in the chlorination reaction of Triclosan through the formation of chlorinated Triclosan derivatives as intermediate reaction species. Although many authors have studied the formation of 2,7/2,8-dichlorodibenzo-p-dioxin in the oxidation of Triclosan by diverse AOPs, no previous studies have investigated the formation of this congener during the electrochemical oxidation treatment. In this work, in order to carry out this research, untreated and electro-oxidized samples at different times, starting with an initial concentration of Triclosan of 100 mg L^{-1}, have been analysed by GC-MS. The chromatograms are depicted in Figure 3.13. The aim of this part of the thesis was to check if the congener 2,7/2,8-dichlorodibenzo-p-dioxin was present in the commercial product (untreated sample) or if it was generated as a consequence of the electrochemical oxidation.

a)

b)

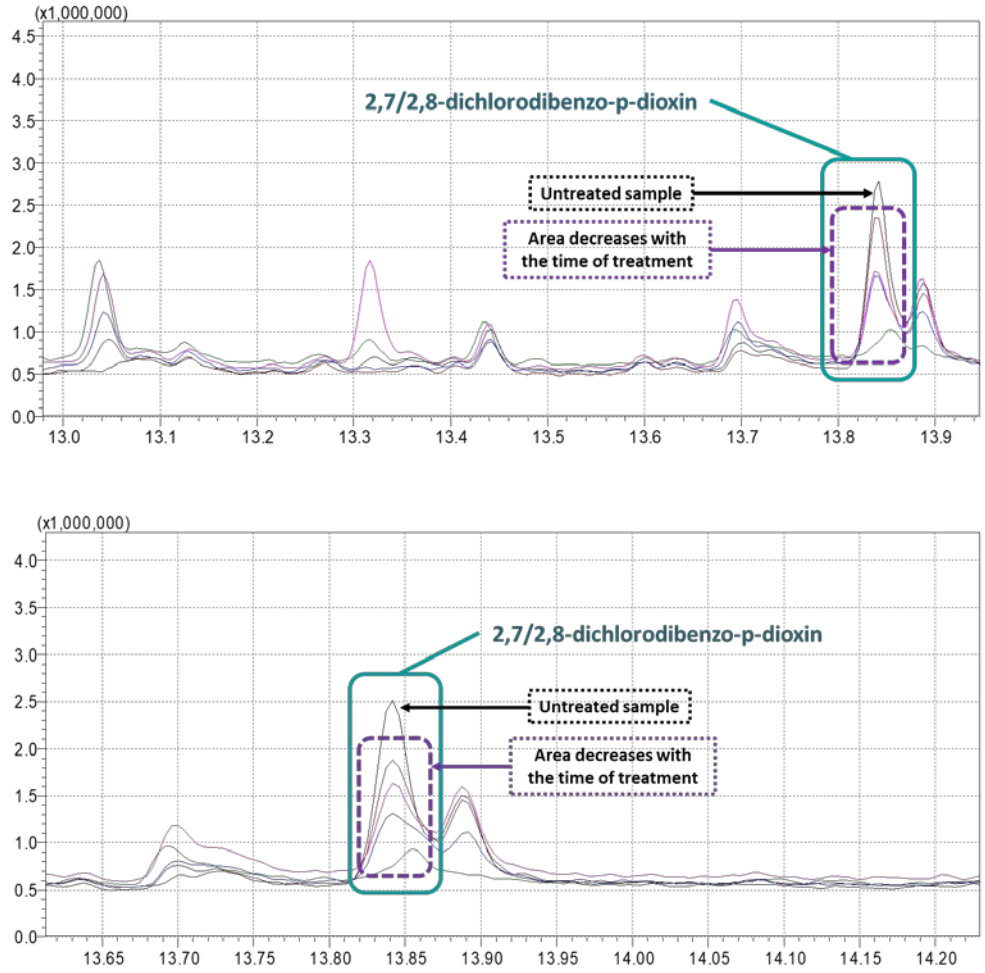

Figure 3.13. 2,7/2,8-Dichlorodibenzo-p-dioxin GC-MS chromatogram in untreated and electro-oxidized 100.0 mg L^{-1} TCS samples working with (a) NaCl and (b) Na_2SO_4 as electrolytes: (-) untreated TCS sample; (-) after 15 min of treatment; (-) after 45 min of treatment; (-) after 75 min of treatment; (-) after 180 min of treatment. $[TCS]_0$= 100.0 mg L^{-1}.

2,7/2,8-dichlorodibenzo-p-dioxin was detected and quantified by GC-MS at a retention time of 13.8 min. As it can be observed in Figure 3.13(a), the highest concentration of 2,7/2,8-dichlorodibenzo-p-dioxin was determined in the untreated sample, where the dioxin reported values up to 6.7×10^{-1} mg L^{-1}. The concentration of this DCDD decreased with the oxidation time. A similar trend in the decrease of DCDD concentration with oxidation time was observed, independently of the electrolyte used in the run (NaCl or Na_2SO_4) (Figure 3.13(b)). In almost all the reported works so far, the analysis of the DCDD has been performed using gas chromatographic techniques were the sample is injected at temperatures higher than 250 °C. In this line of thought, Latch et al. (2003) and Rappe and Nilsson (1972) reported the possible formation of 2,7/2,8-dichlorodibenzo-p-dioxin in the injector of the GC-MS attributed to the high

temperature in this part of the equipment. So, next, the aim was determine whether the formation of 2,7/2,8-dichlorodibenzo-p-dioxin is likely due to the direct cyclization of Triclosan during the analysis via GC–MS in the heated inlet, with an injection temperature set at 285 °C, or if this DCDD compound was contained in the untreated sample.

Here, taking one-step forward, and as a way to support the determination of 2,7/2,8-dichlorodibenzo-p-dioxin, the sample analysis was carried out by High-Performance Liquid Chromatography (HPLC), technique that runs at low temperatures that hinder Triclosan cyclization. With this purpose, an undoped commercial sample containing 100 mg L^{-1} of Triclosan (Figure 3.14(a)), and the same sample doped with 6 mg L^{-1} of 2,7/2,8-dichlorodibenzo-p-dioxin (Figure 3.14(b)), were analysed. As it can be observed in the chromatograms (Figure 3.14), no 2,7/2,8-dichlorodibenzo-p-dioxin was observed; the detection limit of the technique is 2.5×10^{-1} mg L^{-1} (See Figure I included in Annexes III), value below the concentration previously quantified by GC–MS.

a)

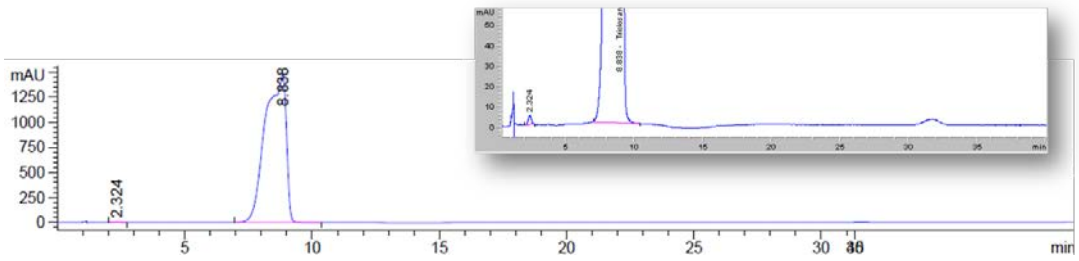

b)

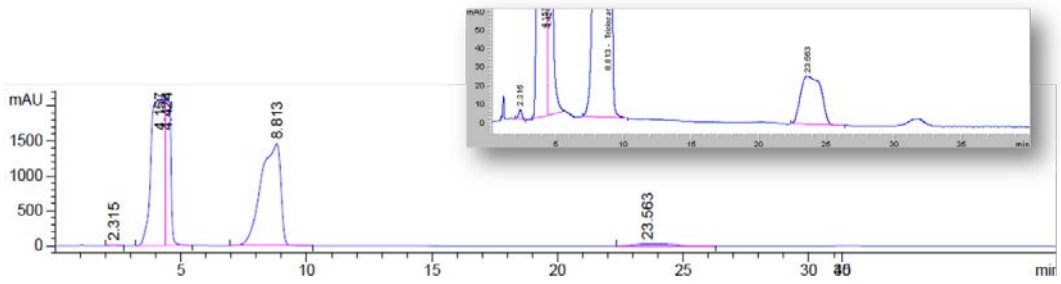

Figure 3.14. High-Performance Liquid Chromatography (HPLC) chromatograms of 100 mg L^{-1} of (a) commercial TCS undoped and (b) doped with 6 mg L^{-1} of 2,7/2,8-dichlorodibenzo-p-dioxin.

Within this analytical assessment, it can be proposed as a possibility that the formation of 2,7/2,8-dichlorodibenzo-p-dioxin may result from the direct cyclization of Triclosan during the analysis via GC–MS in the heated inlet (injection temperature set at 285 °C). The cyclization reaction produced by the high temperature could start with the homolytic carbon–chlorine cleavage, giving a chlorine atom and a phenyl radical, which undergo the formation of the halogenated dibenzo-p-dioxin (Figure 3.15). Thus, the observed decrease of the 2,7/2,8-dichlorodibenzo-p-dioxin concentration over time could be associated to the lower concentration of Triclosan in the analysed samples resulting from the oxidation yield (Figure 3.14(a,b)).

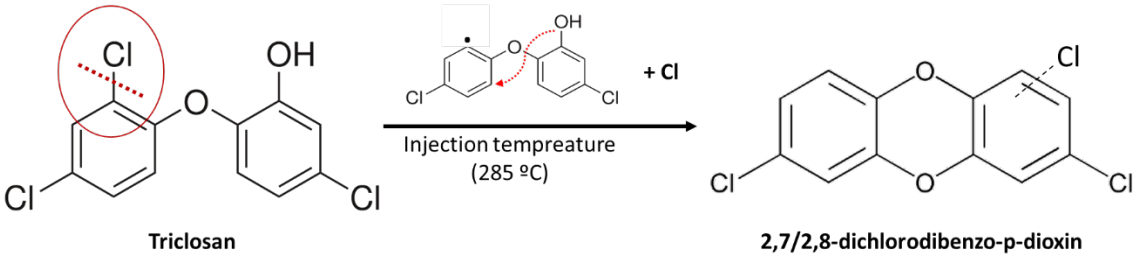

Figure 3.15. Triclosan cyclization to 2,7/2,8-dichlorodibenzo-p-dioxin in the GC-MS injector.

According to the results reported in this section, some conclusions can be taken. The concentration of 2,7/2,8-dichlorodibenzo-p-dioxin for the 100 mg L^{-1} untreated sample of Triclosan analysed by GC-MS (6.7×10^{8} pg L^{-1}) was considerably higher than the concentration obtained for all DCDD homologue groups following the EPA 1613 method (1.2×10^{5} pg L^{-1}). Furthermore, negative results were obtained in the sample analysed by HPLC, where the detection limit was 2.5×10^{-1} mg L^{-1}. Taking this into consideration, the use of GC-MS technique at the conditions used in this work is not a reliable method for the analysis of 2,7/2,8-dichlorodibenzo-p-dioxin in samples where Triclosan is present, and it may lead to inconsistent results. Besides, the EPA 1613 method, extended to analyse unchlorinated and low chlorinated species, resulted in low recoveries percentages, especially when the number of chlorines decreased in the molecule. For this reason, the reliability of this method applied to these species should be questioned. Hence, the analysis of these species under the conditions studied in this work becomes a complex task that requires more analytical research.

3.6. Reaction pathway proposal for the electrochemical oxidation of Triclosan

According to the information collected in relation to the products formed through the oxidation of Triclosan in the reviewed literature (mainly catechol, 4-chlorocatechol, chlorohydroquinone and 2,4-dichlorophenol) (Martín de Vidales et al., 2013; Maharana et al., 2015; Martín de Vidales, 2015;), and in concordance with the experimental results previously reported (2-ethyl-hexanol, 2,4-dichlorophenol, 2-chloro-4-metoxyphenol, 2-chlorohydroquinone, 1-chloro-2,5-dimethoxybenzene, 4-chlorocatechol and diphenyl ether benzene), the reaction mechanisms for the intermediate products and PCDD/Fs from Triclosan degradation are proposed. Besides, this proposal is also corroborate with a theoretical simulation modelling previously reported in the literature for gas and aqueous phase (Gao et al., 2014; Zhang et al., 2015).

·OH radical is considered the main reactive oxidant that is generated during AOPs application, playing a pivotal role in the oxidation of Triclosan (Comninellis et al., 2008; Deng and Zhao, 2015). In this way, Gao et al. (2014) and Zhang et al. (2015), through molecular simulation, have described three possible reaction routes describing the oxidation of Triclosan initiated by the action of a ·OH radical:

(i) OH-addition towards carbon atoms of the benzene or the phenol ring;
(ii) H-abstraction from the phenol ring or a hydrogen atom of either the benzene or the phenol ring;
(iii) Single electron-transfer from Triclosan by ·OH.

Gao et al. (2014), using the software Gaussian, reported that H-abstraction was the route that presented the lowest free energy barrier in comparison to the other possible routes. The reaction mechanism started with a hydrogen abstraction from the position number 2 of the phenolic ring of Triclosan, obtained by the hybrid density functional B3LYP method with the 6-31+G(d,p) basis set, resulting in a free energy barrier of 6.35 kcal mol^{-1} (Figure 3.16). For this reason, the reactions mechanisms that are proposed in this work hereinafter start as is explained in the next Figure.

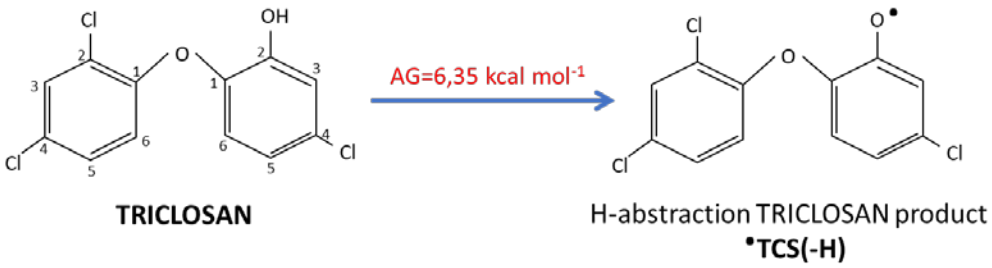

Figure 3.16. H-abstraction from the phenol ring of the Triclosan molecule.

3.6.1. Pathway proposal for the intermediate products

The reaction mechanisms proposed for the intermediate compounds detected in this thesis (2-ethyl-hexanol, 2,4-dichlorophenol, 2-chloro-4-metoxyphenol, 2-chlorohydroquinone, 1-chloro-2,5-dimethoxybenzene, 4-chlorocatechol and diphenyl ether benzene), were corroborated by the theoretical and experimental results reported in the literature.

- With regard to theoretical results, Gao et al. (2014) demonstrated the formation of different intermediate products from Triclosan degradation in aqueous phase through simulation modelling. These results shown that, at higher ·OH concentrations, Triclosan is inclined to produce three stable OH-adducts: R-H$(OH)_1$, R-H$(OH)_2$ and R-H$(OH)_3$ (Figure 3.17). Among the three possible routes, the most energy stable one (R-H $(OH)_1$) tends to form 2,4-dichlorinated phenoxyde radical (DCP(-H)) and 4-chloro-o-semiquinone (o-SQ), with a free energy barrier value up to 9.64 kcal mol^{-1} (Gao et al., 2014). This adduct could lead to the formation of 2,4-dichlorophenol. This theoretical studies could confirm the formation of 2,4-dichlorphenol observed in the experimental results shown in the previous section. There are no other reports so far that explain theoretically the formation of the rest of intermediate products determined.

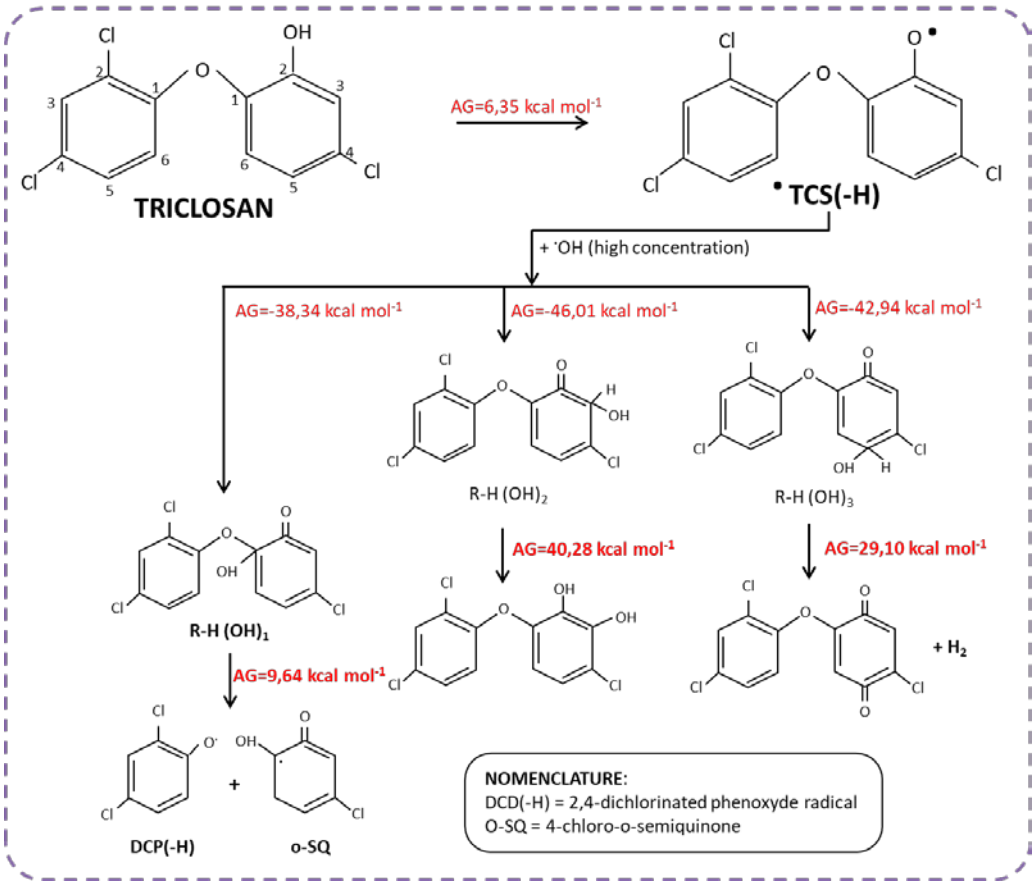

Figure 3.17. Theoretical pathways of intermediate products formation during triclosan H-abstraction route in aqueous phase. Energetic values (kcal mol^{-1}) were calculated by Gao et al. (2014) using the hybrid density functional B3LYP method with the 6-31+G(d,p) basis set and B3LYP/6-311+G(3df,2p).

- Supported with the experimental results reported in the literature, Figure 3.18 displays the reaction mechanisms proposed for the intermediate products detected in this thesis. The pathway starts with a hydrogen atom abstraction from the phenolic ring of the molecule of Triclosan, in accordance with the theoretical results explained above. Then, it can be followed by the attack of ·OH through the addition to the phenolic fraction that leads to the breakage of the molecule and to the formation of 2,4-dichlorophenol and 2-chlorohydroquinone. But it also can be followed by the direct breakage of the molecule by the attack of the OH radical leading to the formation of 2,4-dichlorophenol and 4-chlorocatechol. 2-ethyl-hexanol could be produced by a bond cleavage and successive dechlorination of 2-chlorohydroquinone and 4-chlorocatechol. On the other hand, Triclosan could followed a dechlorination reaction which results in the ether formation.

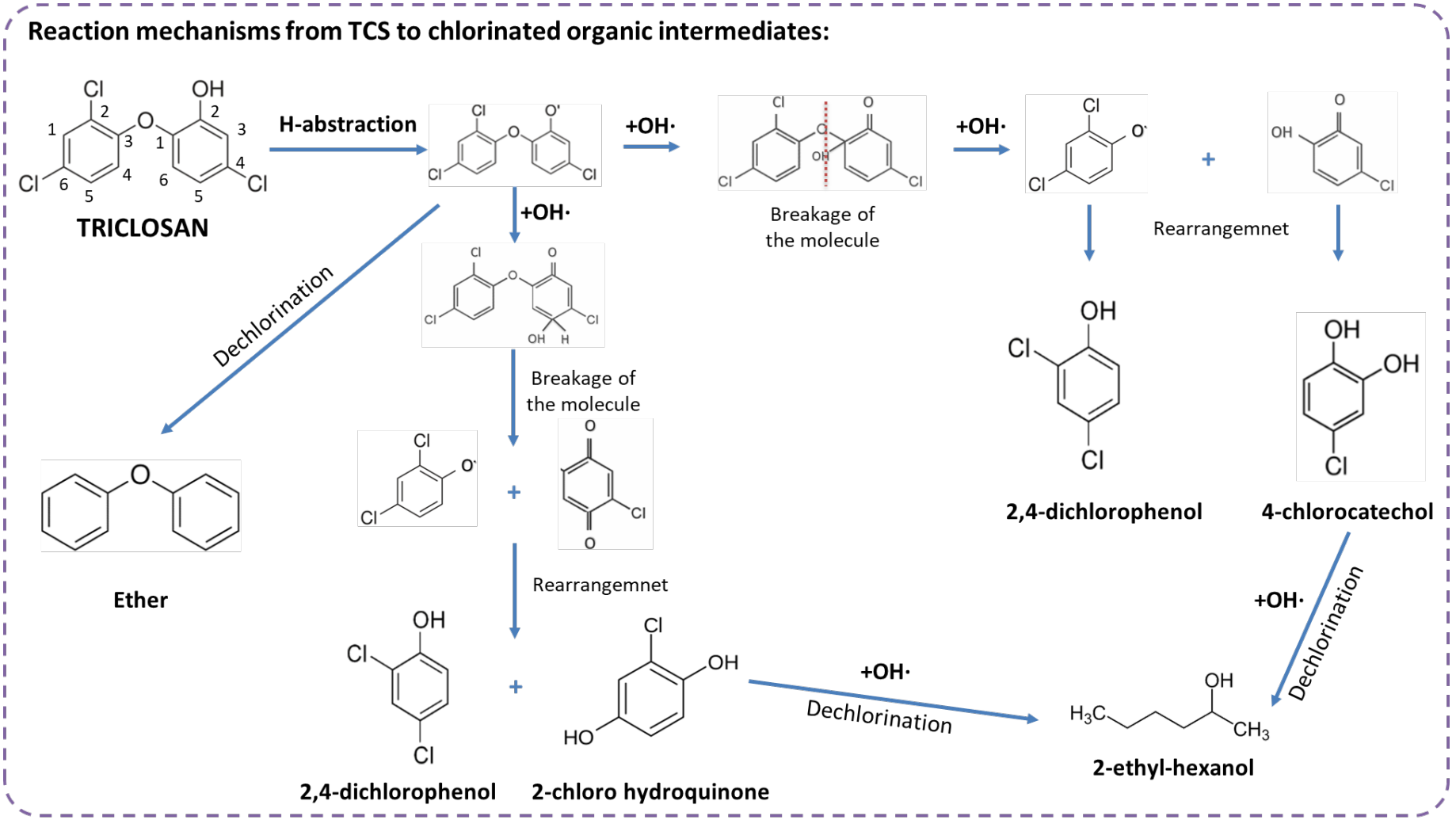

Figure 3.18. Proposed reaction pathway for the formation of organic non-chlorinated and chlorinated products observed in the electrochemical oxidation of aqueous samples of TCS.

3.6.2. Pathway proposal for the PCDD/Fs

With regard to PCDD/Fs reaction pathways, based on theoretical simulating models, Figure 3.19 and Figure 3.20 show the transformation pathways starting with a H-abstraction of Triclosan in aqueous and gas phase, respectively, as reported in the first part of this section (3.6). In aqueous phase (Figure 3.19), the free energy barriers involved in the reaction mechanisms were calculated by Gao et al. (2014) using the Gaussian 03 program and through the use of the hybrid density functional B3LYP method with the 6-31+G(d,p) basis set and B3LYP/6-311+G(3df,2p). On the other hand, and simulating gas phase (Figure 3.20), Zhang et al. (2015) carried out the calculations using also Gaussian 03 program, but through the use of MPWB1K method with the 6-31+G(d,p) basis set.

- As shown in Figure 3.19, two possible cyclization routes are proposed in aqueous phase starting with ·TCS(-H): $R_{cyc,a}H_1$ (first cyclization route in aqueous phase) and $R_{cyc,a}H_2$ (second cyclization route in aqueous phase) routes, with a free energy barrier of 25.33 and 29.45 kcal mol^{-1}, respectively. On the one hand, the first cyclization ($R_{cyc,a}H_1$) can lead to the formation of TrCDD (trichlorodibenzo-p-dioxin). On the other hand, the second cyclization ($R_{cyc,a}H_2$) is likely to form DCDD (dichlorodibenzo-p-dioxin), causing a chlorine loss. This theoretical proposal could confirm the experimental results shown in the previous section 3.5, and TrCDD and DCDD could potentially be formed from the OH-initiated transformation of Triclosan via intermolecular cyclization in aquatic environments.

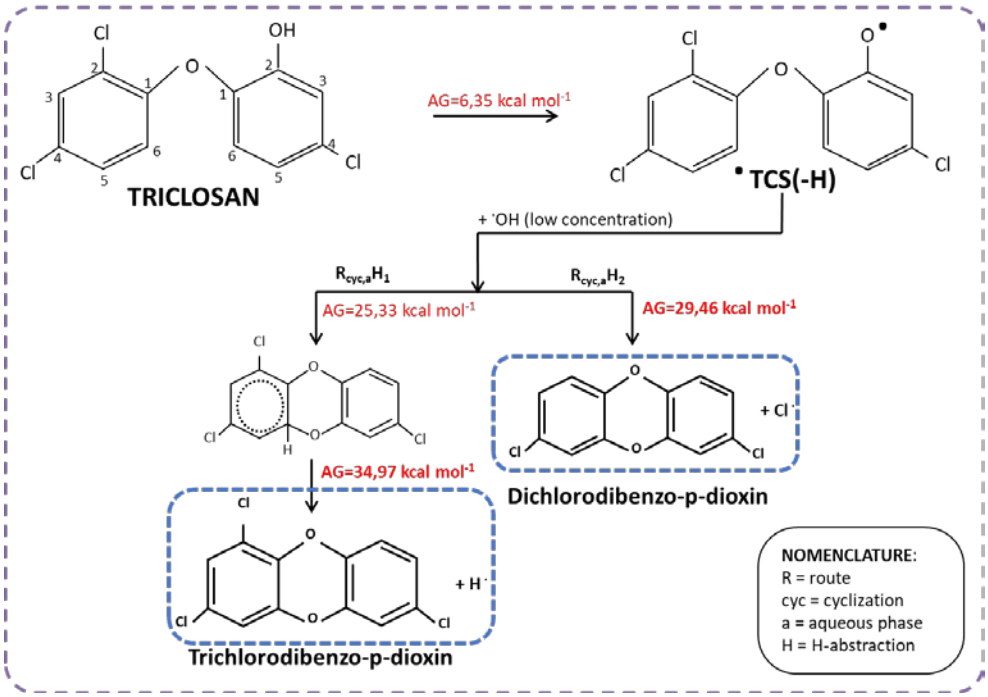

Figure 3.19. Theoretical pathways of PCDD/Fs formation during triclosan H-abstraction route in aqueous phase. Energetic values (kcal mol^{-1}) were calculated by Gao et al. (2014) using the hybrid density functional B3LYP method with the 6-31+G(d,p) basis set and B3LYP/6-311+G(3df,2p).

- The transformation pathway in gas phase, which could explain the formation of PCDFs, is shown in Figure 3.20. Four possible cyclization routes have been proposed (Zhang et al., 2015). In $R_{cyc,g}H_1$ (first cyclization route in gas phase) route, the ·OH radical can attack a carbon atom contiguous to the oxygen atom bridge, overcoming a free energy barrier of 23.93 kcal mol^{-1}. The hydrogen atom can be abstracted by O_2 to form TrCDD (tri-chlorodibenzo-p-dioxin) with a free energy barrier value up to 35.68 kcal mol^{-1}. The next cyclization route, $R_{cyc,g}H_2$ (second cyclization route in gas phase), involves the attack to the carbon atom with a Cl substituent, forming DCDD (di-chlorodibenzo-p-dioxin), achieving energy values of 27.33 kcal mol^{-1}. DCDD and Cl atom are generated more easily than TrCDD in terms of energy. Finally, $R_{cyc,g}H_3$ (third cyclization route in gas phase) and $R_{cyc,g}H_4$ (fourth cyclization route in gas phase) routes are likely to form tri-chlorinated species, starting with an hydrogen abstraction, but, in this case, from the position 6 of the benzene ring (8.6 kcal mol^{-1}). On the one hand, in the $R_{cyc,g}H_3$ route, a carbon atom with an OH substituent is attacked, leading to the formation of TrCDF (tri-chlorodibenzofuran) and ·OH, with 16.14 kcal mol^{-1} of free energy barrier. On the other hand, $R_{cyc,g}H_4$ route leads to the cyclization of the molecule to form TrCDD (tri-chlorodibenzo-p-furan), with a free energy barrier of 30.63 kcal mol^{-1}.

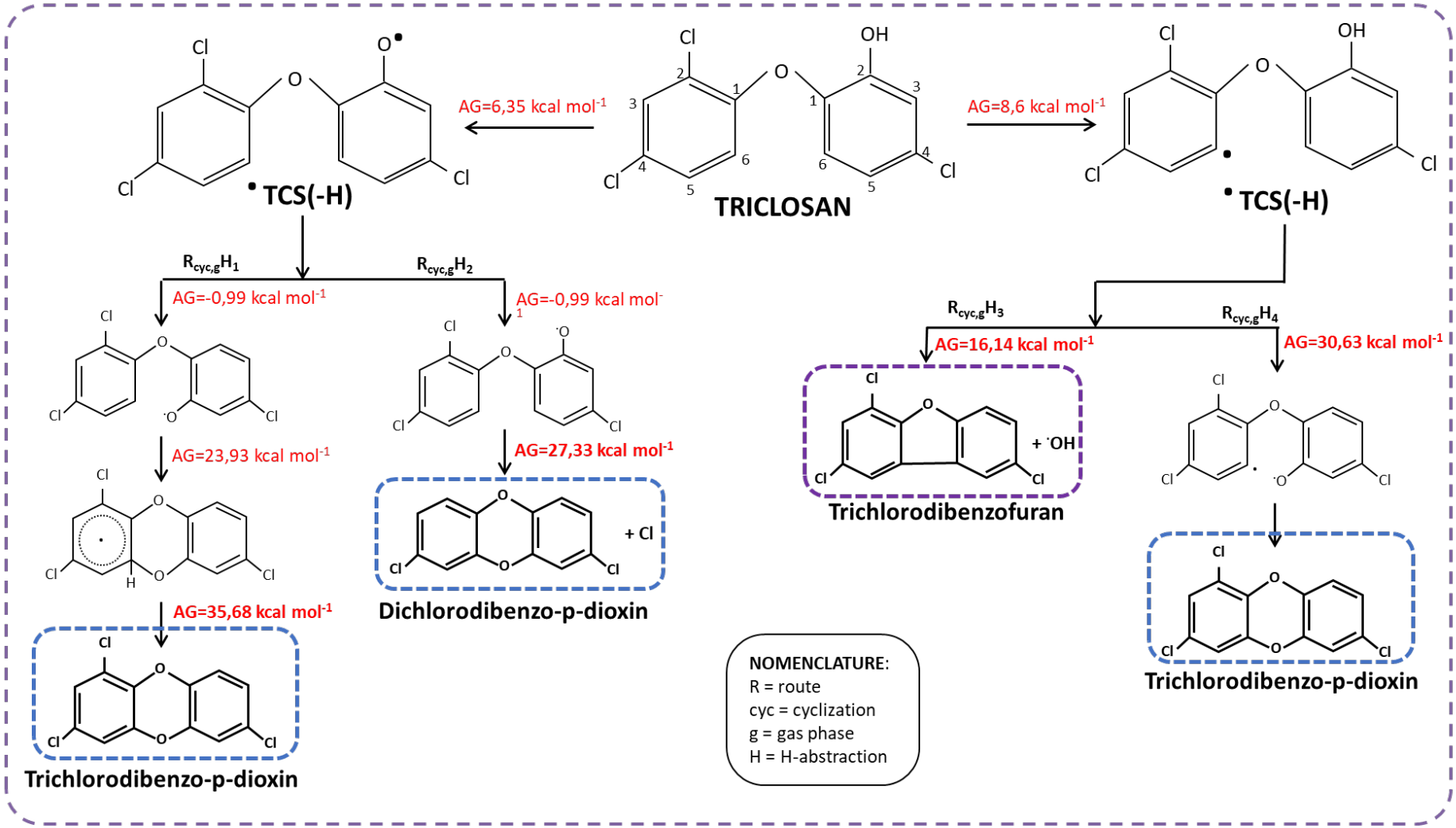

Figure 3.20. Theoretical pathways of PCDD/Fs formation during triclosan H-abstraction route in gas phase. Energetic values (kcal mol^{-1}) were calculated by Zhang et al. (2015) using the density functional theory MPWB1K method with the 6-31+G(d,p) basis set.

The reaction mechanisms of highly chlorinated PCCD/Fs groups that were detected and reported in the previous section are depicted in Figure 3.21. The formation mechanism of these homologues could be explained by the gradual chlorination from low chlorinated dibenzo-p-dioxin and dibenzofurans to higher chlorinated species (Vallejo, 2014; Fernández-Castro et al., 2016). This chlorination process has been also described in gas and aqueous phase experiments when Cl_2 stream was in contact with PCDD/Fs (Wikström and Marklund, 2000; Wang et al., 2014).

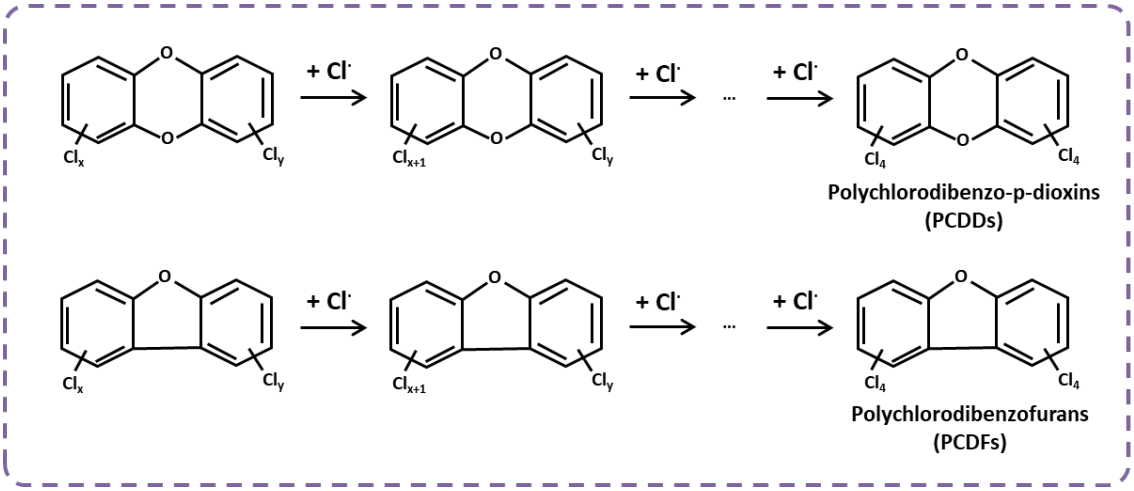

Figure 3.21. Reaction mechanisms from lower chlorinated DD/Fs to PCDD/Fs (Fernández-Castro et al., 2016; Vallejo, 2014).

In this section, the reaction mechanisms of the intermediate products observed in the results sections, including low and high PCDD/Fs, are proposed based on experimental and theoretical results reported in the literature. As explained before, all pathways start with a hydrogen abstraction from the phenol ring of the Triclosan molecule that lead to the formation of a H-abstraction Triclosan product (·TCS(-H)), followed by different mechanisms, such as dechlorination, molecule cleavage or cyclization reactions. On the one hand, smaller molecules, like 2,4-dichlorophenol, 4-chlorocatechol or 2-chlorohydroquinone, also reported in the literature, are formed. On the other hand, the formation of low chlorinated PCDD/Fs due to the cyclization of Triclosan has been corroborated by theoretical simulating models. Finally, once low chlorinated species are formed, chlorination reactions lead to the generation of highly chlorinated PCDD/Fs.

3.8. References

Abdel-Aziz, M.H., Bassyouni, M., Soliman, M.F., Gutub, S.A., Magram, S.F., 2017. Removal of heavy metals from wastewater using thermally treated sewage sludge adsorbent without chemical activation. J. Mater. Environ. Sci. 8, 1737–1747.

Adeli, M., Yamini, Y., Faraji, M., 2017. Removal of copper, nickel and zinc by sodium dodecyl sulphate coated magnetite nanoparticles from water and wastewater samples. Arab. J. Chem. 10, S514–S521. https://doi.org/10.1016/j.arabjc.2012.10.012

Arulmozhi, M., Begun, M.S., Anantharaman, N., Thenmozhi, M., 2014. Continuous foam fractionation of Copper (II) ions from aqueous media and industrial effluents. J. Chem. Pharm. Sci. 2014-Decem, 182–185.

Basha, C.A., Somasundaram, M., Kannadasan, T., Lee, C.W., 2011. Heavy metals removal from copper smelting effluent using electrochemical filter press cells. Chem. Eng. J. 171, 563–571. https://doi.org/10.1016/j.cej.2011.04.031

Beyazit, N., 2014. Copper(II), chromium(VI) and nickel(II) removal from metal plating effluent by electrocoagulation. Int. J. Electrochem. Sci. 9, 4315–4330.

Buth, J.M., Granbois, M., Vikesland, P.J., Mcneill, K., Arnold, W.A., 2009. Pharmaceuticals and Personal Care Products in the Environment. Aquatic photochemistry of chlorinated triclosan derivatives: Potential source of polychlorodibenzo-p-dioxins. Environ. Toxicol. Chem. 28, 2555–2563.

Buth, J.M., McNeill, K., Steen, P.O., Arnold, W.A., Sueper, C., Blumentritt, D., Vikesland, P.J., 2010. Dioxin photoproducts of triclosan and its chlorinated derivatives in sediment cores. Environ. Sci. Technol. 44, 4545–4551. https://doi.org/10.1021/es1001105

Cañizares, P., García-Gómez, J., Fernández de Marcos, I., Rodrigo, M.A., Lobato, J., 2006. Measurement of mass-transfer coefficients by an electrochemical technique. J. Chem. Educ. 83, 1204–1207. https://doi.org/10.1021/ed083p1204

Chan, A., Salsali, H., McBean, E., 2014. Heavy metal removal (copper and zinc) in secondary effluent from wastewater treatment plants by microalgae. ACS Sustain. Chem. Eng. 2, 130–137. https://doi.org/10.1021/sc400289z

Comninellis, C., Kapalka, A., Malato, S., Parsons, S.A., Poulios, I., Mantzavinos, D., 2008. Advanced oxidation processes for water treatment: advances and trends for R&D. J. Chem. Technol. Biotechnol. 83, 769–776. https://doi.org/10.1002/jctb.1873

Comninellis, C., Nerini, A., 1995. Anodic oxidation of phenol in the presence of NaCl for wastewater treatment. J. Appl. Electrochem. 25, 23–28. https://doi.org/10.1007/BF00251260

Deng, Y., Zhao, R., 2015. Advanced Oxidation Processes (AOPs) in wastewater Treatment. Curr. Pollut. Reports 1, 167–176. https://doi.org/10.1007/s40726-015-0015-z

Ding, J., Su, M., Wu, C., Lin, K., 2015. Transformation of triclosan to 2,8-dichlorodibenzo-p-dioxin by iron and manganese oxides under near dry conditions. Chemosphere 133, 41–46. https://doi.org/10.1016/j.chemosphere.2015.03.055

Dong, Y., Liu, J., Sui, M., Qu, Y., Ambuchi, J.J., Wang, H., Feng, Y., 2017. A combined microbial desalination cell and electrodialysis system for copper-containing wastewater treatment and high-salinity-water desalination. J. Hazard. Mater. 321, 307–315. https://doi.org/10.1016/j.jhazmat.2016.08.034

Escudero, C.J., 2017. Avances en la aplicación de las tecnologías ambientales fotocatálisis y oxidación electroquímica para la remediación de agua contaminada por compuestos orgánicos. Doctoral Thesis, University of Cantabria.

Fernández-Castro, P., San Román, M.F., Ortiz, I., 2016. Theoretical and experimental formation of low chlorinated dibenzo-p-dioxins and dibenzofurans in the Fenton oxidation of chlorophenol solutions. Chemosphere 161, 136–144. https://doi.org/10.1016/j.chemosphere.2016.07.011

Gao, Y., Ji, Y., Li, G., An, T., 2014. Mechanism, kinetics and toxicity assessment of OH-initiated transformation of triclosan in aquatic environments. Water Res. 49, 360–370. https://doi.org/10.1016/j.watres.2013.10.027

Govindaraj, M., Rathinam, R., Sukumar, C., Uthayasankar, M., Pattabhi, S., 2013. Electrochemical oxidation of bisphenol-A from aqueous solution using graphite electrodes. Environ. Technol. 34, 503–511. https://doi.org/10.1080/09593330.2012.701333

Hansen, H.K., Lazo, A., Gutierrez, C., Durán, M., Lazo, P., Rojo, A., 2017. Continuous multistage electrodialytic treatment of copper smelter wastewater. Miner. Eng. 100, 187–190. https://doi.org/10.1016/j.mineng.2016.11.006

Kamar, F.H., Nechifor, A.C., Nechifor, G., Mohammed, A.A., Faisal, A.A.H., 2016. Biosorption of lead, copper and cadmium ions from industrial wastewater using fluidized bed of dry cabbage leaves. Rev. Chim. 67, 1039–1046.

Kapałka, A., Joss, L., Anglada, Á., Comninellis, C., Udert, K.M., 2010. Direct and mediated electrochemical oxidation of ammonia on boron-doped diamond electrode. Electrochem. commun. 12, 1714–1717. https://doi.org/10.1016/j.elecom.2010.10.004

Kazeminezhad, I., Mosivand, S., 2017. Elimination of copper and nickel from wastewater by electrooxidation method. J. Magn. Magn. Mater. 422, 84–92. https://doi.org/10.1016/j.jmmm.2016.08.049

Latch, D.E., Packer, J.L., Arnold, W.A., McNeill, K., 2003. Photochemical conversion of triclosan to 2,8-dichlorodibenzo-p-dioxin in aqueous solution. J. Photochem. Photobiol. A Chem. 158, 63–66. https://doi.org/10.1016/S1010-6030(03)00103-5

Lee, C.G., Lee, S., Park, J.A., Park, C., Lee, S.J., Kim, S.B., An, B., Yun, S.T., Lee, S.H., Choi, J.W., 2017. Removal of copper, nickel and chromium mixtures from metal plating wastewater by adsorption with modified carbon foam. Chemosphere 166, 203–211. https://doi.org/10.1016/j.chemosphere.2016.09.093

Lin, Y., Jin, X., Owens, G., Chen, Z., 2019. Simultaneous removal of mixed contaminants triclosan and copper by green synthesized bimetallic iron/nickel nanoparticles. Sci. Total Environ. 695, 133878. https://doi.org/10.1016/j.scitotenv.2019.133878

Lores, M., Llompart, M., Sanchez-Prado, L., Garcia-Jares, C., Cela, R., 2005. Confirmation of the formation of dichlorodibenzo-p-dioxin in the photodegradation of triclosan by photo-SPME. Anal. Bioanal. Chem. 381, 1294–1298. https://doi.org/10.1007/s00216-004-3047-6

Maharana, D., Niu, J., Rao, N.N., Xu, Z., Shi, J., 2015. Electrochemical Degradation of Triclosan at a Ti/SnO_2-Sb/Ce-PbO_2 Anode. Clean - Soil, Air, Water 43, 958–966. https://doi.org/10.1002/clen.201400180

Marcoux, J.F., Doye, S., Buchwald, S.L., 1997. A general copper-catalyzed synthesis of diaryl ethers. J. Am. Chem. Soc. 119, 10539–10540. https://doi.org/10.1021/ja971901j

Martín de Vidales, M.J., 2015. Eliminación de contaminantes orgánicos persistentes de aguas residuales mediante oxidación electroquímica con ánodo de diamante dopado con boro.

Doctoral Thesis, University of Castilla la Mancha.

Martín de Vidales, M.J., Sáez, C., Cañizares, P., Rodrigo, M.A., 2013. Removal of triclosan by conductive-diamond electrolysis and sonoelectrolysis. J. Chem. Technol. Biotechnol. 88, 823–828. https://doi.org/10.1002/jctb.3907

Mezcua, M., Gómez, M.J., Ferrer, I., Aguera, A., Hernando, M.D., Fernández-Alba, A.R., 2004. Evidence of 2,7/2,8-dibenzodichloro-p-dioxin as a photodegradation product of triclosan in water and wastewater samples. Anal. Chim. Acta 524, 241–247. https://doi.org/10.1016/j.aca.2004.05.050

Moneer, A.A., El-Shafei, A.A., Elewa, M.M., Naim, M.M., 2016. Removal of copper from simulated wastewater by electrocoagulation/floatation technique. Desalin. Water Treat. 57, 22824–22834. https://doi.org/10.1080/19443994.2015.1130917

Nawaz, R., Ali, K., Khan, M., 2016. Extraction of copper from wastewater through supported liquid membrane using tri-ethanolamine as a carrier. Desalin. Water Treat. 57, 21827–21841. https://doi.org/10.1080/19443994.2015.1128986

Oduoza, C.F., Wragg, A.A., 2000. Effects of baffle length on mass transfer in a parallel plate rectangular electrochemical cell. J. Appl. Electrochem. 30, 1439–1444. https://doi.org/10.1023/A:1026589226633

Panizza, M., Cerisola, G., 2009. Direct and mediated anodic oxidation of organic pollutants. Chem. Rev. 109, 6541–6569. https://doi.org/10.1007/978-1-4419-6996-5_126

Peng, C., Chai, L.Y., Tang, C.J., Min, X.B., Ali, M., Song, Y.X., Qi, W.M., 2015. Feasibility and enhancement of copper and ammonia removal from wastewater using struvite formation: A comparative research. J. Chem. Technol. Biotechnol. 92, 325-333. https://doi.org/10.1002/jctb.5009

Qiao, X., Zheng, X., Xie, Q., Yang, X., Xiao, J., Xue, W., Chen, J., 2014. Faster photodegradation rate and higher dioxin yield of triclosan induced by cationic surfactant CTAB. J. Hazard. Mater. 275, 210–214. https://doi.org/10.1016/j.jhazmat.2014.05.012

Rappe, C., Nilsson, C.-A., 1972. An artifact in the gas chromatographic determination of impurities in pentachlorophenol. J. Chromatogr. 67, 247–253.

Rodrigues Pires da Silva, J., Merçon, F., Guimarães Costa, C.M., Radoman Benjo, D., 2016.

Application of reverse osmosis process associated with EDTA complexation for nickel and copper removal from wastewater. Desalin. Water Treat. 57, 19466–19474. https://doi.org/10.1080/19443994.2015.1100554

Sanchez-Prado, L., Llompart, M., Lores, M., García-Jares, C., Bayona, J.M., Cela, R., 2006. Monitoring the photochemical degradation of triclosan in wastewater by UV light and sunlight using solid-phase microextraction. Chemosphere 65, 1338–1347. https://doi.org/10.1016/j.chemosphere.2006.04.025

Šerbula, S., Stanković, V., Živković, D., Kamberović, Gorgievski, M., Kalinović, T., 2016. Charasteristics of wastewater streams within the bor copper mine and their influence on pollution of the Timok river, Serbia. Mine Water Environ. 35, 480–485. https://doi.org/10.1007/s10230-016-0392-6

Sirés, I., Oturan, N., Oturan, M.A., Rodríguez, R.M., Garrido, J.A., Brillas, E., 2007. Electro-Fenton degradation of antimicrobials triclosan and triclocarban. Electrochim. Acta 52, 5493–5503. https://doi.org/10.1016/j.electacta.2007.03.011

Solá-Gutiérrez, C., Schröder, S., San Román, M.F., Ortiz, I., 2019. PCDD/Fs traceability during triclosan electrochemical oxidation. J. Hazard Mater. 369, 584–592. https://doi.org/10.1016/j.jhazmat.2019.02.066

Solá-Gutiérrez, C., San Román, M.F., Ortiz, I., 2018. Fate and hazard of the electrochemical oxidation of triclosan. Evaluation of polychlorodibenzo‐p‐dioxins and polychlorodibenzofurans (PCDD/Fs) formation. Sci. Total Environ. 626, 126–133. https://doi.org/10.1016/j.scitotenv.2018.01.082

Tokalıoğlu, Ş., Yavuz, E., Şahan, H., Çolak, S.G., Ocakoğlu, K., Kaçer, M., Patat, Ş., 2016. Ionic liquid coated carbon nanospheres as a new adsorbent for fast solid phase extraction of trace copper and lead from sea water, wastewater, street dust and spice samples. Talanta 159, 222–230. https://doi.org/10.1016/j.talanta.2016.06.022

Tonini, G.A., Ruotolo, L.A.M., 2017. Heavy metal removal from simulated wastewater using electrochemical technology: optimization of copper electrodeposition in a membraneless fluidized bed electrode. Clean Technol. Environ. Policy 19, 403–415. https://doi.org/10.1007/s10098-016-1226-8

Vadiraj, K.T., Belagali, S.L. 2014. Spectrophotometric determination of copper (II) in industrial effluent samples using sulfanilic acid as a ligand system. Bulg. Chem. Commun. 45(3), 447-451.

Vallejo, M., 2014. Assessment of polychlorinated dibenzo-p-dioxins and dibenzofurans, PCDD/Fs, in the application of advanced oxidation processes. Doctoral Thesis, University of Cantabria.

Vallejo, M., San Román, M.F., Ortiz, I., 2013. Quantitative assessment of the formation of polychlorinated derivatives, PCDD/Fs, in the electrochemical oxidation of 2-chlorophenol as function of the electrolyte type. Environ. Sci. Technol. 47, 12400–12408. https://doi.org/10.1021/es403246g

Wang, X., Zhang, H., Ni, Y., Du, Q., Zhang, X., Chen, J., 2014. Kinetics of PCDD/Fs formation from non-wood pulp bleaching with chlorine. Environ. Sci. Technol. 48, 4361–4367. https://doi.org/10.1021/es404347h

Weber, R., 2007. Relevance of PCDD/PCDF formation for the evaluation of POPs destruction technologies - Review on current status and assessment gaps. Chemosphere 67, 109–117. https://doi.org/10.1016/j.chemosphere.2006.05.094

Wikström, E., Marklund, S., 2000. Secondary formation of chlorinated dibenzo-p-dioxins, dibenzofurans, biphenyls, benzenes, and phenols during MSW combustion. Environ. Sci. Technol. 34, 604–609. https://doi.org/10.1021/es9906498

Wu, J. lin, Ji, F., Zhang, H., Hu, C., Wong, M.H., Hu, D., Cai, Z., 2019. Formation of dioxins from triclosan with active chlorine: A potential risk assessment. J. Hazard. Mater. 367, 128–136. https://doi.org/10.1016/j.jhazmat.2018.12.088

Zhang, X., Zhang, C., Sun, X., Kang, L., Zhao, Y., 2015. Chemical conversion pathways and kinetic modeling for the OH-initiated reaction of triclosan in gas-phase. Int. J. Mol. Sci. 16, 8128–8141. https://doi.org/10.3390/ijms16048128

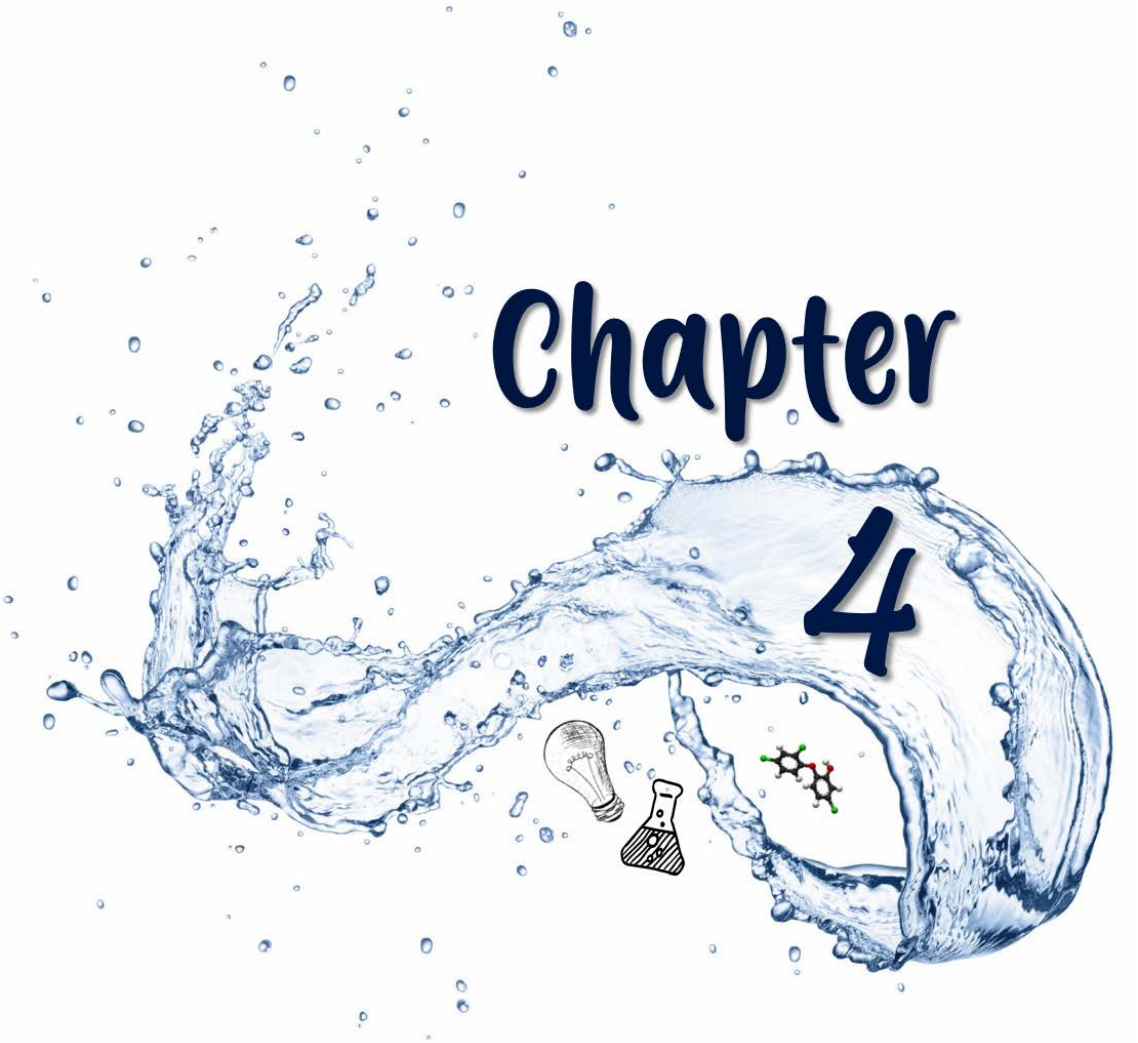

Chapter 4

PHOTOLYTIC OXIDATION OF TRICLOSAN

The effectiveness of photolytic degradation of different organic pollutants, including Triclosan, has been widely studied (Stamatis et al., 2014; Constantin et al., 2015; Chen et al., 2016; Kosera et al., 2017; Chen et al., 2018; Constantin et al., 2018; Iovino et al., 2019) but not the final toxicity after the application of the treatment. In this section, two photolytic oxidation treatments have been applied to synthetic aqueous samples containing Triclosan: photolysis (direct oxidation) and photocatalysis (indirect oxidation). Beforehand, an exhaustive and critical analysis of the state of the art related to the photo-degradation techniques applied to Triclosan solutions as well as to the formation of different intermediate products during the application of these treatments has been performed. This literature analysis provides relevant information about the influence of the operational variables involved in the Triclosan oxidation as well as on the reaction pathways. After this deep review, the experimental phototransformation of Triclosan by photolysis has been assessed, starting with a detailed analysis of UV/Vis light absorbance of Triclosan, followed by photolytic experiments applied to Triclosan aqueous solutions and related compounds, analysing the formation of intermediate products, including dioxins, and finishing with the proposal of a reaction mechanism supported by the obtained results. Finally, photocatalytic experiments have been conducted in order to study the influence of a catalyst on the photo-degradation of Triclosan as well as on its oxidation route, through the analysis of the intermediate products and PCDD/Fs formed during the treatment.

4.1. Main operational conditions involved in the photolytic degradation of Triclosan

The experimental conditions play an important role in the photo-transformation of Triclosan (Latch et al., 2003; Aranami and Readman, 2007), for this reason, this section is focused on the analysis of the conditions reported in previous works devoted to Triclosan photo-degradation, including both direct photolysis and indirect photolysis or photocatalysis. In this way, Figure 4.1 summarizes in conceptual maps the operational conditions found in the literature, such as the wavelength, pH, presence of a catalyst or light source, with the aim to display their relevance in the photo-degradation of Triclosan. In addition to Figure 4.1, more details of the information collected are summarized in Table 4.1, listed by operational condition and in chronologic order within each section.

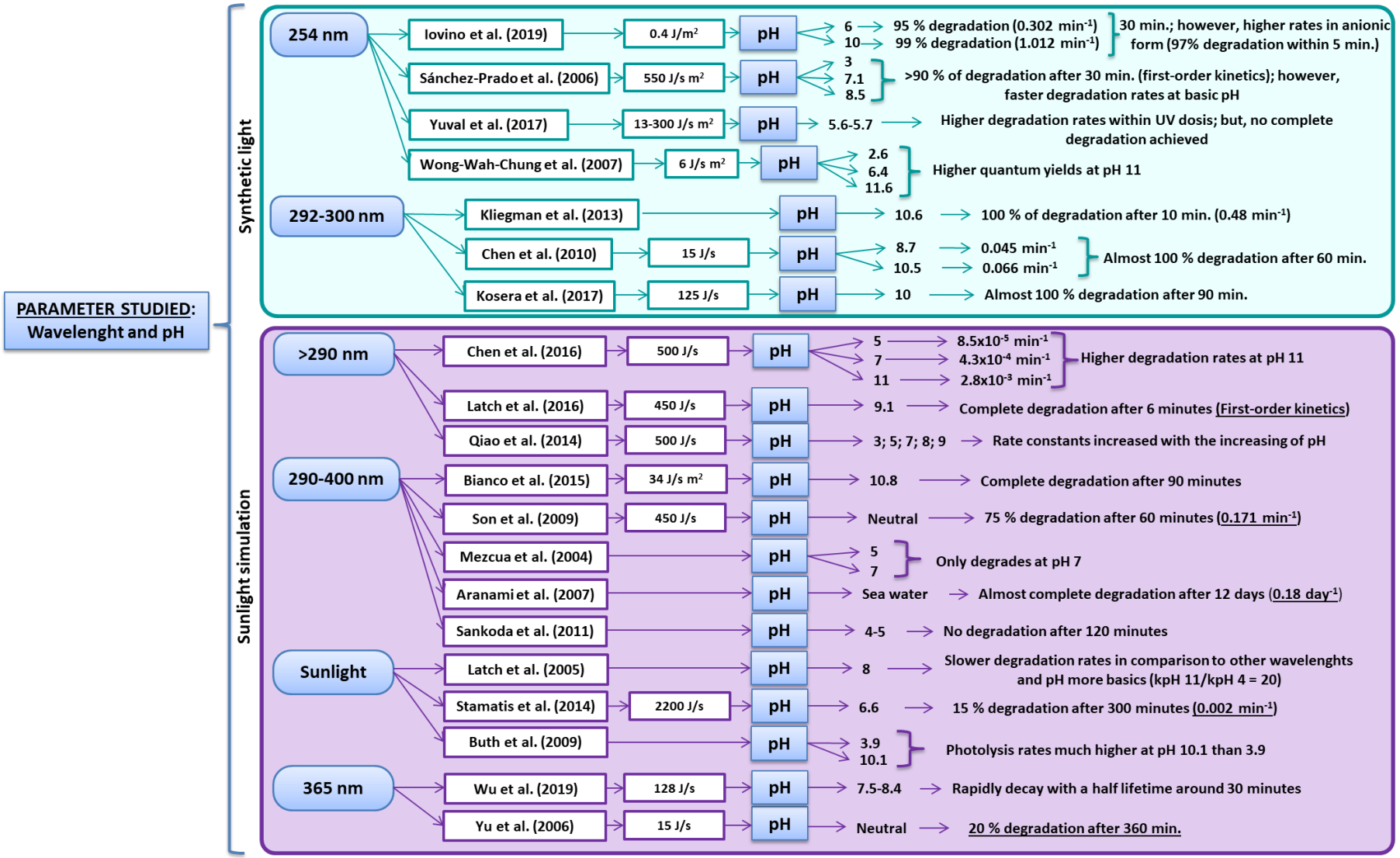

Figure 4.1. Scheme of the principal operational conditions found in the literature and their relevance in the photo-degradation of Triclosan.

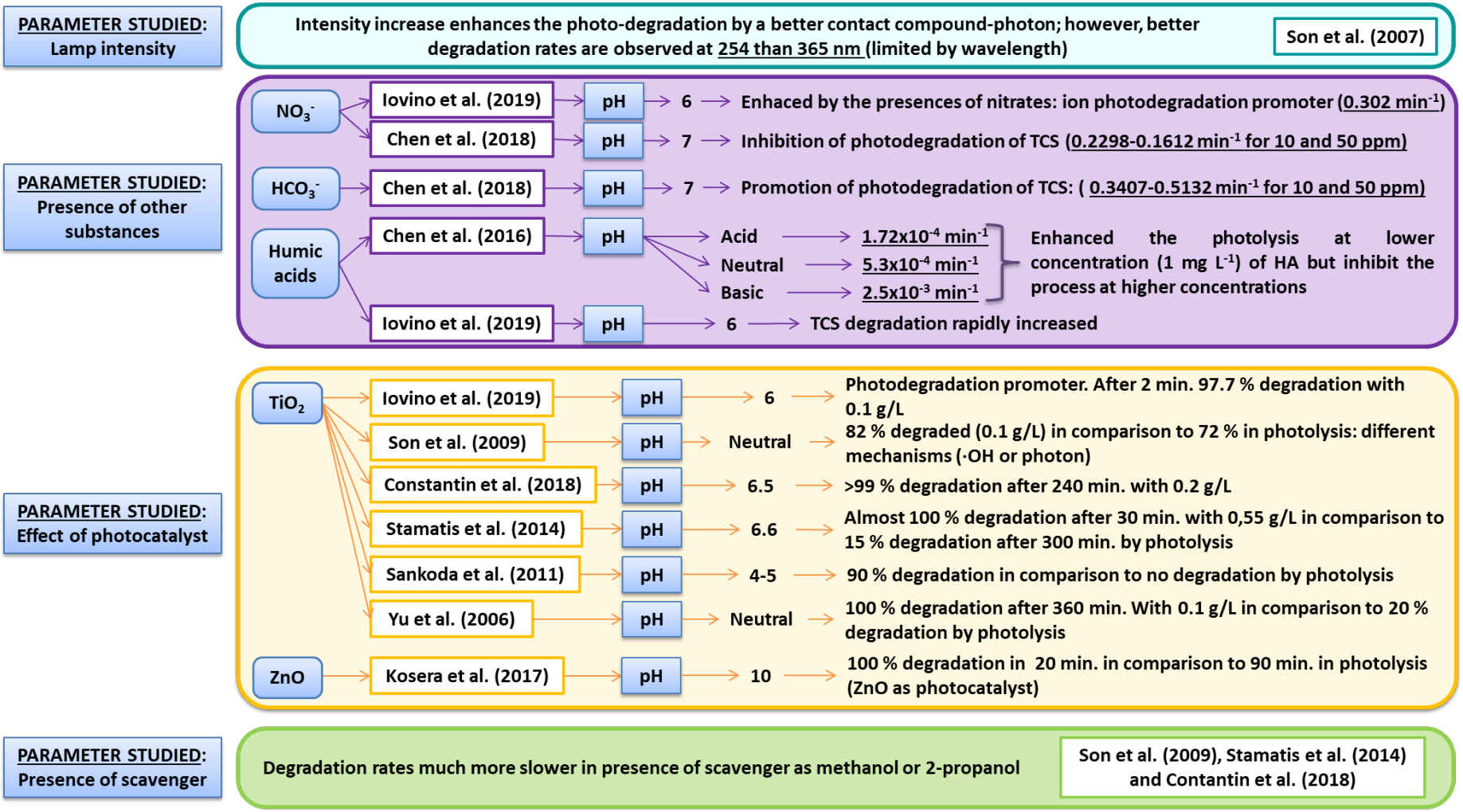

Figure 4.1. Scheme of the principal operational conditions found in the literature and their relevance in the photo-degradation of Triclosan (cont.).

Table 4.1. Main operational conditions applied to photolytic degradation of Triclosan.

Operational condition studied: wavelength and pH of the solution					
References	**Water samples and TCS concentration**	**Wavelength**	**pH**	**k (min^{-1})**	**Main results**
(Sanchez-Prado et al., 2006)	S* and R* ng mL^{-1} levels	254 nm	3	-	> 90 % of TCS degradation after 30 minutes; however, faster TCS removal at basic pH
			7.1		
			8.5		
(Wong-Wah-Chung et al., 2007)	S* 7.8 mg L^{-1}		6.4	-	100 % removed achieved after 30 minutes of irradiation
(Alfiya et al., 2017)	S* 2.5 mg L^{-1}		5.6 - 5.7	0.222	UV dosis has been studied, concluding that higher UV dosis enhance TCS degradation from 20 to 80 % from 0.1 to 0.7 J cm^{-2}, respectively.
(Iovino et al., 2019)	S* 4.5 – 18 mg L^{-1}		6	0.302	95 and 99 % of TCS degradation at an irradiation time lower than 30 minutes for pH of 6 and 10, respectively; however, after 30 minutes 100 % degradation rates for both cases.
			10	1.012	
(Chen et al., 2010)	S* 30 mg L^{-1}	292 – 300 nm	8.7	0.045	Almost 100 % degradation after 60 minutes; however, higher removal rates for pH 10.5
			10.5	0.066	
(Kliegman et al., 2013)	S* (10:90 Methanol: water buffer solution) 15 mg L^{-1}		10.6	0.480	100 % removed achieved after 10 minutes of irradiation
(Kosera et al., 2017)	S* 10 mg L^{-1}		10	-	Almost 100 % removals after 90 minutes

S*: synthetic aqueous solution; R*: real urban wastewater.

Table 4.1. Main operational conditions applied to photolytic degradation of Triclosan (cont.).

Operational condition studied: wavelength and pH of the solution					
References	**Water samples and TCS concentration**	**Wavelength**	**pH**	**k (min^{-1})**	**Main results**
(Mezcua et al., 2004)	S* 8.2 mg L^{-1}	290 – 400 nm	5	-	TCS degradation only observed at pH 7
			7		
(Aranami and Readman, 2007)	Sea water -		8	1.250×10^{-4}	Almost complete degradation of TCS after 12 days
(Son et al., 2009)	S* 0.5 – 8.7 mg L^{-1}		Neutral	-	75 % degradation of TCS after 60 minutes
(Sankoda et al., 2011)	S* 1 mg L^{-1}		4 - 5	-	No degradation observed after 120 minutes
(Bianco et al., 2015)	S* 15 mg L^{-1}		10.8	-	Complete degradation of TCS after 90 minutes
(Latch et al., 2003)	S* 1 – 22 mg L^{-1}	>290 nm	9.1	-	Complete degradation of TCS after 6 minutes
(Qiao et al., 2014)	S* 1 mg L^{-1}		3 - 9	1.17×10^{-4} – 0.030	The rate constants of TCS degradation increased with the increasing of pH
(Chen et al., 2016)	S* 1 mg L^{-1}		5	8.500×10^{-5}	At pH 5 (TCS almost in molecular form) very slow photolysis of TCS. At pH 7 (TCS is both in molecular and anionic form) TCS photolysis is enhanced. At pH 11 (TCS almost in anionic form) higher photolysis degradation rates
			7	4.300×10^{-4}	
			11	2.800×10^{-4}	

S*: synthetic aqueous solution; R*: real urban wastewater.

Table 4.1. Main operational conditions applied to photolytic degradation of Triclosan (cont.).

Operational condition studied: wavelength and pH of the solution					
References	**Water samples and TCS concentration**	**Wavelength**	**pH**	**k (min^{-1})**	**Main results**
(Yu et al., 2006)	S* 9 mg L^{-1}	365 nm	Neutral	-	20 % TCS removal after 360 minutes
(Wu et al., 2019)	Sea water $2 \times 10^{-4} – 2 \times 10^{-3}$ mg L^{-1}		7.5 - 8.4	-	Rapidly decay with a half lifetime around 30 minutes
Operational condition studied: lamp intensity					
References	**Matrices and TCS concentration**	**Wavelength**	**Lamp intensities studied**	**k (min^{-1})**	**Main results**
(Son et al., 2007)	S* 1 mg L^{-1}	254 and 365 nm	0.34×10^{-4} - 2.26×10^{-4} Einstein min^{-1} L^{-1}	-	Better degradation rates obtained at highest intensities working with wavelenght of 254 nm (0.72×10^{-4} and 1.08×10^{-4} Eintein min^{-1} L^{-1})
Operational condition studied: presence of other substances					
References	**Matrices and TCS concentration**	**Substance**	**pH**	**k (min^{-1})**	**Main results**
(Chen et al., 2018)	S* 1 mg L^{-1}	NO_3^-	7	0.23 – 0.16 (10 – 50 mg L^{-1} NO_3^-)	Inhibition of TCS degradation due to the scavenging process, more pronounced at higher concentrations of $NaNO_3$
(Iovino et al., 2019)	S* 4.5 – 18 mg L^{-1}		6	0.302	TCS degradation enhaced by the presence of nitrates: the ion acts as a photo-degradation promoter

S*: synthetic aqueous solution; R*: real urban wastewater.

Table 4.1. Main operational conditions applied to photolytic degradation of Triclosan (cont.).

Operational condition studied: presence of other substances					
References	**Matrices and TCS concentration**	**Substance**	**pH**	**k (min^{-1})**	**Main results**
(Chen et al., 2018)	S* 1 mg L^{-1}	HCO_3^-	7	0.341 – 0.513 (10 – 50 mg L^{-1} HNO_3^-)	The promotion of TCS removal is observed: CO_3^- radicals are formed. However, the coexistence of more inorganic anions in the solution inhibit its degradation due to its scavenging activity.
(Chen et al., 2016)	S* 1 mg L^{-1}	Humic acids	Acid	1.720 x 10^{-4}	TCS degradation rates are enhanced by the presence of humic acids at low concentrations independently of the pH (1 mg L^{-1}); however, at higher concentrations the removal process is inhibited.
			Neutral	5.300 x 10^{-4}	
			Basic	2.500 x 10^{-3}	
(Iovino et al., 2019)	S* 4.5 – 18 mg L^{-1}		6	-	TCS degradation rates rapidly increased (0.10 mg L^{-1} of humic acids)

Operational condition studied: presence of scavengers					
References	**Matrices and TCS concentration**	**Scavenger**	**Scavenger concentration**	**k (min^{-1})**	**Main results**
(Chen et al., 2016)	S* 1 mg L^{-1}	2,4,6-trimethylphenol	5 x 10^{-4} mol L^{-1}	1.35 x 10^{-4} – 2.46 x 10^{-3}	Significantly inhibition of TCS degradation at pH 5 and 7, especially with 2-propanol. However, slight variation in the results was observed at pH 11.
		β-carotene	1 x 10^{-3} mol L^{-1}	1.48 x 10^{-4} – 2.45 x 10^{-3}	
		2-propanol	2 %, V/V	1.28 x 10^{-4} – 2.56 x 10^{-3}	
		Furfuryl alcohol	5 x 10^{-4} mol L^{-1}	1.63 x 10^{-4} – 2.47 x 10^{-3}	

S*: synthetic aqueous solution; R*: real urban wastewater.

Table 4.1. Main operational conditions applied to photolytic degradation of Triclosan (cont.).

Operational condition studied: presence of scavengers					
References	**Matrices and TCS concentration**	**Scavenger**	**Scavenger concentration**	**k (min^{-1})**	**Main results**
(Son et al., 2009)	S* 0.5 – 8.7 mg L^{-1}	2-propanol	2 x 10^{-3} mol L^{-1}	-	Degradation rates of TCS in both direct and indirect photolysis were reduced in the presence of 2-propanol as scavenger
(Stamatis et al., 2014)	S* 1 mg L^{-1}		1.7 x 10^{-2} mol L^{-1}	0.0473	Around 68.8 % of inhibition of TCS degradation rate was observed
(Constantin et al., 2018)	S* 31.8 mg L^{-1}		3 x 10^{-3} mol L^{-1}	0.008	Highly decreased on the degradation of TCS in the presence of 2-propanol, TCS degradation decreased with about 60 %
(Kliegman et al., 2013)	S* (10:90 Methanol:water buffer solution) 15 mg L^{-1}	d_8-isopropanol	1 mol L^{-1}	-	Not highly differences were observed in the degradation of TCS
(Son et al., 2007)	S* 1 mg L^{-1}	Methanol	0.1 x 10^{-3} - 10 x 10^{-3} mol L^{-1}	-	13.9, 33.0, and 62.9 % of TCS reduction was observed after 60 minutes of treatment at 10 x 10^{-3}, 1 x 10^{-3} and 0.1 x 10^{-3} mol L^{-1}, respectively. Only 8.2 % of degradation observed in methanol used as solvent instead of water.
(Alfiya et al., 2017)	S* 2.5 mg L^{-1}		0.15 mol L^{-1}	-	Considerably inhibition of TCS degradation rates were obtained when methanol was added to the solution as scavenger

S*: synthetic aqueous solution; R*: real urban wastewater.

Table 4.1. Main operational conditions applied to photolytic degradation of Triclosan (cont.).

Operational condition studied: presence of catalyst					
References	**Matrices and TCS concentration**	**Catalyst**	**Catalyst concentration**	**k (min^{-1})**	**Main results**
(Yu et al., 2006)	S* 9 mg L^{-1}	TiO_2	0.1 g L^{-1}	-	A complete degradation of TCS observed after 360 minutes in comparison to 20 % of degradation by direct photolysis
(Son et al., 2009)	S* 0.5 – 8.7 mg L^{-1}			0.167 – 0.216 (8.686 – 0.869 mg L^{-1} TCS)	82 % removed in comparison to 72 % by direct photolysis
(Iovino et al., 2019)	S* 4.5 – 18 mg L^{-1}			-	Strongly influenced observed, TiO_2 acts as a photo-degradation promoter. 97.7 % of TCS degradation after 2 minutes
(Constantin et al., 2018)	S* 31.8 mg L^{-1}		0.2 g L^{-1}	0.025	>99 % of TCS degraded after 240 minutes
(Stamatis et al., 2014)	S* 1 mg L^{-1}		0.55 g L^{-1}	0.1504	Almost a complete degradation of TCS observed after 30 minutes in contrats with 15 % of removal by direct photolysis
(Sankoda et al., 2011)	S* 1 mg L^{-1}		-	-	90 % removed compared to any degradation of TCS by direct photolysis
(Kosera et al., 2017)	S* 10 mg L^{-1}	ZnO	0.03 g L^{-1}	-	Complete degradation shown in 20 minutes as compared to 90 minutes needed by direct photolysis

S*: synthetic aqueous solution; R*: real urban wastewater.

Most of the studied solutions are synthetic samples spiked with Triclosan and prepared in pure water, with concentrations in the range of mg L^{-1}. Since the maximum Triclosan solubility in water is 10 mg L^{-1} at 20 °C (Yu et al., 2006), the initial concentration of Triclosan in the samples studied and dissolved in pure water is usually below its solubility limit (Sanchez-Prado et al., 2006; Wong-Wah-Chung et al., 2007; Alfiya et al., 2017; Kosera et al., 2017; Mezcua et al., 2004; Son et al., 2009; Sankoda et al., 2011; Qiao et al., 2014; Chen et al. 2016; Yu et al., 2006; Son et al., 2007; Chen et al., 2018; Stamatis et al., 2014). Some authors have also applied photochemical treatments to real wastewater (Sanchez-Prado et al., 2006; Mezcua et al., 2004; Wu et al., 2019). Next, the principal operational variables involved in the photo-degradation of Triclosan listed in Table 1.4 are analyzed separately.

(i) Solution pH. The effect of the solution pH on Triclosan photo-degradation has been extensively analyzed. Triclosan has a pK_a between 7.9 and 8.1 as reported by several authors (Tixier et al., 2002; Latch et al., 2005; Wong-Wah-Chung et al., 2007). Thus, this compound may exist in two different molecular forms depending on the pH: anionic form (when the pH is above the pK_a) or molecular form (the pH is below the pK_a). It has been demonstrated by many authors that the anionic form of Triclosan (pH > 7.9 – 8.1) absorbs light preferentially when compared to the neutral form (Tixier et al., 2002; Kliegman et al., 2013). 100 % degradation of Triclosan was reported by many authors working under alkaline conditions (Iovino et al., 2019; Chen et al., 2010; Kliegman et al., 2013; Kosera et al., 2017; Bianco et al., 2015; Latch et al., 2003; Qiao et al., 2014; Chen et al., 2016). Lower degradation rates have been observed at neutral pH (Sanchez-Prado et al., 2006; Alfiya et al., 2017; Mezcua et al., 2004; Iovino et al., 2019; Son et al., 2009; Chen et al., 2016). In contrast to the very low or even no degradation observed when working at acid pH (Mezcua et al., 2004; Sankoda et al., 2011; Qiao et al., 2014; Chen et al., 2016). Thus, in order to enhance the photo-degradation of Triclosan, many authors have selected alkaline values of pH (preferably above 8) as reported in Table 4.1 (Sanchez-Prado et al., 2006; Iovino et al., 2019; Chen et al., 2010; Kliegman et al., 2013; Kosera et al., 2017; Aranami and Readman, 2007; Bianco et al., 2015; Latch et al., 2003; Qiao et al., 2014; Chen et al., 2016; Wu et al., 2019).

(ii) Wavelength. Together with the pH, the wavelength selection is a factor that has to be taken into consideration. A wide range of wavelengths has been applied to the degradation of Triclosan. Weatherly and Gosse (2017) reported that the anionic form of Triclosan strongly absorbs light at wavelengths close to 300 nm. In the same way, Lindström et al. (2002)

reported that the absorbance of Triclosan increased considerably at wavelengths between 300 and 320 nm when it was dissociated (pH > pK_a) in comparison to a very weak absorbance when it was in a non-dissociated form (pH < pK_a). This fact was corroborated by Latch et al. (2005) and Kliegman et al. (2013). Thus, most of the authors have applied wavelengths between 254 and 400 nm as summarized in Table 4.1. Iovino et al. (2019) carried out the photolysis of Triclosan under UV irradiation (254 nm) achieving a removal rate of 99 % after 30 minutes when the solution was set to pH 10; however, working at the same conditions but decreasing the pH to 6, Triclosan degradation was reduced to 95 %. Similar results were obtained by Sanchez-Prado et al. (2006); higher degradation rates were obtained at basic pH (8.5) working at 254 nm (more than 90 % removal after 30 minutes). Complete degradation of Triclosan was also observed by Wong-Wah-Chung et al. (2007) working at the same wavelength (254 nm) and at a neutral pH. In the same way, working at wavelengths between 292 and 300 nm and at basic pH, 100 % degradation rates have been reported (Chen et al., 2010; Kliegman et al., 2013; Kosera et al., 2017). Some authors have been applied wavelengths in the range of 290 – 400 nm, observing a complete Triclosan degradation rates when working at neutral and basic pH (Mezcua et al., 2004; Aranami and Readman, 2007; Son et al., 2009; Bianco et al., 2015), or achieving no removal rates when working at acidic pH (Mezcua et al., 2004; Sankoda et al., 2011). In the same way, working at a wide range of wavelengths, but above 290 nm, several authors have observed complete degradation rates of Triclosan at neutral and basic pH, in contrast to, as well expected, no removal rates at an acidic pH (Latch et al., 2003; Qiao et al., 2014; Chen et al., 2016).

(iii) Light intensity. Although the literature on this variable is scarce, the intensity of the ultraviolet lamp is another parameter with great influence on the Triclosan degradation rate. Son et al. (2007) applied different light intensities at wavelengths of 254 and 365 nm; resulting in higher removal rates at the highest intensities when working at 254 nm (0.72×10^{-4} and 1.08×10^{-4} Einstein min^{-1} L^{-1}) (see Table 4.1). These authors emphasized that the intensity of the lamp is an important factor that plays a decisive role on the degradation kinetics of Triclosan; however, the photo-degradation of Triclosan is also limited by the UV wavelength as previously described.

(iv) Presence of other substances. The presence of other substances might alter the composition of the aqueous medium and cause different effects in the photolytic process (Chen et al., 2016; Iovino et al., 2019). For instance, the presence of humic acids (HA) or inorganic salts in the solution enhanced the yield of the photo-degradation reactions due

to their photosensitizer action, namely compounds that can be activated by light in order to generate reactive oxygen species (ROS) (Chen et al., 2016, 2018) (see Table 4.1). Iovino et al. (2019) demonstrated the enhancement of the degradation rates of Triclosan by the presence of nitrate anions NO_3^- (50 mg L^{-1}) and HA (10 mg L^{-1}), obtaining a complete removal after 10 minutes; these achievements were attributed to the formation of highly reactive radicals from the anions that were present in the solution. However, opposite results were reported by Chen et al. (2018) working with higher concentrations of NO_3^-. This effect was attributed to the UV light absorption by NO_3^- which competed with Triclosan leading to a slight inhibition of the photolysis of Triclosan. The influence of HCO_3^- in the aqueous solution was studied by Chen et al. (2018); in this case, this anion enhanced the photolysis of Triclosan. Although HCO_3^- could not absorb UV light as in the case of NO_3^-, HCO_3^- could react with the active radicals of Triclosan formed from the direct photolysis of Triclosan and produce CO_3^- radicals, powerful oxidants, which enhanced the Triclosan oxidation (Chen et al., 2018). The degradation rates enhance by the presence of HA has been reported; however, high concentration of these species could cause an inhibition of Triclosan degradation (Chen et al., 2016; Iovino et al., 2019). With regard to the presence of chloride, no effect on the degradation of Triclosan was observed. The same study showed that the photolysis of Triclosan was inhibited when the three anions, NO_3^-, HCO_3^- and Cl^-, coexisted in the solution. These results highlight the complexity and coupled influence of anions of different nature in the photolysis of Triclosan.

(v) Presence of scavengers. In order to investigate the quantum yield for the photo-degradation of Triclosan as well as the possible pathway involved in the photo-degradation (·OH radical or photon (h^+)), several authors have studied the effect of different scavengers which might compete with Triclosan for the photons or radicals present in the reaction medium (see Table 4.1) (Chen et al., 2016; Son et al., 2009; Stamatis et al., 2014; Constantin et al., 2018; Kliegman et al., 2013; Son et al., 2007; Alfiya et al., 2017). 2-propanol, being the photon scavenger most frequently used, suppressed the photo-degradation efficiency of Triclosan according to many authors (Son et al., 2009; Stamatis et al., 2014; Constantin et al., 2015; Chen et al., 2016). In a similar way, methanol has been also used as photo-scavenger by different researchers (Son et al., 2007; Alfiya et al., 2017), obtaining similar results; that is considerable inhibition of Triclosan degradation rates occurred when methanol was added to the treated solution. 2,4,6-trimethylphenol (TMP), β-carotene and furfuryl alcohol (FFA), different scavengers studied by Chen et al. (2016), also reported an inhibitory effect on Triclosan degradation when they are dissolved in aqueous solution.

(vi) Presence of catalyst. The indirect photolysis by the presence of a catalyst, or photocatalysis, has been successfully applied to the remediation of a variety of organic compounds (Hoffmann et al., 1995; Ibhadon and Fitzpatrick, 2013; Ribao et al., 2018). With respect to the photocatalyst on Triclosan degradation, TiO_2 is the most commonly used material in concentrations that range from 0.10 to 0.55 g L^{-1} (Rafqah et al., 2006; Yu et al., 2006; Son et al., 2009; Sankoda et al., 2011; Stamatis et al., 2014; Constantin et al., 2015, 2018; Iovino et al., 2019), with the exception of the work of Kosera et al. (2017) that employed ZnO as catalyst, achieving a complete degradation of Triclosan after 20 minutes of treatment with a dose of 0.03 g L^{-1} (Table 4.1). This table also collects the rate enhancement in the photocatalytic degradation of Triclosan in comparison to direct photolysis (Stamatis et al., 2014; Alfiya et al., 2017; Kosera et al., 2017); in some cases, the presence of the catalyst promoted the degradation achieving removals of 100.0 % (Yu et al., 2006; Stamatis et al., 2014; Kosera et al., 2017; Constantin et al., 2018).

To summarize, the studies collected in Table 4.1 show that Triclosan degradation rates are enhanced working at conditions where Triclosan is present in its anionic form (pH > pK_a: 7.9 – 8.1). Thus, pH is an important parameter that plays an important role in the photo-degradation of Triclosan. In the same way, wavelengths operating in the region of 300 nm strongly enhance the photolytic process at conditions where Triclosan is present in its phenolate form (pH > pK_a), achieving its complete degradation. Furthermore, accompanied by the wavelength, the intensity of the lamp could be a decisive factor with a great influence on the photo-treatment of Triclosan, increasing its degradation rate. In relation with the presence of other substances in the reaction medium, the results displayed in Table 4.1 highlight the complexity and coupled influence of anions of different nature in the photolysis of Triclosan, such as NO_3^- and HCO_3^-, which could enhance or inhibit the degradation process. On the other hand, it could be concluded that the presence of photo-scavengers in the treated samples, like 2-propanol or methanol, might inhibit the photolytic degradation of Triclosan; this inhibition has been reported to be as high as 70.0 %. Finally, with regard to the influence of a catalyst on the solution, the reported studies showed that its presence strongly enhances the kinetics of Triclosan degradation independently of the catalyst used or dose employed, achieving removal rates of 100 %.

4.2. Main reaction mechanisms involved in the photo-degradation of Triclosan

The formation of Triclosan photo-oxidation products has been widely studied by many authors, being 2,8-dichlorodibenzo-p-dioxin, 2,4-dichlorophenol and 4-chlorocatechol some of the most common by-products reported in the literature. Triclosan photo-transformation pathways have been reviewed and a summary is illustrated in Figures 4.2, 4.3 and 4.4.

Figure 4.2 shows the products formed in the photo-degradation of Triclosan in aqueous phase formed through a molecule cleavage, chlorination or dechlorination reactions. 2,4-dichlorophenol has been demonstrated to be one of the main photo-products observed in the degradation of Triclosan (route 1). It might be produced by a photo-induced hydrolysis due to the effect of the UV light that produce an ether cleavage (Sanchez-Prado et al., 2006; Kliegman et al., 2013; Chen et al., 2016; Iovino et al., 2019). In the same way, as shown in Figure 4.2, 2,4-dichlorophenol might be formed by the action of OH radicals that cause a homolytic scission of the carbon-oxygen bond (Latch et al., 2003; Rafqah et al., 2006; Son et al., 2007, 2009; Sankoda et al., 2011; Stamatis et al., 2014; Constantin et al., 2018). Furthermore, chlorophenol (route 2) and 4-chlorocatechol (route 3) might be provoked by the action of OH radical on the molecule of Triclosan (Son et al., 2007, 2009) or by the action of the photo-induced hydrolysis of Triclosan under UV light (Sanchez-Prado et al., 2006). Furthermore, the formation of 4-chlorocatechol has been described as a result of a disproportionation reaction of the phenoxyl radical that came from the breakage of the Triclosan molecule when forming 2,4-dichlorophenol (route 4) (Rafqah et al., 2006; Stamatis et al., 2014; Chen et al., 2016; Constantin et al., 2018). The formation of chlorinated Triclosan has been also observed as a consequence of several chlorination reactions (route 5) (Sankoda et al., 2011). The formation of hydrodehalogenation products of Triclosan has been also described as a consequence of a dechlorination reaction (route 6) (Kliegman et al., 2013; Iovino et al., 2019). Route 7 described the formation of 2,4-dichlophenol from a the chlorinated Triclosan cleavage (Iovino et al., 2019). In addition, the formation of chlorophenols as a consequence of a dechlorination reaction of 2,4-dichlorophenol has been observed (route 8). Finally, the successive dechlorination reactions of chlorophenols, as shown in Figure 4.2, may lead to the formation of phenol (route 9) (Sanchez-Prado et al., 2006; Chen et al., 2016).

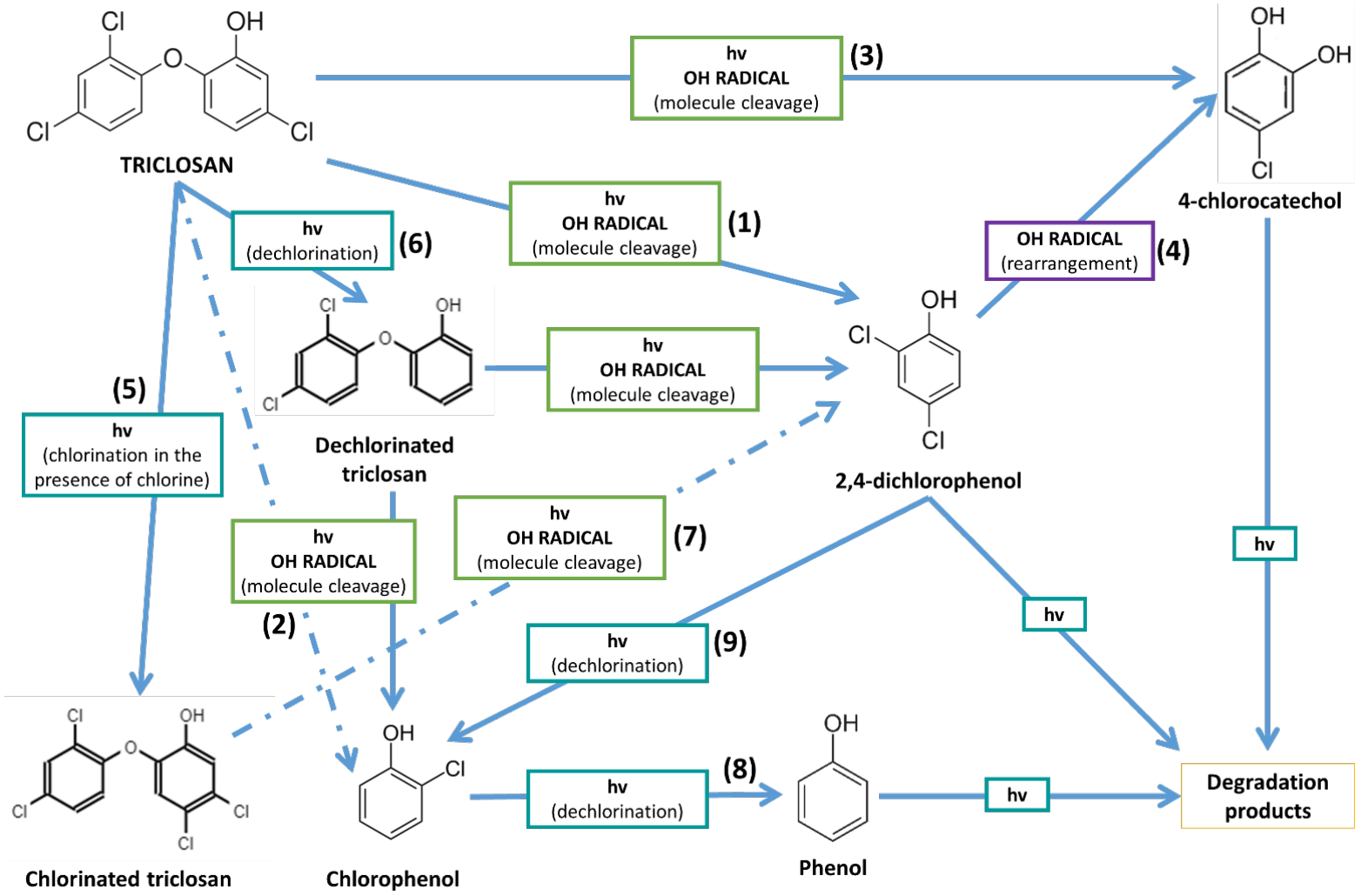

Figure 4.2. Summary of the main TCS photo-degradation pathways: molecule cleavage, dechlorination and chlorination mechanisms. Adapted from the literature (Latch et al., 2005; Son et al., 2007, 2009; Sankoda et al., 2011; Kliegman et al., 2013; Chen et al., 2016; Constantin et al., 2018; Iovino et al., 2019). *hv*: photolysis; *OH RADICAL*: photocatalysis.

On the other hand, Chen et al. (2010) reported polymerization reactions at higher Triclosan concentrations leading to Triclosan polymers, which are the sum of various Triclosan molecules. The reaction between two molecules of Triclosan could be explained by the interaction between the hydroxy and chlorine groups (Figure 4.3) (route 1). In the same way, the formation of hydroxyl-chlorinated-PCBs have been explained through the generation of a biradical intermediate that leads to their formation (route 2) (Kliegman et al., 2013). Furthermore, several authors have observed the presence of Triclosan-quinones and Triclosan-catechols as displayed in Figure 4.3 (route 3 and 4). The reaction mechanisms that lead to the formation of these species could proceed through the attack of OH radicals to form an ·OH adduct, which due to the unstable state, decays to a semi-quinone radical. The semi-quinone disproportionation leads to the formation of the semi-quinone radical that, finally, yielded TCS-quinone and TCS-catechol (Rafqah et al., 2006; Yu et al., 2006). The formation of 2,4-dichlophenol from Triclosan quinone produced by a molecule cleavage has been also reported (route 5) (Latch et al., 2005).

Finally, the potential formation of 2,8-dichlorodibenzo-p-dioxin has been considered in different works. The formation of this compound by a photochemical rearrangement reaction is favoured under certain operation conditions (Figure 4.4). Wong-Wah-Chung et al. (2007), Buth et al. (2009), Kliegman et al. (2013), Bianco et al. (2015) and Iovino et al. (2019) observed the formation of 2,8-dichlorodibenzo-p-dioxin at pH above 10. Furthermore, the presence of this specie has been also observed in the presence of NO_3^- (Iovino et al., 2019). In the same way, Son et al. (2007) studied the influence of the light intensity on the formation of 2,8-dichlorodibenzo-p-dioxin; this specie was only observed at the highest light intensities studied working at 365 nm. Nevertheless, it has been reported that the inhibition in the formation of 2,8-dichlorodibenzo-p-dioxin might occur working at acidic pH (Mezcua et al., 2004; Wong-Wah-Chung et al., 2007; Chen et al., 2016), low light intensities (Son et al., 2007), or in the presence of HA (Chen et al., 2016). In photocatalytic processes (likely through OH radicals), the formation of 2,8-dichlorodibenzo-p-dioxin might be inhibited through the action of OH radicals (Yu et al., 2006; Son et al., 2009) (Figure 4.4). As it has been explained in section 2.1.1, the reaction mechanisms present in a photocatalytic oxidation consist on the formation of ·OH radicals that likely provoke an ether cleavage of Triclosan molecule, which, consequently, avoids the cyclization that generates 2,8-dichlorodibenzo-p-dioxin. In contrast to the photolytic oxidation, which is produced via the adsorption of a photon, that, as it has been demonstrated, likely provokes the cyclization of the molecule under certain conditions. On the other hand, 2,8-dichlorodibenzo-p-dioxin could be transformed into other products by the action of the light (photolysis) or by the action of OH radicals (photocatalysis). The formation of dibenzo-p-dioxin (route 1 in Figure 4.4) has been described by Son et al. (2009) as a dechlorination reaction produced by the action of the photons produced in the

photolysis of 2,8-dichlorodibenzo-p-dioxin. 4-chlorocatechol and 2,4-dichlorophenol might be formed by the action of the photo-induced hydrolysis of 2,8-dichlorodibenzo-p-dioxin or by the action of OH radicals, which produce the dioxin bond splitting (route 2 and 3 of Figure 4.4) (Son et al., 2009; Constantin et al., 2018). In the same way, chlorophenol and phenol has been reported as by-products of 2,8-dichlorodibenzo-p-dioxin, which might be attacked by the action of OH radicals that cause its cleavage (route 4 and 5 of Figure 4.4) (Son et al., 2007, 2009). In the same way, the formation of phenol might be produced by the dibenzo-p-dioxin cleavage by the action of OH radicals (route 6 of Figure 4.4) (Son et al., 2007). Finally, PCDD/Fs from 2,8-dichlorodibenzo-p-dioxin has been described as a chlorination reaction in the presence of chlorine in a photolytic treatment (route 7 of Figure 4.4) (Fernández-Castro et al., 2016).

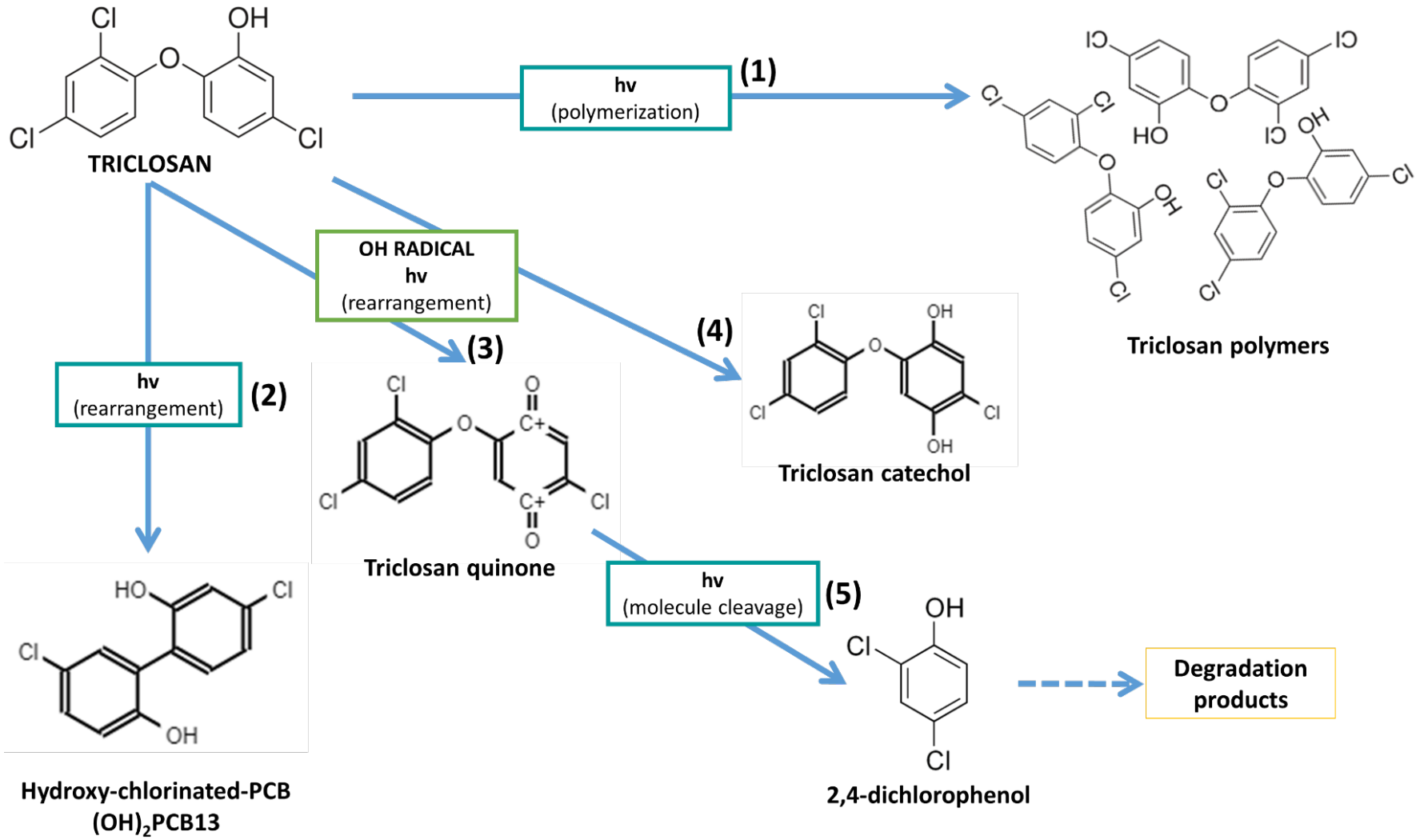

Figure 4.3. Summary of the main TCS photo-degradation pathways: polymerization and rearrangement mechanisms. Adapted from the literature (Rafqah et al., 2006; Yu et al., 2006; Chen et al., 2010; Kliegman et al., 2013). *hv*: photolysis; *OH RADICAL*: photocatalysis.

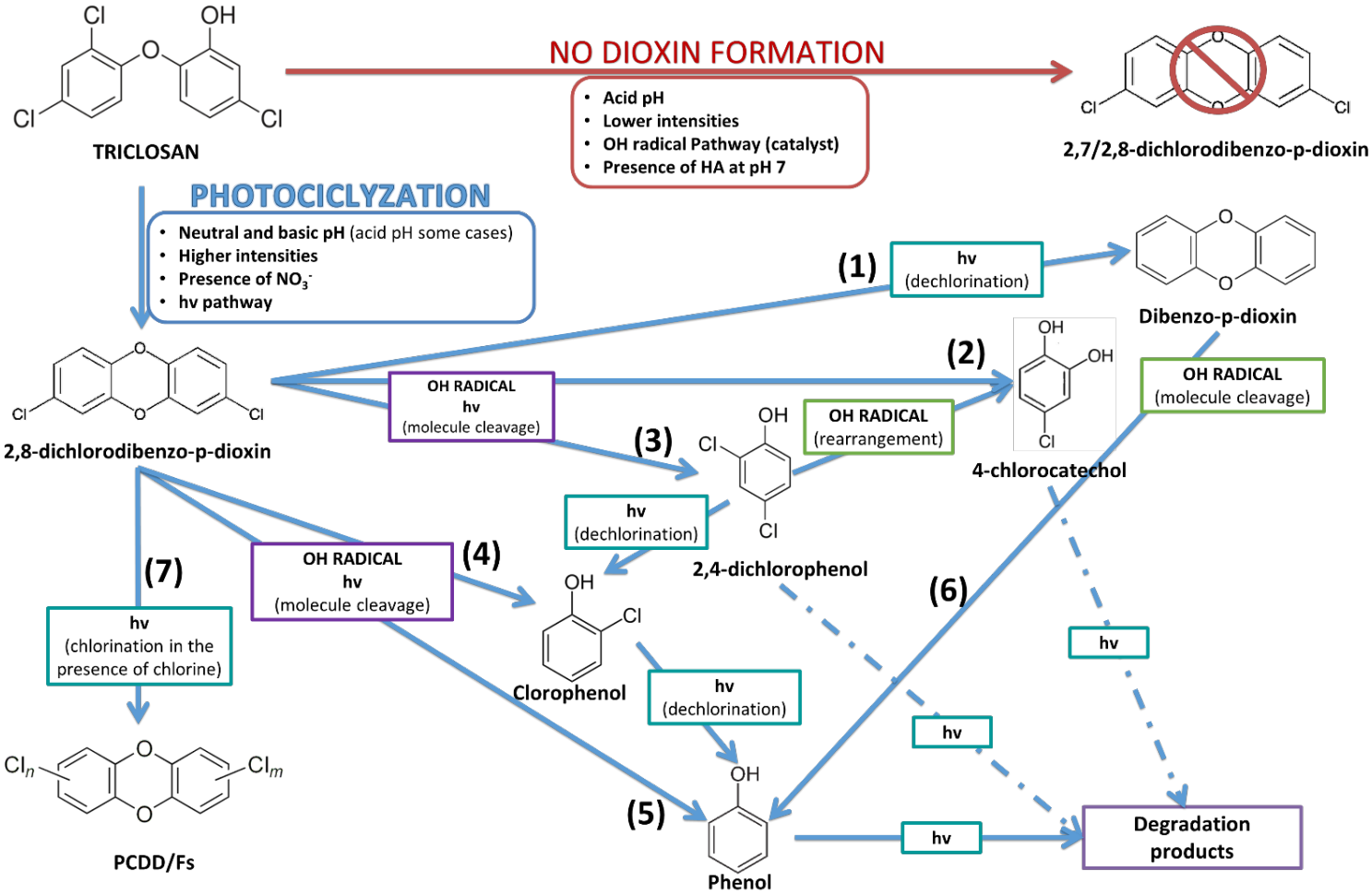

Figure 4.4. Scheme of TCS photodegradation pathways: formation of 2,8-dichlorodibenzo-p-dioxin and its degradation leading to the formation of other by-products. Adapted from the literature (Latch et al., 2005; Son et al., 2007; Wong-Wah-Chung et al., 2007; Son et al., 2009; Kliegman et al., 2013; Constantin et al., 2018; Iovino et al., 2019; Wu et al., 2019). *hv*: photolysis; *OH RADICAL*: photocatalysis.

As a summary, Table 4.2 collects all the products of Triclosan photo-degradation observed in the literature.

Table 4.2. Products formed in the photo-degradation of Triclosan reported in the literature.

Molecule structure of the products of Triclosan photo-degradation observed in the literature		
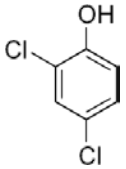	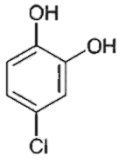	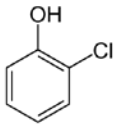
2,4-dichlorophenol	4-chlorocatechol	Chlorophenol
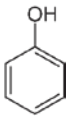	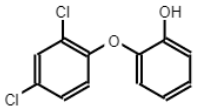	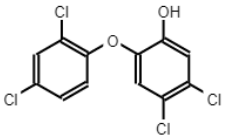
Phenol	Dechlorinated Triclosan	Chlorinated Triclosan
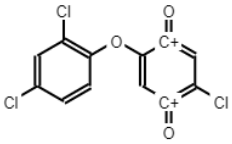	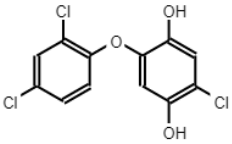	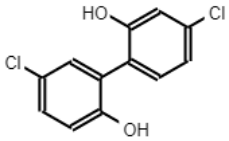
Triclosan quinone	Triclosan catechol	Hydroxy-chlorinated-PCB ($(OH)_2$PCB13)
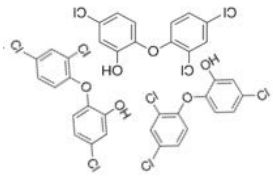	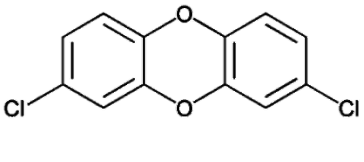	
Triclosan polymers	2,8-dichlorodibenzo-p-dioxin	

4.3. Direct oxidation of Triclosan: photolysis

In this part of the work, the photolysis of Triclosan as well as the by-products formed during the treatment has been investigated. In order to deepen into the reaction mechanisms involved in the photo-transformation of Triclosan and its toxicity, photolysis experiments of its hydrodehalogenation derivatives (Triclosan molecules with less chlorine atoms placed in the three different positions of the Triclosan molecule (Figure 4.5)), have been carried out. The aim of this study is to determine the reaction mechanisms that are behind the photolysis of Triclosan,

achieving a better understanting of the reaction pathways that lead to the formation of PCDD/Fs.

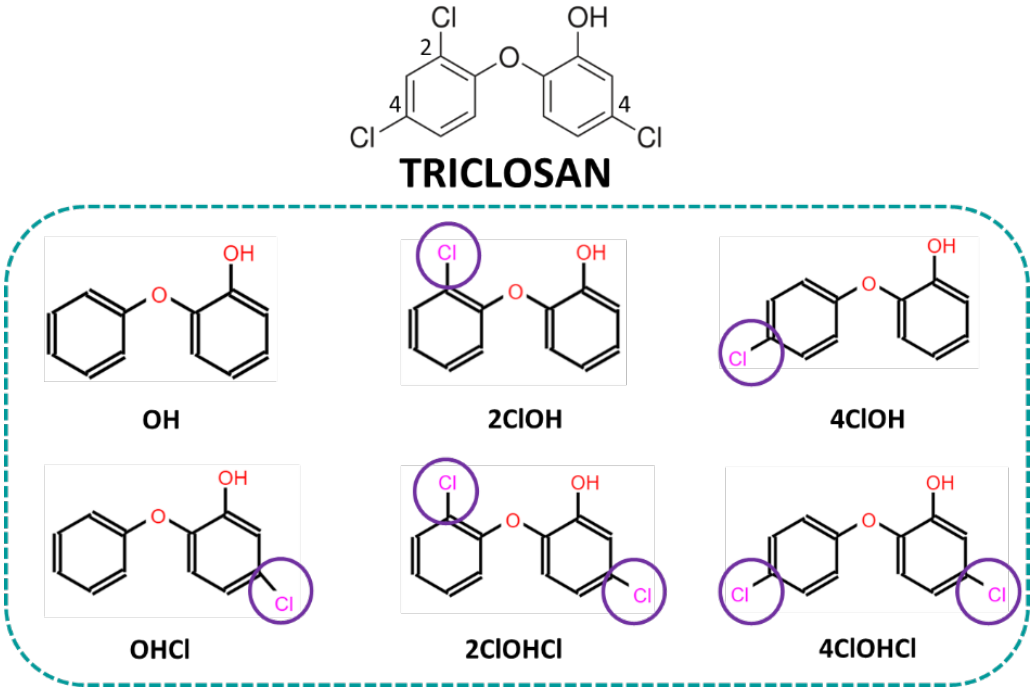

Figure 4.5. Molecular structure of Triclosan and its hydrodehalogenated derivatives.

As explained in the first part of this chapter, it has been reported that the absorbance of Triclosan is higher when it is present in its anionic form, namely when the pH solution is above its pK_a. For this reason, before starting the experiments, in order to ensure the anionic form of the compounds studied (Triclosan and their hydrodehalogenation derivatives), the pK_a of Triclosan and its derivatives were determined.

4.3.1. pK_a determination

In order to get the absorbance spectra of Triclosan at different wavelengths, UV-Vis light spectroscopy of a 5 µM (1.45 mg L^{-1}) synthetic aqueous solution was scanned from 800 to 200 nm in a Varian Cary 100 Bio UV-Visible spectrophotometer was carried out. To stabilize the pH during the measurement, the solutions were made in a 5 mM phosphate buffer solution. Since the measurements were made from acid to basic pH and the initial pH solution of Triclosan was closed to 7, some drops of 1 M HCl were added to the initial solution of Triclosan, adjusting the initial pH of the solution to a value close to 5. Then, the procedure consisted of a slight increase of the pH by adding drops of 0.1 M NaOH and monitoring the absorbance under each pH until the absorbance remained stable, which indicated that the maximum absorbance of the target

compound is reached (Figure 4.6). In the case of Triclosan, the final pH was 10.59. Above this pH the absorbance of Triclosan remained constant. Finally, results displayed in Figure 4.6 demonstrated that Triclosan absorbed more light in the UV region, specifically at 300 nm, at a pH equal or above 10.59. These measurements were made for the hydrodehalogenation derivatives of Triclosan at concentrations of 10 µM (concentration ranging from 1.86 to 2.55 mg L^{-1} depending on the molecular weight of the compound), showing the same behaviour observed for Triclosan; the maximum light absorbance took place at wavelengths of 300 nm for pH above 10.5. Results can be found in Figure 4.7.

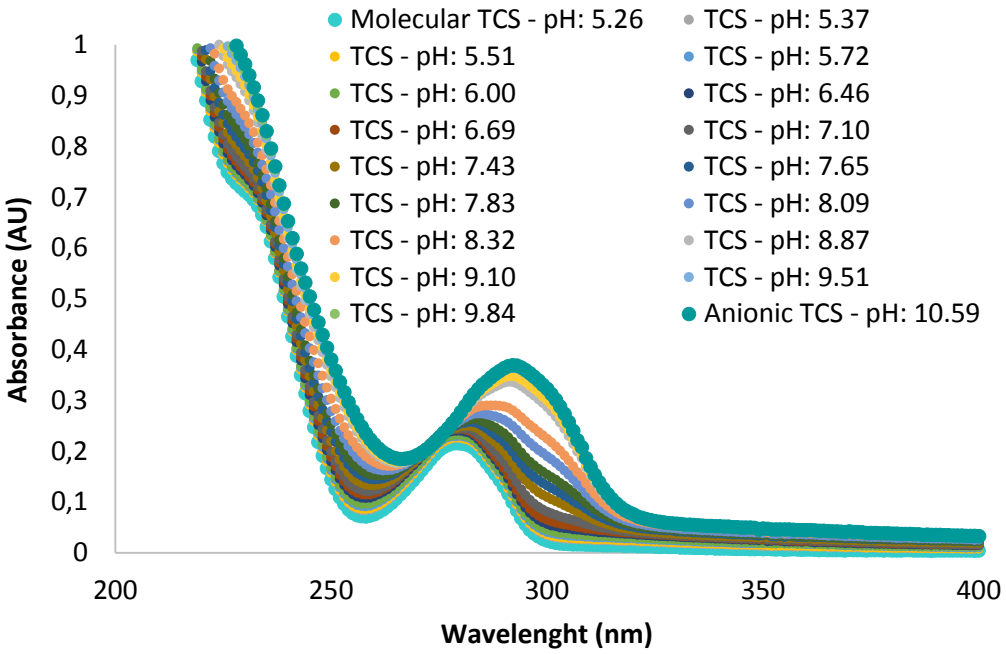

Figure 4.6. Absorbance versus wavelength spectra of anionic (pH: 10.59) and molecular (pH: 7.10) TCS. [TCS]= 5 µM (1.45 mg L^{-1}).

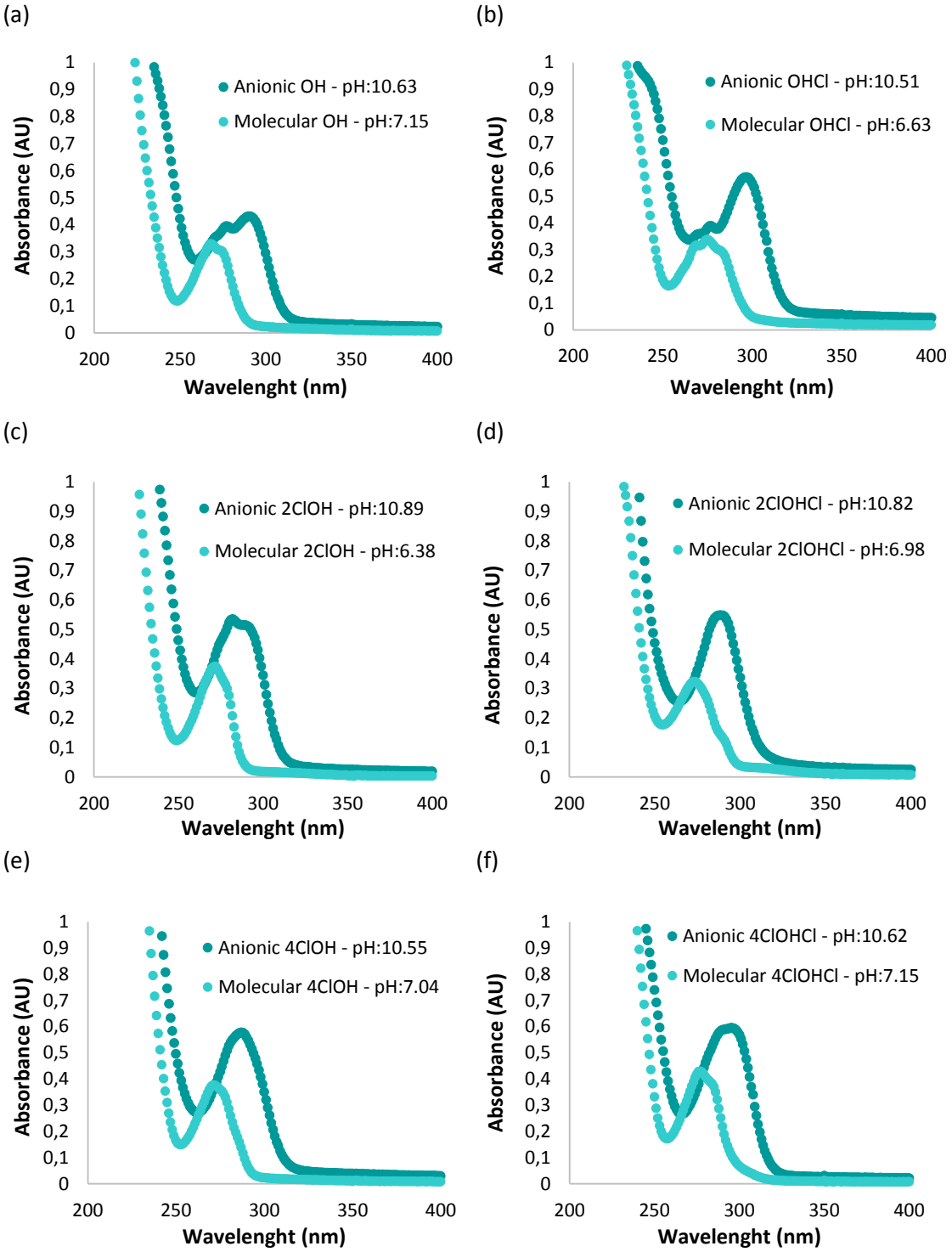

Figure 4.7. Absorbance versus wavelength spectra of anionic and molecular form of hydrodehalogenation derivatives of TCS: (a) OH; (b) OHCl; (c) 2ClOH; (d) 2ClOHCl; (e) 4ClOH; (f) 4ClOHCl. [Hydrodehalogenation derivatives of TCS]= 10 µM (concentration ranging from 1.86 to 2.55 mg L^{-1} depending on the molecular weight of the compound).

To obtain pKa values of Triclosan and its derivatives a graphical method developed by Salgado and Vargas-Hernández (2014) has been applied. The procedure started plotting the absorbance at a wavelength of 300 nm, since it was the maximum light absorbance (anionic Triclosan form), versus pH (Figure 4.8). Then, the curve of the absorbance at 274 nm (molecular Triclosan form) versus the pH was added. The pKa value was determined by the intersection point of the two linear zones of both curves. In the case of Triclosan resulted in a pKa value of 8.31. The same procedure was followed for Triclosan derivatives. Table 4.3 summarizes the pKa values obtained for all the compounds studied.

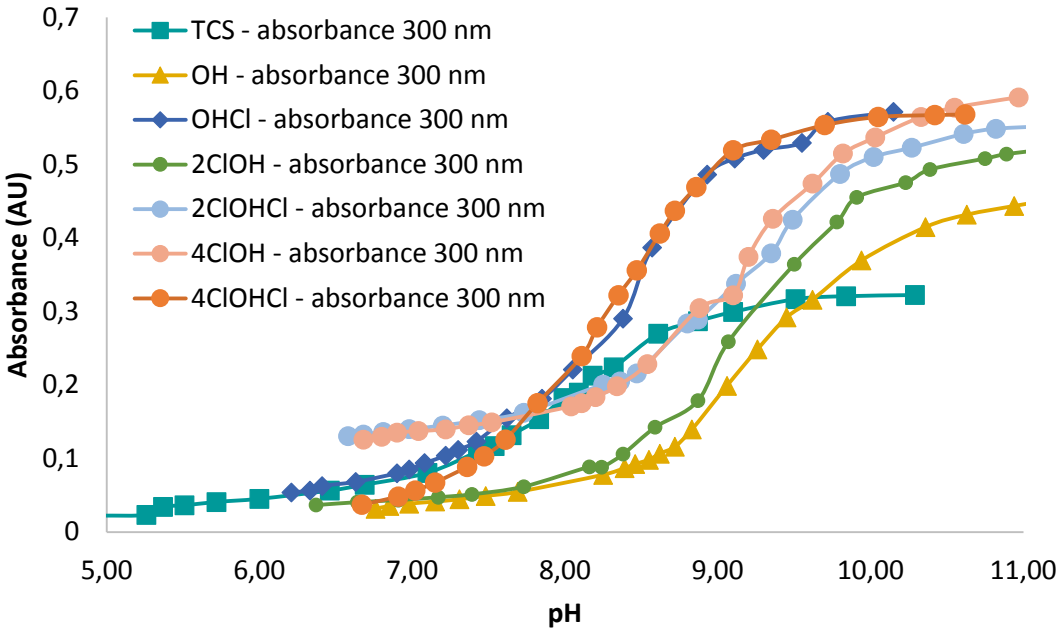

Figure 4.8. Absorbance of TCS and its hydrodehalogenation derivatives at a wavelength of 300 nm at different pH. [TCS]= 5 µM (1.45 mg L^{-1}); [Hydrodehalogenation derivatives of TCS]= 10 mM (concentration ranging from 1.86 to 2.55 mg L^{-1}).

Table 4.3. pK_a values of triclosan and its hydrodehalogenation derivatives.

Name	pKa
Triclosan	8.31
OH	9.83
OHCl	8.66
2ClOH	9.39
4ClOH	9.44
2ClOHCl	9.23
4ClOHCl	8.60

To ensure the maximum light absorbance of Triclosan and its derivatives when photolysis experiments were carried out, they had to be present in their anionic forms. In this way, the pH of the solution had to be above the pK_a values shown in Table 4.2 for each compound.

4.3.2. Photolysis of Triclosan and its derivatives

The photolytic experiments of Triclosan and its hydrodehalogenation derivatives, with an initial concentration of each compound of 50 µM (equivalent to 14.48 mg L^{-1} in the case of Triclosan and ranging from 9.30 to 12.75 mg L^{-1} for its hydrodehalogenation derivatives) dissolved in a carbonate buffer solution (0.01 M, pH 10.6; $NaHCO_3$ (121.3 mg), Na_2CO_3 (293.1 mg) in 1 L ultrapure water) containing 10 % acetonitrile, have been carried out in a photoreactor Rayonet Srinivasan-Griffin with 300 nm wavelengths bulbs (Institute of Biogeochemistry and Pollutant Dynamics, ETH, Zürich). A carbonate buffer solution was used to maintain a constant pH of 10.6, monitored along the oxidation treatment. In this way, Triclosan and their hydrodehalogenation derivatives were in anionic form during the time of experiments. Acetonitrile was used to ensure the complete dissolution of Triclosan in the aqueous sample due to its low solubility as mentioned in the previous chapter. Figure 4.9 shows the results of Triclosan degradation as well as the intermediate products, which were identified without further processing by HPLC (Dionex Ultimate 3000).

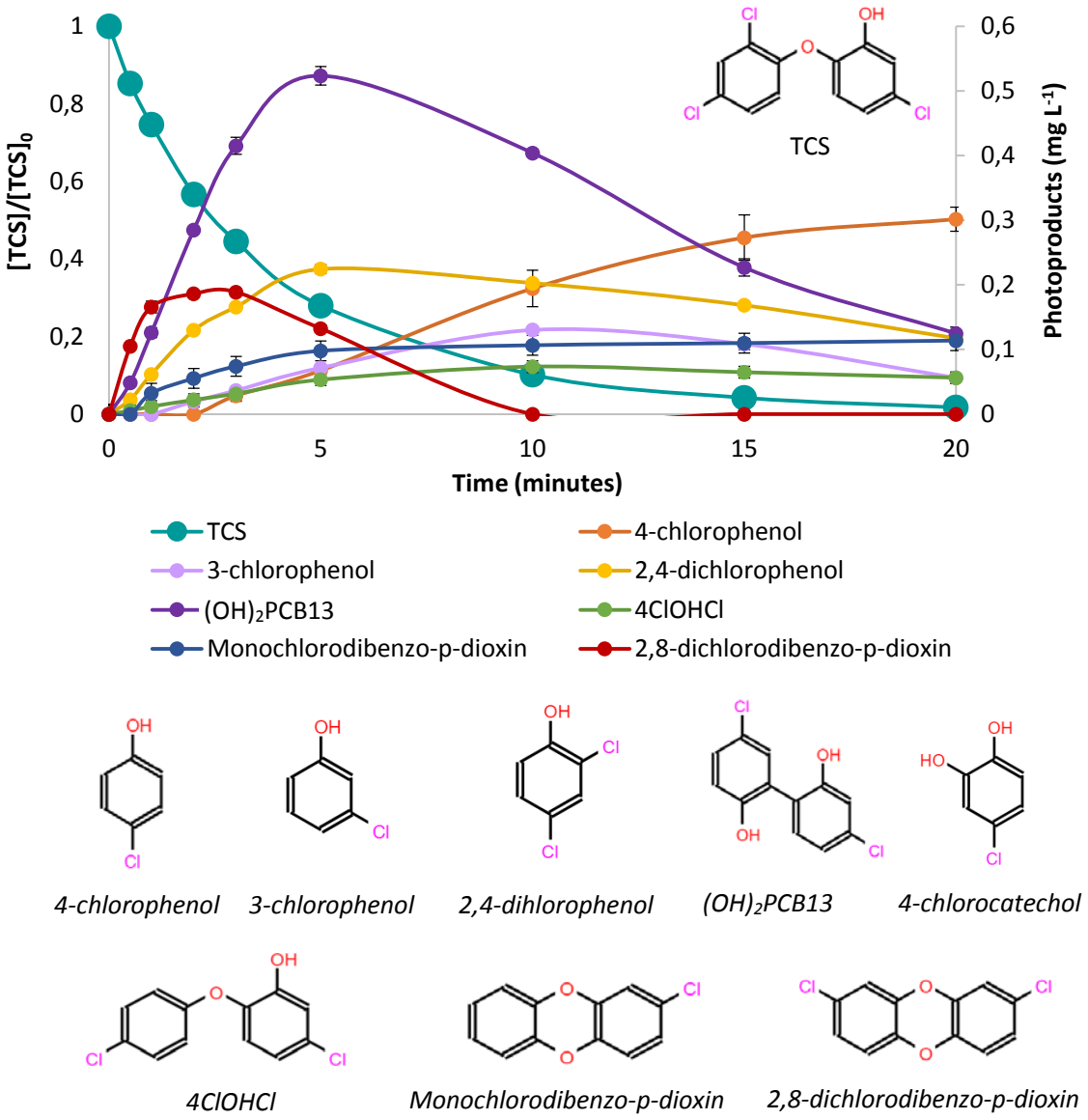

Figure 4.9. Photolysis degradation of TCS and formation of TCS photoproducts. $[TCS]_0$= 50 µM (14.48 mg L^{-1}).

As it can be observed in the Figure 4.9, 3 minutes were required to reduce the initial Triclosan concentration by 50 %. In order to completely degrade Triclosan, the photolytic treatment took 20 minutes. Three phenols were observed as photoproducts of Triclosan: 3-chlorophenol, 4-chlorophenol and 2,4-dichlorophenol. 3-chlorophenol and 2,4-dichlorophenol were identified as intermediate products, reaching a maximum concentration value of 0.13 and 0.22 mg L^{-1} at 10 and 5 minutes, respectively, and decreased to 0.06 and 0.12 mg L^{-1} at the end of the photolytic treatment. However, the concentration of 4-chlorophenol increased along the oxidation treatment, reaching a value of 0.30 mg L^{-1} at the end of the experiment (Figure 4.9). $(OH)_2$PCB13 (4,5´-dichloro-[1,1´-biphenyl]-2,2´-diol) was also identified as an intermediate photoproduct of Triclosan; the highest concentration was observed at 5 minutes of treatment

with a value of 0.52 mg L^{-1}, then it decreased to 0.12 mg L^{-1} after 20 minutes, final point of the experiment. Figure 4.9 also shows that 4ClOHCl, hydrodehalogenation derivative of Triclosan, remained constant at an average concentration of 0.06 mg L^{-1} after 5 minutes. Finally, monochlorodibenzo-p-dioxin and 2,8-dichlorodibenzo-p-dioxin were observed as photoderivative products of Triclosan. However, 2,8-dichlorodibenzo-p-dioxin acted as an intermediate product, achieving its maximum concentration value of 0.19 mg L^{-1} at 3 minutes, and, then, decreasing to zero at 10 minutes. On the other hand, monochlorodibenzo-p-dioxin remained constant after 5 minutes with an average concentration of 0.1 mg L^{-1}. Finally, 4-chlorocatechol was qualitatively identified after 10 minutes as a photoproduct of Triclosan; however, the quantification method was not developed. Experimental data are depicted together with error bars, which have been obtained after replication of the experiments.

Then, photolytic experiments of hydrodehalogenation derivatives of Triclosan have been carried out and results are shown below following the scheme displayed in Figure 4.5. Firstly, results for OH derivative photolysis are represented in Figure 4.10.

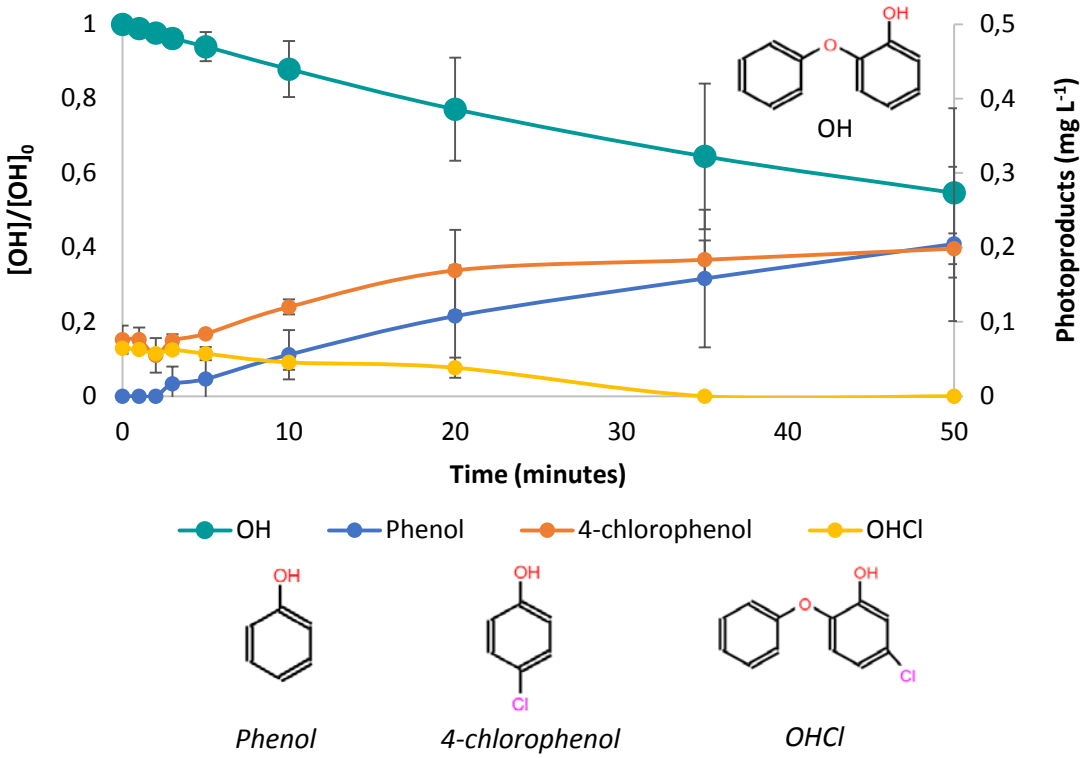

Figure 4.10. Photolysis degradation of OH and formation of OH photoproducts. $[OH]_0$= 50 µM (9.30 mg L^{-1}).

In comparison to Triclosan, OH degradation rates were slower, requiring 50 minutes to reduce its concentration by almost 50 %. These experimental results indicated that chlorine-carbon bonds of the molecule of Triclosan presented the lowest bond dissociation energies of the molecule, resulting in a quicker photo-transformation of Triclosan. In the photolysis of the OH derivative, phenol and 4-chorophenol were found at the highest concentrations (0.2 mg L^{-1}) at the end of the experiment. However, 4-chlorophenol was observed in the initial OH solution with a concentration of 0.08 mg L^{-1}, indicating that it might have been produced as an impurity in the synthesis of the target compound. Then, along the oxidation of OH, 4-chlorophenol may have been formed as a consequence of OH photo-degradation. In the same way, the OHCl derivative was observed in the initial OH solution, associated to an impurity formed during the synthesis of OH. Its concentration decreased along the treatment as a result of the photolytic oxidation.

Next, the photolysis of OHCl hydrodehalogenation derivative (molecular structure displayed in Figure 4.5) has been assessed and depicted in Figure 4.11.

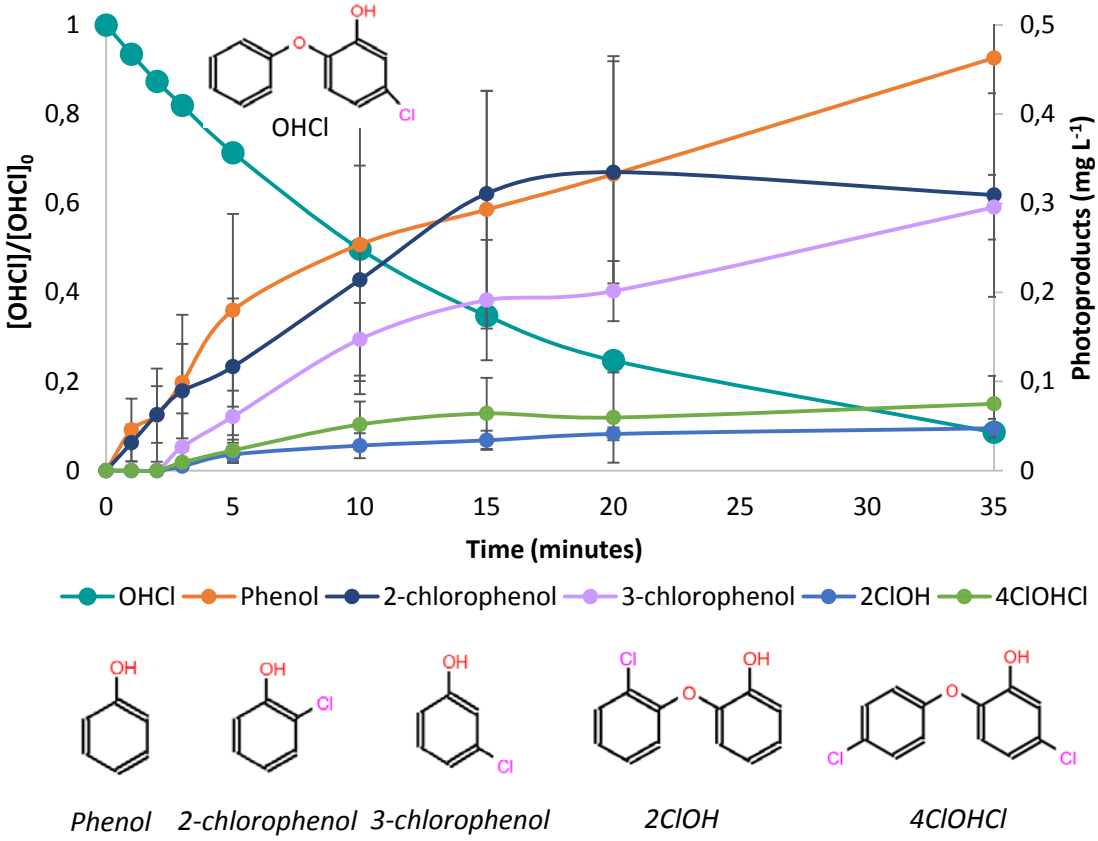

Figure 4.11. Photolysis degradation of OHCl and formation of OHCl photoproducts. $[OHCl]_0$= 50 µM (11.02 mg L^{-1}).

It took 10 minutes to reduce the concentration of OHCl by 50 %. Nevertheless, almost complete degradation was produced after 35 minutes. Phenol, 2-chlorophenol, 3-chlorophenol, 2ClOH and 4ClOHCl were observed as photoproducts of OHCl. Among them, phenol was the product observed at the highest concentration, achieving a value as high as 0.45 mg L^{-1} at 35 minutes, followed by 2-chlorophenol and 3-chlorophenol, which reached a maximum concentration of 0.33 mg L^{-1} at 20 minutes and 0.30 mg L^{-1} at 35 minutes, respectively. Lastly, 2ClOH and 4ClOHCl derivatives were found at concentrations below 0.1 mg L^{-1} at the end of the experiment. Furthermore, catechol was qualitatively identified as an intermediate photoderivative product of Triclosan with a maximum concentration at 20 minutes; however, the quantification method was not developed. Finally, no dioxin congeners were observed on the degradation of OH derivative.

These results were followed by the photolysis of 2ClOH hydrodehalogenation derivative (molecular structure displayed in Figure 4.5) (Figure 4.12).

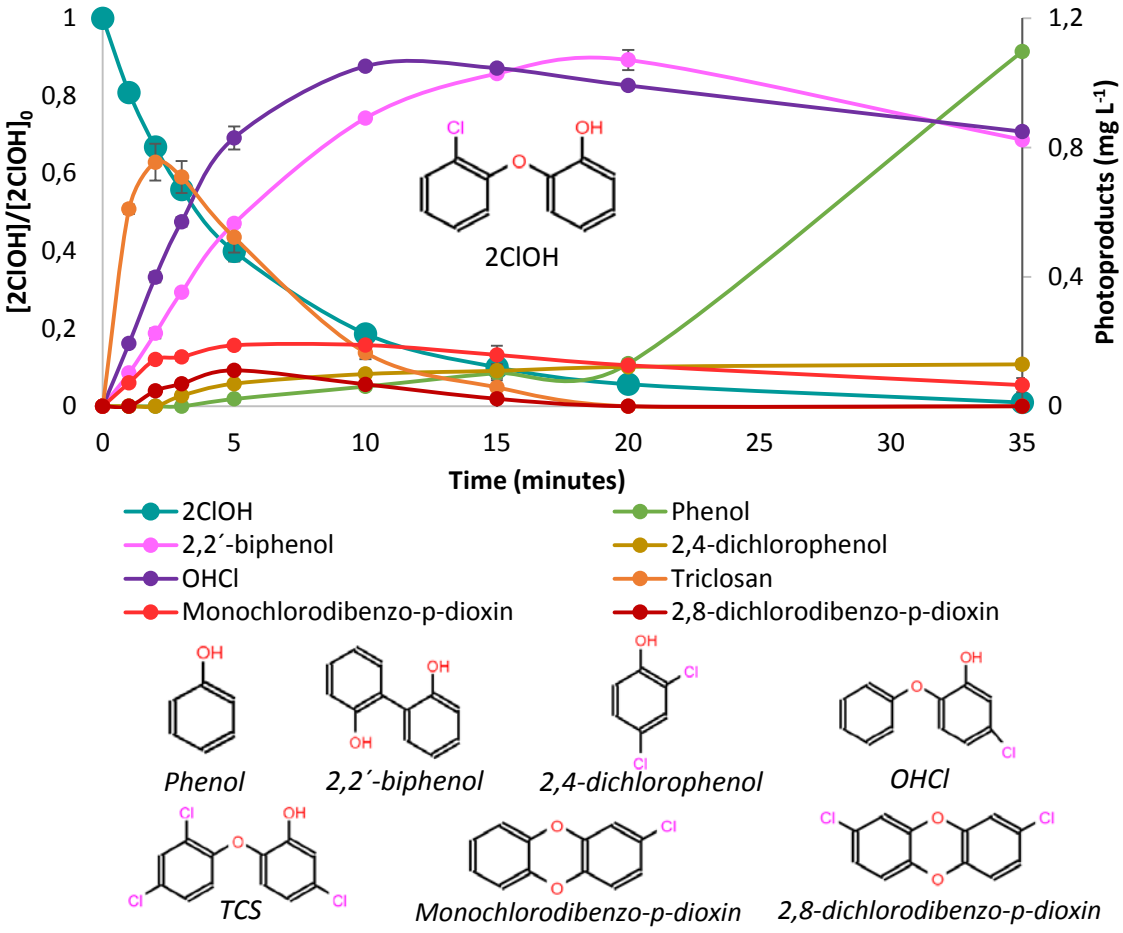

Figure 4.12. Photolysis degradation of 2ClOH and formation of 2ClOH photoproducts. $[2ClOH]_0$= 50 µM (11.02 mg L^{-1}).

Between 3 and 5 minutes were required to eliminate 50 % of the target compound and 35 minutes to reduce its concentration to zero. OHCl derivative and 2,2´-biphenol were observed as the main intermediate products of 2ClOH photolysis: 1.05 mg L^{-1} at 10 minutes and 1.07 mg L^{-1} at 20 minutes, respectively. Triclosan was also observed as an intermediate product of 2ClOH, achieving the highest concentration at 2 minutes (0.75 mg L^{-1}), and associated to a chlorination reaction of 2ClOH. As final photoderivative product, phenol achieved a final concentration of 1.10 mg L^{-1} after 35 minutes. Finally, it has to be highlighted the formation of monochlorodibenzo-p-dioxin and 2,8-dichlorodibenzo-p-dioxin. A similar behaviour was observed on the photolytic degradation of Triclosan; monochlorodibenzo-p-dioxin remained constant along the treatment with an average concentration of 0.19 mg L^{-1}, however, 2,8-dichlorodibenzo-p-dioxin acted as an intermediate photoderivative product that achieved a maximum concentration value of 0.11 mg L^{-1} after 5 minutes. Furthermore, hydroquinone was qualitatively identified as a photoproduct of Triclosan after 5 minutes; however, the quantification method was not developed.

Next, the photolysis of 2ClOHCl hydrodehalogenation derivative (molecular structure displayed in Figure 4.5) has been assessed and depicted in Figure 4.13.

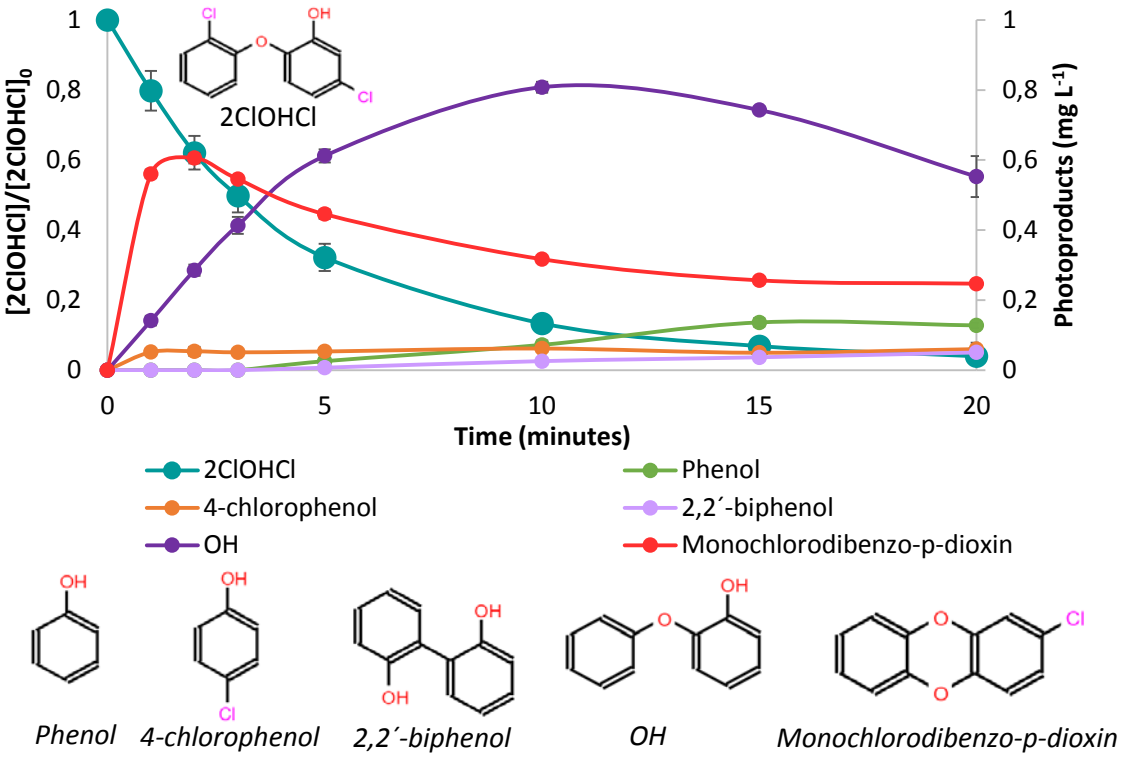

Figure 4.13. Photolytic degradation of 2ClOHCl and formation of 2ClOHCl photoproducts. $[2ClOHCl]_0$= 50 µM (12.75 mg L^{-1}).

2ClOHCl hydrodehalogenation derivative required 20 minutes to achieve an almost complete elimination. Nevertheless, after 3 minutes the concentration of 2ClOHCl was reduced by 50 %. OH derivative, found as an intermediate product, reached values of 0.81 mg L^{-1} at 10 minutes, then, it decreased to 0.55 mg L^{-1} at the end of the experiment. Monochlorodibenzo-p-dioxin was also identified as one of the main intermediate products of the photolysis of 2ClOHCl. Its maximum concentration was found at 2 minutes (0.61 mg L^{-1}). Then, it remained constant at an average concentration of 0.25 mg L^{-1} between 15 and 20 minutes. Phenol, 4-chlorophenol and 2,2´-biphenol were identified as photoderivative products of 2ClOHCl at low concentrations, below 0.2 mg L^{-1}. Furthermore, hydroquinone was qualitatively identified as a photoderivative product of Triclosan, however, the quantification method was not developed.

Then, Figure 4.14 shows the results related to 4ClOH derivative (molecular structure displayed in Figure 4.5) during the photolysis treatment.

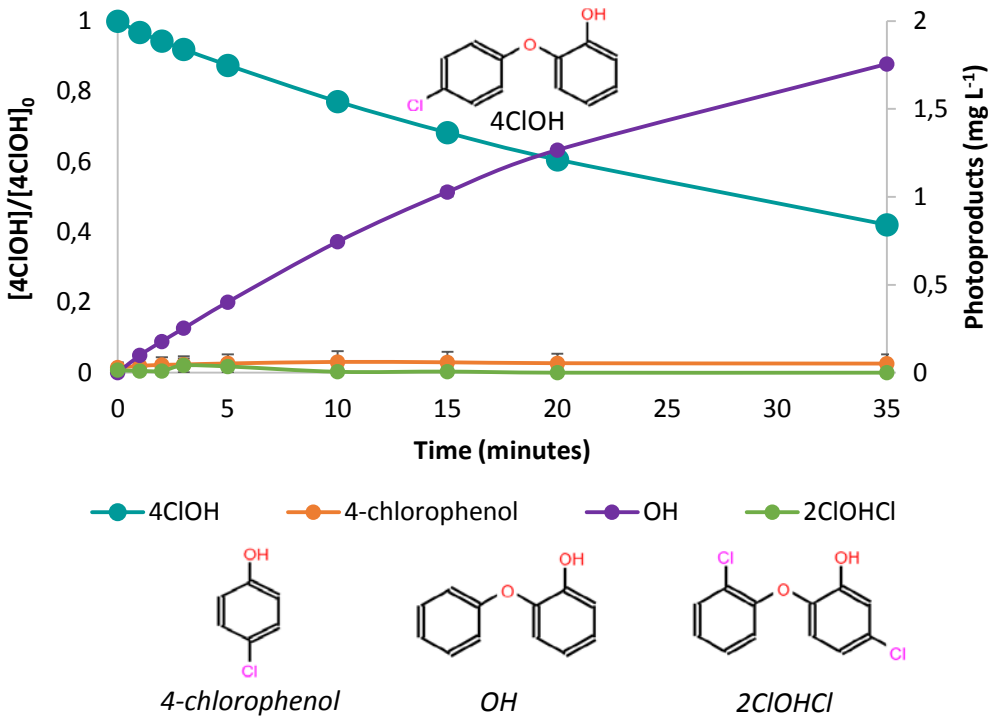

Figure 4.14. Photolysis degradation of 4ClOH and formation of 4ClOH photoproducts. $[4ClOH]_0$= 50 µM (11.02 mg L^{-1}).

After 35 minutes, 42 % of the target compound was removed from the solution. In this case, OH hydrodehalogenation derivative was the main photoproduct observed, with a concentration of 1.76 mg L^{-1} at the end of the experiment. 4-chlorophenol and 2ClOHCl were

found at very low concentration, less than 0.01 mg L^{-1}. Furthermore, no dioxin congeners were observed on the photolysis of 4ClOH derivative.

Finally, the last hydrodehalogenation derivative of Triclosan studied was 4ClOHCl (molecular structure displayed in Figure 4.5) (Figure 4.15).

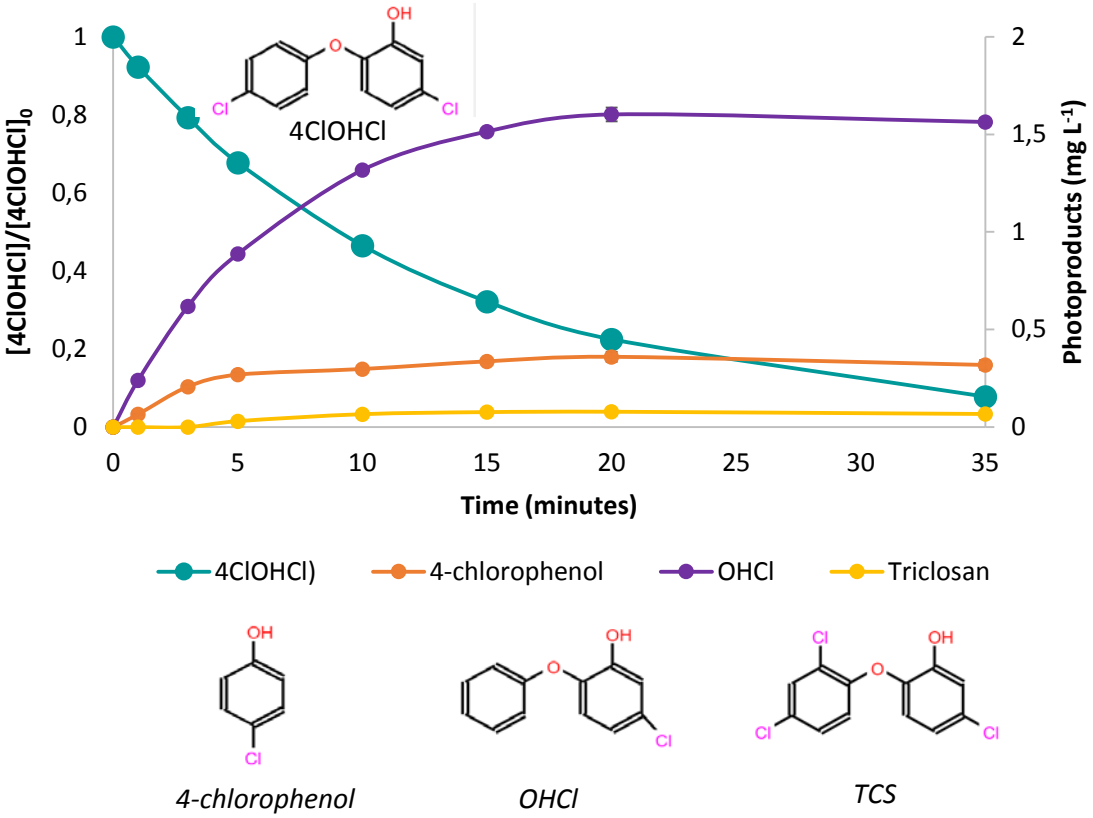

Figure 4.15. Photolytic degradation of 4ClOHCl and formation of 4ClOHCl photoproducts. $[4ClOHCl]_0$= 50 µM (12.75 mg L^{-1}).

More than 90 % 4ClOHCl was eliminated after 35 minutes. Furthermore, 10 minutes were required to reduce its concentration by 50 %. 4-chlorophenol, OHCl and Triclosan were identified as photoproducts of 4ClOHCl derivative. OH was observed at the highest concentration (1.60 mg L^{-1}), followed by 4-chlorophenol (0.36 mg L^{-1}) and Triclosan (0.08 mg L^{-1}). It has to be highlighted that no dioxin congener was observed in the photolysis of 4ClOHCl. Furthermore, hydroquinone was qualitatively identified but the quantification method was not developed.

A summary of by-products observed in the photo-degradation of Triclosan and its hydrodehalogenation derivatives is presented in Table 4.4.

Table 4.4. Summary of the by-products detected on the photolysis of Triclosan and its hydrodehalogenation derivatives.

			TARGET COMPOUND						
			TCS 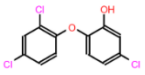	OH 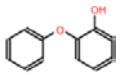	OHCl 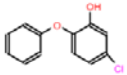	2ClOH 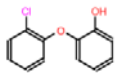	2ClOHCl 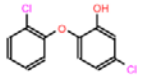	4ClOH 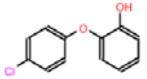	4ClOHCl 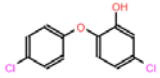
			Literature	*Experimentally observed*					
BY-PRODUCTS	Phenol		X		X	X	X	X		
	2-chlorophenol		X			X				
	3-chlorophenol		X	X		X				
	4-chlorophenol		X	X	X			X	X	X
	2,4-dichlorophenol		X	X			X			
	$(OH)_2$PCB13		X	X						
	2,2´-biphenol						X	X		
	Hydroquinone						X	X		X
	Catechol					X				
	4-chlorocatechol		X	X						
	2,8-dichlorodibenzo-p-dioxin		X	X			X			
	Monochlorodibenzo-p-dioxin			X			X	X		
	TCS						X			X
	Dechlorinated TCS	OH	X					X	X	
		OHCl			X		X			X
		2ClOH				X				
		2ClOHCl							X	
		4ClOH								
		4ClOHCl		X		X				
	Chlorinated TCS		X							
	TCS polymers		X							
	TCS quinone/TCS catechol		X							

To conclude, in this section the study of the photolytic treatment of Triclosan and their hydrodehalogenation derivatives has been carried out. The following conclusions are drawn after the analysis of the experimental results,

(i) The time required to achieve high degradation rates increased as the number of chlorine atoms present in the molecule decreased. For this reason, Triclosan presented the highest degradation rate in comparison to their hydrodehalogenation derivatives;

(ii) The main photoproducts observed in the photolysis of Triclosan were 4-chlorophenol, 2,4-dichlorophenol and $(OH)_2$PCB13 (4,5´-dichloro-[1,1´-biphenyl]-2,2´-diol);

(iii) The presence of dioxins (monochlorodibenzo-p-dioxin and/or 2,8-dichlorodibenzo-p-dioxin) was only observed when the target molecule presented a chlorine atom in the position number 2 of the benzene ring, that is Triclosan, 2ClOH and 2ClOHCl derivatives, verifying the suspicion that the chlorine placed in position 2 of the benzene ring is the responsible of the formation of these species.

(iv) Finally, the formation of chlorophenols, 2,4-dichlorophenol, $(OH)_2$PCB13, 4-chlorocatechol, 2,8-dichlorodibenzo-p-dioxin and dechlorinated Triclosan products were also observed in the literature. Monochlorodibenzo-p-dioxin was detected in this work, but not observed in the literature. However, although phenol, chlorinated Triclosan, Triclosan polymers, Triclosan quinone and Triclosan catechol were products identified by some authors, they were not detected in this work.

4.3.3. Photolysis of the intermediate products in Triclosan degradation

In order to make the most of the pieces of the puzzle fit together and achieve a better understanding of the reaction mechanisms involved in the photolysis of Triclosan, photolytic experiments of the main intermediate products observed at the highest concentrations in the photolysis of Triclosan and its derivatives have been carried out. With this purpose, initial solutions of 20 µM of $(OH)_2$PCB13 (5.10 mg L^{-1}), 2,2´-biphenol (3.72 mg L^{-1}), phenol (1.88 mg L^{-1}), 2,-chlorophenol (2.57 mg L^{-1}), 3-chorophenol (2.57 mg L^{-1}), 4-chlorophenol (2.57 mg L^{-1}) and 2,4-dichlorophenol (3.26 mg L^{-1}) dissolved in a carbonate buffer solution (0.01 M, pH 10.6; $NaHCO_3$ (121.3 mg), Na_2CO_3 (293.1 mg) in 1 L ultrapure water) containing 10 % acetonitrile were

prepared and photolize in a photoreactor Rayonet Srinivasan-Griffin with 300 nm wavelengths bulbs. Results are shown in Figures 4.16 and 4.17.

(a)

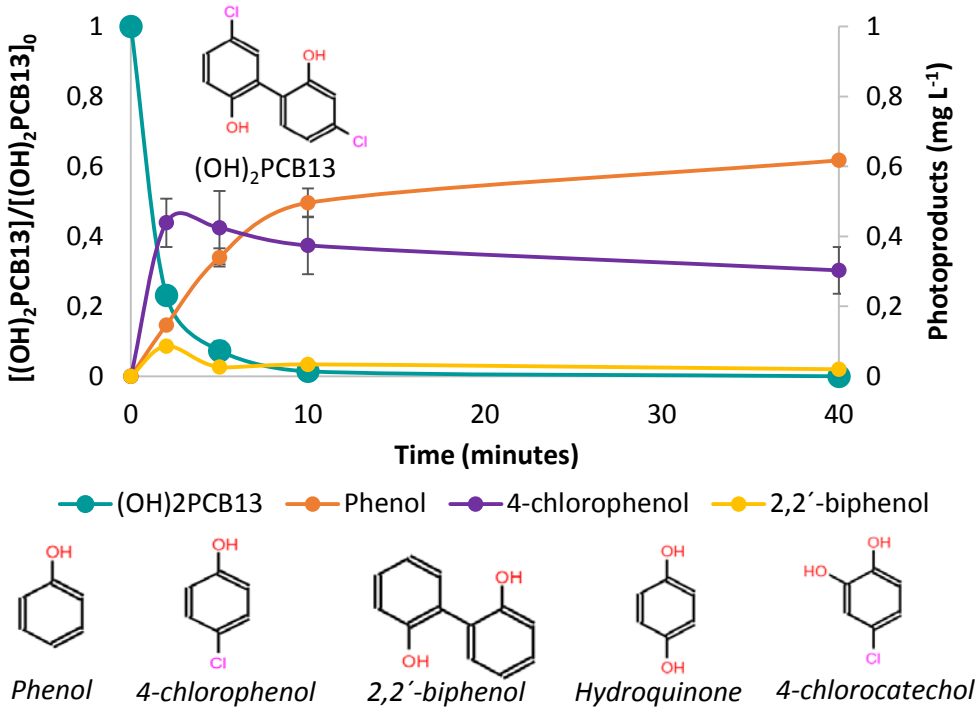

(b)

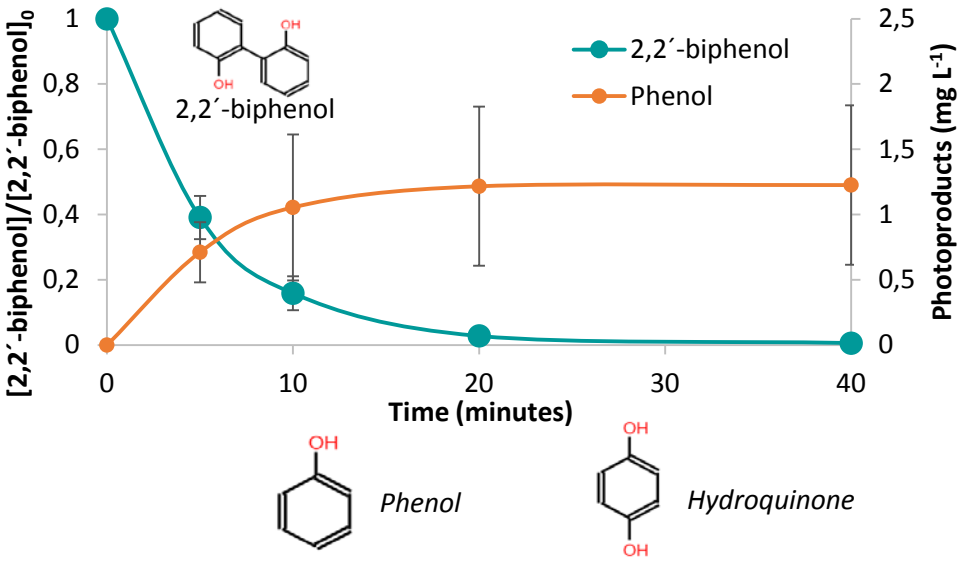

Figure 4.16. Photolytic degradation of $(OH)_2PCB13$ (a) and 2,2´-biphenol (b) and their photoproducts formation. $[(OH)_2PCB13]_0$= 20 µM (5.10 mg L^{-1}); $[2,2´biphenol]_0$= 20 µM (3.72 mg L^{-1}).

Figure 4.16(a) displays the photolysis of $(OH)_2$PCB13, which was the main intermediate product formed in the photo-degradation of Triclosan. As it has been previously shown in Figure 4.9, $(OH)_2$PCB13 achieved its maximum concentration after 5 minutes of Triclosan treatment, and then, its concentration decreased until the end of the treatment, leading to the formation of their own photo-products as shown in Figure 4.16(a). In this way, it can be observed that the photodegradation of this biphenyl gave rise to the formation of phenol, 4-chlorophenol and 2,2´-biphenol. After 10 minutes of treatment, when no $(OH)_2$PCB13 remained in the solution, the concentration of their photo-products varied very slightly. After 40 minutes, the concentration of 4-chlorophenol slightly decreased from 0.37 to 0.30 mg L^{-1} while phenol concentration slowly increased from 0.50 to 0.62 mg L^{-1}. The photodegradation of $(OH)_2$PCB13 also led to the formation of the 2,2´-biphenol intermediate at a very low concentration; achieving the highest concentration value after 2 minutes (0.09 mg L^{-1}). Furthermore, 4-chlorocatechol and hydroquinone were qualitatively identified as intermediate products in the degradation of $(OH)_2$PCB13, however, the quantification method was not developed. On the other hand, Figure 4.16(b) depicts the results obtained for the photolysis of 2,2´-biphenol, being phenol the main photo-product identified, achieving values up to 1.23 mg L^{-1}. Finally, hydroquinone was also qualitatively observed as an intermediate product of 2,2´-biphenol.

Next, photolysis results obtained for phenol, 2-chlorophenol, 3-chlorophenol, 4-chlorophenol and 2,4-dichlorophenol are shown in Figure 4.17(a-e).

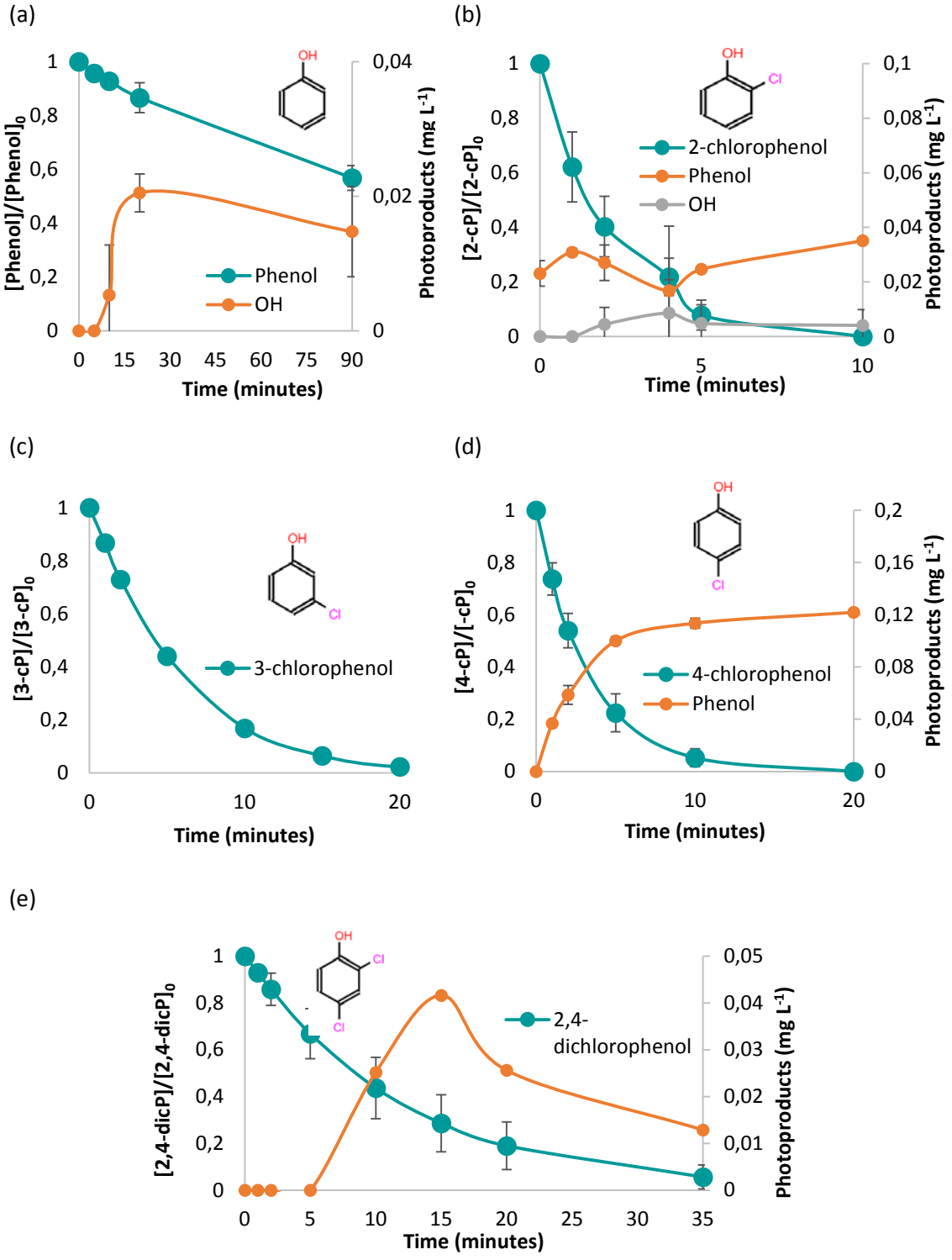

Figure 4.17. Photolysis degradation of phenols and their photoproducts formation: phenol (a); 2-cP (2-chlorophenol) (b); 3-cP (3-chlorophenol) (c); 4-cP (4-chlorophenol) (d); 2,4-dichlorophenol (2,4-dicP) (e). $[Phenol]_0$= 20 µM (1.9 mg L^{-1}); $[2\text{-cP}]_0$, $[3\text{-cP}]_0$, $[4\text{-cP}]_0$ = 20 µM (2.6 mg L^{-1}); $[2,4\text{-dicP}]_0$= 20 µM (3.3 mg L^{-1}).

Firstly, phenol (Figure 4.17(a)) showed a slow photo-degradation, requiring 90 minutes to decrease its concentration by almost 50 %. Along the photolytic treatment, the formation of OH (hydrodehalogenation derivative of Triclosan) has been observed. Furthermore, catechol and hydroquinone were qualitatively observed. In the same way, the photolysis of 2-chlorophenol (Figure 4.17(b)) has been assessed, achieving a complete elimination after 10 minutes. Phenol was observed in the initial solution, associated to an impurity present in the 2-chlorophenol solution. Furthermore, phenol remained constant along the photolytic treatment of the target compound. OH was identified at a very low concentration, reaching values up to $8.6 \cdot 10^{-3}$ mg L^{-1} after 4 minutes. The formation of hydroquinone as an intermediate product of 2-chlorophenol was qualitatively observed. Next, Figure 4.17(c) displayed the results obtained for the photolysis of 3-chlorophenol, showing a fast photo-degradation (complete degradation observed after 20 minutes). In this case, only catechol and hydroquinone were qualitatively determined. Similar behaviour was observed for 4-chorophenol photolysis (Figure 4.17(d)), and a complete removal was achieved at 20 minutes. Phenol was the main photo-product identified, with a concentration of 0.12 mg L^{-1} after 20 minutes of treatment. In addition, hydroquinone was also qualitatively observed as an intermediate product. Finally, the photolysis of 2,4-dichlorophenol was carried out (Figure 4.17(e)). In this case, 35 minutes were required to decrease its concentration by almost 100 %. 3-chlorophenol was identified as the main intermediate product of 2,4-dichlorophenol, with a maximum concentration of 0.04 mg L^{-1} at 15 minutes. Furthermore, hydroquinone was qualitatively determined as an intermediate of 2,4-dichlorophenol photolysis. A summary of the by-products observed in the photo-degradation of the main photo-products of Triclosan is presented in Table 4.5.

To sum up, the photolysis of the main intermediate products of Triclosan has been assessed in order to complete the reaction mechanisms involved in the photolysis of Triclosan. $(OH)_2$PCB13 and 2,2´-biphenol presented faster photo-degradation rates, resulting in a complete removal at 10 and 20 minutes, respectively. In the same way, the three chlorophenols and 2,4-dichlorophenol proved to be highly photo-sensitive, presented very fast removal rates. However, in the case of phenol, and with similar behaviour than OH (hydrodehalogenation derivative of Triclosan), due to the absence of a chlorine-carbon bond in the molecule (which has the lowest bond dissociation energy in the molecules studied in this thesis), the degradation rates were very slow in comparison to the phenols that had a chlorine atom in the phenol ring. For this reason, the time required to degrade phenol was higher. Regarding to the photo-products formed during the oxidation of the main intermediate products of Triclosan, hydroquinone was observed in all of them, followed by phenol, which was observed in almost

all of them, except for 3-chlorophenol and 2,4-dichlorophenol. Catechol was observed in the oxidation of phenol and 3-chlorophenol, whereas OH (hydrodehalogenation derivative of Triclosan) was observed for phenol and 2-chlorophenol oxidation. With the experimental results shown above, a reaction mechanism describing the photolysis of Triclosan has been proposed and it is developed in the next section.

Table 4.5. Summary of the by-products observed on the photolysis of the main photo-products of Triclosan and its derivatives.

		TARGET COMPOUND						
		$(OH)_2$PCB13 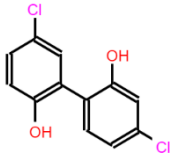	**2,2´-biphenol** 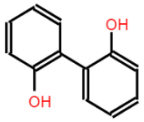	**Phenol** 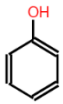	**2-chlorophenol** 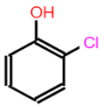	**3-chlorophenol** 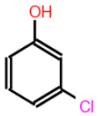	**4-chlorophenol** 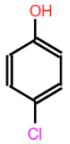	**2,4-dichlorophenol** 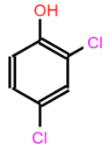
BY-PRODUCTS	**Phenol**	X	X		X		X	
	2-chlorophenol							
	3-chlorophenol							X
	4-chlorophenol	X						
	2,4-dichlorophenol							
	Catechol			X		X		
	4-chlorocatechol	X						
	2,2´-biphenol	X						
	Hydroquinone	X	X	X	X	X	X	X
	OH			X	X			

4.3.4. Formation pathway of the intermediate products of Triclosan photo-degradation

Based on the literature as well as on the experimental results obtained in section 1.3.2 (photolysis of Triclosan and its hydrodehalogenation derivatives) and in section 1.3.3 (photolysis of the main intermediate products resulting from Triclosan oxidation), the pathways involved in the photolytic degradation of Triclosan are presented. $(OH)_2$PCB13, observed in the literature as an intermediate product of Triclosan photolysis (section 4.2 in Figure 4.3 (route 2)), might be formed through a biradical intermediate, involving an initial cleavage of a carbon-oxygen bond. Then, an spirobenzoxetane is formed from the rearrangement of the biradical to, finally, be reduced to give the hydroxylated biphenyl product (Kliegman et al., 2013) (see Figure 4.18). $(OH)_2$PCB13 was observed as an intermediate product that is also degraded along the treatment, which might lead to the formation of chlorophenols through its bond cleavage.

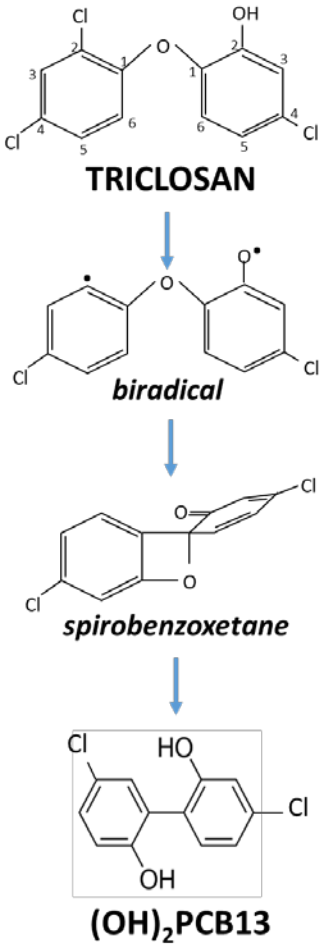

Figure 4.18. Reaction mechanism that describe the formation of $(OH)_2$PCB13 from TCS during the photolytic treatment.

In addition, 2,4-dichlorophenol was experimentally identified as one of the main intermediate products in the photolysis of Triclosan. The formation of this phenol has been reported by many authors as previously detailed (Sanchez-Prado et al., 2006; Kliegman et al., 2013; Chen et al., 2016; Iovino et al., 2019). It might be produced by a photo-induced hydrolysis of Triclosan due to the effect of the UV light that produces an ether cleavage leading to the formation of 2,4-dichlorophenol (Figure 4.19). This pathway was previously addressed in the literature and displayed in Figure 4.2 (route 1). Then, 2,4-dichlorophenol might be dechlorinated to generate chlorophenols (pathway reported also in the literature in Figure 4.2 (route 9)). In the same way, a dechlorination reaction of Triclosan might formed hydrodehalogenation derivatives of Triclosan, such as 4ClOHCl and OHCl (pathway previously addressed in the literature and displayed in Figure 4.2 (route 6). Then, 4ClOHCl and OHCl molecules could be broken to form chlorophenols (pathway reported in the literature in Figure 4.2 (routes 9 and 10)). The formation of catechol, hydroquinone and phenol could be explained as a dechlorination reaction followed by rearrangement of the molecule. In this case, catechol pathway was reported in the literature as the rearrangement of 2,4-dichlorophenol molecule (Figure 4.2, route 4), whereas the formation of phenol as a dechlorination reaction of chlorophenol (Figure 4.2, route 11). However, the generation of hydroquinone was not previously reported in the literature. Furthermore, 2,2´-biphenol, observed in the photolysis of $(OH)_2$PCB13, led also to the formation of phenol and hydroquinone (Figure 4.19), pathways not reported in the literature. On the other hand, some compounds were identified in the literature as by-products on the photolysis of Triclosan, but not detected in this work, such as phenol (corresponding to route 8 of Figure 4.2), chlorinated Triclosan (corresponding to route 5 of Figure 4.2), Triclosan polymers (route 1 of Figure 4.3) and Triclosan quinone and Triclosan catechol (routes 3 and 4 of Figure 4.3).

During the photolysis of Triclosan, the formation of 2,8-dichlorodibenzo-p-dioxin and monochlorodibenzo-p-dioxin was observed. As it was displayed in Figure 4.9, 2,8-dichlorodibenzo-p-dioxin was an intermediate product that achieved its maximum concentration after 3 minutes and then it was completely degraded. However, monochlorodibenzo-p-dioxin remained constant along the treatment. The formation of 2,8-dichlorodibenzo-p-dioxin has been previously reported by many authors (Wong-Wah-Chung et al., 2007; Kliegman et al., 2013; Bianco et al., 2015; Iovino et al., 2019). The formation of this congener might be explained by a cyclization reaction of Triclosan. Furthermore, the formation of dioxins was only observed for those hydrodehalogenation derivatives of Triclosan that had a chlorine atom in the position number 2 of the benzene ring (Figure 4.20). This could explain that

the reaction mechanism involved in the formation of this congener started with a breakage of the chloro-carbon bond located in the position 2 of the benzene ring of Triclosan, which then leads to the formation of a biradical. Then, the reaction is followed by an spirobenzoxetane formation, as occurred with the $(OH)_2$PCB13 formation. Finally, this specie cycles to form 2,8-dichlorodibenzo-p-dioxin. As this congener is an intermediate photo-product, the formation of monochlorodibenzo-p-dioxin might be produced due to the dechlorination reaction of the dichlorodibenzo-p-dioxin congener. This pathway was also reported by Kliegman et al. (2013).

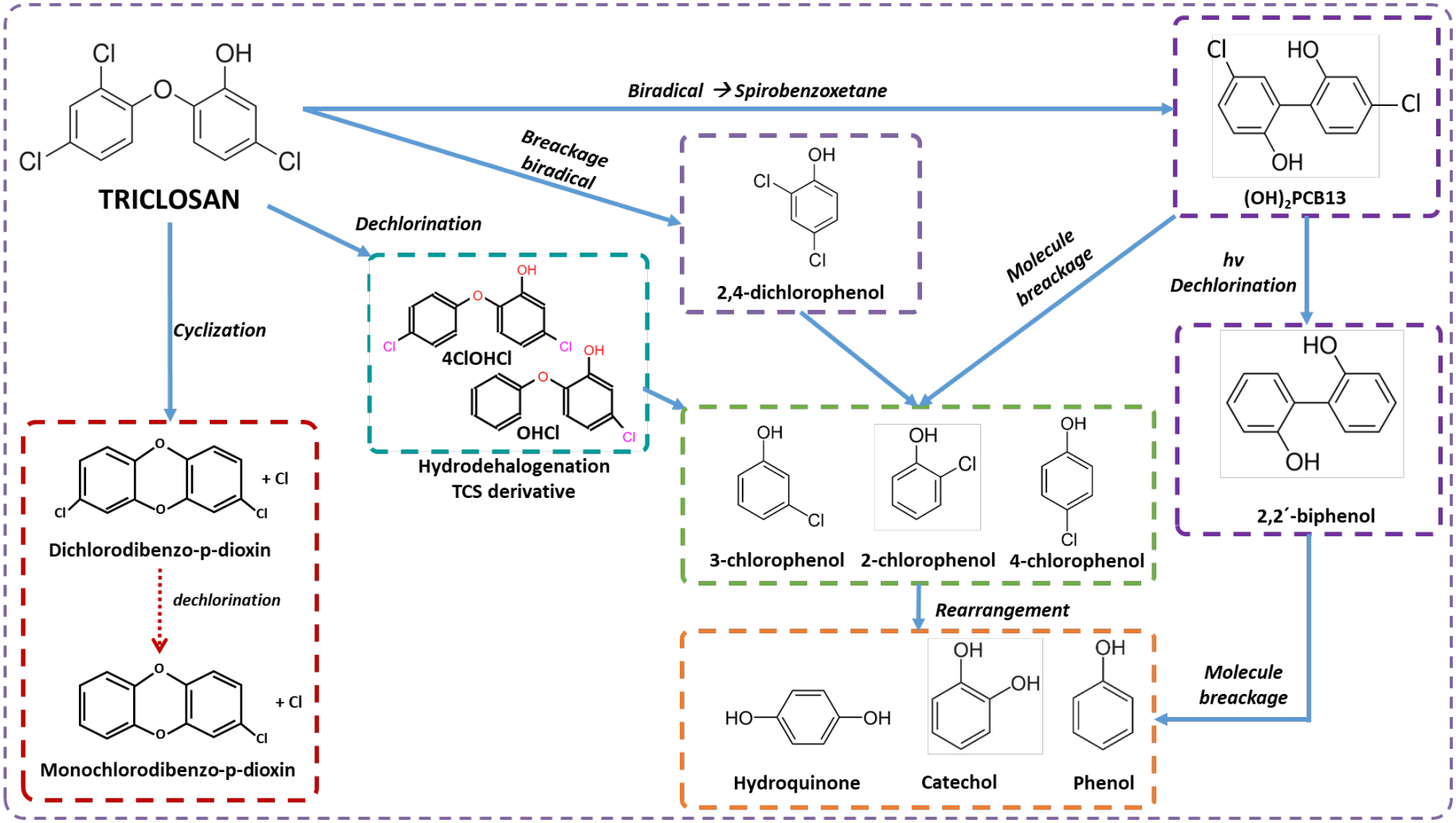

Figure 4.19. Reaction mechanisms proposal for the photolysis of TCS.

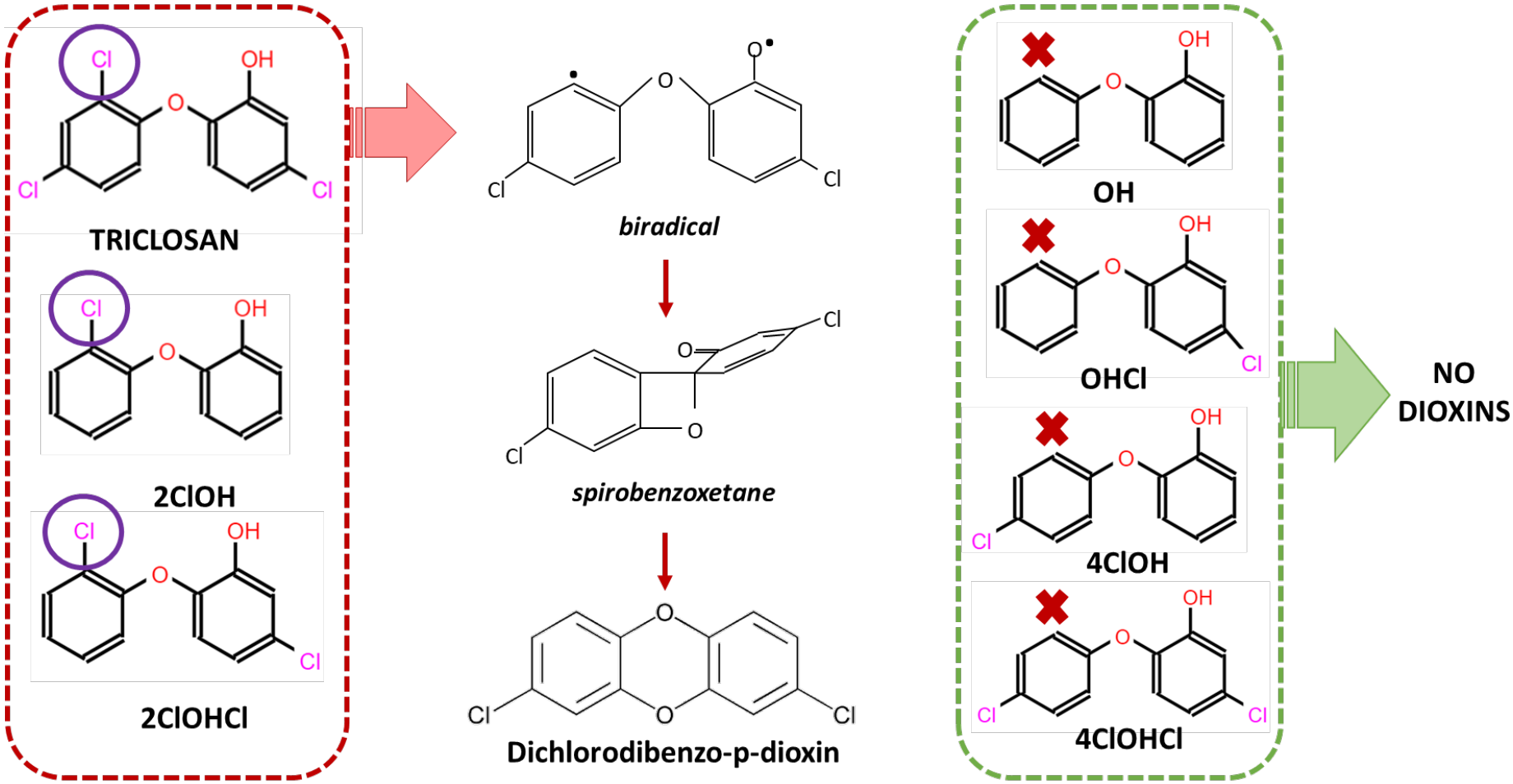

Figure 4.20. Scheme representing the formation of dichlorodibenzo-p-dioxin from TCS and their hydrodehalogenation derivatives.

4.4. Indirect oxidation of Triclosan: photocatalysis

In this part of the work, in order to deepen into the effect of a catalyst on the photolysis of Triclosan, the photocatalytic treatment of Triclosan and the potential formation of by-products has been investigated. The experiments, with an initial concentration of 10 mg L^{-1} containing 1 % of acetonitrile and neutral pH, have been carried out in a UV LED photoreactor (APRIA System S.L.; section 2.3). LEDs had an emission wavelength between 375 and 380 nm. The acetonitrile aliquot was the minimum volume required to ensure the complete dissolution of Triclosan in the aqueous sample. In order to study the influence of the catalyst, three different concentrations of TiO_2 were employed: 0.75, 1.0 and 1.5 g L^{-1}. The treated sample was filtered before analysis. Triclosan was monitored by HPLC, while the intermediate products were qualitatively analysed by GC-MS and quantitatively measured by HPLC. Finally, the analysis of PCDD/Fs was analysed by HRGC-HRMS following the EPA 1613 method.

Figure 4.21 shows the influence of the catalyst doses employed in the rate of degradation of Triclosan.

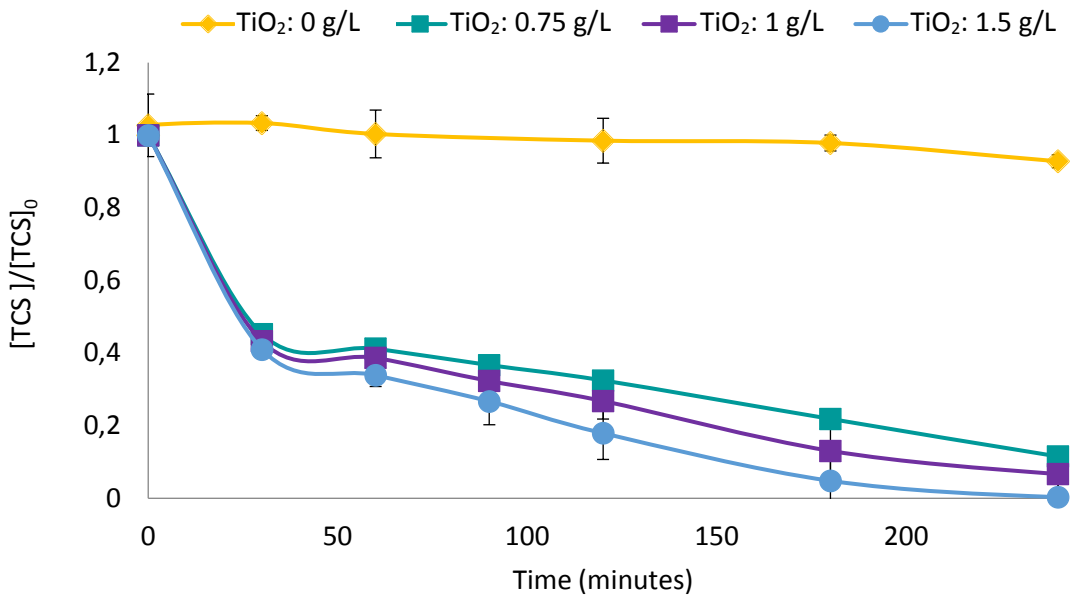

Figure 4.21. Influence of the TiO_2 loading on the change of TCS concentration with time. $[TCS]_0$= 10 mg L^{-1}.

Firstly, an experiment without catalyst was carried out. As it can be observed, no degradation of Triclosan was produced. This fact is associated to the wavelength applied; Triclosan did not absorb light at the wavelength employed (375 – 380 nm). However, this wavelength was applied to optimize the TiO_2 photocatalyst activity, since wavelengths between

300 and 400 nm activate TiO_2 (Kanakaraju et al., 2014). As it can be observed in Figure 4.21, no differences between the three photocatalyst loadings were found when the initial concentration of Triclosan was reduced by 50 %. However, after 30 minutes of treatment, 1.5 g L^{-1} TiO_2 led to faster degradation rates, indicating that the light screening phenomena was not achieved at this concentration of TiO_2. For this reason, for the three photocatalyst loadings studied in this work, 1.5 g L^{-1} of TiO_2 was considered as the optimum dose taking 4 hours to achieve a complete Triclosan removal. Nevertheless, the differences were not very large when using doses of 0.75 and 1 g L^{-1} and 5 hours were required to eliminate nearly 100 %. Experimental data are depicted together with error bars, which have been obtained after replication of the experiments.

4.4.1. Major intermediate products in the photocatalysis of Triclosan

Although Triclosan disappeared completely during the photocatalytic treatment, different oxidation by-products could be formed, which could give rise to an increase of the final toxicity. As reported in the first part of the chapter, the reaction mechanisms involved in a photocatalytic treatment consist on the formation of OH radicals, which likely provoke an ether cleavage of Triclosan molecule and lead to the formation of smaller molecules. In this work, along with the quantitative determination of the change in Triclosan concentration, GC–MS analysis were performed to identify intermediate products formed during the photocatalytic oxidation of 10 mg L^{-1} of Triclosan. The qualitative analysis confirmed the formation of 2,4-dichlorophenol as an intermediate product (Figure 4.22). Furthermore, it was quantified by HPLC and results are shown in Figure 4.23. The maximum concentration was observed after 30 minutes for the three TiO_2 doses studied, reaching an average concentration of 0.70 mg L^{-1}. Then, when using 1.5 g L^{-1} of photocatalyst, 2,4-dichlorophenol decreased to zero after 4 hours of oxidation. Nevertheless, as the concentration of TiO_2 decreased, the rate of formation of 2,4-dichlorophenol kinetics was lower, associated to the slower removal of Triclosan. The formation of 2,4-dichlorophenol was supported by the literature and it was reported as one of the main products observed in the photocatalysis of Triclosan, formed through a homolytic scission of the carbon-oxygen bond (Latch et al., 2003; Rafqah et al., 2006; Son et al., 2007, 2009; Sankoda et al., 2011; Stamatis et al., 2014; Constantin et al., 2018). Although the formation of chlorophenol and 4-chlorocatechol has been reported in the literature (Rafqah et al., 2006; Son et al., 2009; Sankoda et al., 2011; Stamatis et al., 2014; Constantin et al., 2018), they have been not detected in this work. In the same way, and supported by the literature (Rafqah et al., 2006; Son et al., 2009; Stamatis et al., 2014), the formation of 2,8-dichlorodibenzo-p-dioxin was not observed.

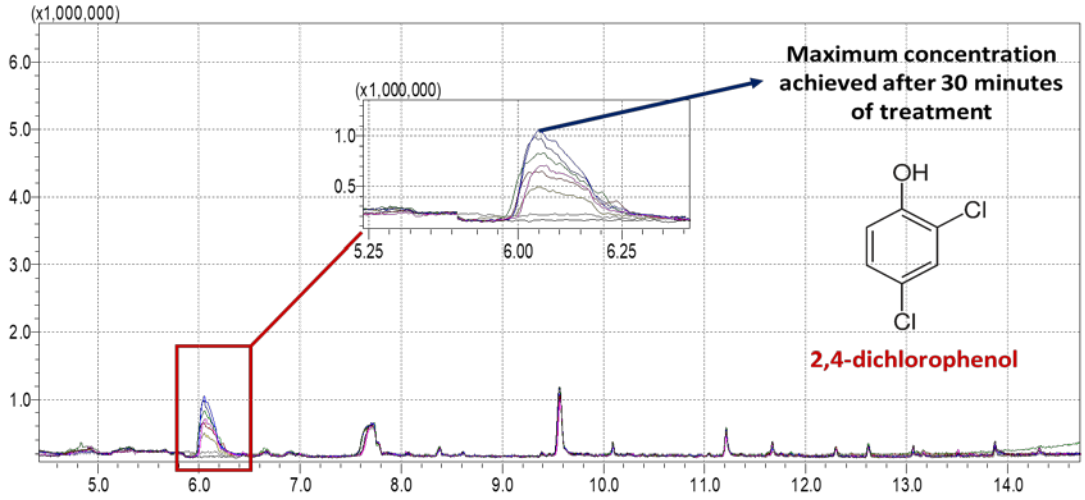

Figure 4.22. GC-MS chromatogram of the photocatalytic oxidized samples with time.

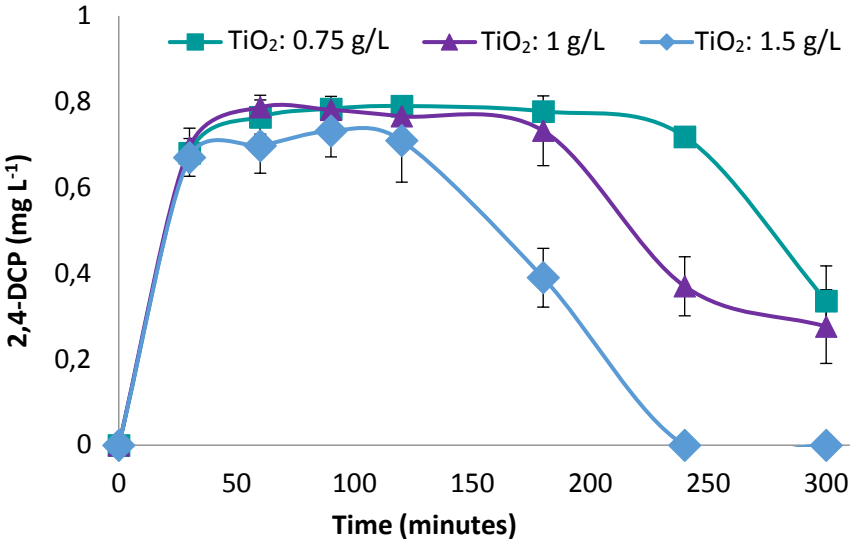

Figure 4.23. Influence of the TiO_2 loading on the formation of 2,4-dichlorophenol during TCS photocatalytic treatment with time.

4.4.2. Formation of highly chlorinated PCDD/Fs in the photocatalysis of Triclosan

With the aim of deepen on to the final toxicity of the treated samples, in this section, the formation of highly chlorinated PCDD/Fs in the photocatalysis of Triclosan has been analysed. The analytical method is detailed in the experimental section and followed EPA 1613 method (section 2.5). Although the samples contained TiO_2 as catalyst, it remained in the aqueous phase in the first steps of the preparation and purification method. In order to avoid the possible

contamination of the experimental system by the accumulation of PCDD/Fs, a blank solution was analysed before the experiments. The results obtained for the blank solution showed very low concentrations of PCDD/Fs. Figure 4.24 shows the concentration of the homologues, from TCDD/Fs to OCDD/Fs (tetra to octachlorinated dibenzo-p-dioxins and dibenzofurans), that have been identified in the untreated and photocatalytic oxidized Triclosan samples when Triclosan has completely disappeared, that is at 5 hours (time selected to ensure that no Triclosan remained in the solution). Experimental data are depicted together with error bars, which have been obtained after replication of the experiments.

According to the results depicted in Figure 4.24, low concentrations of PCDD/Fs have been found in the untreated sample, being TCDF the group of homologues that presents the highest concentration ($1.8 \cdot 10^{1}$ pg L^{-1}), accounted for 46.0 % of the total PCDD/Fs profile. The total PCDD/Fs concentration increased from $2.3 \cdot 10^{1}$ pg L^{-1} for the untreated sample to $1.0 \cdot 10^{5}$, $1.2 \cdot 10^{5}$ and $9.8 \cdot 10^{2}$ pg L^{-1} for the three TiO_2 concentrations studied in this thesis. TCDD increased from 2.4 pg L^{-1} for the untreated sample to $2.0 \cdot 10^{3}$, $7.9 \cdot 10^{2}$ and $8.6 \cdot 10^{1}$ pg L^{-1} for those samples treated with 0.75, 1 and 1.5 g L^{-1} of TiO_2, respectively, accounted for 1.9, 0.6 and 8.9 % of the total PCDD/Fs concentration. As shown in Figure 4.25 (a), the homologues concentration from PeCDD to OCDD slightly increased in comparison to the untreated sample when 0.75 and 1 g L^{-1} of TiO_2 doses were used. However, when 1.5 g L^{-1} was used as catalyst loading, the concentration of these homologues (from PeCDD to OCDD) showed a decrease in comparison to the untreated sample. Regarding to PCDFs profile (Figure 4.25 (b)), it was certainly the group of homologues which presented the highest concentration, accounted for more than 90.4 % of the total PCCD/Fs concentration, specifically, 98.0, 99.3 and 90.4 % when using 0.75, 1 and 1.5 g L^{-1} of TiO_2, respectively. Within this groups, TCDF increased considerably from $1.8 \cdot 10^{1}$ pg L^{-1} for the untreated sample to $1.0 \cdot 10^{5}$, $1.2 \cdot 10^{5}$ and $8.8 \cdot 10^{2}$ pg L^{-1} for those samples treated with 0.75, 1 and 1.5 g L^{-1} of TiO_2, respectively; accounted for 98.0, 99.3 and 90.4 % of the total PCDD/Fs concentration. For the rest of furan homologues (from PeCDF to OCDF) the concentration did not substantially increase, maintaining a concentration ranging from $2.5 \cdot 10^{-1}$ to 8.1 pg L^{-1} for both the untreated and treated samples. For both profiles, PCDDs and PCDFs, the concentration of the homologue groups decreased as the chlorination degree increased and as the concentration of catalyst increased.

a)

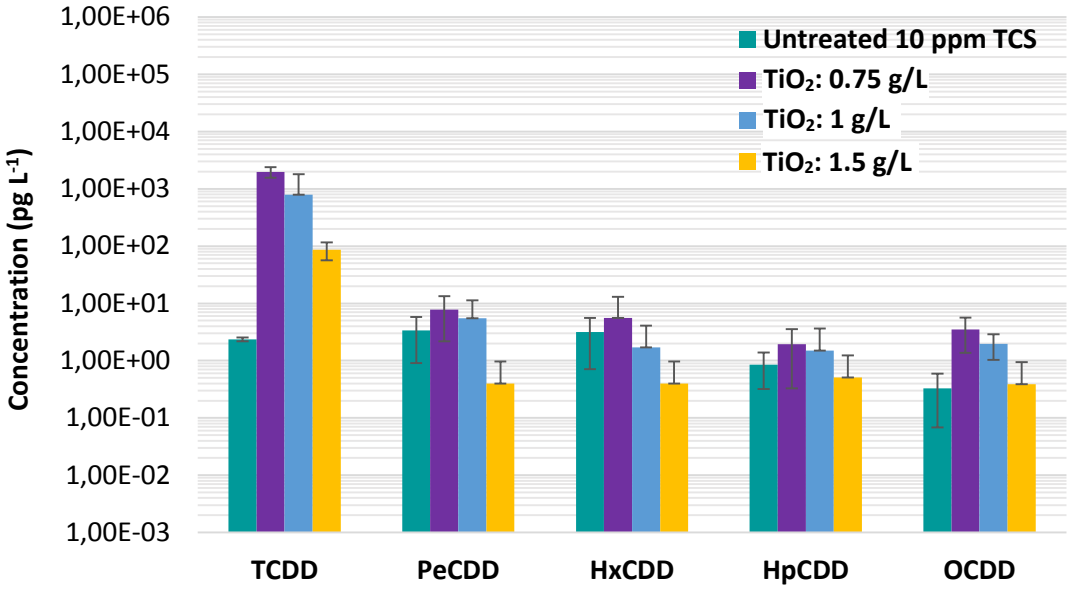

b)

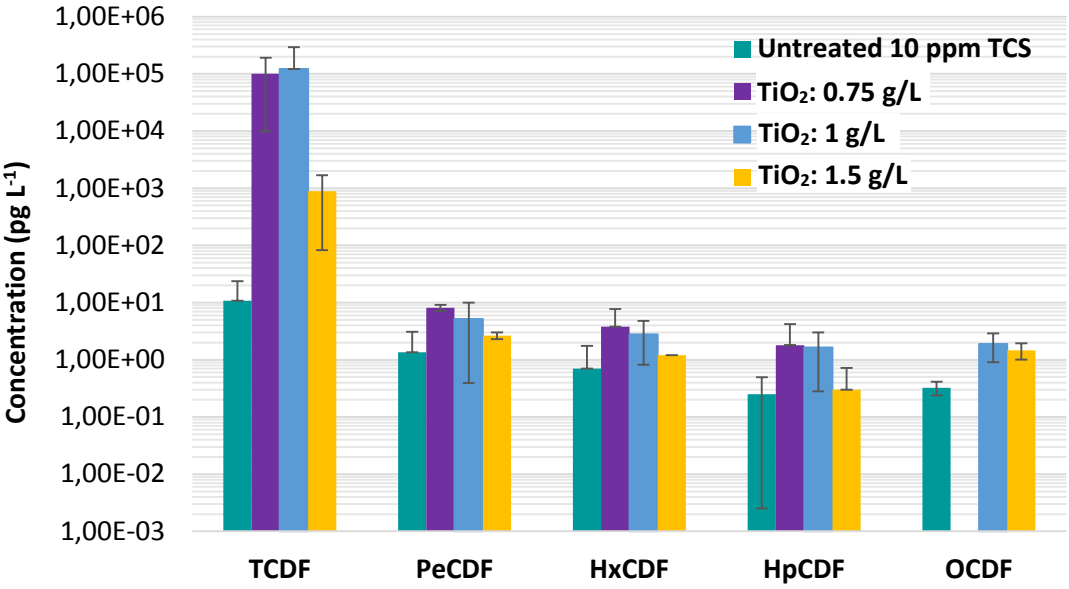

Figure 4.24. Concentration of highly chlorinated dioxins (a) and furans (b) as function of TiO_2 concentration (0.75, 1 and 1.5 g L^{-1}), oxidation time of 5 h.

Congeners with chlorine atoms at 2,3,7,8 positions, recognised as the most toxic ones, are depicted in Figure 4.25. This analysis was also made when Triclosan had completely disappeared, that is after 5 hours. EPA 1613 recoveries obtained for these analysis are presented in the annexes (Table II.7 and II.8).

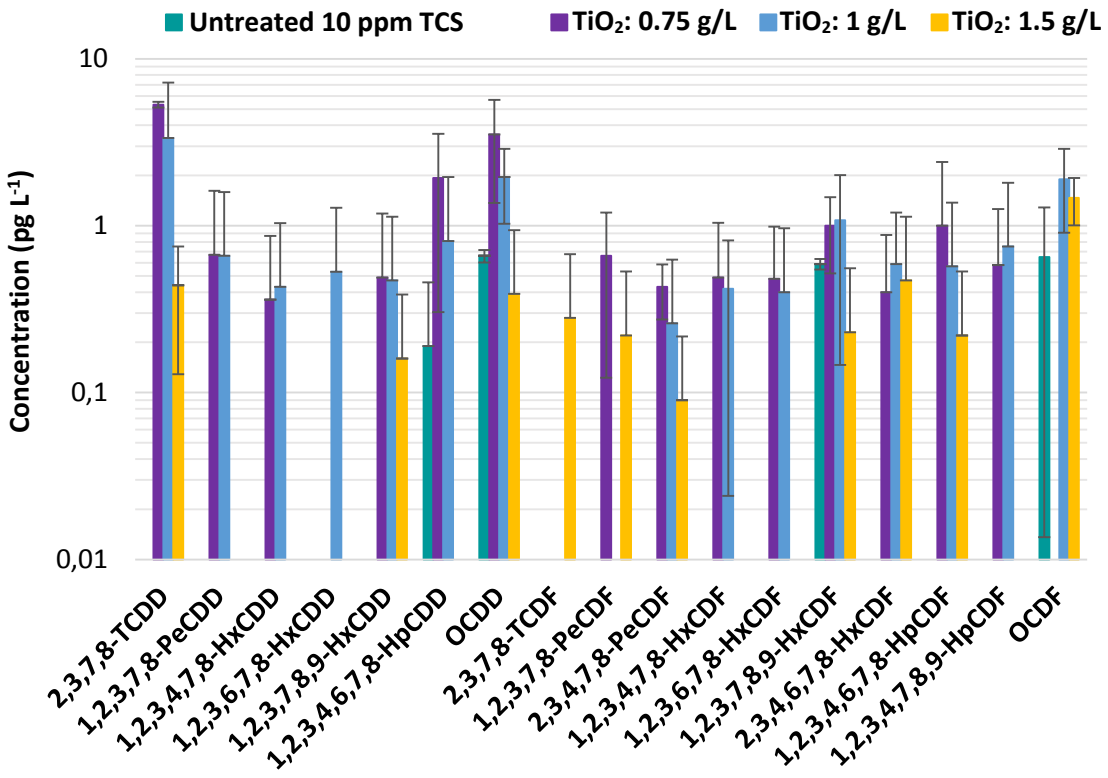

Figure 4.25. Concentration of 2,3,7,8-PCDD/Fs congeners as function of TiO_2 concentration (0.75, 1 and 1.5 g L^{-1}), oxidation time of 5 h.

The concentration of 2,3,7,8-PCDD/Fs congeners for these runs has been also analysed and results are depicted in Figure 4.25. Firstly, in the untreated sample, 1,2,3,4,6,7,8-HpCDD, OCDD, 1,2,3,7,8,9-HxCDF and OCDF congeners were detected at very low concentrations (0.2 – 0.7 pg L^{-1}). As it can be observed, the total concentration of 2,3,7,8-PCDD/Fs congeners increased for all the three TiO_2 concentrations studied after the treatment, with the exception of OCDD and 1,2,3,7,8,9-HxCDF when applying 1.5 g L^{-1} of catalyst. But, the total concentration of 2,3,7,8-PCDD/Fs decreased as the TiO_2 loading increased, from 17.3 pg L^{-1} for a dose of TiO_2 of 0.75 g L^{-1} to 4.0 pg L^{-1} for a dose of 1.5 g L^{-1}. 2,3,7,8-TCDD, 1,2,3,4,6,7,8-HpCDD and OCDD were the congeners that presented the highest concentrations when the TiO_2 loading was 0.75 g L^{-1}, achieving values up to 5.3, 1.9 and 3.5 pg L^{-1}, respectively, accounting for 30.7, 11.1 and 20.3 % of the total 2,3,7,8-PCDD/Fs. When the dose of catalyst applied was 1 g L^{-1}, 2,3,7,8-TCDD, OCDD and OCDF were the predominant congeners, reaching values between 1.9 and 3.4 pg L^{-1} (13.4 – 23.7 % of the total 2,3,7,8-PCDD/Fs). Finally, although the concentrations of 2,3,7,8-PCDD/Fs congeners were very low when using 1.5 g L^{-1} as TiO_2 loading, OCDF was the predominant congener, with a value of 1.5 pg L^{-1} (37.0 % of the total 2,3,7,8-PCDD/Fs).

In addition, the toxicity equivalent index (TEQ) has been calculated as previously detailed in chapter 2. As it can be observed in Figure 4.26, TEQ values slightly increased in comparison to the untreated sample. However, these values decreased as the concentration of TiO_2 employed in the treatment decreased. It has to be highlighted that for the three photocatalyst doses used, all the values are below the limit of 30.0 pg L^{-1} recommended by the U.S. EPA for drinking water.

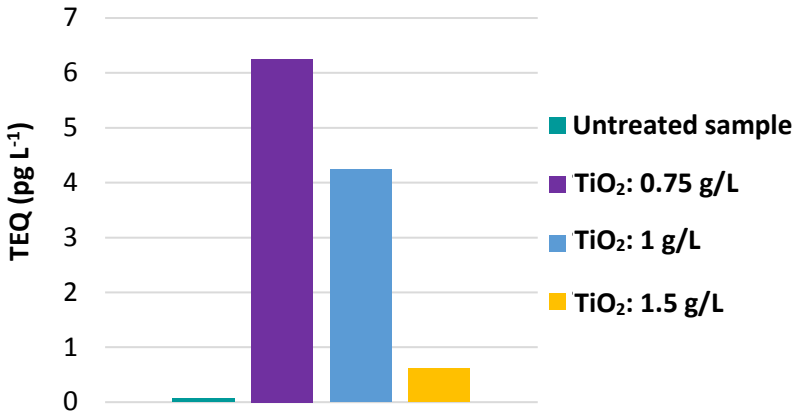

Figure 4.26. TEQ values as function of the TiO_2 loading (0.75, 1 and 1.5 g L^{-1}), oxidation time of 5 h.

4.4.3. Pathway proposal for the intermediate products of Triclosan

Based on the experimental results obtained in the previous section, the pathways involved in the photocatalytic degradation of Triclosan have been summarized. As shown in section 4.4.1, 2,4-dichlorophenol has been demonstrated to be one of the main photo-products observed in the degradation of Triclosan by photocatalysis. The generation of this compound has been explained by the action of OH radicals that cause an homolytic scission of the carbon-oxygen bond (as reported in Figure 4.2, route 1) (Latch et al., 2003; Rafqah et al., 2006; Son et al., 2007, 2009; Sankoda et al., 2011; Stamatis et al., 2014; Constantin et al., 2018). In the case of PCDD/Fs formation, 2,8-dichlorodibenzo-p-dioxin was not observed neither in the literature (Rafqah et al., 2006; Son et al., 2009; Stamatis et al., 2014) nor on the experimental results obtained in this work after the application of a photocatalytic treatment to Triclosan solutions. For this reason, the reliability of the analytical technique employed, explained in section 3.5, remains a concern. For the first time, the qualitatively and quantitatively formation of highly chlorinated PCDD/Fs from the photocatalytic oxidation of Triclosan has been demonstrated. It has been reported that the reaction mechanisms involved in a photocatalytic treatment in aqueous phase occurred through the formation of OH radicals, same pathway as in electrochemical oxidation treatment, described in section 3.6. A hydrogen abstraction from the

molecule of Triclosan is produced throught the action of OH radicals, forming Triclosan radical (·TCS(-H)). Then, different cyclizations led to the formation of low chlorinated dioxins and furans: dichlorodibenzo-p-dioxins (DCDD), trichlorodibenzo-p-dioxins (TrCDD) and trichlorodibenzofurans (TrCDFs) (Figure 3.19 and 3.20 of section 3.6.2). The formation of highly chlorinated PCDD/Fs might be also explained by the fast chlorination of low chlorinated PCDD/Fs. A brief scheme explaining the reaction mechanisms that describe the formation of PCDD/Fs by the photocatalytic oxidation of Triclosan is shown below (Figure 4.27).

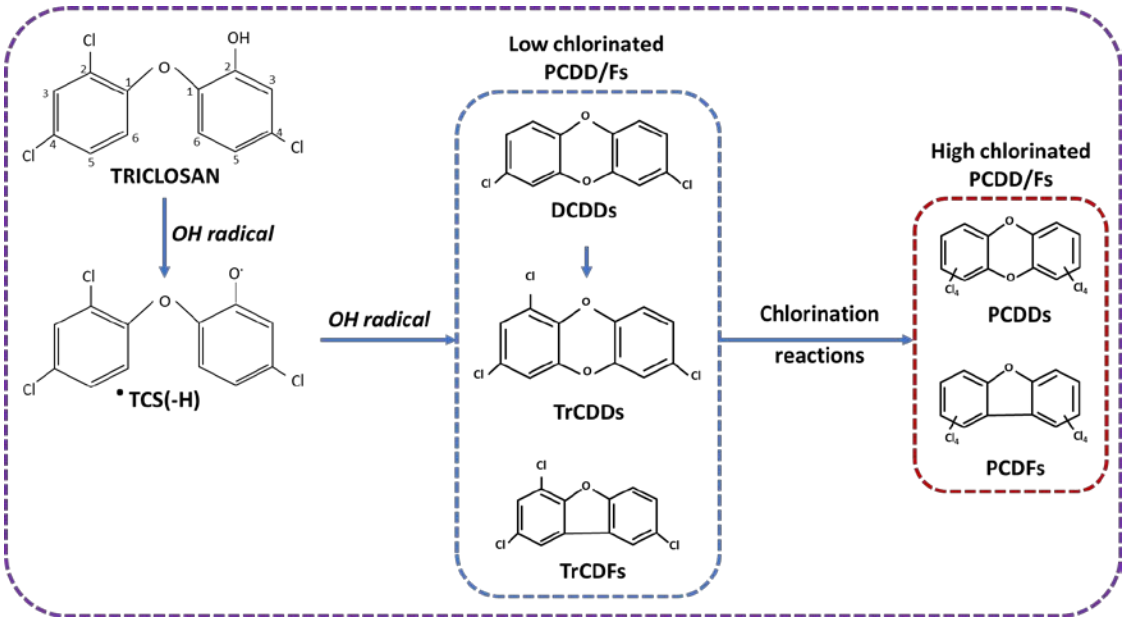

Figure 4.27. Reaction mechanisms for the photocatalysis of TCS: PCDD/Fs formation.

4.5. Electrochemical vs. photocatalytic oxidation

The application of efficient AOP methods to remove Triclosan from polluted waters must be supported with the adequate assessment of the formation of byproducts and final toxicity of the remediated waters; thus the latter constitutes the second objective that has driven this work. In order to compare electrochemical and photocatalytic technologies in terms of toxicity, the experiments with an initial concentration of 10 mg L^{-1} of Triclosan were selected. When electrochemical oxidation treatment was applied, TEQ values increased from 0.4 pg L^{-1} for the untreated sample to 4.4 and 4.7 pg L^{-1} when NaCl and Na_2SO_4 were present in the solution, respectively. TEQ values increased from 0.1 pg L^{-1} for the untreated sample to 0.6 pg L^{-1} when applying a photocatalytic treatment with a TiO_2 loading of 1.5 g L^{-1}. This catalyst dose was

demonstrated to be the optimum among the doses studied in this work in terms of TCS degradation kinetics, applied for the same Triclosan initial concentration. However, TEQ had a value of 6.3 pg L^{-1} when the catalyst dose was 0.75 g L^{-1} and no Triclosan remained in the solution. Thus, the conditions that facilitate the degradation of TCS with minimum increase in the toxicity of remediated waters were: Na_2SO_4 as electrolyte in the electrochemical oxidation treatment; and 1.5 g L^{-1} as TiO_2 loading in the photocatalytic treatment.

First, a comparison between the formation of highly chlorinated PCCD/Fs (from TCDD/F to OCDD/F) has been carried out and results are shown in Figure 4.28. This Figure collects and compares the results for the untreated sample together with the results obtained for 10 mg L^{-1} of Triclosan treated with Na_2SO_4 as electrolyte type in the electrochemical oxidation treatment, and the results obtained for the untreated sample together with the results obtained working with 1.5 g L^{-1} of TiO_2 doses in the photocatalytic oxidation of Triclosan. The analysis of highly chlorinated PCDD/Fs at times when Triclosan was completely removed from the solution, that is after 1 and 5 hours of electrochemical and photolytic oxidation treatment, respectively, has been performed. Figure 4.28(a) shows the concentrations of the PCDDs profile, whereas Figure 4.28(b) displays the concentrations determined for PCDDFs species.

The total concentration of PCDD/Fs increased from $8.2 \cdot 10^1$ pg L^{-1} for the untreated sample to $2.9 \cdot 10^2$ pg L^{-1} for the electrochemically oxidized sample with Na_2SO_4. For the photocatalytic treatment, the total concentration of PCDD/Fs increased from $2.3 \cdot 10^1$ pg L^{-1} for the untreated sample to $9.8 \cdot 10^2$ pg L^{-1} after the oxidation of Triclosan. The PCDDs profile (Figure 4.28(a)) shows higher concentrations resulting in the electrochemical oxidation ($2.6 \cdot 10^2$ pg L^{-1}) in comparison to the photocatalytic treatment ($8.8 \cdot 10^1$ pg L^{-1}). In this way, when the samples were electrochemically oxidized, TCDD was the predominant group of the total PCDD/Fs, reaching a value of $1.8 \cdot 10^2$ pg L^{-1} (accounting for 62.3 %). On the other hand, PCDF profile showed higher concentrations when applying the photocatalytic treatment ($8.8 \cdot 10^2$ pg L^{-1}) than for the electrochemical oxidation ($4.0 \cdot 10^1$ pg L^{-1}). Hence, the predominant homologue group when applying a photocatalytic treatment was TCDF, reaching a value of $8.8 \cdot 10^2$ pg L^{-1} of the total PCDD/Fs concentration (accounting for 90.4 %).

(a)

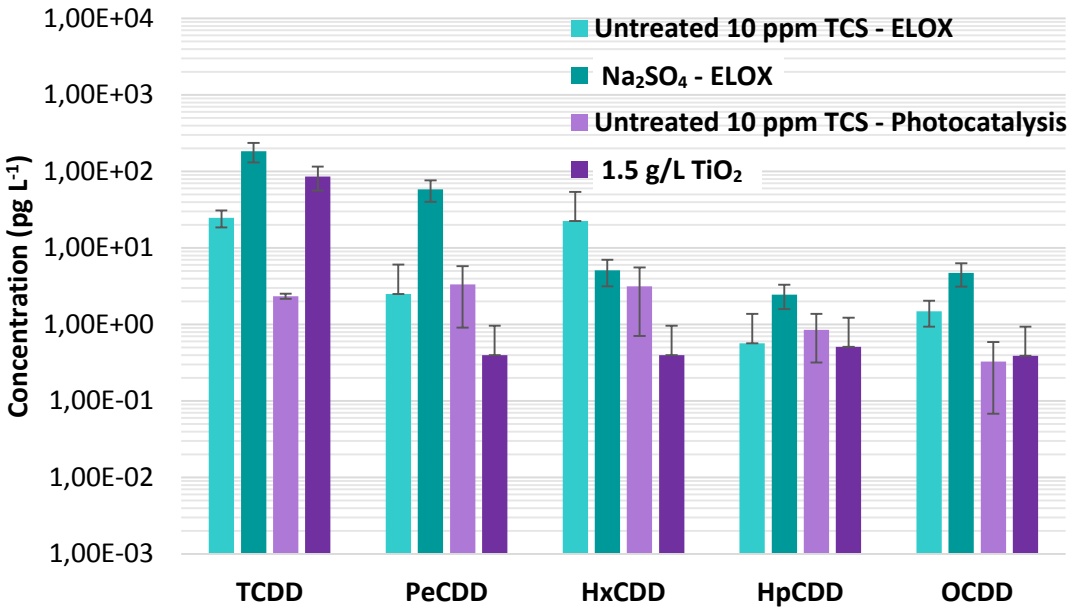

(b)

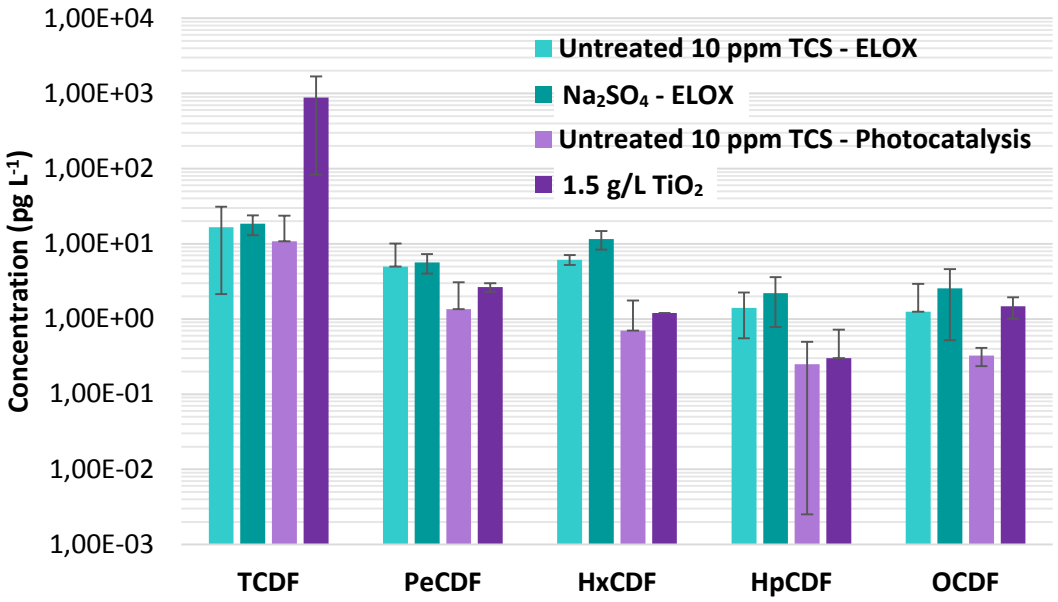

Figure 4.28. Concentration of highly chlorinated dioxins (a) and furans (b) as function of the technology applied: electrochemical and photocatalytic oxidation treatment. Initial concentration of TCS: 10.0 mg L^{-1}. Oxidation time of 1 and 5 h for electrochemical and photocatalytic oxidation treatment, respectively.
Supporting electrolyte: Na_2SO_4; TiO_2 doses: 1.5 g L^{-1}.

Congeners with chlorine atoms at 2,3,7,8 positions, recognised as the most toxic species, are depicted in Figure 4.29. Firstly, in the blank analysed before the electrochemical oxidation, 1,2,3,4,6,7,8-HpCDD, OCDD and OCDF congeners were detected at the highest concentrations (1.2 – 2.0 pg L^{-1}). On the other hand, for the blank performed for the photocatalytic oxidation treatment, OCDD, 1,2,3,7,8,9-HxCDF and OCDF congeners were detected at the highest concentrations (0.6 – 0.7 pg L^{-1}). After the electrochemical treatment, the total concentration of 2,3,7,8-PCDD/Fs accounted for 6.7 % of the total PCDD/Fs concentration, whereas for the photocatalytic treatment the total concentration of 2,3,7,8-PCDD/Fs accounted for 0.4 % of the total PCDD/Fs concentration. For electrochemically oxidized samples, 2,3,7,8-TCDD, 1,2,3,6,7,8-HxCDD, OCDD and OCDF were the congeners that presented the highest concentrations, achieving average values up to 4.7 pg L^{-1}. Specifically, the 2,3,7,8-congener profile was dominated by OCDD (23.6 % of the total 2,3,7,8-PCDD/Fs concentration). Whereas after the photocatalytic treatment, 2,3,7,8-TCDD, 2,3,4,6,7,8-HxCDD and OCDF were the congeners that presented the highest concentrations, achieving average values up to 1.5 pg L^{-1}. Specifically, the 2,3,7,8-congener profile was dominated by OCDD (37.0 % of the total 2,3,7,8-PCDD/Fs).

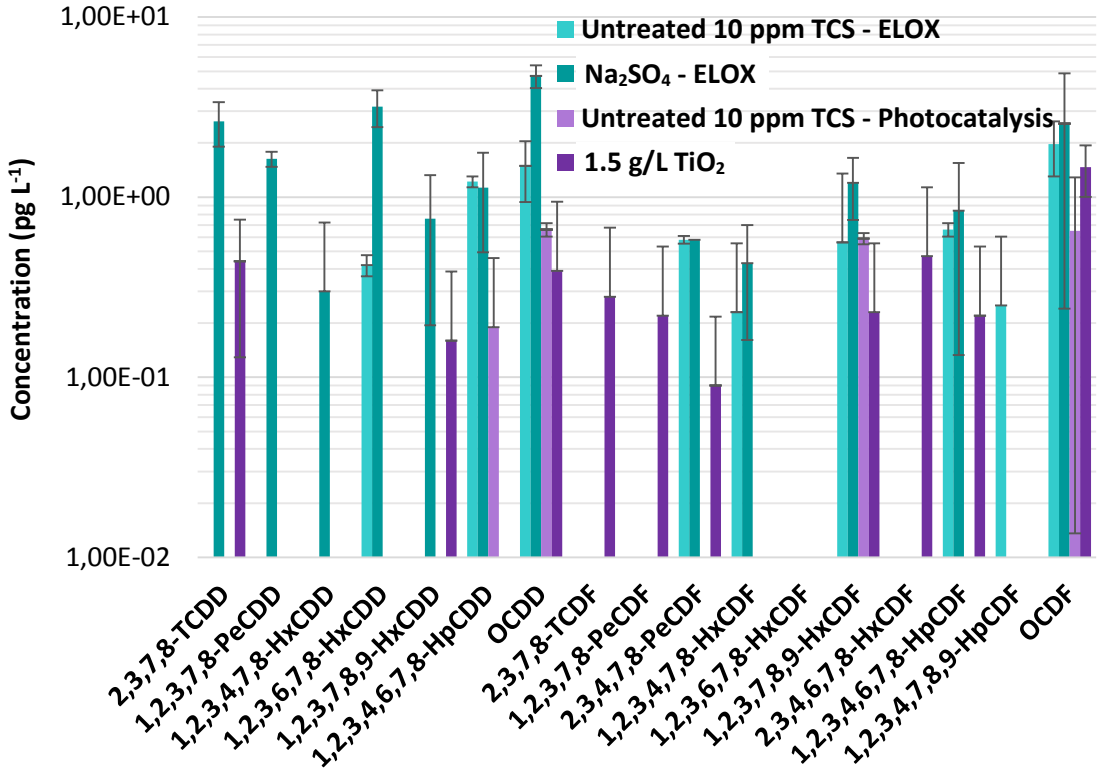

Figure 4.29. Concentration of 2,3,7,8-PCDD/Fs congeners as a function of the remediation technology electrochemical and photocatalytic oxidation. Initial concentration of TCS: 10.0 mg L^{-1}. Oxidation time of 1 and 5 h, respectively. Supporting electrolyte: Na_2SO_4; TiO_2 doses: 1.5 g L^{-1}.

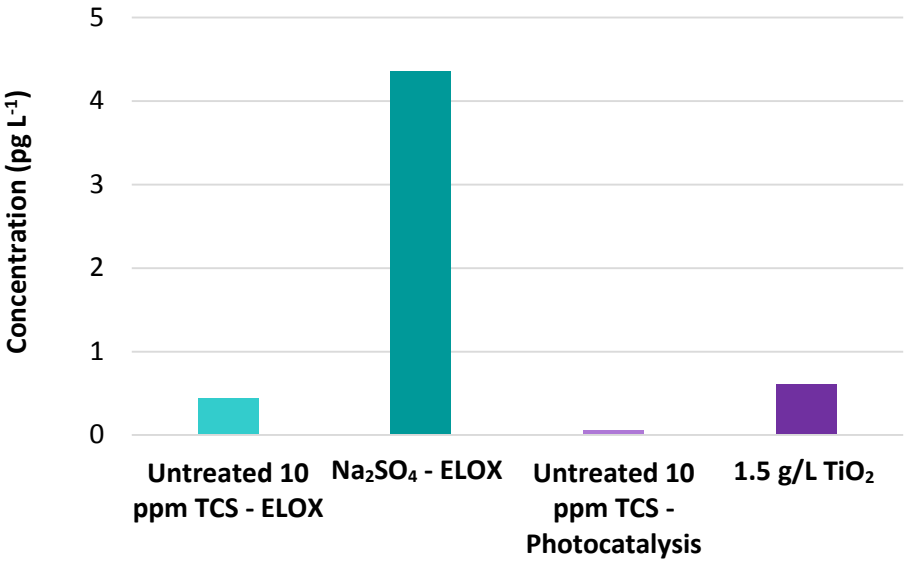

Figure 4.30. TEQ values calculated for the untreated and treated samples when applying both technologies, electrochemical and photocatalytic technologies.

TEQ values increased from 0.4 pg L^{-1} for the untreated sample to 4.4 pg L^{-1} when applying an electrochemical oxidation treatment with Na_2SO_4 as electrolyte. Whereas TEQ values increased from 0.1 pg L^{-1} for the untreated sample to 0.6 pg L^{-1} when applying a photocatalytic treatment with a TiO_2 loading of 1.5 g L^{-1}. Thus, although the total PCDD/Fs concentration resulted higher for the photo-treatment application, the final toxicity increased after electrochemical remediation; this is explained by the higher contribution of 2,3,7,8 species to the total PCDD/Fs concentration that are associated to high toxicity levels. Besides, TEQ did not take high values that were below the maximum value established by the U.S. EPA for drinking water (30 pg L^{-1}). These results highlight the relevance of including the toxicity analysis in selecting the experimental conditions for the application of oxidation remediation technologies to polluted wastewaters with persistent chlorinated compounds, adding this information to the technical performance of the treatment.

A summary reporting all the results obtained in this section section is shown in the next table.

Table 4.5. Summary of highly chlorinated PCDD/Fs and TEQ concentrations in the electrochemically and photocatalytic oxidized samples.

	Total highly PCDD/Fs concentration (pg L^{-1})	**Total highly PCDDs (dioxins) concentration (pg L^{-1})**	**Total highly PCDFs (furans) concentration (pg L^{-1})**	**2,3,7,8-PCDD/Fs congeners concentration (pg L^{-1})**	**TEQ (pg L^{-1})**
Untreated 10 ppm TCS - ELOX	82.28	51.83	30.45	7.38	0.44
ELOX Na_2SO_4	295.53	255.09	40.44	19.97	4.36
Untreated 10 ppm TCS - Photocatalysis	23.45	10.03	13.42	2.09	0.06
1,5 g L^{-1} TiO_2	975.12	88.10	887.02	3.97	0.61

4.6. References

Alfiya, Y., Friedler, E., Westphal, J., Olsson, O., Dubowski, Y., 2017. Photodegradation of micropollutants using V-UV/UV-C processes; Triclosan as a model compound. Sci. Total Environ. 601–602, 397–404. https://doi.org/10.1016/j.scitotenv.2017.05.172

Aranami, K., Readman, J.W., 2007. Photolytic degradation of triclosan in freshwater and seawater. Chemosphere 66, 1052–1056. https://doi.org/10.1016/j.chemosphere.2006.07.010

Bianco, A., Fabbri, D., Minella, M., Brigante, M., Mailhot, G., Maurino, V., Minero, C., Vione, D., 2015. New insights into the environmental photochemistry of 5-chloro-2-(2,4-dichlorophenoxy)phenol (triclosan): Reconsidering the importance of indirect photoreactions. Water Res. 72, 271–280. https://doi.org/10.1016/j.watres.2014.07.036

Chen, L., Wang, Z., Qian, C., He, Y., 2018. Effects of inorganic anions on the photolysis of triclosan under UV irradiation. Water Sci. Technol. 78, 1476–1480. https://doi.org/10.2166/wst.2018.421

Chen, L., Wang, Zheng, Wang, Zhulai, Gu, X., 2016. Influence of humic acid on the photolysis of Triclosan in different dissociation forms. Water. Air. Soil Pollut. 227, 1–7. https://doi.org/10.1007/s11270-016-3024-7

Chen, Z., Cao, G., Song, Q., 2010. Photo-polymerization of triclosan in aqueous solution induced by ultraviolet radiation. Environ. Chem. Lett. 8, 33–37. https://doi.org/10.1007/s10311-008-0187-5

Constantin, L., Nitoi, I., Cristea, I., Oancea, P., Orbeci, C., Nechifor, A.C., 2015. Degradation of triclosan by TiO_2 - UV irradiation in aqueous solutions. Rev. Chim. 66, 597–600.

Constantin, L.A., Nitoi, I., Cristea, N.I., Constantin, M.A., 2018. Possible degradation pathways of triclosan from aqueous systems via TiO_2 assisted photocatalyis. J. Ind. Eng. Chem. 58, 155–162. https://doi.org/10.1016/j.jiec.2017.09.020

Fernández-Castro, P., San Román, M.F., Ortiz, I., 2016. Theoretical and experimental formation of low chlorinated dibenzo-p-dioxins and dibenzofurans in the Fenton oxidation of chlorophenol solutions. Chemosphere 161, 136–144. https://doi.org/10.1016/j.chemosphere.2016.07.011

Hoffmann, M.R., Martin, S.T., Choi, W., Bahnemann, D.W., 1995. Environmental Applications of Semiconductor Photocatalysis. Chem. Rev. 95, 69–96. https://doi.org/10.1021/cr00033a004

Ibhadon, A., Fitzpatrick, P., 2013. Heterogeneous photocatalysis: recent advances and

applications. Catalysts 3, 189–218. https://doi.org/10.3390/catal3010189

Iovino, P., Chianese, S., Prisciandaro, M., Musmarra, D., 2019. Triclosan photolysis: operating condition study and photo-oxidation pathway. Chem. Eng. J. https://doi.org/10.1016/j.cej.2019.02.132

Kanakaraju, D., Glass, B.D., Oelgemöller, M., 2014. Titanium dioxide photocatalysis for pharmaceutical wastewater treatment. Environ. Chem. Lett. 12, 27–47. https://doi.org/10.1007/s10311-013-0428-0

Kliegman, S., Eustis, S.N., Arnold, W.A., McNeill, K., 2013. Experimental and theoretical insights into the involvement of radicals in triclosan phototransformation. Environ. Sci. Technol. 47, 6756–6763. https://doi.org/10.1021/es3041797

Kosera, V.S., Cruz, T.M., Chaves, E.S., Tiburtius, E.R.L., 2017. Triclosan degradation by heterogeneous photocatalysis using ZnO immobilized in biopolymer as catalyst. J. Photochem. Photobiol. A Chem. 344, 184–191. https://doi.org/10.1016/j.jphotochem.2017.05.014

Latch, D., Packer, J., Stender, B., VanOverbeke, J., Arnold, W., McNeill, K., 2005. Aqueous photochemistry of Triclosan: formation of oligomerization products. Environ. Toxicol. Chem. 24, 517–525.

Latch, D.E., Packer, J.L., Arnold, W.A., McNeill, K., 2003. Photochemical conversion of triclosan to 2,8-dichlorodibenzo-p-dioxin in aqueous solution. J. Photochem. Photobiol. A Chem. 158, 63–66. https://doi.org/10.1016/S1010-6030(03)00103-5

Lindström, A., Buerge, I.J., Poiger, T., Bergqvist, P.A., Müller, M.D., Buser, H.R., 2002. Occurrence and environmental behavior of the bactericide triclosan and its methyl derivative in surface waters and in wastewater. Environ. Sci. Technol. 36, 2322–2329. https://doi.org/10.1021/es0114254

Lores, M., Llompart, M., Sanchez-Prado, L., Garcia-Jares, C., Cela, R., 2005. Confirmation of the formation of dichlorodibenzo-p-dioxin in the photodegradation of triclosan by photo-SPME. Anal. Bioanal. Chem. 381, 1294–1298. https://doi.org/10.1007/s00216-004-3047-6

Mezcua, M., Gómez, M.J., Ferrer, I., Aguera, A., Hernando, M.D., Fernández-Alba, A.R., 2004. Evidence of 2,7/2,8-dibenzodichloro-p-dioxin as a photodegradation product of triclosan in water and wastewater samples. Anal. Chim. Acta 524, 241–247. https://doi.org/10.1016/j.aca.2004.05.050

Qiao, X., Zheng, X., Xie, Q., Yang, X., Xiao, J., Xue, W., Chen, J., 2014. Faster photodegradation

rate and higher dioxin yield of triclosan induced by cationic surfactant CTAB. J. Hazard. Mater. 275, 210–214. https://doi.org/10.1016/j.jhazmat.2014.05.012

Rafqah, S., Wong-Wah-Chung, P., Nelieu, S., Einhorn, J., Sarakha, M., 2006. Phototransformation of triclosan in the presence of TiO_2 in aqueous suspension: mechanistic approach. Appl. Catal. B Environ. 66, 119–125. https://doi.org/10.1016/j.apcatb.2006.03.004

Ribao, P., Rivero, M.J., Ortiz, I., 2018. Enhanced photocatalytic activity using GO/TiO_2 catalyst for the removal of DCA solutions. Environ. Sci. Pollut. Res. 25, 34893–34902. https://doi.org/10.1007/s11356-017-0901-6

Salgado, L.E.V., Vargas-Hernández, C., 2014. Spectrophotometric Determination of the pK_a, isosbestic point and equation of absorbance vs. pH for a universal pH indicator. Am. J. Anal. Chem. 05, 1290–1301. https://doi.org/10.4236/ajac.2014.517135

Sanchez-Prado, L., Llompart, M., Lores, M., García-Jares, C., Bayona, J.M., Cela, R., 2006. Monitoring the photochemical degradation of triclosan in wastewater by UV light and sunlight using solid-phase microextraction. Chemosphere 65, 1338–1347. https://doi.org/10.1016/j.chemosphere.2006.04.025

Sankoda, K., Matsuo, H., Ito, M., Nomiyama, K., Arizono, K., Shinohara, R., 2011. Identification of triclosan intermediates produced by oxidative degradation using TiO_2 in pure water and their endocrine disrupting activities. Bull. Environ. Contam. Toxicol. 86, 470–475. https://doi.org/10.1007/s00128-011-0249-4

Son, H.S., Choi, S.B., Zoh, K.D., Khan, E., 2007. Effects of ultraviolet intensity and wavelength on the photolysis of triclosan. Water Sci. Technol. 55, 209–216. https://doi.org/10.2166/wst.2007.034

Son, H.S., Ko, G., Zoh, K.D., 2009. Kinetics and mechanism of photolysis and TiO_2 photocatalysis of triclosan. J. Hazard. Mater. 166, 954–960. https://doi.org/10.1016/j.jhazmat.2008.11.107

Stamatis, N., Antonopoulou, M., Hela, D., Konstantinou, I., 2014. Photocatalytic degradation kinetics and mechanisms of antibacterial triclosan in aqueous TiO_2 suspensions under simulated solar irradiation. J. Chem. Technol. Biotechnol. 89, 1145–1154. https://doi.org/10.1002/jctb.4387

Tixier, C., Singer, H.P., Canonica, S., Müller, S.R., 2002. Phototransformation of triclosan in surface waters: a relevant elimination process for this widely used biocide - Laboratory studies, field measurements, and modeling. Environ. Sci. Technol. 36, 3482–3489.

https://doi.org/10.1021/es025647t

Weatherly, L.M., Gosse, J.A., 2017. Triclosan exposure, transformation, and human health effects. J. Toxicol. Environ. Heal. - Part B Crit. Rev. 20(8), 447–469.

Wong-Wah-Chung, P., Rafqah, S., Voyard, G., Sarakha, M., 2007. Photochemical behaviour of triclosan in aqueous solutions: kinetic and analytical studies. J. Photochem. Photobiol. A Chem. 191, 201–208. https://doi.org/10.1016/j.jphotochem.2007.04.024

Wu, J. lin, Ji, F., Zhang, H., Hu, C., Wong, M.H., Hu, D., Cai, Z., 2019a. Formation of dioxins from triclosan with active chlorine: a potential risk assessment. J. Hazard. Mater. 367, 128–136. https://doi.org/10.1016/j.jhazmat.2018.12.088

Wu, J. lin, Ji, F., Zhang, H., Hu, C., Wong, M.H., Hu, D., Cai, Z., 2019b. Formation of dioxins from triclosan with active chlorine: a potential risk assessment. J. Hazard. Mater. 367, 128–136. https://doi.org/10.1016/j.jhazmat.2018.12.088

Yu, J.C., Kwong, T.Y., Luo, Q., Cai, Z., 2006. Photocatalytic oxidation of triclosan. Chemosphere 65, 390–399. https://doi.org/10.1016/j.chemosphere.2006.02.011

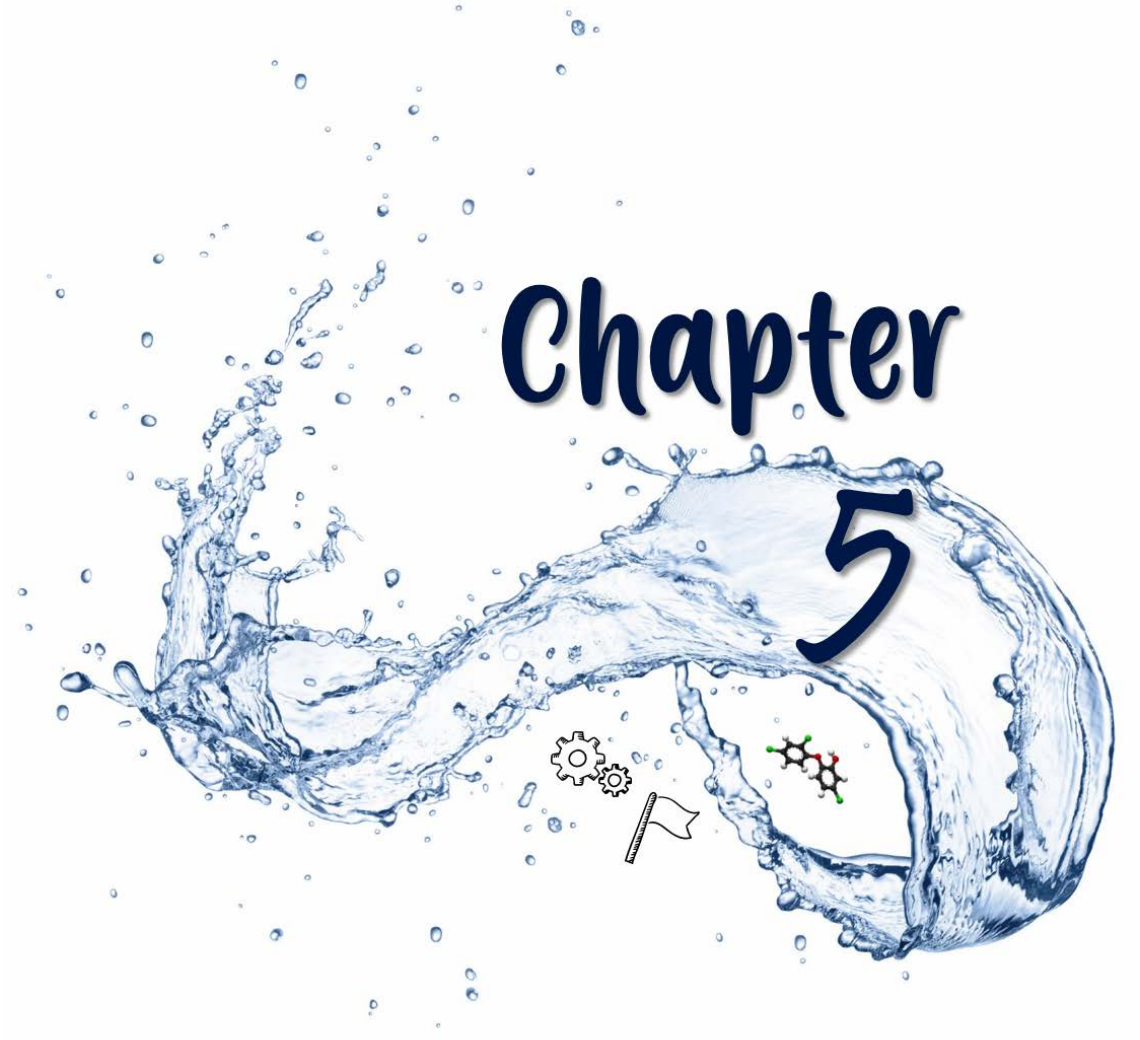

Chapter 5

CONCLUSIONS

This thesis has been focused on the application of advanced oxidation processes (AOPs) to aqueous samples containing Triclosan (TCS); in addition to the analysis of the oxidation performance in terms of Triclosan degradation, special attention has been paid to the formation of intermediate products, especially to the potential formation of polychlorinated dibenzo-p-dioxins and dibenzofurans (PCDD/Fs) and their inherent toxicity. In particular, the electrochemical oxidation and photolytic treatments applied to model solutions containing Triclosan have been assessed. After the analysis of the state-of-the-art and the obtained experimental results, this study has led to the following conclusions,

Electrochemical oxidation of Triclosan

In chapter 3, the electrochemical oxidation of Triclosan solutions (with initial concentrations of 10, 100 and 150 mg L^{-1}) using BDD anodes was carried out under galvanostatic mode (J = 6, 60 and 90 A m^{-2}, respectively). The influence of two widely used electrolytes, NaCl (56.3 mM) and Na_2SO_4 (21.1 mM), and the presence of copper on the degradation of Triclosan, by adding 10 mg L^{-1} of the metal in the target solution, has been studied.

Triclosan was completely removed but the specific electrical charge needed to achieve a complete degradation of Triclosan increased with its initial concentration. 1, 3 and 4 hours were required to completely eliminate the target compound for the thee Triclosan concentrations studied, 10, 100 and 150 mg L^{-1}, respectively. The degradation kinetics were independent of the supporting electrolyte employed as well as of the presence of copper in the aqueous solution.

Besides Triclosan, the presence of different oxidation by-products was determined. GC-MS analysis was carried out for the 100 mg L^{-1} Triclosan solution. Independently of the supporting electrolyte, the analysis confirmed the formation of chloro-aromatic intermediate species, such as 2,4-dichlorophenol, 4-chlorocatechol, 2-chlorohydroquinone, 2-chloro-4-methoxyphenol and 1-chloro-2,5-dimethoxybenzene. In addition, the formation of non-chlorinated products was also detected: 2-ethyl-hexanol and diphenyl ether benzene.

The analysis of the formation of highly chlorinated PCDD/Fs was determined following the EPA 1613 method in samples where Triclosan had completely disappeared.

- Firstly, the analysis of PCDD/Fs in the untreated samples has been determined, resulting in a total concentration of PCCD/Fs of $8.2 \cdot 10^1$, $9.1 \cdot 10^1$ and $2.2 \cdot 10^2$ pg L^{-1} for 10, 100 and 150 mg L^{-1} of Triclosan. TEQ took values of 0.4, 0.6 and 1.3 pg L^{-1} for three three initial Triclosan concentrations.

- The use of NaCl as electrolyte resulted in a total PCDD/Fs concentration in the oxidized samples of $3.7 \cdot 10^2$, $3.4 \cdot 10^4$ and $1.6 \cdot 10^5$ pg L^{-1} with a PCDD profile (dioxins profile) accounting for 82.5, 91.2 and 99.5 % for the initial Triclosan concentrations studied in this work (10, 100 and 150 mg L^{-1}). However, and although the low contribution of the 2,3,7,8-PCDD/Fs concentration in the total PCDD/Fs (accounting by 0.8, 1.8 and 5.2 %), TEQ levels increased from values close to zero for the untreated samples to concentrations under the studied conditions of 4.7, $2.8 \cdot 10^2$ and $3.8 \cdot 10^2$ pg L^{-1} (for 10, 100 and 150 mg L^{-1} Triclosan samples, respectively). In particular, TEQ values were 11, 320 and 300 times higher than the untreated samples for the three concentrations of Triclosan studied. These TEQ values are several times higher for the last two cases than the maximum contaminant level established by the U.S. EPA for drinking water (30 pg L^{-1}), specifically, 9 and 13 times higher than the maximum permitted.

- Regarding the use of Na_2SO_4 as electrolyte type, the total PCDD/Fs increased to $2.9 \cdot 10^2$, $8.6 \cdot 10^3$ and $8.4 \cdot 10^4$ pg L^{-1}, of which PCDD profile (dioxins profile) accounted for 86.3, 80.9 and 97.9 %. Concentration of 2,3,7,8-PCDD/Fs accounted for 6.7, 1.7 and 0.7 % of the total PCDD/Fs for the three Triclosan concentrations studied (10, 100 and 150 mg L^{-1}). TEQ values slightly increased in comparison to the untreated sample, specifically, these values were 10, 97 and 20 times higher, corresponding to concentrations of 4.4, $5.3 \cdot 10^1$ and $2.5 \cdot 10^1$ pg L^{-1} for 10, 100 and 150 mg L^{-1} Triclosan samples, respectively.

  A summary reporting all the results obtained is presented below (Table 5.1).

Table 5.1. Summary of high chlorinated PCDD/Fs and TEQ concentrations in the untreated and oxidized samples.

	Total highly PCDD/Fs concentration (pg L^{-1})			**Total highly PCDDs (dioxins) concentration (pg L^{-1})**			**2,3,7,8-PCDD/Fs congeners concentration (pg L^{-1})**			**TEQ (pg L^{-1})**		
	Initial Triclosan concentration (mg L^{-1})											
	10	100	150	10	100	150	10	100	150	10	100	150
Untreated sample	**82.3**	**90.9**	**221.9**	**51.8**	**28.1**	**105.5**	**7.4**	**13.6**	**11.2**	**0.4**	**0.5**	**1.3**
$\frac{NaCl}{Untreated\ sample}$*	5	376	739	6	1109	1546	3	45	119	11	501	301
$\frac{Na_2SO_4}{Untreated\ sample}$*	4	75	38	5	196	78	3	11	5	10	97	20

* The table expresses the ratio of the concentration determined in these samples with respect to the concentration in the untreated samples.

- On the other hand, the influence of copper on the potential formation of highly chlorinated PCDD/Fs has been studied for 100 mg L^{-1} Triclosan solution. The total concentration of PCDD/Fs was $1.5 \cdot 10^4$ and $5.6 \cdot 10^3$ pg L^{-1} in the presence of NaCl and Na_2SO_4, decreasing by 55.8 and 35.1 % when copper was present in the reaction medium, respectively. PCDD profile (dioxins profile) accounted for 89.9 and 70.4 % for NaCl and Na_2SO_4, respectively. In addition, the concentration of 2,3,7,8-PCDD/Fs only accounted for 2.3 and 2.5 % of the total PCDD/Fs for the two electrolytes studied, which led to a decrease of TEQ values in the presence of copper: $1.7 \cdot 10^2$ and $4.5 \cdot 10^1$ pg L^{-1} for the two electrolytes studied. Considering these results,it is possible to conclude that copper may act as catalyst in the electrochemical oxidation of Triclosan, having a significant influence on the decrease of PCDD/Fs formation, independently of the electrolyte employed. Therefore, toxicity values were lower in the presence of copper, decreasing by 5 and 15 % in comparison to the samples without copper for NaCl and Na_2SO_4, respectively.

Next, the analysis of non-chlorinated and low chlorinated PCDD/Fs has been carried out for oxidized Triclosan samples (10, 100 and 150 mg L^{-1}) when Triclosan had disappeared completely. To this end, the EPA 1613 method has been expanded. With NaCl, the total concentration of low chlorinated PCDD/Fs increased from $8.33 \cdot 10^3$, $1.56 \cdot 10^5$ and $2.23 \cdot 10^5$ pg L^{-1} for the untreated samples to $6.75 \cdot 10^4$, $2.04 \cdot 10^5$ and $1.01 \cdot 10^6$ pg L^{-1} for the three Triclosan concentration studied. However, in the presence of Na_2SO_4, the total concentration of low

chlorinated species remained constant or decreased slightly to $8.47 \cdot 10^3$, $1.48 \cdot 10^5$ and $1.61 \cdot 10^5$ pg L^{-1}.

A summary reporting all the results obtained is presented below (Table 5.2).

Table 5.2. Summary of low chlorinated PCDD/Fs concentrations in the untreated and oxidized samples.

	Total low PCDD/Fs concentration (pg L^{-1})			**Total low PCDDs (dioxins) concentration (pg L^{-1})**		
	Initial Triclosan concentration (mg L^{-1})					
	10	100	150	10	100	150
Untreated sample	**8326.6**	**156624.5**	**222761.0**	**5647.7**	**139235.8**	**205926.1**
$\frac{\text{NaCl}}{\text{Untreated sample}}$*	8	1	5	12	1	0.5
$\frac{\text{Na}_2\text{SO}_4}{\text{Untreated sample}}$*	1	1	0.5	1	1	1

* The table expresses the ratio of the concentration determined in these samples with respect to the concentration in the untreated samples.

In the same way, when the sample contained NaCl, the presence of copper led to a decrease of the total concentration of low chlorinated PCDD/Fs from $2.04 \cdot 10^5$ to $7.01 \cdot 10^4$ pg L^{-1} (accounting for 65.6 %). In the presence of Na_2SO_4 as electrolyte, this value was reduced from $1.48 \cdot 10^5$ to $6.50 \cdot 10^4$ pg L^{-1} (accounting for 56.1 %).

The high concentration of low chlorinated PCCD/Fs in the untreated samples as well as in the oxidized samples draw our attention. Besides, the likely formation of 2,7/2,8-dichlorodibenzo-p-dioxin during Triclosan oxidation has caught the attention of many authors. For this reason, an exhaustive analysis of the formation of this congener during the electrochemical oxidation of Triclosan was developed. The results obtained by GC-MS showed the decrease in the concentration of 2,7/2,8-dichlorodibenzo-p-dioxin along the oxidation time, being the highest concentration observed that corresponding to the untreated sample. However, these results were not corroborated using HPLC. With this analytical assessment, it can be proposed that the formation of 2,7/2,8-dichlorodibenzo-p-dioxin may result from the direct cyclization of Triclosan during the analysis via GC–MS in the heated inlet. Thus, the use of GC-MS technique at the conditions used in this work might not be a reliable method for the analysis of 2,7/2,8-dichlorodibenzo-p-dioxin in samples where Triclosan is present, and it might

lead to inconsistent results. Besides, the extension of the EPA 1613 method, applied to unchlorinated and low chlorinated species, resulted in low recovery percentages. For this reason, the reliability of this method applied to the quantitative traceability of the formation of 2,7/2,8-dichlorodibenzo-p-dioxin was not consistent. Hence, it was concluded that the analysis of this compound under the conditions studied in this work becomes a complex task that requires more analytical efforts.

Lastly, the reaction mechanisms that described the formation of the by-products identified in this work has been proposed. The reaction pathways are based on the experimental results obtained in this thesis and supported by precious literature references containing either experimental or modelling results obtained using Gaussian computational chemistry software. The reaction mechanism started with a hydrogen abstraction from the phenol ring of the Triclosan molecule, reported as the lower free energy barrier route in comparison to the other possible routes calculated by simulation modelling. Then, Triclosan pathway followed different reactions that led to the formation of the by-products observed in the experimental results obtained in this work, supported by experimental and modelling data already reported: (i) breakage of the molecule, dechlorination, or rearrangement reactions, which led to the formation of smaller molecules such as 2,4-dichlorophenol, 4-chlorocatechol or 2-chlorohydroquinone; and (ii) cyclization reactions that led to the formation of low chlorinated PCDD/Fs, once the hydrogen was abstracted from the phenol ring, Triclosan molecule was transformed to low chlorinated species, followed by successive chlorination reactions that generated high chlorinated PCDD/Fs.

Photolytic oxidation of Triclosan

In chapter 4, two photolytic oxidation treatments have been applied to model aqueous solutions containing Triclosan: photolysis and photocatalysis. First of all, an exhaustive and critical analysis of the state-of-the-art related to the photo-degradation techniques applied to Triclosan solutions as well as to the formation of different intermediate products during the application of these treatments has been carried out.

Conclusions after the review of the state of the art of Triclosan photolysis

As reported in the literature, pH was a decisive parameter that played an important role in the photo-degradation of Triclosan. Wavelengths in the region of 300 nm strongly enhanced the photolytic process of Triclosan at conditions where Triclosan was present in its phenolate

form (pH > pK_a: 7.9 – 8.1). Together with the wavelength, the intensity of the lamp was also a decisive factor with high influence on the photo-degradation of Triclosan. In relation to the presence of other substances in the reaction medium, the results highlighted the complexity and coupled influence of anions of different nature in the photolysis of Triclosan, such as humic acids or inorganic salts. Besides, the presence of photo-scavengers in the treated samples, like 2-propanol or methanol, might inhibit the photolytic degradation of Triclosan because they competed for the photons or radicals presented in the reaction medium. Finally, with regard to the influence of a catalyst on the solution, in most cases TiO_2, the reported studies showed that its presence strongly enhanced the kinetics of Triclosan degradation independently of the catalyst used or dose employed.

Critical analysis of the by-products of Triclosan

Although photolytic treatments have been shown very effective for the degradation of Triclosan, the formation of different photo-products has been reported. Two main reaction pathways have been described: direct oxidation by the action of a photon (photolysis) and indirect oxidation by the action of OH radicals (photocatalysis). 2,4-dichlorophenol has been highlighted as one of the main products in the photo-degradation of Triclosan; its formation is associated to the photo-induced hydrolysis of Triclosan due to the effect of the UV light that produces an ether cleavage (photolysis) or by the action of ·OH that cause a homolytic scission of the carbon-oxygen bond (photocatalysis). In the same way, chlorophenol and 4-chlorocatechol might be formed by the action of ·OH or by the action of the photo-induced hydrolysis of Triclosan under UV light. Furthermore, the successive dechlorination reactions of chlorophenols led to the formation of phenol. Although the literature was scarce, the formation of Triclosan polymers, hydroxyl-chlorinated-PCBs, Triclosan-quinones and Triclosan-catechols has been found in Triclosan photo-oxidation. Finally, the formation of 2,8-dichlorodibenzo-p-dioxin has been widely reported. The formation of this congener by a cyclization reaction of Triclosan is favored under certain operation conditions: solution pH above 10, in the presence of NO_3^-, and at higher light intensities. However, in samples at acidic pH or in the presence of humic acids the inhibition in the formation of 2,8-dichlorodibenzo-p-dioxin has been reported to occur. In the same way, the formation of 2,8-dichlorodibenzo-p-dioxin might be inhibited in photocatalytic processes thanks to the action of OH radicals, which provoke a ether cleavage of Triclosan molecule.

On the Triclosan photolysis: experiments

Then, the photolytic experiments of Triclosan and its six hydrodehalogenation derivatives (Triclosan molecules with less chlorines placed in the three different positions of the Triclosan molecule), with an initial concentration of each compound of 50 µM (equivalent to 14.5 mg L^{-1} in the case of Triclosan) was carried out with 300 nm bulbs. The aim of the study was to acquire better understanding of the reaction mechanisms that led to the formation of PCDD/Fs and related compounds in the photolysis of Triclosan, and more specifically, identifying the chlorine that led to the formation of 2,8-dichlorodibenzo-p-dioxin. Firstly, the pK_a was determined for all the compounds studied, and, to ensure the maximum light absorbance of Triclosan and its derivatives, the pH solution was maintained above the pK_a.

- The photolysis of Triclosan took 20 minutes to achieve a complete removal. However, the formation of several photo-products was observed. 3-chlorophenol, 4-chlorophenol, 2,4-dichlorophenol, $(OH)_2$PCB13 ((4,5´-dichloro-[1,1´-biphenyl]-2,2´-diol), monochlorodibenzo-p-dioxin and 2,8-dichlorodibenzo-p-dioxin were the main products observed on the photolysis of Triclosan, achieving values up to 0.5 mg L^{-1}. Furthermore, a hydrodehalogenation derivative of Triclosan was also found: 4ClOHCl (5-chloro-2-(4-chlorophenoxy) phenol).

- The photolysis of the six hydrodehalogenation derivatives of Triclosan has been performed: OH (2-phenoxy phenol), OHCl (5-chloro-2-phenoxy phenol), 2ClOH (2-(2-chlorophenoxy) phenol), 2ClOHCl (5-chloro-2-(2-chlorophenoxy) phenol), 4ClOH (2-(4-chlorophenoxy) phenol) and 4ClOHCl (5-chloro-2-(4-chlorophenoxy) phenol). The intermediate products mainly observed in the photolysis of Triclosan derivatives were phenol, 4-chlorophenol and hydroquinone. In addition, it is noted that the formation of dioxins was only found in the photolysis of 2ClOH and 2ClOHCl, reaching values up to 1.8 mg L^{-1}.

- The photolysis of Triclosan and six of its hydrodehalogenation derivatives led to the following conclusions: the time required to achieve high degradation rates increased as the number of chlorine atoms present in the molecule decreased, for this reason, Triclosan presented the highest degradation rate in comparison to their hydrodehalogenation derivatives; and, the presence of dioxins (monocholorodibenzo-p-dioxin and/or 2,8-dichlorodibenzo-p-dioxin) was only observed when the target molecule

presented a chlorine atom in the position number 2 of the benzene ring, that is Triclosan, 2ClOH and 2ClOHCl derivatives, achieving values up to 0.6 mg L^{-1}.

- In order to put together most of the pieces of the puzzle and achieve a better understanding of the reaction mechanisms involved in the photolysis of Triclosan, the photolysis of the intermediates found at the highest concentrations was carried out. These compounds were: $(OH)_2$PCB13 ((4,5´-dichloro-[1,1´-biphenyl]-2,2´-diol), 2,2´-biphenol, phenol, 2-chlorophenol, 3-chlorophenol, 4-chlorophenol and 2,4-dichlorophenol. The time required to achieve a complete degradation of the intermediates ranged between 10 and 90 minutes. Thanks to the photolysis of the main intermediate products of Triclosan and its derivatives, useful knowledge about the reaction mechanisms involved in the photo-degradation of Triclosan was obtained.

- Then, based on the experimental results, a complete reaction pathway that described the photolysis of Triclosan was proposed. $(OH)_2$PCB13 was proposed as an intermediate product of Triclosan that was also was degraded along the treatment, leading to the formation of chlorophenols through a breakage cleavage. 2,4-dichlorophenol, produced by a photo-induced hydrolysis of Triclosan, might be dechlorinated to generate chlorophenols. Besides, a dechlorination reaction of Triclosan might form hydrodehalogenation derivatives of Triclosan, such as 4ClOHCl and OHCl. Then, 4ClOHCl and OHCl molecules could be broken to form chlorophenols. The formation of catechol, hydroquinone and phenol as Triclosan photo-products could be explained by dechlorination reactions followed by rearrangement of the molecule. On the other hand, 2,8-dichlorodibenzo-p-dioxin was an intermediate product, whereas monochlorodibenzo-p-dioxin remained constant along the Triclosan treatment. However, the formation of these congeners was only observed for those hydrodehalogenation derivatives of Triclosan that had a chlorine atom in the position number 2 of the benzene ring. This could explain the reaction mechanism involved in the formation of this congener, which started with a breakage of the chloro-carbon bond located at the position 2 of the benzene ring of Triclosan.

On the Triclosan photocatalysis: experiments

In the last section of chapter 4, the photocatalysis of Triclosan has been assessed. Experiments, with an initial concentration of 10 mg L^{-1} of Triclosan, have been carried out with emission wavelength between 375 and 380 nm. Three different concentration of TiO_2 have been

studied: 0.75, 1.0 and 1.5 g L^{-1}. For the three photocatalyst loadings studied in this work, a complete removal of Triclosan was achieved, reaching the highest degradation rate with 1.5 g L^{-1} of TiO_2. 2,4-dichlorophenol was found as an intermediate compound with values up to 0.8 mg L^{-1} for all the three catalyst loadings studied; its formation is associated to the homolytic scission of the carbon-oxygen bond of Triclosan molecule. Finally, the analysis of highly chlorinated PCDD/Fs when Triclosan was completely removed was determined.

The total PCDD/Fs concentration increased from $2.3 \cdot 10^1$ pg L^{-1} for the untreated sample to $1.0 \cdot 10^5$, $1.2 \cdot 10^5$ and $9.8 \cdot 10^2$ pg L^{-1} for the three TiO_2 concentrations studied in this thesis. Actually, the PCDF profile accounted for more than 90.4 % of the total PCCD/Fs concentration, specifically, 98.0, 99.3 and 90.4 % when using 0.75, 1 and 1.5 g L^{-1} of TiO_2, respectively. 2,3,7,8-TCDD, 1,2,3,4,6,7,8-HpCDD and OCDD were the congeners that presented the highest concentrations when the TiO_2 loading was 0.75 g L^{-1}, accounting for 30.7, 11.1 and 20.3 % of the total 2,3,7,8-PCDD/Fs. When the dose of catalyst applied was 1 g L^{-1}, 2,3,7,8-TCDD, OCDD and PCDF were the predominant congeners (13.4 – 23.7 % of the total 2,3,7,8-PCDD/Fs). Finally, for 1.5 g L^{-1} as TiO_2 loading, OCDF was the predominant congener, accounting for 37.0 % of the total 2,3,7,8-PCDD/Fs. Furthermore, TEQ values increased in comparison to the untreated sample, being 104, 71 and 10 times higher than the untreated sample. However, these values decreased as the concentration of TiO_2 employed in the treatment increased (6.3, 4.2 and 0.6 pg L^{-1}, respectively).

A summary reporting all the results obtained is presented below (Table 5.3).

Table 5.3. Summary of highly chlorinated PCDD/Fs and TEQ concentrations in the untreated and photocatalytic oxidized samples.

	Total highly PCDD/Fs concentration (pg L^{-1})			**Total highly PCDFs (furans) concentration (pg L^{-1})**			**2,3,7,8-PCDD/Fs congeners concentration (pg L^{-1})**			**TEQ (pg L^{-1})**		
Untreated sample	**82.3**	**90.8**	**221.9**	**51.8**	**28.1**	**105.5**	**7.3**	**13.6**	**11.2**	**0.4**	**0.5**	**1.3**
	TiO_2 loading (g L^{-1})											
	0.75	1	1.5	0.75	1	1.5	0.75	1	1.5	0.75	1	1.5
$\frac{\text{Treated sample}}{\text{Untreated sample}}$*	43772	5208	42	7499	9040	66	8	7	2	104	71	10

* the table expresses the ratio of the concentration determined in these samples with respect to the concentration in the untreated samples

Electrochemical oxidation vs. Photocatalysis oxidation

Summarizing, in order to compare both technologies (electrochemical and photochemical oxidation treatments) in terms of toxicity, the experiments with an initial concentration of 10 mg L^{-1} of Triclosan were used as reference. When electrochemical oxidation treatment was applied, TEQ values increased from 0.4 pg L^{-1} for the untreated sample to 4.7 and 4.4 pg L^{-1} when NaCl and Na_2SO_4 was present in the solution medium, respectively. On the other hand, TEQ values increased from 0.1 pg L^{-1} for the untreated sample to 0.6 pg L^{-1} when applying a photocatalytic treatment with a TiO_2 loading of 1.5 g L^{-1}, which was demonstrated to be the optimum dose of catalyst among the doses studied in this work. However, TEQ had a value of 6.3 pg L^{-1} when the catalyst dose was 0.75 g L^{-1}. To conclude, in these cases in which the initial concentration of Triclosan was 10 mg L^{-1}, TEQ did not take high values, being below the maximum value established by the U.S. EPA for drinking water (30 pg L^{-1}). However, and as reported and demonstrated along this work, the importance of considering the operational conditions when applying AOPs could have a great influence on the formation of by-products, and, as a consequence, on the final toxicity of the sample after the treatment, which may be higher than the initial wastewater toxicity.

Conclusiones

La Tesis Doctoral aquí presentada tiene como objetivo la aplicación de procesos de oxidación avanzada (POAs) a muestras acuosas que contienen Triclosán (TCS); además del análisis del rendimiento oxidativo en términos de degradación de Triclosán, se ha prestado especial atención a la formación de productos intermedios, especialmente a la potencial formación de dibenzo-p-dioxinas y dibenzofuranos policlorados (PCDD/Fs) y su intrínseca toxicidad. En particular, se han evaluado la oxidación electroquímica y fotoquímica aplicadas a soluciones modelo de Triclosán. Una vez analizado el estado del arte y los resultados obtenidos de manera experimental, las siguientes conclusiones han sido tomadas,

Oxidación electroquímica del Triclosán

En el capítulo 3, la oxidación electroquímica de disoluciones acuosas de Triclosán (con concentraciones iniciales de 10, 100 y 150 mg L^{-1}) empleando ánodos de diamante dopado con

boro (BDD) fue llevada a cabo bajo condiciones galvanostáticas (J= 6, 60 y 90 A m^{-2}, respectivamente). Además, se estudió la influencia de dos electrolitos comúnmente utilizados, NaCl (56.3 mM) y Na_2SO_4 (21.1 mM), así como la presencia de cobre (10 mg L^{-1}) en la degradación de Triclosán.

Aunque se consiguió una completa eliminación del Triclosán para todas las concentraciones iniciales estudiadas, la carga eléctrica específica aumentó con la concentración inicial de Triclosán. El tiempo necesario para alcanzar la completa eliminación fue de 1, 3 y 4 horas para las tres concentraciones de Triclosán estudiadas, 10, 100 y 150 mg L^{-1}, respectivamente. Las cinéticas de degradación fueron independientes del electrolito empleado así como de la presencia de cobre en la disolución acuosa.

Además de la degradación de Triclosán, se determinó la presencia de diferentes subproductos de oxidación. El análisis en cromatografía de gases (GC-MS) se determinó para la disolución de 100 mg L^{-1} Triclosán, confirmando la formación de compuestos intermedias cloro-aromáticos, tales como 2,4-diclorofenol, 4-clorocatecol, 2-clorohidroquinona, 2-cloro-4-metoxifenol y 1-cloro-2,5-dimetoxibenceno, independientemente del electrolito empleado. Además, también se detectó la formación de productos no clorados: 2-etil-hexanol y difenil éter benceno.

El análisis de la formación de PCDD/Fs altamente clorados se determinó a través del método EPA 1613 cuando se consiguió una completa eliminación del Triclosán.

- En primer lugar, se llevó a cabo el análisis de PCDD/Fs en las muestras sin tratar, dando lugar a una concentración total de PCCD/Fs de $8.2 \cdot 10^1$, $9.1 \cdot 10^1$ y $2.2 \cdot 10^2$ pg L^{-1} para 10, 100 y 150 mg L^{-1} de Triclosán, respectivamente. La toxicidad expresada como Equivalente Tóxico (TEQ) fue de 0.4, 0.6 y 1.3 pg L^{-1} para las tres concentraciones iniciales de Triclosán.

- El uso de NaCl como electrolito dio lugar a una concentración total de PCDD/Fs en las muestras oxidadas de $3.7 \cdot 10^2$, $3.4 \cdot 10^4$ y $1.6 \cdot 10^5$ pg L^{-1}, siendo del total el 82.5, 91.2 y 99.5 % el porcentaje correspondiente al perfil de PCDD (perfil de dioxinas) para las concentraciones iniciales de Triclosán estudiadas en este trabajo (10, 100 y 150 mg L^{-1}). Sin embargo, aunque la contribución de los congéneres 2,3,7,8-clorosustituídos al total de PCDD/Fs fue muy baja (representando el 0.8, 1.8 y 5.2 %), los niveles de TEQ aumentaron desde valores cercanos a cero para las muestras sin tratar, hasta

concentraciones de 4.7, $2.8 \cdot 10^2$ y $3.8 \cdot 10^2$ pg L^{-1} para las muestras tratadas (10, 100 y 150 mg L^{-1} de TCS, respectivamente). En particular, los valores de TEQ fueron 11, 320 y 300 veces mayor que en las muestras sin tratar para las tres disoluciones de Triclosán estudiadas. Estos valores fueron mucho más altos en los dos últimos casos que el límite establecido por la EPA en aguas de bebida (30 pg L^{-1}), en concreto, 9 y 13 veces mayor que el máximo permitido.

- Respecto al uso de Na_2SO_4 como electrolito, la concentración total de PCDD/Fs aumentó a $2.9 \cdot 10^2$, $8.6 \cdot 10^3$ y $8.4 \cdot 10^4$ pg L^{-1}, de los cuales, el perfil de PCDD (perfil de dioxinas) representó el 86.3, 80.9 y 97.9 %. La concentración de los congéneres 2,3,7,8-clorosustituídos representó el 6.7, 1.7 y 0.7 % del total de PCDD/Fs para las tres concentraciones iniciales de Triclosán estudiadas (10, 100 y 150 mg L^{-1}). Los valores de TEQ aumentaron ligeramente en comparación con los de la muestra sin tratar, en concreto los valores fueron 10, 97 y 20 veces mayor, correspondiendo a concentraciones de 4.4, $5.3 \cdot 10^1$ y $2.5 \cdot 10^1$ pg L^{-1} para 10, 100 y 150 mg L^{-1} de Triclosán en las muestras, respectivamente.

A continuación, se presenta un resumen que recoge todos los resultados obtenidos (Tabla 5.1).

Tabla 5.1. Resumen de las PCDD/Fs más clorados y de las concentraciones TEQ en las muestras sin tratar y en las muestras oxidadas.

	Concentración total de las PCDD/Fs más clorados (pg L^{-1})			**Concentración total de PCDDs (dioxinas) (pg L^{-1})**			**Concentración de los congéneres 2,3,7,8-PCDD/Fs (pg L^{-1})**			**TEQ (pg L^{-1})**		
	Concentración inicial de Triclosán (mg L^{-1})											
	10	100	150	10	100	150	10	100	150	10	100	150
Muestra sin tratar	**82.3**	**90.9**	**221.9**	**51.8**	**28.1**	**105.5**	**7.4**	**13.6**	**11.2**	**0.4**	**0.5**	**1.3**
$\frac{NaCl}{\text{Muestra sin tratar}}$*	5	376	739	6	1109	1546	3	45	119	11	501	301
$\frac{Na_2SO_4}{\text{Muestra sin tratar}}$*	4	75	38	5	196	78	3	11	5	10	97	20

* La tabla expresa el ratio de concentración determinado en las muestras con respecto a la concentración de las muestras sin tratar.

- Por otra parte, se estudió la influencia del cobre en la potencial formación de PCDD/Fs altamente clorados para disoluciones que contenían 100 mg L^{-1} de Triclosán. La concentración total de PCDD/Fs fue de $1.5 \cdot 10^4$ y $5.6 \cdot 10^3$ pg L^{-1} en presencia de NaCl y Na_2SO_4, disminuyendo un 55.8 y 35.1 % cuando el cobre estaba presente en el medio de reacción, respectivamente. El perfil de PCDD (perfil de dioxinas) representó el 89.9 y 70.4 % empleando NaCl y Na_2SO_4, respectivamente. Además, la concentración de los congéneres 2,3,7,8-clorosustituídos solo representó el 2.3 y el 2.5 % del total de PCDD/Fs para los dos electrolitos empleados, lo que condujo a una disminución de los valores de TEQ en presencia de cobre: $1.7 \cdot 10^2$ y $4.5 \cdot 10^1$ pg L^{-1} para ambos electrolitos. Teniendo en cuenta estos resultados, se puede concluir que el cobre puede actuar como catalizador en la oxidación electroquímica del Triclosán, teniendo una importante influencia en el decrecimiento de la formación de PCDD/Fs, independientemente del electrolito empleado. Por lo tanto, los valores de toxicidad fueron menores en presencia del cobre, disminuyendo un 5 y 15 % en comparación con aquellas muestras en las que no se empleó cobre y se usó NaCl y Na_2SO_4, respectivamente.

A continuación, el análisis de las PCDD/Fs no clorados y de baja cloración se llevó a cabo para las muestras oxidadas de Triclosán (10, 100 y 150 mg L^{-1}), cuando el Triclosán se había eliminado completamente, extendiendo el método EPA 1613. Cuando se usó NaCl como electrolito, la concentración total de las PCDD/Fs menos clorados aumentó desde $8.33 \cdot 10^3$, $1.56 \cdot 10^5$ y $2.23 \cdot 10^5$ pg L^{-1} para las muestras sin tratar, hasta $6.75 \cdot 10^4$, $2.04 \cdot 10^5$ y $1.01 \cdot 10^6$ pg L^{-1} para las tres concentraciones de Triclosán estudiadas. Sin embargo, en presencia de Na_2SO_4, la concentración total de estas especies permaneció constante o se redujo ligeramente a $8.47 \cdot 10^3$, $1.48 \cdot 10^5$ y $1.61 \cdot 10^5$ pg L^{-1}.

Un resumen conteniendo todos los resultados obtenidos en esta sección se presenta a continuación (Tabla 5.2).

Tabla 5.2. Resumen de las concentraciones de PCDD/Fs menos clorados tanto en las muestras sin tratar como en las muestras oxidadas.

	Concentración total de PCDD/Fs menos clorados (pg L^{-1})			**Concentración total de PCDDs (dioxinas) menos cloradas (pg L^{-1})**		
	Concentración inicial de Triclosán (mg L^{-1})					
	10	100	150	10	100	150
Muestra sin tratar	**8326.6**	**156624.5**	**222761.0**	**5647.7**	**139235.8**	**205926.1**
$\frac{\mathbf{NaCl}}{\mathbf{Muestra\ sin\ tratar}}$ *	8	1	5	12	1	0.5
$\frac{\mathbf{Na_2SO_4}}{\mathbf{Muestra\ sin\ tratar}}$ *	1	1	0.5	1	1	1

* La tabla expresa el ratio de concentración determinado en las muestras tratadas con respecto a la concentración de las muestras sin tratar.

De este modo, cuando la muestra contiene NaCl, la presencia de cobre conduce a una disminución de la concentración de las PCDD/Fs menos clorados, desde $2.04 \cdot 10^5$ hasta $7.01 \cdot 10^4$ pg L^{-1} (representando una reducción del 65.6 %). En presencia de Na_2SO_4 como electrolito, este valor se redujo desde $1.48 \cdot 10^5$ hasta $6.50 \cdot 10^4$ pg L^{-1} (representando una reducción del 56.1 %).

Cabe destacar la elevada concentración de las PCCD/Fs de baja cloración en las muestras sin tratar, así como en las muestras oxidadas. Además, la formación de 2,7/2,8-diclorodibenzo-p-dioxina durante la oxidación del Triclosán ha estado en el punto de mira de muchos autores. Por esta razón, se desarrolló un análisis exhaustivo de la formación de este congéner durante la oxidación electroquímica del Triclosán. Los resultados obtenidos por cromatografía de gases (GC-MS) mostraron una disminución en la concentración de 2,7/2,8-diclorodibenzo-p-dioxina a lo largo del tratamiento oxidativo, siendo la concentración más alta observada la correspondiente a la muestra sin tratar. Sin embargo, estos resultados no fueron corroborados cuando se empleó cromatografía líquida (HPLC). Con esta evaluación analítica, se puede proponer que la formación del congéner 2,7/2,8-diclorodibenzo-p-dioxina puede producirse debido a la ciclación directa del Triclosán durante el análisis a través de GC-MS, más concretamente en la etapa inyección a altas temperaturas dentro del equipo. Por tanto, el uso de la técnica de GC-MS en las condiciones empleadas en este trabajo puede no ser un método fiable para el análisis de 2,7/2,8-diclorodibenzo-p-dioxina en muestras en las que el Triclosán está presente, y puede dar lugar a resultados inciertos. Además, la expansion del método EPA 1613 aplicado a las especies no clorados y de baja cloración dio lugar a porcentajes de recuperación bajos. Por esta razón, la fiabilidad de este método aplicado a la trazabilidad

cuantitativa en la formación de 2,7/2,8-diclorodibenzo-p-dioxina no es consistente. Por lo tanto, se puede concluir que el análisis de este compuesto bajo las condiciones estudiadas en este trabajo es una tarea compleja que requiriendo profundizar en los métodos analíticos.

Por último, se han propuesto los mecanismos de reacción que describen la formación de los subproductos identificados en este trabajo. Los mecanismos de reacción propuestos se basan en los resultados experimentales obtenidos en esta tesis, además de estar respaldados por la literaura, la cual contiene resultados experimentales o de simulación molecular (empleando el software de química computacional *Gaussian*). El mecanismo de reacción propuesto comienza con la abstracción de un hidrógeno del anillo fenólico de la molécula de Triclosán, reportada como la ruta que presentaba una energía libre más baja en comparación con las otras rutas calculadas por simulación molecular. A continuación, los diferentes mecanismos de reacción describieron la formación de subproductos, los cuales fueron observados en los resultados experimentales obtenidos en este trabajo, y respaldados con la literatura tanto con datos experimentales como de simulación molecular: (i) la ruptura de la molécula, decloración, o reacciones de reordenación, condujeron a la formación de moléculas más pequeñas como el 2,4-diclorofenol, 4-clorocatecol or 2-clorohidroquinona; y (ii) reacciones de ciclación condujeron a la formación de PCDD/Fs de baja cloración, que con sucesivas reacciones de cloración, dan lugar a PCDD/Fs altamente clorados.

Oxidación fotocatalítica del Triclosán

En el capítulo 4, se han aplicado dos tratamientos de oxidación fotolítica (fotólisis y fotocatálisis) a disoluciones acuosas sintéticas de Triclosán. En primer lugar, se ha llevado a cabo un análisis exhaustivo y crítico de los últimos avances reportados en la literatura relacionados con las técnicas de fotodegradación aplicadas a las disoluciones de Triclosán, así como a la formación de diferentes productos intermedios.

Conclusiones después de la revision del estado del arte en la fotólisis de TCS

Como se reporta en la literatura, el pH fue un parámetro decisivo que jugó un papel importante en la fotodegradación de Triclosán. Longitudes de onda de 300 nm mejoraron el proceso fotolítico de Triclosán en condiciones donde éste se encontró en su forma fenolato (pH > pK_a: 7.9 – 8.1). Junto con la longitud de onda, la intensidad de la lámpara también fue un factor decisivo en la fotodegradación del Triclosán. En relación a la presencia de otras sustancias en el medio de reacción, tales como ácidos húmicos o sales inorgánicas, los resultados resaltaron la

complejidad añadida al estudio de degradación fotoquímica. Además, la presencia de scavengers en las muestras tratadas, como el 2-propanol o el metanol, podrían inhibir la degradación fotolítica del Triclosán debido a la competencia por los fotones o radicales presentes en el medio de reacción. Finalmente, con respecto a la influencia del catalizador en la solución, en la mayoría de los casos TiO_2, los estudios reportados mostraron que su presencia mejoraba altamente la cinética de la degradación de Triclosán independientemente del catalizador utilizado o la dosis empleada.

Análisis crítico de los subproductos del Triclosán

Aunque los tratamientos fotolíticos han presentado una alta eficacia en la degradación de Triclosán, se ha demostrado la formación de diferentes subproductos durante el tratamiento. Se han descrito dos vías principales de reacción: oxidación directa por acción de un fotón (fotólisis) y oxidación indirecta por acción de radicales ·OH (fotocatálisis). 2,4-diclorofenol ha sido uno de los principales productos de la fotodegradación del Triclosán; su formación está asociada a la hidrólisis fotoinducida del Triclosán debido al efecto de la luz UV que produce la ruptura del éter (fotólisis) o por la acción de ·OH, causando una ruptura homolítica del enlace carbono-oxígeno (fotocatálisis). Además, el clorofenol y el 4-clorocatecol pueden formarse por la acción de los radicales ·OH o por la hidrólisis foto-inducida de Triclosán bajo luz UV. Las sucesivas reacciones de decloración de los clorofenoles produjeron la formación de fenoles. La formación de Triclosan polimerizado, 4,5´-dicloro-[1,1´-bifenil]-2,2´-diol ($(OH)_2$PCB13), Triclosán-quinona y Triclosán-catecol han sido también determinados en la oxidación fotoquímica del Triclosán. Finalmente, la formación de 2,8-diclorodibenzo-p-dioxina ha sido ampliamente estudiada. Su formación proviene de una reacción de ciclación del Triclosán favorecida bajo ciertas condiciones de operación: pH básicos, en presencia de aniones NO_3^-, y bajo elevadas intensidades de luz. Por el contrario, su formación se inhibe a pH ácidos y en presencia de ácidos húmicos. Además, la formación de 2,8-diclorodibenzo-p-dioxina podría inhibirse en procesos fotocatalíticos debido a la acción de radicales ·OH, que provocan la ruptura de la molécula de Triclosán.

Fotólisis del Triclosán: experimentos

A continuación, la oxidación fotolítica del Triclosán y sus seis derivados hidrodeshalogenados (moléculas de Triclosán que presentan menos átomos de cloro y están situados en las tres diferentes posiciones de la molécula de Triclosán), con una concentración inicial de cada compuesto de 50 µM (equivalente a 14.5 mg L^{-1} en el caso de Triclosán) fue

realizada a 300 nm. El objetivo de este estudio consisitó en mejorar la comprensión de los mecanismos de reacción que condujeron a la formación de PCDD/Fs y compuestos relacionados en la fotólisis de Triclosán, y más específicamente, identificar el cloro que conduce a la formación de 2,8-diclorodibenzo-p-dioxina. Primero, se determinó el pK_a de todos los compuestos estudiados, y, para asegurar la máxima absorbancia de luz por parte del Triclosán y sus derivados, el pH de la disolución se mantuvo por encima de su pK_a.

- La fotólisis del Triclosán tuvo una duración de 20 minutos, momento en el que se alcanzó su completa eliminación. Sin embargo, se formaron varios subproductos. 3-clorofenol, 4-clorofenol, 2,4-diclorofenol, $(OH)_2$PCB13, monoclorodibenzo-p-dioxina y 2,8-diclorodibenzo-p-dioxina fueron los principales productos observados en la fotólisis del Triclosán, alcanzando valores por encima de 0.5 mg L^{-1}. Asimismo, se observó un derivado hidrodeshalogenado del Triclosán: 4ClOHCl (5-cloro-2-(4-clorofenoxi)fenol).

- A continuación, se realizó la fotólisis de los seis derivados de hidrodeshalogenación del Triclosán: OH (2-fenoxifenol), OHCl (5-cloro-2-fenoxifenol), 2ClOH (2-(2-clorofenoxifenol), 2ClOHCl (5-cloro-2-(2-clorofenoxifenol), 4ClOH (2-(4-clorofenoxifenol) y 4ClOHCl (5-cloro-2-(4-clorofenoxifenol). Los principales productos intermedios observados en la fotólisis de los derivados del Triclosán fueron fenol, 4-clorofenol e hidroquinona. Además, se observa que la formación de dioxinas solo fue encontrada en la fotólisis del 2ClOH y 2ClOHCl, alcanzando valores de hasta 1.8 mg L^{-1}.

- La fotólisis del Triclosán y de sus seis derivados de hidrodeshalogenación permitieron llegar a las siguientes conclusiones: el tiempo requerido para lograr altas tasas de degradación aumentó a medida que disminuyó el número de átomos de cloro presentes en la molécula, y por esta razón, el Triclosán presentó la mayor tasa de degradación en comparación con sus derivados de hidrodeshalogenación; y, la presencia de dioxinas (monoclorodibenzo-p-dioxina y/o 2,8-diclorodibenzo-p-dioxina) solo fue observada cuando la molécula presentaba un átomo de cloro en la posición número 2 del anillo bencénico, correspondiente al Triclosán y sus derivados 2ClOH y 2ClOHCl, alcanzando valores de hasta 0.6 mg L^{-1}.

- Con el fin una mejor comprensión de los mecanismos de reacción involucrados en la fotólisis del Triclosán, se llevó a cabo la oxidación fotolítica de los intermedios

encontrados a concentraciones más elevadas. Estos compuestos fueron: $(OH)_2$PCB13, 2,2´-bifenol, fenol, 2-clorofenol, 3-clorofenol, 4-clorofenol y 2,4-diclorofenol. Los tiempos requeridos para alcanzar la completa degradación de éstos fueron de entre 10 y 90 minutos. Gracias a la fotólisis de los principales productos intermedios del TCS y sus derivados, se obtuvo información de gran utilidad acerca de los mecanismos de reacción involucrados en la fotodegradación del TCS.

- A continuación, basados en los resultados obtenidos experimentalmente, se propusieron los mecanismos de reacción que describen la oxidación fotolítica del Triclosán. $(OH)_2$PCB13, producto intermedio de degradación del Triclosán, fue también oxidado, dando lugar a la formación de clorofenoles a través de la ruptura de la molécula. 2,4-diclorofenol, producido por hidrólisis fotoinducida del Triclosán, puede generar clorofenoles a través de reacciones de decloración. Además, una reacción de decloración de Triclosán podría generar derivados de hidrodeshalogenación, como 4ClOHCl y OHCl, para, a continuación, romperse y formar clorofenoles. La formación de catecol, hidroquinona y fenol como fotoproductos del Triclosán podrían producirse por reacciones de decloración seguidas de un reordenamiento de la molécula. Por otra parte, 2,8-diclorodibenzo-p-dioxina fue determinado como un producto intermedio, mientras que la monoclorodibenzo-p-dioxina permaneció constante a lo largo del tratamiento del Triclosán. Sin embargo, la formación de estos congéneres solo fue observada para aquellos derivados hidrodeshalogenados del Triclosán que tienen un átomo de cloro en la posición número 2 del anillo bencénico. Esto podría explicar el mecanismo de reacción involucrado en la formación de este congéner, comenzando con la ruptura del enlace cloro-carbono situado en la posición 2 del anillo bencénico del Triclosán.

Fotocatálisis del Triclosán: experimentos

En la última sección del capítulo 4, se realiza una evaluación de la oxidación fotocatalítica del Triclosán. Los experimentos fueron llevados a cabo con una concentración inicial de Triclosán de 10 mg L^{-1} aplicando una longitud de onda de entre 375 y 380 nm. Se estudiaron tres concentraciones diferentes de TiO_2: 0.75, 1.0 y 1.5 g L^{-1}. Se obtuvo una completa eliminación de Triclosán para las 3 cargas de catalizador estudiadas en este trabajo, alcanzándose el mayor ratio de degradación con 1.5 g L^{-1} de TiO_2. 2,4-diclorofenol se observó como un compuesto intermedio con valores de hasta 0.8 mg L^{-1} para las 3 cargas de catalizador estudiadas; su formación está asociada con la ruptura homolítica del enlace carbono-oxígeno de la molécula del Triclosán.

Finalmente, se determinó el análisis de las PCDD/Fs más clorados cuando el Triclosán fue eliminado completamente.

La concentración total de PCDD/Fs aumentó desde $2.3 \cdot 10^1$ pg L^{-1} para la muestra sin tratar hasta $1.0 \cdot 10^5$, $1.2 \cdot 10^5$ y $9.8 \cdot 10^2$ pg L^{-1} para las tres concentraciones de TiO_2 estudiadas en esta tesis. En efecto, el perfil de PCDF representó más del 90.4 % de la concentración total de PCCD/Fs, concretamente, 98.0, 99.3 y 90.4 % cuando se empleó 0.75, 1 y 1.5 g L^{-1} de TiO_2, respectivamente. 2,3,7,8-TCDD, 1,2,3,4,6,7,8-HpCDD y OCDD fueron los congérenes que presentaron las concentraciones más elevadas cuando para concentración de TiO_2 de 0.75 g L^{-1}, representando el 30.7, 11.1 y 20.3 % del total de 2,3,7,8-PCDD/Fs. Cuando la cantidad de catalizador empleada fue de 1 g L^{-1}, 2,3,7,8-TCDD, OCDD y PCDF fueron los congéneres predominantes (13.4 – 23.7 % del total de 2,3,7,8-PCDD/Fs). Finalmente, para 1.5 g L^{-1} de TiO_2, OCDF fue el congéner predominante, representando el 37.0 % del total de 2,3,7,8-PCDD/Fs. Además, los valores de TEQ aumentaron en comparación con respecto a la muestra sin tratar, siendo 104, 71 y 10 veces mayor. No obstante, estos valores disminuyeron a medida que la concentración de TiO_2 empleada en el tratamiento aumentó (6.3, 4.2 and 0.6 pg L^{-1}, respectivamente).

A continuación, se presenta un resumen presentando todos los resultados obtenidos en esta sección (Tabla 5.3).

Table 5.1. Resumen de las PCDD/Fs más clorados y las concentraciones de TEQ en las muestras sin tratar y fotocatalíticamente oxidadas.

	Concentración total de PCDD/Fs más clorados (pg L^{-1})			**Concentración total de PCDFs (furanos) más clorados (pg L^{-1})**			**Concentración de los congéneres 2,3,7,8-PCDD/Fs (pg L^{-1})**			**TEQ (pg L^{-1})**		
Muestra sin tratar	**82.3**	**90.8**	**221.9**	**51.8**	**28.1**	**105.5**	**7.3**	**13.6**	**11.2**	**0.4**	**0.5**	**1.3**
	Cantidad de TiO_2 (g L^{-1})											
	0.75	1	1.5	0.75	1	1.5	0.75	1	1.5	0.75	1	1.5
$\frac{\text{Muestra tratada}}{\text{Muestra sin tratar}}$ *	43772	5208	42	7499	9040	66	8	7	2	104	71	10

* La tabla expresa el ratio de concentración determinado en estas muestras con respecto a la concentración de las muestras sin tratar.

Oxidación electroquímica vs. oxidación fotocatalítica

Con el obejtivo de comparar ambas tecnologías (oxidación electroquímica y fotocatalítica) en términos de toxicidad, los experimentos con una concentración inicial de 10 mg L^{-1} de Triclosán fueron empleados como referencia. Cuando se aplicó la oxidación electroquímica, los valores de TEQ incrementaron desde 0.4 pg L^{-1} para la muestra sin tratar hasta 4.7 y 4.4 pg L^{-1} cuando se empleó NaCl y Na_2SO_4 como electrolitos, respectivamente. Por otra parte, los valores de TEQ aumentaron desde 0.1 pg L^{-1} para la muestra sin tratar hasta 0.6 pg L^{-1} cuando se aplicó un tratamiento fotocatalítico con una cantidad de TiO_2 de 1.5 g L^{-1}, la cual fue la cantidad óptima de catalizador de entre todas las dosis estudiadas en este trabajo. Sin embargo, el TEQ aumentó hasta 6.3 pg L^{-1} cuando la dosis de catalizador fue de 0.75 g L^{-1}. Para concluir, en los casos en los que la concentración de TCS fue de 10 mg L^{-1}, el TEQ no tuvo valores excesivamente altos, siendo menores que el máximo establecido por la U.S. EPA para el agua potable (30 pg L^{-1}). No obstante, como se describió y demostró a lo largo de todo este trabajo, la importancia de tener en consideración las condiciones operacionales a la hora de aplicar POAs puede tener una gran influencia en la formación de subproductos, y, en consecuencia, en la toxicidad final de la muestra después del tratamiento, la cual puede ser mayor que la toxicidad inicial del agua de partida.

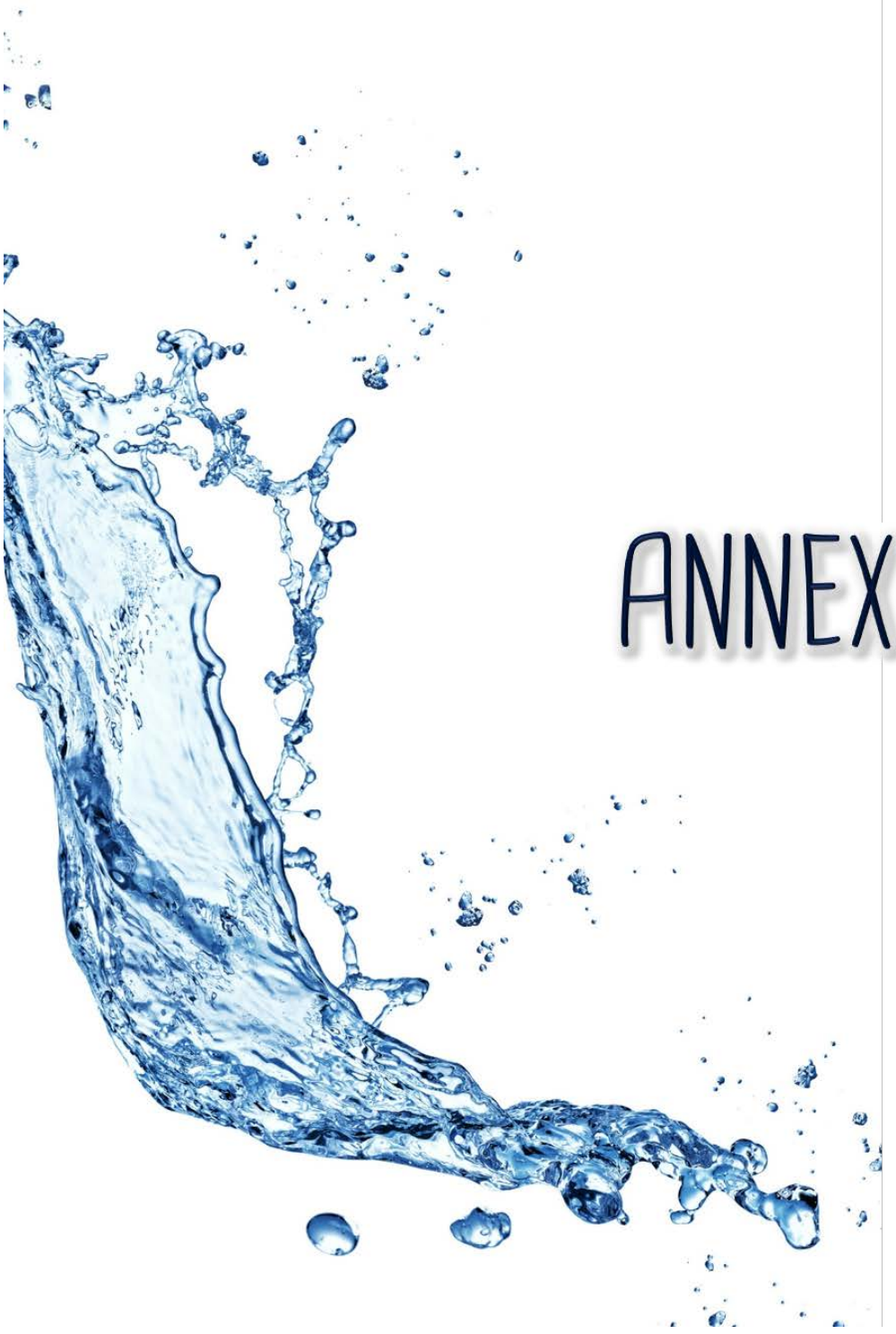

ANNEXES

ANNEX I. Concentration of labelled EPA 1613 solutions

Table I.1. Concentration of PCDD/Fs in labelled EPA 1613 LCS standard solution from Wellington Laboratories Inc. It contains the PCDD/Fs isotopically labelled with $^{13}C_{12}$.

	Concentration (ng mL^{-1})
	LCS (Labelled compound stock solution)
2,3,7,8-Tetrachloro[$^{13}C_{12}$]dibenzo-p-dioxin	100
1,2,3,7,8-Pentachloro[$^{13}C_{12}$]dibenzo-p-dioxin	100
1,2,3,4,7,8-Hexachloro[$^{13}C_{12}$]dibenzo-p-dioxin	100
1,2,3,6,7,8-Hexachloro[$^{13}C_{12}$]dibenzo-p-dioxin	100
1,2,3,4,6,7,8-Heptachloro[$^{13}C_{12}$]dibenzo-p-dioxin	100
Octachloro[$^{13}C_{12}$]dibenzo-p-dioxin	200
2,3,7,8-Tetrachloro[$^{13}C_{12}$]dibenzofuran	100
1,2,3,7,8-Pentachloro[$^{13}C_{12}$]dibenzofuran	100
2,3,4,7,8-Pentachloro[$^{13}C_{12}$]dibenzofuran	100
1,2,3,4,7,8-Hexachloro[$^{13}C_{12}$]dibenzofuran	100
1,2,3,6,7,8-Hexachloro[$^{13}C_{12}$]dibenzofuran	100
1,2,3,7,8,9-Hexachloro[$^{13}C_{12}$]dibenzofuran	100
2,3,4,6,7,8-Hexachloro[$^{13}C_{12}$]dibenzofuran	100
1,2,3,4,6,7,8-Heptachloro[$^{13}C_{12}$]dibenzofuran	100
1,2,3,4,7,8,9-Heptachloro[$^{13}C_{12}$]dibenzofuran	100

Table I.2. Concentration of non-chlorinated and low chlorinated PCDD/Fs (mono to tri-) in native standard solutions from Wellington Laboratories Inc.

	Concentration (µg mL^{-1})
	DDF-MDT (Native PCDD/PCDF solution/mixture)
Dibenzo-p-dioxin	1.0
2-Chlorodibenzo-p-dioxin	1.0
2,3-Dichlorodibenzo-p-dioxin	1.0
2,3,7-Trichlorodibenzo-p-dioxin	1.0
Dibenzofuran	1.0
2-Chlorodibenzofuran	1.0
2,3-Dichlorodibenzofuran	1.0
2,3,8-Trichlorodibenzofuran	1.0

Table I.3. Concentration of non-chlorinated and low chlorinated PCDD/Fs (mono to tri-) in labelled standard solutions from Wellington Laboratories Inc. It contains the PCDD/Fs isotopically labelled with $^{13}C_{12}$.

	Concentration (µg mL^{-1})
	MDDF-MDT (Mass-labelled PCDD/PCDF solution/mixture)
[$^{13}C_{12}$]Dibenzo-p-dioxin	1.0
2-Chloro[$^{13}C_{12}$]dibenzo-p-dioxin	1.0
2,3-Dichloro[$^{13}C_{12}$]dibenzo-p-dioxin	1.0
2,3,7-Trichloro[$^{13}C_{12}$]dibenzo-p-dioxin	1.0
[$^{13}C_{12}$]Dibenzofuran	1.0
2-Chloro[$^{13}C_{12}$]dibenzofuran	1.0
2,3-Dichloro[$^{13}C_{12}$]dibenzofuran	1.0
2,3,8-Trichloro[$^{13}C_{12}$]dibenzofuran	1.0

Table I.4. Concentration of PCDD/Fs in labelled EPA 1613ISS standard solution from Wellington Laboratories Inc. It contains the PCDD/Fs isotopically labelled with $^{13}C_{12}$.

	Concentration (ng mL^{-1})
	ISS (Internal standard spiking solution)
2,3,7,8-Tetrachloro[$^{13}C_{12}$]dibenzo-p-dioxin	200
1,2,3,7,8,9-Hexachloro[$^{13}C_{12}$]dibenzo-p-dioxin	200

Table I.5. EPA Method 1613 calibration and verification solutions CSL and CS1-CS4 from Wellington Laboratories Inc.

	Concentration (ng mL^{-1})				
	1613CSL	1613CS1	1613CS2	1613CS3	1613CS4
2,3,7,8-Tetrachlorodibenzo-p-dioxin	0.1	0.5	2	10	40
1,2,3,7,8-Pentachlorodibenzo-p-dioxin	0.5	2.5	10	50	200
1,2,3,4,7,8-Hexachlorodibenzo-p-dioxin	0.5	2.5	10	50	200
1,2,3,6,7,8-Hexachlorodibenzo-p-dioxin	0.5	2.5	10	50	200
1,2,3,7,8,9-Hexachlorodibenzo-p-dioxin	0.5	2.5	10	50	200
1,2,3,4,6,7,8-Heptachlorodibenzo-p-dioxin	0.5	2.5	10	50	200
Octachlorodibenzo-p-dioxin	1.0	5	20	100	400
2,3,7,8-Tetrachlorodibenzofuran	0.1	0.5	2	10	40
1,2,3,7,8-Pentachlorodibenzofuran	0.5	2.5	10	50	200
2,3,4,7,8-Pentachlorodibenzofuran	0.5	2.5	10	50	200
1,2,3,4,7,8-Hexachlorodibenzofuran	0.5	2.5	10	50	200
1,2,3,6,7,8-Hexachlorodibenzofuran	0.5	2.5	10	50	200
1,2,3,7,8,9-Hexachlorodibenzofuran	0.5	2.5	10	50	200
2,3,4,6,7,8-Hexachlorodibenzofuran	0.5	2.5	10	50	200
1,2,3,4,6,7,8-Heptachlorodibenzofuran	0.5	2.5	10	50	200
1,2,3,4,7,8,9-Heptachlorodibenzofuran	0.5	2.5	10	50	200
Octachlorodibenzofuran	1.0	5	20	100	400
2,3,7,8-Tetrachloro[$^{13}C_{12}$]dibenzo-p-dioxin	100	100	100	100	100
1,2,3,7,8-Pentachloro[$^{13}C_{12}$]dibenzo-p-dioxin	100	100	100	100	100
1,2,3,4,7,8-Hexachloro[$^{13}C_{12}$]dibenzo-p-dioxin	100	100	100	100	100
1,2,3,6,7,8-Hexachloro[$^{13}C_{12}$]dibenzo-p-dioxin	100	100	100	100	100
1,2,3,4,6,7,8-Heptachloro[$^{13}C_{12}$]dibenzo-p-dioxin	100	100	100	100	100
Octachloro[$^{13}C_{12}$]dibenzo-p-dioxin	200	200	200	200	200
2,3,7,8-Tetrachloro[$^{13}C_{12}$]dibenzofuran	100	100	100	100	100
1,2,3,7,8-Pentachloro[$^{13}C_{12}$]dibenzofuran	100	100	100	100	100
2,3,4,7,8-Pentachloro[$^{13}C_{12}$]dibenzofuran	100	100	100	100	100
1,2,3,4,7,8-Hexachloro[$^{13}C_{12}$]dibenzofuran	100	100	100	100	100

Table I.5. EPA Method 1613 calibration and verification solutions CSL and CS1-CS4 from Wellington Laboratories Inc (cont.).

	Concentration (ng mL^{-1})				
	1613CSL	1613CS1	1613CS2	1613CS3	1613CS4
1,2,3,6,7,8-Hexachloro[$^{13}C_{12}$]dibenzofuran	100	100	100	100	100
1,2,3,7,8,9-Hexachloro[$^{13}C_{12}$]dibenzofuran	100	100	100	100	100
2,3,4,6,7,8-Hexachloro[$^{13}C_{12}$]dibenzofuran	100	100	100	100	100
1,2,3,4,6,7,8-Heptachloro[$^{13}C_{12}$]dibenzofuran	100	100	100	100	100
1,2,3,4,7,8,9-Heptachloro[$^{13}C_{12}$]dibenzofuran	100	100	100	100	100
2,3,7,8-[$^{37}Cl_4$]Tetrachlorodibenzo-p-dioxin	0.1	0.5	2	10	40
1,2,3,4-Tetrachloro[$^{13}C_{12}$]dibenzo-p-dioxin	100	100	100	100	100
1,2,3,7,8,9-Hexachloro[$^{13}C_{12}$]dibenzo-p-dioxin	100	100	100	100	100

ANNEX II. Recoveries of labelled EPA 1613 solutions

A. PCDD/Fs analysis in the electrochemical oxidation of Triclosan

Table II.1. Recoveries of labelled PCDD/Fs in 10, 100 and 150 mg L^{-1} Triclosan blank solutions performed in duplicate (I and II).

	Initial concentration of Triclosan (mg L^{-1})					
	10		100		150	
	Recovery (%)					
	I	II	I	II	I	II
2,3,7,8-TCDD^{13}C	83	87	81	82	76	87
1,2,3,7,8-PeCDD^{13}C	112	111	96	109	96	111
1,2,3,4,7,8-HxCDD^{13}C	102	103	91	99	83	97
1,2,3,6,7,8-HxCDD^{13}C	97	97	87	96	80	89
1,2,3,7,8,9-HxCDD^{13}C	100	100	100	100	100	100
1,2,3,4,6,7,8-HpCDD^{13}C	104	103	94	105	95	98
OCDD^{13}C	88	76	26	101	77	87
2,3,7,8-TCDF^{13}C	95	96	34	94	88	100
1,2,3,7,8-PeCDF^{13}C	100	101	95	96	85	100
2,3,4,7,8-PeCDF^{13}C	108	108	100	101	90	103
1,2,3,4,7,8-HxCDF^{13}C	89	98	81	86	87	95
1,2,3,6,7,8-HxCDF^{13}C	87	93	84	92	81	89
1,2,3,7,8,9-HxCDF^{13}C	104	100	92	99	84	92
2,3,4,6,7,8-HxCDF^{13}C	89	91	83	94	80	85
1,2,3,4,6,7,8-HpCDF^{13}C	101	88	89	103	83	95
1,2,3,4,7,8,9-HpCDF^{13}C	102	98	90	110	87	104

Table II.2. Recoveries of labelled PCDD/Fs in 10, 100 and 150 mg L^{-1} Triclosan electrochemical oxidized samples performed in duplicate (I and II). Electrolyte type: NaCl.

	Initial concentration of Triclosan (mg L^{-1})							
	10		100		100 (Presence copper)		150	
	Recovery (%)							
	I	II	I	II	I	II	I	II
2,3,7,8-TCDD^{13}C	78	80	83	89	86	73	65	76
1,2,3,7,8-PeCDD^{13}C	97	109	108	112	114	95	88	95
1,2,3,4,7,8-HxCDD^{13}C	90	93	102	106	106	88	74	90
1,2,3,6,7,8-HxCDD^{13}C	85	89	97	97	101	81	66	80
1,2,3,7,8,9-HxCDD^{13}C	100	100	100	100	100	100	100	100
1,2,3,4,6,7,8-HpCDD^{13}C	85	105	97	106	107	85	79	83
OCDD^{13}C	67	101	78	87	98	74	69	90
2,3,7,8-TCDF^{13}C	86	90	93	98	95	78	76	89
1,2,3,7,8-PeCDF^{13}C	88	91	97	104	102	85	74	86
2,3,4,7,8-PeCDF^{13}C	95	103	104	89	109	92	86	90
1,2,3,4,7,8-HxCDF^{13}C	87	92	97	93	100	86	77	94
1,2,3,6,7,8-HxCDF^{13}C	83	88	92	98	94	81	67	86
1,2,3,7,8,9-HxCDF^{13}C	87	96	104	103	108	84	71	82
2,3,4,6,7,8-HxCDF^{13}C	81	88	93	98	97	79	66	80
1,2,3,4,6,7,8-HpCDF^{13}C	78	99	106	101	111	82	79	84
1,2,3,4,7,8,9-HpCDF^{13}C	84	115	99	110	110	87	81	84

Table II.3. Recoveries of labelled PCDD/Fs in 10, 100 and 150 mg L^{-1} Triclosan electrochemical oxidized samples performed in duplicate (I and II). Electrolyte type: Na_2SO_4.

	Initial concentration of Triclosan (mg L^{-1})							
	10		100		100 (Presence copper)		150	
	Recovery (%)							
	I	II	I	II	I	II	I	II
2,3,7,8-TCDD^{13}C	92	84	86	77	91	75	78	86
1,2,3,7,8-PeCDD^{13}C	117	105	112	98	117	94	100	114
1,2,3,4,7,8-HxCDD^{13}C	108	96	108	90	110	87	86	95
1,2,3,6,7,8-HxCDD^{13}C	101	89	103	85	106	82	77	86
1,2,3,7,8,9-HxCDD^{13}C	100	100	100	100	100	100	100	100
1,2,3,4,6,7,8-HpCDD^{13}C	106	102	104	91	110	76	90	98
OCDD^{13}C	83	90	104	80	88	55	79	84
2,3,7,8-TCDF^{13}C	102	97	99	83	103	84	89	99
1,2,3,7,8-PeCDF^{13}C	110	92	100	91	113	88	92	106
2,3,4,7,8-PeCDF^{13}C	114	101	106	95	117	91	97	109
1,2,3,4,7,8-HxCDF^{13}C	100	95	103	85	90	69	85	95
1,2,3,6,7,8-HxCDF^{13}C	97	92	98	80	90	74	77	85
1,2,3,7,8,9-HxCDF^{13}C	107	98	111	90	110	86	83	92
2,3,4,6,7,8-HxCDF^{13}C	97	88	99	79	93	74	75	84
1,2,3,4,6,7,8-HpCDF^{13}C	99	97	112	82	108	79	85	94
1,2,3,4,7,8,9-HpCDF^{13}C	103	108	106	89	100	72	93	102

Table II.4. Recoveries of labelled non-chlorinated and low chlorinated PCDD/Fs (mono to tri-) in 10, 100 and 150 mg L^{-1} Triclosan blank solutions performed in duplicate (I and II).

	Initial concentration of Triclosan (mg L^{-1})					
	10		100		150	
	Recoveries (%)					
	I	II	I	II	I	II
D-p-D^{13}C	-	-	-	-	-	-
2-D-p-D^{13}C	1	11	12	0	7	0
2,3-D-p-D^{13}C	29	87	39	27	31	22
2,3,7-D-p-D^{13}C	83	91	76	78	65	68
D-F^{13}C	-	-	-	-	-	-
2-D-F^{13}C	0	22	3	1	2	0
2,3-D-D-F^{13}C	27	87	63	21	26	35
2,3,8-D-D-F^{13}C	83	87	124	82	72	67

Table II.5. Recoveries of labelled non-chlorinated and low chlorinated PCDD/Fs (mono to tri-) in 10, 100 and 150 mg L^{-1} Triclosan electrochemical oxidized samples performed in duplicate (I and II). Electrolyte type: NaCl.

	Initial concentration of Triclosan (mg L^{-1})							
	10		100		100 (Presence copper)		150	
	Recoveries (%)							
	I	II	I	II	I	II	I	II
D-p-$D^{13}C$	-	0	-	-	-	-	-	-
2-D-p-$D^{13}C$	6	0	7	2	3	-	0	0
2,3-D-p-$D^{13}C$	56	16	116	40	-	18	3	9
2,3,7-D-p-$D^{13}C$	82	78	122	85	10	59	51	61
D-$F^{13}C$	-	0	-	-	-	-	-	-
2-D-$F^{13}C$	11	1	14	1	-	-	0	0
2,3-D-D-$F^{13}C$	56	14	62	31	4	6	10	6
2,3,8-D-D-$F^{13}C$	78	78	93	81	-	57	55	69

Table II.6. Recoveries of labelled non-chlorinated and low chlorinated PCDD/Fs (mono to tri-) in 10, 100 and 150 mg L^{-1} Triclosan electrochemical oxidized samples performed in duplicate (I and II). Electrolyte type: Na_2SO_4.

	Initial concentration of Triclosan (mg L^{-1})							
	10		100		100 (presence copper)		150	
	Recoveries (%)							
	I	II	I	II	I	II	I	II
D-p-$D^{13}C$	-	0	-	-	-	-	-	-
2-D-p-$D^{13}C$	2	3	13	3	19	-	0	0
2,3-D-p-$D^{13}C$	44	54	116	41	-	38	3	1
2,3,7-D-p-$D^{13}C$	91	98	113	80	77	80	59	47
D-$F^{13}C$	-	0	-	-	-	-	-	-
2-D-$F^{13}C$	5	9	49	2	19	2	0	0
2,3-D-D-$F^{13}C$	46	61	85	33	66	34	3	1
2,3,8-D-D-$F^{13}C$	87	102	109	78	81	81	78	67

B. PCDD/Fs analysis in the photocatalytic oxidation of Triclosan

Table II.7. Recoveries of labelled PCDD/Fs in 10 mg L^{-1} Triclosan blank solutions performed in duplicate (I and II).

	Recovery (%)	
	I	II
2,3,7,8-TCDD^{13}C	90	64
1,2,3,7,8-PeCDD^{13}C	108	91
1,2,3,4,7,8-HxCDD^{13}C	99	84
1,2,3,6,7,8-HxCDD^{13}C	96	84
1,2,3,7,8,9-HxCDD^{13}C	100	100
1,2,3,4,6,7,8-HpCDD^{13}C	104	90
OCDD^{13}C	109	69
2,3,7,8-TCDF^{13}C	85	70
1,2,3,7,8-PeCDF^{13}C	91	83
2,3,4,7,8-PeCDF^{13}C	104	89
1,2,3,4,7,8-HxCDF^{13}C	90	77
1,2,3,6,7,8-HxCDF^{13}C	87	75
1,2,3,7,8,9-HxCDF^{13}C	96	75
2,3,4,6,7,8-HxCDF^{13}C	90	76
1,2,3,4,6,7,8-HpCDF^{13}C	100	86
1,2,3,4,7,8,9-HpCDF^{13}C	105	63

Table II.8. Recoveries of labelled PCDD/Fs in 10 mg L^{-1} Triclosan photocatalytic oxidized samples performed in duplicate (I and II). TiO_2 loading: 0.75, 1 and 1.5 g L^{-1}.

	TiO_2 concentration (g L^{-1})					
	0.75		1		1.5	
	Recovery (%)					
	I	II	I	II	I	II
2,3,7,8-TCDD^{13}C	69	70	62	62	63	65
1,2,3,7,8-PeCDD^{13}C	71	78	74	94	90	92
1,2,3,4,7,8-HxCDD^{13}C	72	79	70	82	80	76
1,2,3,6,7,8-HxCDD^{13}C	70	79	69	78	79	76
1,2,3,7,8,9-HxCDD^{13}C	100	100	100	100	100	100
1,2,3,4,6,7,8-HpCDD^{13}C	63	89	78	84	77	75
OCDD^{13}C	53	87	76	86	79	74
2,3,7,8-TCDF^{13}C	79	83	73	71	71	72
1,2,3,7,8-PeCDF^{13}C	73	78	70	80	81	79
2,3,4,7,8-PeCDF^{13}C	76	82	74	90	90	88
1,2,3,4,7,8-HxCDF^{13}C	72	75	65	70	76	72
1,2,3,6,7,8-HxCDF^{13}C	71	74	64	73	74	71
1,2,3,7,8,9-HxCDF^{13}C	76	83	71	79	78	73
2,3,4,6,7,8-HxCDF^{13}C	69	74	63	73	78	70
1,2,3,4,6,7,8-HpCDF^{13}C	65	88	74	82	79	75
1,2,3,4,7,8,9-HpCDF^{13}C	59	89	73	82	82	75

ANNEX III. Supplementary experimental data

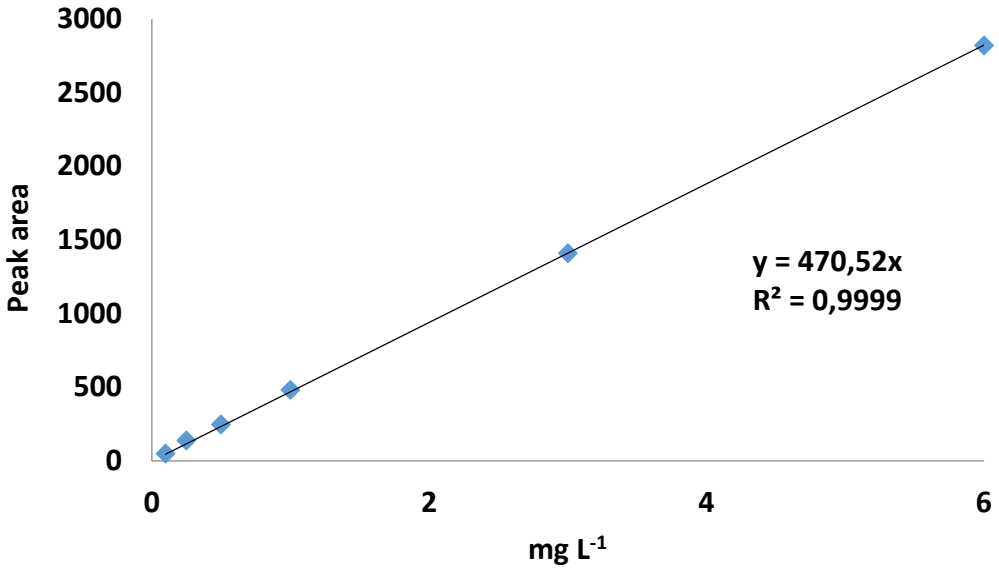

Figure I. Calibration curve representing the peak area vs. the concentration of the standard 2,7/2,8-dichlorodibenzo-p-dioxin used in the data analysis of High-Performance Liquid Chromatography (HPLC) results.

ANNEX IV. List of papers published in indexed journals

1. Fate and hazard of the electrochemical oxidation of triclosan. Evaluation of polychlorodibenzo‐p‐dioxins and polychlorodibenzofurans (PCDD/Fs) formation. Solá-Gutiérrez, C., San Román, M.F., Ortiz, I. Sci. Total Environ. 626 (2018) 126-133. (JCR Impact Factor (2018): 5.589, Q1).

2. PCDD/Fs traceability during triclosan electrochemical oxidation. Solá-Gutiérrez, C., Schröder, S., San Román, M.F., Ortiz, I. J. Hazard Mater. 369 (2019) 584-592. (JCR Impact Factor (2018): 7.650, Q1).

3. Shedding light into the mechanistic photolytic and photocatalytic degradation of Triclosan. Solá-Gutiérrez, C., Schröder, S., San Román, M.F., Ortiz, I. J. Environ. Manage. *Under review*. (JCR Impact Factor (2018): 4.865, Q1).

4. Overall toxicity assessment of treating wastewater containing organic pollutants under a life cycle approach. San Román, M.F., Solá-Gutiérrez, C., Laso, J., Schröder, S., Margallo, M., Vazquez, I., Ortiz, I., Irabien, A., Aldaco, R. Sci. Total Environ. *Submitted*. (JCR Impact Factor (2018): 5.589, Q1).

ANNEX V. Congress contributions

Solá-Gutiérrez, C., San Román, M.F., Ortiz, I. Research of polychlorodibenzo-p-dioxin and dibenzofurans (PCDD/Fs) precursors in the application of Advanced Oxidation Processes. 6th EuCheMS-Chemistry Congress. Seville (Spain), September 11-15, 2016. *Poster presentation*

Fernández-Castro, P., **Solá-Gutiérrez, C.**, San Román, M.F., Ortiz, I. Formation of low and high chlorinated dibenzo-p-dioxins and dibenzofurans during the Fenton oxidation of 2-chlorophenol. V Reunión Nacional de Dioxinas, Furanos y Compuestos Orgánicos Persistentes Relacionados. Barcelone (Spain), June 14-16, 2017. *Poster presentation*

Solá-Gutiérrez, C., San Román, M.F., Ortiz, I. The potential formation of polychlorinated dibenzo-p-dioxins and dibenzofurans (PCCD/Fs) during the electrochemical oxidation of Triclosan. V Reunión Nacional de Dioxinas, Furanos y Compuestos Orgánicos Persistentes Relacionados. Barcelone (Spain), June 14-16, 2017. *Poster presentation*

Fernández-Castro, P., **Solá-Gutiérrez, C.**, San Román, M.F., Ortiz, I. Formation of PCDD/Fs during the Fenton oxidation of 2-CP. 10th World Congress of Chemical Engineering. Barcelone (Spain), October 1-5, 2017. *Poster presentation*

Solá-Gutiérrez, C., Schröder, S., San Román, M.F., Ortiz, I. Aqueous oxidation of Triclosan: The potential formation of PCDD/Fs. 38th International Symposium on Halogenated Persistent Organic Pollutants (POPs) & 10th International PCB Workshop: Dioxin 2018. Cracow (Poland), August 26-31, 2018. *Poster presentation*

Solá-Gutiérrez, C., San Román, M.F., Ortiz, I. Dioxins and furans as by-products in the Advanced Oxidation of Triclosan. 38th International Symposium on Halogenated Persistent Organic Pollutants (POPs) & 10th International PCB Workshop: Dioxin 2018. Cracow (Poland), August 26-31, 2018. *Lecture*

Solá-Gutiérrez, C., San Román, M.F., Ortiz, I. Formation of chlorinated organic compounds during the electrochemical oxidation: Determination of PCDD/Fs. ANQUE-ICCE-CBIQ 2019. Santander (Spain), June 19-21, 2019. *Lecture*

Solá-Gutiérrez, C., Schröder, S., San Román, M.F., Ortiz, I. Potential formation of PCDD/Fs during the TCS electrochemical oxidation. Influence of the operational variables. ECCE12, The 12th European Congress of Chemical Engineering. Florence (Italy), September 15-19, 2019. *Lecture*

Solá-Gutiérrez, C., Schröder, S., San Román, M.F., Ortiz, I. Photocatalytic degradation of Triclosan. 14th Conference on sustainable development of energy, water and environment system (SDEWES). Dubrovnik (Croatia), October 1-6, 2019. *Poster presentation*

Solá-Gutiérrez, C., Schröder, S., San Román, M.F., Ortiz, I. Determination of chlorinated organic compounds and PCDD/Fs during Triclosan electrochemical oxidation. 14th Conference on sustainable development of energy, water and environment system (SDEWES). Dubrovnik (Croatia), October 1-6, 2019. *Lecture*

ANNEX VI. Dissemination activities

Solá-Gutiérrez, C. European Researchers' Night. Diffusion activities of the Research Groups: DEPRO, PAS, IPS y TAB. Santander, September 2016, 2017, 2019.

Solá-Gutiérrez, C. Diffusion activities in the Scientific Week at the University of Cantabria.
Santander, November 7-1, 2016, November 6-17, 2017.

Solá-Gutiérrez, C. Mini-lecture: own experiences as Chemical Engineer. International Day of Women and Girls in Science. ETSIIT, University of Cantabria. February 11, 2019.

About the author

Claudia Solá Gutiérrez was born in Santander (Spain) on September 21st, 1991. She obtained a BSc and MSc in Chemical Engineering in 2015 at the University of Cantabria. After finishing her studies, she joined to the Chemical and Biomolecular Engineering Department to start her research career. In 2015, she started her PhD in "Chemical Engineering, Energy and Processes" under the supervision of Prof. Inmaculada Ortiz and Dr. Mª Fresnedo San Román. To this end, she was granted with a Personnel Research Training Program of the Spanish Ministry of Science, Innovation and Universities.

During her PhD, she performed a research stay of four months at the Institute of Biogeochemistry and Pollutants Dynamics (ETH Zürich) under the supervision of Prof. Kristopher McNeill and Dr. Jennifer Apell.

At the time of working, she is author of 2 scientific articles in indexed journals as well as 10 contributions in international and national conferences. Two more articles have been submitted to international journals, which are expected to be published in the near future.